Mécanismes moléculaires impliqués dans l'adaptation de Francisella tularensis à sa niche intracellulaire

Jason Ziveri

Université Paris Descartes

Thèse de Doctorat en sciences présentée par

Jason ZIVERI

Pour obtenir le grade de Docteur de l'Université Paris Descartes

Ecole Doctorale Bio Sorbonne Paris Cité

Science de la vie et de la santé

Spécialité : Microbiologie

Mécanismes moléculaires impliqués dans l'adaptation de *Francisella tularensis* à sa niche intracellulaire

Soutenue publiquement le 17 septembre 2018, devant le jury composé de :

Dr. Alain Charbit	Directeur de thèse
Pr. Xavier Nassif	Président du jury
Dr. Patricia Renesto	Rapporteur
Dr. Eric Cascales	Rapporteur
Dr. Javier Pizzaro-Cerda	Examinateur
Pr. Eric Valade	Examinateur

Université Paris Descartes

Thèse de Doctorat en sciences présentée par

Jason ZIVERI

Pour obtenir le grade de Docteur de l'Université Paris Descartes

Ecole Doctorale Bio Sorbonne Paris Cité

Science de la vie et de la santé

Spécialité : Microbiologie

Mécanismes moléculaires impliqués dans l'adaptation de *Francisella tularensis* à sa niche intracellulaire

Soutenue publiquement le 17 septembre 2018, devant le jury composé de :

Dr. Alain Charbit	Directeur de thèse
Pr. Xavier Nassif	Président du jury
Dr. Patricia Renesto	Rapporteur
Dr. Eric Cascales	Rapporteur
Dr. Javier Pizzaro-Cerda	Examinateur
Pr. Eric Valade	Examinateur

Unité de pathogénie des infections systémiques, Inserm 1151 équipe 11

Institut Necker Enfant Malade, Université Paris Descartes

Bâtiment Leriche – Porte 9

14 rue Maria Helena Viera Da Silva

75014 Paris

« *Le sentiment de mystère est le plus beau qu'il nous soit donné d'éprouver. Il est la source de tout art et de toute science véritable.* »

Albert Einstein

« *Tout ce que nous avons à décider, c'est ce que nous devons faire du temps qui nous est imparti.* »

J. R. R. Tolkien (1954)

Remerciements

Je tiens avant toute chose à remercier mon directeur de thèse, le Dr Alain Charbit, de m'avoir accueilli dans son équipe *Francisella*, pour son aide précieuse, ses conseils avisés, sa patience, la liberté et l'autonomie dont j'ai pu faire preuve tout au long de ces trois ans de thèse et de m'avoir fait confiance dès le début.

Je remercie aussi le Pr Xavier Nassif de m'avoir accueilli dans son laboratoire et d'avoir accepté de prendre la direction de mon jury de thèse.

Un grand remerciement à la Direction Général de l'Armement (DGA) et à l'INSERM, sans qui cette thèse n'aurait pas été possible.

Je remercie également les rapporteurs, le Dr Patricia Renesto et le Dr Eric Cascales, ainsi que les examinateurs, le Docteur Javier Pizzaro-Cerda et le Professeur Eric Valade pour avoir accepté d'évaluer ce travail et pour l'intérêt qu'ils y ont porté.

Comment ne pas remercier l'intégralité de l'équipe 11, présente et passée, pour leurs aides, leurs bonnes humeurs, ces bons moments passés ensemble et parce que « la vérité n'intéresse personne ». Daniel Euphrasie pour tous ces kilomètres de courses, Xin Tan pour tes « chinoiseries », Fabiola Tros pour ton aide pendant ces 3 ans mais surtout pour l'organisation des repas d'équipe, Marion Dupuis pour ton aide et ton soutient pendant ces 3 ans, Mathilde pour tes soufflements et ta motivation défaillante, Julie pour toutes nos discussions cinématographique et Zoé pour tes talents musicaux. Je remercie aussi Jean-Philippe, Anne, Mathieu, Emmanuelle, Hervé et Gaël pour tous ces moments passés à table et surtout nos discussions et débats du midi. Je remercie tous les autres membres de l'équipe, Elena, Sophia, Elodie, Eric, Jean, David, Christine et Baptiste.

Parce qu'il n'y a pas que la science, je me dois aussi de remercier tout ceux qui m'ont soutenu durant toutes mes années d'études. Je remercie tous mes supers copains, Joffrey, Alex, Valou, Denis, Le Roi Pipou, Manon, Flora et Charlène pour tous nos délires, tous ces moments passés ensemble et sans qui tout aurait été très différent. Un merci à tous ceux qui m'ont soutenu de près ou de loin pendant toutes ces années (Victoria, Salomé, Elyane, Catherine, Matthieu, Michot et Baptiste). Et tous ceux que j'oublie ...

J'aimerais terminer ces remerciements en dédiant ma thèse à ma fabuleuse famille sans qui tout cela aurait été impossible. A mes parents, pour l'exemple qu'ils représentent et pour m'avoir transmit ce goût du travail, à ma sœur et mon frère pour à peu près tout...

Résumé

Francisella tularensis est l'agent étiologique responsable de la tularémie, une zoonose endémo-épidémique dans l'hémisphère Nord, capable d'infecter un grand nombre d'espèces animales (mammifères, oiseaux, insectes,…) et potentiellement hautement pathogène pour l'homme. Cette pathologie encore mal connue a des manifestations très polymorphes, pouvant aller de formes bénignes jusqu'à des formes pulmonaires mortelles.

Lors de l'infection de mammifères, *Francisella* se multiplie principalement à l'intérieur des cellules macrophagiques. Cependant, au cours de sa dissémination systémique, elle est capable d'infecter de nombreux autres types cellulaires, y compris non phagocytaires (épithéliales, hépatocytes,…). Pour cela, *Francisella* a développé des mécanismes lui permettant d'échapper à la lyse dans le phagosome et de se multiplier dans le cytoplasme des cellules infectées où elle obtient certains éléments essentiels à sa croissance.

Dans une première partie, nous nous sommes intéressés à l'adaptation métabolique de *Francisella* au cours de son cycle intracellulaire et notamment au rôle d'une enzyme clé de la Glycolyse/Gluconéogenèse, la fructose-1,6-biphosphate aldolase (FBA). Au-delà de son rôle ménager dans le métabolisme, nous démontrons que FBA est importante pour la multiplication bactérienne dans les macrophages en présence de substrats gluconéogèniques. De plus, nous mettons en évidence un rôle direct de cette enzyme métabolique dans la régulation de la transcription des gènes *katG* et *rpoA*, codant respectivement pour la catalase et une sous-unité de l'ARN polymérase. Nous proposons un modèle dans lequel FBA participe au contrôle de l'homéostasie redox de l'hôte et à la réponse immunitaire inflammatoire.

Dans une seconde partie, nous nous sommes intéressés au système de sécrétion de type VI (SST6) de *Francisella*. De nombreuses bactéries à Gram négatif utilisent le SST6 pour transloquer des protéines effectrices dans des cellules eucaryotes ou procaryotes. *Francisella* possède un SST6 non-canonique codé sur l'îlot de pathogénicité FPI qui est essentiel pour la sortie du phagosome et permet à la bactérie de se multiplier dans le cytosol de la cellule hôte. En utilisant une approche phosphoprotéomique globale chez la sous-espèce *novicida*, nous avons identifié un site de phosphorylation unique sur la tyrosine 139 de IglB, un composant clé de la gaine contractile du SST6. Nos résultats suggèrent que le statut de phosphorylation de IglB joue un rôle important dans l'assemblage d'un SST6 fonctionnel. Nous proposons que cette modification post-traductionnelle du composant majeur de la gaine pourrait constituer un nouveau mécanisme permettant de moduler la dynamique d'assemblage/désassemblage du SST6.

Mots Clés : *Francisella tularensis*, Métabolisme, Fructose-1,6-biphosphate aldolase, Système de Sécrétion de Type VI, IglB, Modification post-traductionnelle.

Abstract

Francisella tularensis is the etiological agent responsible for tularemia, an endemo-epidemic zoonosis in the northern hemisphere, capable of infecting a large number of animal species (mammals, birds, insects, ...) and potentially highly pathogenic for the man. This pathology, still poorly known, has very polymorphous manifestations, ranging from mild to deadly lung forms.

During mammalian infection, *Francisella* multiplies mainly within macrophage cells. However, during its systemic dissemination, it is able to infect many other cell types, including non-phagocytic (epithelial, hepatocytes, ...). For this, *Francisella* has developed mechanisms to escape lysis in the phagosome and to multiply in the cytoplasm of infected cells where it gets some essential elements for its growth.

In a first part, we focused on the metabolic adaptation of *Francisella* during its intracellular cycle and in particular the role of a key enzyme of Glycolysis / Gluconeogenesis, fructose-1,6-biphosphate aldolase (FBA). Beyond its housekeeping role in metabolism, we demonstrate that FBA is important for bacterial multiplication in macrophages in the presence of gluconeogenic substrates. In addition, we highlight a direct role of this metabolic enzyme in the regulation of transcription of the genes katG and rpoA, coding respectively for catalase and a subunit of RNA polymerase. We propose a model in which FBA participates in the control of host redox homeostasis and inflammatory immune response.

In a second part, we were interested in the Type VI secretion system (T6SS) of *Francisella*. Many Gram-negative bacteria use T6SS to translocate effector proteins into eukaryotic or prokaryotic cells. *Francisella* has a non-canonical T6SS encoded on the pathogenicity FPI island that is essential for phagosome release and allows the bacterium to multiply in the cytosol of the host cell. Using a global phosphoproteomic approach in *novicida* subspecies, we identified a unique phosphorylation site on IglB tyrosine 139, a key component of the contractile sheath of T6SS. We demonstrate that the phosphorylation status of IglB plays an important role in the assembly of a functional T6SS. We propose that this post-translational modification of the major component of the sheath may constitute a regulation mechanism for modulating the assembly / disassembly dynamics of the T6SS.

Key words : *Francisella tularensis*, Metabolism, Fructose-1,6-biphosphate aldolase, Type VI Secretion System, IglB, Post-translational modification.

Liste des Abréviations

ABC : ATP binding cassette
AIM2 : Absent In Melanoma 2
Atg : Autophagy related genes
Bcl-2 : B-cell lymphoma 2
BCV : *Brucella* Containing Vacuole
CryoEM : cryo-electro-microscopie
DAMPs : Danger-associated molecular patterns
ED : Voie Entner-Doudoroff
EMP : Embden-Meyerhof-Parnas
Fba : Fructose-1,6-biphosphate aldolase
FCP : Francisella-containing phagosome
FPI : *Fancisella* Pathogenicity Island
GlpX : Fructose biphosphatase de classe II
Igl : Intracellular Growth Locus
IS : Séquences d'insertion
LAMP-1 : Lysosomal-associated membrane protein
LC3 : Microtubule –associated protein light chain 3
LCV : *Legionella* Containing Vacuole
LLO : Listeriolysine O
LPS : Lipopolysaccharide
LVS : Live vaccine strain
NRAMP1 : Natural resistance-associated macrophage protein 1
PAM : Peptides anti-microbiens
PAMPs : Pathogen-associated molecular patterns
ppGpp : Guanosine tétraphosphate
Mpb : Mega paire de base
MDP : Muramyl dipeptide
MigR : Macrophage Intracellular Growth Regulator
NADPH : nicotinamide adenine dinucléotide phophate
NLR : NOD-Like receptors
OMV : Vésicules de membrane externe
PEP : phosphoénolpyruvate
PGN : Peptidoglycane
PI(3)P : Phosphatidylinositol-3-Phosphate
PlcA : Phospholipase bactérienne C
PP : Voie des pentoses phosphates
PRR : Pattern Recognition Receptors
RE : Réticulum Endoplasmique
RLR : RIG-I -like receptors
ROS : Reactive oxygen species
SNARE : N-ethylmaleimide-sensitive factor attachment protein receptor
ssp. : Sous-espèce
SST3 : Système de sécrétion de type 3
SST6 : Système de sécrétion de type 6
TCA : Tricarboxilic acid cycle
TFP : Pili de type 4
TLR : Toll-like receptor
Tss : Type six secretion
UFC : Unités formant des colonies

Table des matières

INTRODUCTION BIBLIOGRAPHIQUE

Une introduction bibliographique présentera, dans un premier chapitre, les bactéries à multiplication intracellulaire. A l'aide de quelques exemples choisis, nous nous intéresserons plus particulièrement aux bactéries à multiplication intracellulaire facultative, en insistant sur leurs stratégies pour échapper aux mécanismes d'élimination de l'hôte ainsi qu'aux différentes stratégies d'adaptation métabolique qu'elles mettent en oeuvre. Puis, nous discuterons plus en détail le cas particulier de *Francisella tularensis*, la bactérie pathogène qui est utilisée comme modèle d'étude au laboratoire.

Un deuxième chapitre présentera les deux articles qui ont constitué mon principal travail de thèse. Le premier article (déjà publié) porte sur l'identification d'une enzyme clé pour le métabolisme des carbohydrates importante pour la virulence de *Francisella.* Le second article (en préparation) porte sur une modification post-traductionnelle d'une protéine du fourreau de l'appareil de sécrétion de Type VI de *Francisella,* impliquée dans sa dynamique d'assemblage.

Enfin, les autres travaux auxquels j'ai participé, et qui ont donné lieu à des publications, seront regroupés en annexe.

Chapitre 1 :

Adaptation des bactéries à multiplication intracellulaire et leur niche

Partie I : La vie intracellulaire: un monde à part

Les bactéries pathogènes constituent un des dangers majeurs pour la santé humaine à travers le monde et l'émergence sans cesse croissante de résistances multiples aux antibiotiques nécessite le développement de nouvelles approches pour pouvoir combattre les maladies infectieuses causées par ces pathogènes. Parmi les bactéries dite « à multiplication intracellulaire », on distingue généralement deux catégories : les bactéries à multiplication intracellulaire facultative et les bactéries à multiplication intracellulaire obligatoire.

1. Généralités

Les bactéries à multiplication intracellulaire obligatoire (comme les *Chlamydia, les Rickettsia* …) ont perdu la capacité de se multiplier en dehors de leurs hôtes, contrairement aux bactéries à multiplication intracellulaire facultative (comme par exemple *Francisella tularensis*, *Listeria monocytogenes*, ou *Legionella pneumophila* …) qui ont gardé la capacité de se multiplier dans différents milieux extracellulaires. Cette capacité de ne pas strictement dépendre d'un hôte pour survivre peut leur conférer un avantage lors de leur cycle infectieux (Casadevall, 2008a; Suter, 1956).

Il existe également des bactéries à multiplication essentiellement extracellulaire mais qui, de façon occasionnelle ou dans des conditions d'infection très spécifiques, peuvent survivre et se multiplier à l'intérieur de cellules eucaryotes. C'est notamment le cas de *Staphylococcus aureus* (Rollin et al., 2017; Surewaard et al., 2016). Nous ne discuterons pas ici de cette dernière catégorie.

En général, la vie intracellulaire s'accompagne d'un phénomène de réduction du génome, de perte de gènes et d'apparition de pseudogènes (Andersson and Andersson; Martínez-Cano et al., 2015; Wernegreen, 2015). Ces pertes de gènes peuvent parfois avoir une ampleur plus importante et être associées à des pertes de voies métaboliques complètes, comme de voies nécessaires à l'acquisition de nutriments que la bactérie va être capable de récupérer directement chez son hôte. Par exemple, *Rickettsia* a perdu

de nombreux gènes nécessaires à plusieurs voies métaboliques, notamment du métabolisme des sucres, des purines et des acides aminés (Merhej et al., 2014; Renesto et al., 2005). On parle alors de «patho-adaptation». Des travaux récents émettent l'hypothèse que ce phénomène de perte de matériel génétique est à l'origine de la transition de la multiplication intracellulaire facultative vers la multiplication intracellulaire obligatoire. En effet, à terme, la perte de certaines séquences génomiques empêcherait les bactéries de survivre à l'extérieur de leurs hôtes (Casadevall, 2008b; Eisenreich et al., 2017; Weinert and Welch, 2017). La vie intracellulaire peut aussi s'accompagner d'acquisition d'un certain nombre de gènes de l'hôte. Par exemple, l'équipe de Carmen Buchrieser a démontré en 2004 l'existence de nombreuses protéines de type eucaryote chez *L. pneumophila*, un phénomène probablement lié à une évolution étroite et prolongée de cette bactérie avec les amibes de l'environnement (Cazalet et al., 2004).

Les bactéries à multiplication intracellulaire stricte dépendent de leurs hôtes et ont une relation très intime avec ceux-ci. Ces pathogènes ont appris à maitriser l'art d'échapper aux mécanismes de réponse aux infections de l'hôte et, quand la maladie se déclare, celle-ci est très souvent liée à une perturbation de la relation entre l'hôte et le pathogène. Les bactéries à multiplication intracellulaire facultative ont des relations beaucoup plus variées avec leurs hôtes. Certains de ces pathogènes ne vont causer la maladie que dans une minorité d'hôtes et n'infecter qu'un nombre limité de types cellulaires. Très souvent, le résultat de l'interaction de ces pathogènes avec leurs hôtes dépend de l'état immunologique de l'hôte.

Nous avons choisi de discuter dans cette première partie introductive le cas de quelques bactéries à multiplication intracellulaires, en insistant plus particulièrement sur leur style de vie, leurs stratégies pour échapper aux mécanismes d'élimination de l'hôte, ainsi que de leurs différentes stratégies d'adaptation métabolique. Le cas particulier de ***Francisella tularensis*** sera discuté séparément et fera l'objet de la deuxième partie.

2. Le cycle infectieux des bactéries intracellulaires

Quelque soit l'espèce bactérienne, on peut très schématiquement diviser le cycle

intracellulaire en quatre phases principales : l'*entrée*, la *survie*, la *multiplication* et la *sortie*.

L'étape d'*entrée* peut être réalisée par le pathogène de façon active ou passive (par un processus de phagocytose). Pour les processus actifs, on distingue trois grands mécanismes d'entrée, les mécanismes dits « Trigger », « Zipper » et « Looping », respectivement. Lors du mécanisme Trigger, les bactéries (ex. *Shigella*, *Salmonella*...) interagissent directement avec le cytosquelette des cellules, en injectant des effecteurs par le biais d'un système de sécrétion dédié (**Figure 1A**). Ces effecteurs provoquent des réarrangements du cytosquelette pour engloutir la bactérie dans une vacuole. Lors du mécanisme d'entrée de type « Zipper », les bactéries (ex. *Yersinia pestis, Listeria monocytogenes …*) entrent en contact et adhèrent à la cellule par la liaison spécifique entre une protéine de surface bactérienne et un récepteur cellulaire (**Figure 1B**). Les extensions membranaires et les réarrangements du cytosquelette engloutissent ensuite la bactérie dans une vacuole. Enfin, le mécanisme d'entrée ici appelé « looping » correspond à la formation de larges protrusions membranaires (loops ; **Figure 1C**). Il est à ce jour spécifique de *Francisella* et sera rediscuté plus bas (Cossart and Sansonetti, 2004; Pizarro-Cerdá et al., 2016).

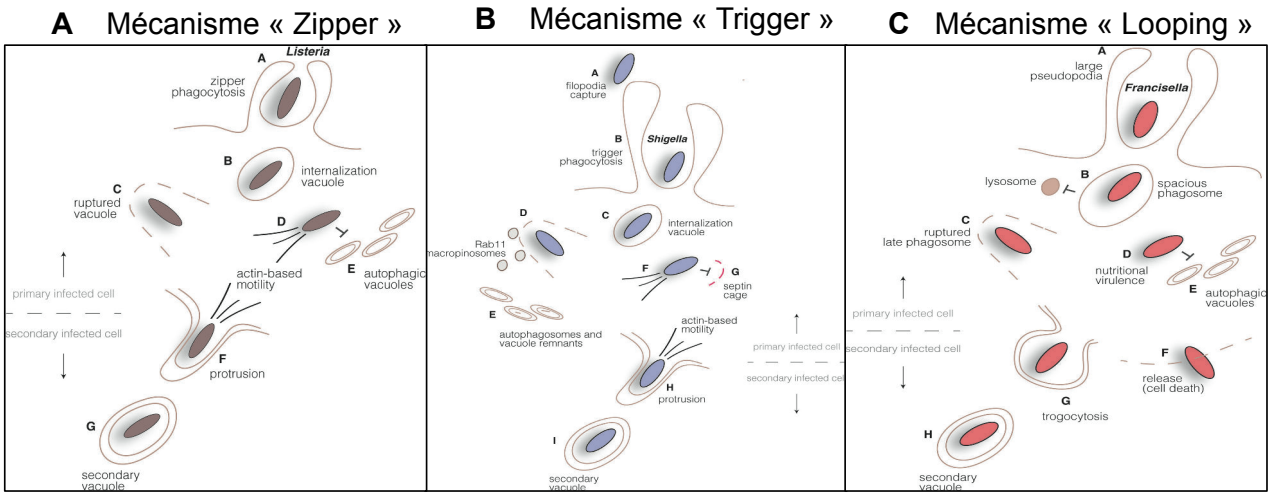

Figure 1 : Mécanismes d'entrée des bactéries à multiplication intracellulaire. A) Mécanisme « Zipper » et l'exemple de *L. monocytogenes* ; **B)** Mécanisme « Trigger » réalisé par *Shigella et Salmonella* ; **C)** Mécanisme « Looping » avec *F. tularensis*. Adapté de (Pizarro-Cerdá et al., 2016).

Dans le cas de *Pseudomonas aeruginosa,* bien que cette bactérie ait été très longtemps considérée comme une bactérie à multiplication extracellulaire, on sait désormais qu'elle est capable d'infecter des cellules non phagocytaires telles que des cellules épithéliales ou endothéliales (Engel and Eran, 2011). Cette bactérie va utiliser des systèmes de sécrétions pour rentrer et survivre dans les cellules non phagocytaires (Kroken et al., 2018; Sana et al., 2015). La bactérie va utiliser un de ces systèmes de sécrétion de Type VI (H2-T6SS) pour sécréter dans le cytoplasme des cellules cibles des effecteurs, et notamment la protéine VgrG2b qui va s'associer avec le complexe de la tubuline γTuRC, provoquer des réarrangements microtubulaires et ainsi permettre l'internalisation de la bactérie (Sana et al., 2015). La bactérie va utiliser un autre système de sécrétion (SST3) pour sécréter d'autres effecteurs (comme l'effecteur ExoS), qui seront quant à eux important pour la survie intracellulaire (Kroken et al., 2018).

La deuxième étape du cycle intracellulaire est l'étape la plus délicate pour les bactéries qui doivent *survivre* dans un environnement défavorable puisque la vacuole dans laquelle ils se trouvent va progressivement s'acidifier au fur et à mesure qu'elle se mature en phagolysosome et contenir divers composés microbicides puissants. Pour cela, certains pathogènes ont évolué de façon à être capables de sortir dans le cytosol très rapidement (en moins de 30 minutes suivant l'étape d'entrée ; **Tableau 1**). Pour ces bactéries, cette rapidité de lyse des vacuoles est essentielle à leur survie. Prenons l'exemple du mécanisme de lyse des vacuoles de *L. monocytogenes* qui a été caractérisé de façon extensive (Hamon et al., 2012; Pizarro-Cerdá et al., 2016). L'échappement est médié par la Listeriolysin O (LLO) et la phospholipase de type C. La LLO s'insère dans la membrane vacuolaire en liant le cholestérol et forme des pores, entraînant la rupture de cette membrane (Cossart et al., 1989; Osborne et al.; Seveau, 2014; Smith et al., 1995) (Cossart et al., 1989; Smith et al., 1995; **Tableau 1**). Chez *Shigella flexneri*, la sortie du compartiment phagosomal est facilitée par l'utilisation d'un système de sécrétion de Type III (SST3) et plus précisément grâce à un effecteur sécrété, IpaB (Mellouk et al., 2014).

	Shigella flexneri	***Listeria monocytogenes***	***Burkholderia pseudomallei***	***Rickettsia* spp.**
Gène bactérien	IpaB, SST3, Mxi-Spa	Listeriolysine O, Phospholipase C	Gène de fonction inconnu : BPSS1539	Phospholipases, haemolysin C
Facteurs de l'hôte	Inconnu	GILT	Inconnu	Inconnu
Condition de la vacuole nécessaire	Inconnu	pH 5,5	Inconnu	Inconnu
Cinétique d'échappement	15-30 min	17 min	Inconnu	12 minutes pour *Rickettsia coronii*

Tableau 1 : Mécanisme d'échappement phagosomal des bactéries cytosolique. Adapté de (Katrina Ray et al., 2009).

La troisième étape du cycle est la *multiplication intracellulaire*. Tandis que certaines bactéries ont acquis la capacité de sortir du phagosome pour se multiplier directement dans le cytoplasme des cellules infectées, de nombreuses autres bactéries (*e.g. Legionella, Salmonella, Mycobacteria*, *Brucella…)* ont évolué de façon à être capables de résider dans une vacuole modifiée propice à leur développement intracellulaire. Par exemple, *L. pneumophila,* une fois internalisée, va éviter la dégradation induite par les lysosomes et va remodeler le phagosome naissant en une niche réplicative (So et al., 2015). Dès le début de l'infection, la bactérie manipule le trafic membranaire de l'hôte permettant le recrutement de vésicules dérivées du réticulum endoplasmique (RE) qui vont libérer leur contenu dans les LCV (« *Legionella containing vacuole* »), fournissant le nécessaire nutritionnelle pour la réplication de la bactérie (Robinson and Roy).

Une fois internalisée par la cellule, *Brucella* réside dans une vacuole, la BCV. Cette vacuole va suivre la voie endocytique normale et devient mature au cours du temps et va donc s'acidifier. La bactérie va ensuite être capable de faire migrer la BCV jusqu'au reticulum endoplasmique. Un certain nombre de facteur de l'hôte seront utilisés par la

bactérie pour permettre à celle-ci d'établir une niche réplicative dans le RE, présentant des conditions plus favorable pour sa multiplication (Bargen et al., 2011; Celli, 2015).

Pour la dernière étape du cycle, la *dissémination*, on peut citer l'exemple de bactéries à multiplication cytosolique, comme *S. flexneri*, *L. monocytogenes*, *Burkholderia pseudomallei* et *Rickettsia,* qui vont polymériser l'actine de l'hôte au pôle bactérien pour former des queues de comètes d'actine (Stevens et al., 2006; Welch and Way, 2013). Les « comètes d'actines » propulsent les bactéries à travers le cytoplasme, permettant le passage entre cellules, en évitant le passage par le milieu extracellulaire potentiellement bactéricide (**Figure 1 et 2**). D'autres pathogènes vont tout simplement provoquer la mort cellulaire (apoptose ou pyroptose) et permettre le relargage des bactéries dans le milieux extracellulaire (*e.g. F. tularensis,* voir ci-dessous ou encore *Bacillus anthracis,*) (Henry et al., 2007; Mariathasan et al., 2005; Popov et al., 2002).

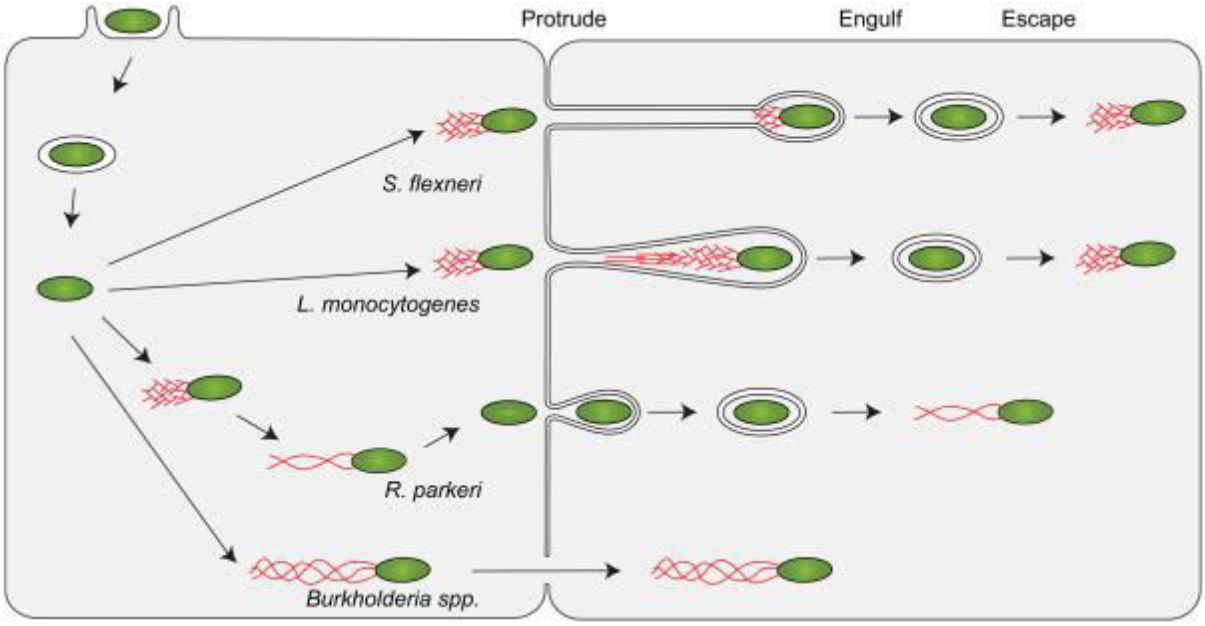

Figure 2 : Cycles de vie des bactéries à multiplication intracellulaires qui exploitent la motilité à base d'actine pour permettre le passage de cellule à cellule. Ici l'exemple de 4 bactéries intracellulaires : *S. flexneri*, *L. monocytogenes*, *Rickettsia spp.* et *Burkholderia spp*). Actine, rouge ; bactéries, vert. D'après (Lamason and Welch, 2017).

3. Les réponses de l'hôte et stratégies de contre-attaque des pathogènes intracellulaires

L'efficacité d'une réponse immunitaire face aux infections dépend de la rapidité et des moyens mis en place par les cellules du système immunitaire innée (tels que les macrophages, les cellules dendritiques et les neutrophiles). Les macrophages possèdent différents mécanismes de destruction des bactéries dont quelques exemples vous seront présentés dans cette partie.

3.1 Dans le phagosome

La première stratégie d'élimination des pathogènes se situe au niveau de l'étape phagosomale. La phagocytose des bactéries par les macrophages entraîne leur élimination lors de la maturation du phagosome grâce à trois phénomènes principaux : le «Burst oxydatif», provoqué par la production d'espèces réactives de l'oxygène (ROS), son acidification et la libération d'enzymes ou de peptides cytotoxiques contenus dans les lysosomes (Sies, 1991; Weiss and Schaible, 2015).

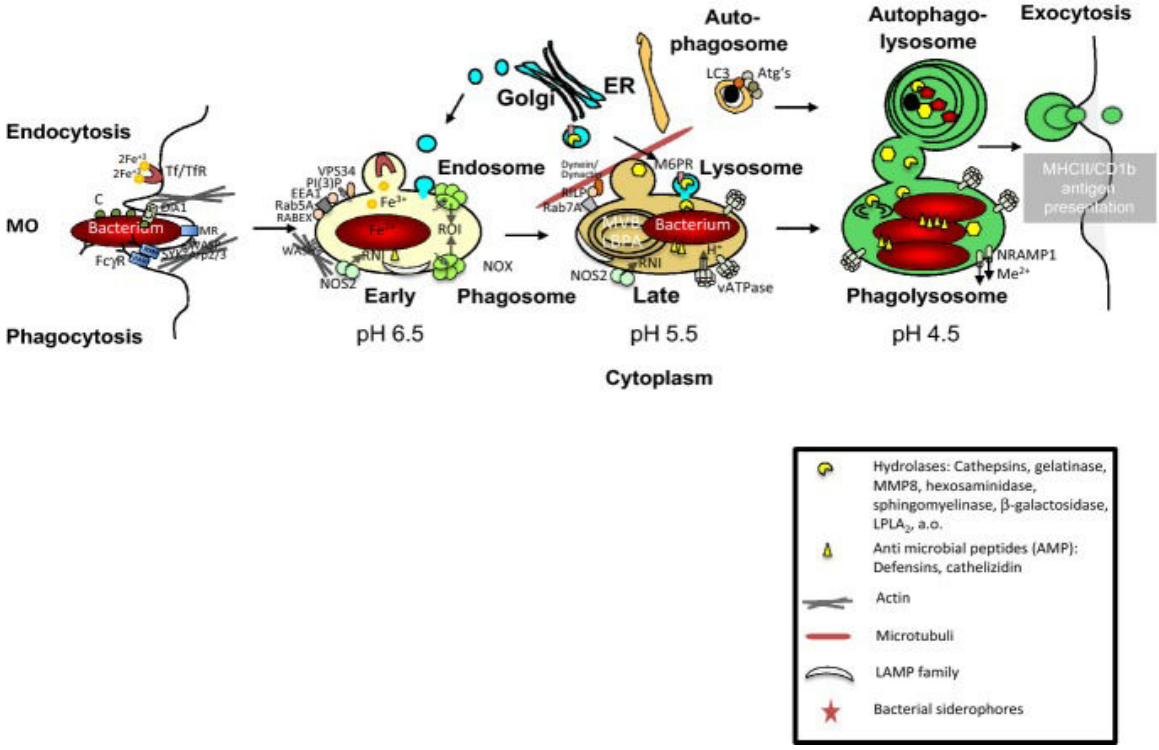

Figure 3 : Représentation des différentes étapes de la maturations des phagosomes et des autophagosomes dans les macrophages. La formation des phagosomes commence à gauche par l'étape de Phagocytose/Endocytose et se poursuit dans le cytoplasme par le recrutement des différents marqueurs. Adapté de (Weiss and Schaible, 2015).

La maturation du phagosome conduit à un remodelage et une acquisition successive de marqueurs biochimiques, donnant naissance à une vacuole microbicide (Pitt et al., 1992). Cette maturation se fait en trois étapes (**Figure 3**). Elle débute par la fusion de la vacuole nouvellement formée avec des endosomes précoces, permettant la formation du phagosome précoce. Cette fusion vésiculaire est coordonnée par une famille de protéines, les Rab GTPases (Stenmark, 2009). Ces protéines jouent un rôle important dans le trafic vésiculaire, la fusion entre les vésicules et la fission. Cette première étape se caractérise par l'acquisition d'un certain nombre de marqueurs membranaires spécifiques tels que : Rab5, la protéine initiatrice de la maturation (Vieira et al., 2003), la molécule EEA-1 (Early Endosome Antigen 1), la molécule VPS45 ou du PI(3)P (Christoforidis et al., 1999; Ohya et al., 2009). On retrouve aussi une autre grande famille de molécules intervenant dans ce processus, la famille des SNARE (N-ethylmaleimide-sensitive factor attachment protein receptor), comme par exemple les protéines VAMP4, syntaxin13, Vit1A et Syntaxin6 (Bethani et al., 2007; McBride et al., 1999). Ces molécules sont importantes puisqu'elles vont apporter l'énergie nécessaire à la modification des membranes lipidiques. C'est à cette étape que vont être produites des ROS par la NADPH oxydase, un complexe enzymatique au niveau de la membrane phagosomale. Chez les macrophages non activés, ce complexe est inactif et s'assemble lors de l'activation des macrophages. La NADPH oxydase est constituée des protéines gp91phox et p22phox et de 4 protéines cytoplasmiques : p40phox, p47phox, p67phox et Rac (**Figure** 4) qui s'assemblent à la membrane du phagosome lors de sa formation (Nunes et al.,2013). Ce complexe va produire une grande quantité d'anion superoxyde (O^{2-}) grâce à l'oxygène moléculaire. Spontanément, l'O^{2-} est transformé en peroxyde d'hydrogène qui sera transformé en un autre radical toxique, l'hydroxyle. Cette production de ROS est appelée le « burst oxydatif ».

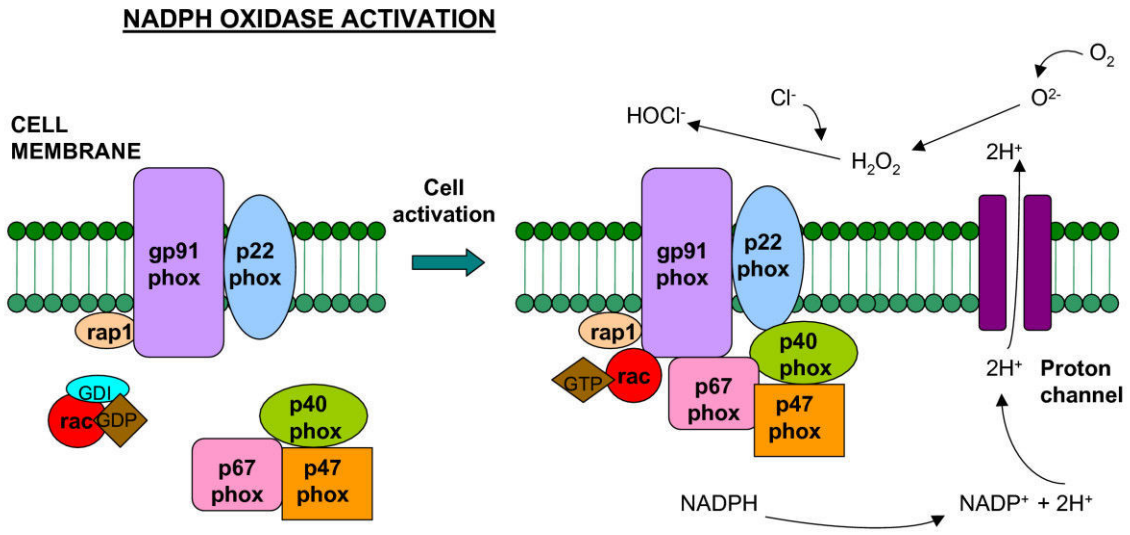

Figure 4 : Représentation schématique de l'activation de la NADPH oxydase. D'après (Assari, 2006).

On assiste ensuite à la deuxième étape de la maturation du phagosome. Le phagosome précoce se transforme en phagosome tardif qui résulte de la fusion des phagosomes précoces avec les endosomes tardifs. La caractéristique principal de ce compartiment est l'acquisition de pompes à protons, appelées vATPases, permettant un abaissement du pH autour de 5,5 (Maxfield and Yamashiro, 1987). On assiste à nouveau à l'acquisition d'autres marqueurs phagosomaux et notamment à l'acquisition de Rab7, Rab9, les molécules LAMP (LAMP-1 et LAMP-β) et la perte de Rab5 qui va être recyclée (Rink et al., 2005; Vonderheit and Helenius, 2005).

Dans ce compartiment, on observe aussi l'arrivée en grande quantité de peptides antimicrobiens (PAM) destinés à détruire les bactéries. C'est le deuxième phénomène d'élimination phagosomal. Il existe deux principales familles de PAM qui sont les défensines et les cathélicidines. Ces deux familles vont agir en formant des pores dans la membrane et endommager l'ADN et induire la lyse bactérienne (Hancock and Diamond, 2000). L'activité antimicrobienne des cathélicidines est particulièrement puissante sur *Shigella* spp, *S. aureus* et les *Streptocoques* (Guaní-Guerra et al., 2010). Les PAM peuvent jouer aussi un rôle pro-inflammatoire et chimio-attractant permettant ainsi la mise en place d'une réponse immunitaire innée et adaptative (van der Does et al., 2010; Méndez-Samperio, 2008).

Dans ce compartiment, on retrouve d'autres éléments impliqués dans

l'élimination des bactéries phagocytées, parmi lesquels des protéines qui vont séquestrer des nutriments essentiels pour les bactéries. On peut citer l'exemple des lactoferrines qui vont séquestrer le fer, un élément essentiel pour la survie bactérienne (Cassat and Skaar, 2013). On retrouve aussi la protéine membranaire NRAMP1 (natural resistance-associated macrophage protein 1) qui exerce un effet bactériostatique et permet l'excrétion des ions Fe^{2+}, Zn^{2+} et Mn^{2+} de la vacuole phagosomale (Cellier et al., 2007). Les ions Fe^{2+} et Zn^{2+} sont des cofacteurs enzymatiques importants et le Mn2+ est requis pour l'activité de la superoxyde dismutase.

Enfin, on retrouve des enzymes de dégradation comme des endopeptidases (cystéine and aspartate protéases), des exopeptidases (cystéine and sérine protéases) et des hydrolases qui vont dégrader les sucres (α-hexosaminidase et -glucuronidase) et les lipides (phospholipase A2) (Pillay et al., 2002).

La dernière étape de maturation est la transformation du phagosome tardif en phagolysosome qui résulte de la fusion du premier avec des lysosomes provenant de l'appareil de Golgi. On assiste cette fois à une forte diminution du pH (autour de 4,5) due à l'acquisition massive de vATPases. Ces lysosomes contiennent des protéases et des lipases, des molécules LAMP et de la cathepsine D (marqueur spécifiquement utilisé en immunofluorescence). La cathepsine D est une protéase impliquée dans la dégradation des protéines mais aussi dans la présentation de peptides au complexe majeur d'histocompatibilité (Deussing et al., 1998). Le phagolysosome dirige les particules dégradées vers des compartiments de recyclage comme le réticulum endoplasmique ou vers la membrane plasmique pour les présenter au système immunitaire).

3.2 L'autophagie

L'autophagie est un processus important d'adaptation de la cellule eucaryote qui se produit en réponse à différentes formes de stress, y compris la privation de nutriments, l'épuisement des facteurs de croissance, l'activation de signaux immunitaires (PAMPs, DAMPs, PRRs, TLR,...), les infections intracellulaires (virus,

parasites, bactéries) et l'hypoxie. L'autophagie permet la dégradation d'organelles endommagées, comme les mitochondries, d'agrégats de protéines trop gros pour être pris en charge par le protéasome ou encore éliminer des micro-organismes. En cas d'infection, l'autophagie permet une forme de protection contre les micro-organismes, on parle alors de xénophagie (Bauckman et al., 2015).

Lorsque ce processus est activé, dans le cytoplasme, apparaîssent des vésicules à doubles membranes appelées autophagosomes provenant du RE, de l'appareil de golgi ou des mitochondries (**Figure 3**) (Rubinsztein et al., 2012). Ces autophagosomes vont pouvoir fusionner avec les lysosomes et ainsi permettre la dégradation de leur contenu (Randow and Münz, 2012). Un certain nombre de protéines vont être recrutées lors de l'induction de cette voie et notamment les protéines Atg qui vont permettre la mise en place de ce processus. La présence de PI(3)P (Phosphatidylinositol-3-Phosphate) par le recrutement de Vsp34 (He et al., 2009) permet l'activation des protéines Atg5, Atg12 et Atg16 et provoquer la formation d'une vésicule autour des produits à dégrader. Ensuite, par l'intermédiaire de LC3 et d'un mécanisme dépendant de la protéine Rab7, cette vésicule va être adressée vers les lysosomes pour en dégrader son contenu (Dunn, 1990). Pour améliorer l'efficacité de ce processus, les cellules de l'immunité innée ont mis au point une machinerie capable de reconnaître spécifiquement des molécules caractéristiques de chaque bactérie. Par exemple dans le cytosol la protéine p62 va reconnaître *L. monocytogenes* ou *S. typhimurium* (Yoshikawa et al., 2009; Zheng et al., 2009). Dans le cas de *Shigella*, ce sont les senseurs cytosoliques Nod1 and Nod2 (voir paragraphe suivant) qui jouent un rôle crucial dans la détection de la bactérie et l'induction de l'autophagie, en induisant le recrutement de la protéine ATG16L1 au site d'entrée de la bactérie (Travassos et al., 2010).

A leur tour, les bactéries à multiplication intracellulaire ont développé des stratégies soit pour éviter l'autophagie, soit pour l'utiliser dans certains contextes infectieux, comme une niche alternative et/ou une source de nutriments. Par exemple, *L. pneumophila*, va inhiber l'autophagie par la sécrétion de facteurs de virulence qui vont cliver les protéines pro-autophagiques, comme la protéine LC3 (Choy et al., 2012). D'autres pathogènes, comme *L. monocytogenes*, qui une fois dans le cytosol de la cellule, exprime la protéine ActA à sa surface pour permettre la polymérisation d'actine

(grâce au recrutement des protéines cellulaires Arp2/3 et Ena/VASP), utilise également ActA pour protéger sa surface de la reconnaissance par les ubiquitines ligases et les adaptateurs d'autophagie. La phospholipase bactérienne C (PlcA), interfère également avec l'autophagie, en réduisant les niveaux intracellulaires de phosphatidylinositol 3-phosphate (PI3P), une molécule de signalisation nécessaire pour les processus de macro-autophagie (Tattoli et al., 2013; Yoshikawa et al., 2009).

3.3 L'immunité nutritionnelle

Les bactéries intracellulaires ont évolué afin d'optimiser leur production d'énergie à partir des nutriments mis à leur disposition dans la cellule hôte. Une partie des défenses immunitaires innées des cellules passe donc par une restriction de l'accès aux nutriments pour les pathogènes. On parle alors « d'immunité nutritionnelle ».

Par exemple, les macrophages sont capables d'utiliser des transporteurs phagosomaux comme le transporteur de cations divalents (manganèse, fer et cobalt) NRAMP1 (SLC11A1), pour « affamer » les pathogènes intracellulaires et limiter leur capacité de multiplication intracellulaire. En effet, il a été démontré que l'expression du gène codant pour ce transporteur était augmentée chez des macrophages activés par de l'IFNγ (Forbes, 2003; Jabado et al., 2000; Juttukonda and Skaar, 2015). Un autre exemple de stratégie est la production de protéines liant le fer comme la transferrine, la ferritine et la calprotectine, ou des protéines de liaison au manganèse, au calcium et au zinc, pour séquestrer ces ions métalliques afin d'inhiber la croissance microbienne (Hood and Skaar, 2012).

3.4 Les Pattern recognition receptors (PRR)

Lorsque les bactéries se retrouvent dans le cytoplasme des cellules immunitaires innées, ce qui signifie qu'elles ont survécu à l'étape phagosomale, et qu'elles ont échappé à la reconnaissance et la dégradation par l'autophagie, il existe encore une

ligne de défense cytosolique à affronter, les Pattern Recognition Receptors (PRR). Les PRR vont détecter des composants microbiens conservés appelés des « pathogen-associated molecular patterns » ou PAMP tels que la flagelline, les acides nucléiques uniques aux bactéries et aux virus (ADN CpG, ARNdb), le lipopolysaccharides (LPS), l'acide lipotéichoïque ou le peptidoglycane. Parmi ces PRR, on peut citer l'exemple des Toll-Like receptors (TLR, dont certains, comme les TLR2 et TLR4, sont déjà mis en jeu dans la détection des bactéries à la surface des cellules, lors de l'étape d'entrée), les NOD-Like receptors (NLR) ou les RIG-I -like receptors (RLR). La détection des PAMP par les TLR, NLR et RLR active de multiples voies de signalisation pro-inflammatoires pour monter une réponse bactéricide efficace ciblant le pathogène (Akira et al., 2006).

Rappelons que NOD1 et NOD2 détectent des molécules bactériennes produites au cours de la synthèse et / ou de la dégradation du peptidoglycane (PGN). NOD1 reconnaît l'acide dipeptidique γ-D-glutamyl-méso-diaminopimélique (iE-DAP), produit par la plupart des bactéries Gram-positives et Gram-positives. En revanche, NOD2 est activé par le muramyl dipeptide (MDP), un composant de pratiquement tous les types de PGN (Chamaillard et al., 2003; Girardin et al., 2003a, 2003b; Inohara et al., 2003). La reconnaissance directe ou indirecte du ligand NOD1 et/ou NOD2 permet l'activation des voies NF-KB et MAP kinase, permettant la translocation des facteurs de transcription dans le noyau et permettre la transcription de gènes cibles. Ces voies vont activer la transcription de gènes codant pour des molécules pro-inflammatoires qui stimulent à la fois les réponses immunitaires innée et adaptative.

3.5 Induction de la mort cellulaire

La mort cellulaire, ou apoptose, est un phénomène de sénescence programmée, sans inflammation et sans fuite de contenu cytosolique dans le milieu extérieur. C'est aussi un processus utilisé pour lutter contre certaines bactéries intracellulaires. L'apoptose se caractérise par la segmentation de l'ADN et le maintien de l'intégrité membranaire, en permettant de restreindre la dissémination des bactéries intracellulaires dans l'organisme et de faciliter leur dégradation. Ces corps apoptotiques

serviront ainsi à la présentation antigénique et l'activation de l'immunité adaptative (Lai and Sjöstedt, 2003; Lai et al., 2004). Il existe deux voies d'activation de l'apoptose, la voie intrinsèque et la voie extrinsèque.

La voie intrinsèque est la voie de mort cellulaire dépendant des mitochondries. Dans une cellule infectée, il va y avoir relargage de facteurs de signalisation mitochondriale, activation de la sécrétion de protéines pro-inflammatoires (telles que BH3, Bcl-2 homology 3) qui vont induire l'oligomérisation des facteurs pro-apoptotiques Bax et Bak, provoquer la formation de pores dans la membrane mitochondriale et le relargage du cytochrome C. On assiste alors à l'activation des pro-caspases 9 en caspases 9 et l'activation du processus d'apoptose (Arnoult et al., 2011).

La voie extrinsèque est initiée par l'activation d'un récepteur de mort au niveau de la membrane plasmique (FasL, TNF-R1, Apo2/Apo3,...). Ce récepteur va transmettre un signal apoptotique externe, activant la machinerie de mort programmée de la cellule, entraînant l'activation des caspases-3 et 7 et menant à l'apoptose (Ashida et al., 2011).

Il existe un autre mécanisme de mort cellulaire, appelé pyroptose, décrit plus récemment (Mariathasan et al., 2004; Sansonetti et al., 2000)**.** C'est un mécanisme dépendant de l'activation de l'inflammation. Lorsque que certain PAMPs vont être reconnus par les PRRs et plus précisément par les NLR, il va y avoir activation d'un complexe protéique appelé l'inflammasome (Malik and Kanneganti, 2017; Yilmaz et al., 2010). L'activation de ce complexe protéique composé du NLR, de la protéine adaptatrice Asc et de la pro-caspase-1, permet l'activation de la caspase-1. Cette caspase va cliver les précurseurs de cytokines pro-inflammatoire pro-IL-1β et proIL-18, qui vont être sécrétées dans le milieu extracellulaire et permettre la mise en place d'une réponse inflammatoire et l'activation de la pyroptose (Ashida et al., 2011; Schroder and Tschopp, 2010). La pyroptose va induire la mort de la cellule et ainsi permettre la libération des bactéries intracellulaires, les exposant à nouveau à l'élimination par les cellules de l'immunité et notamment aux polynucléaires neutrophiles (Miao et al., 2010) (**Figure 5**).

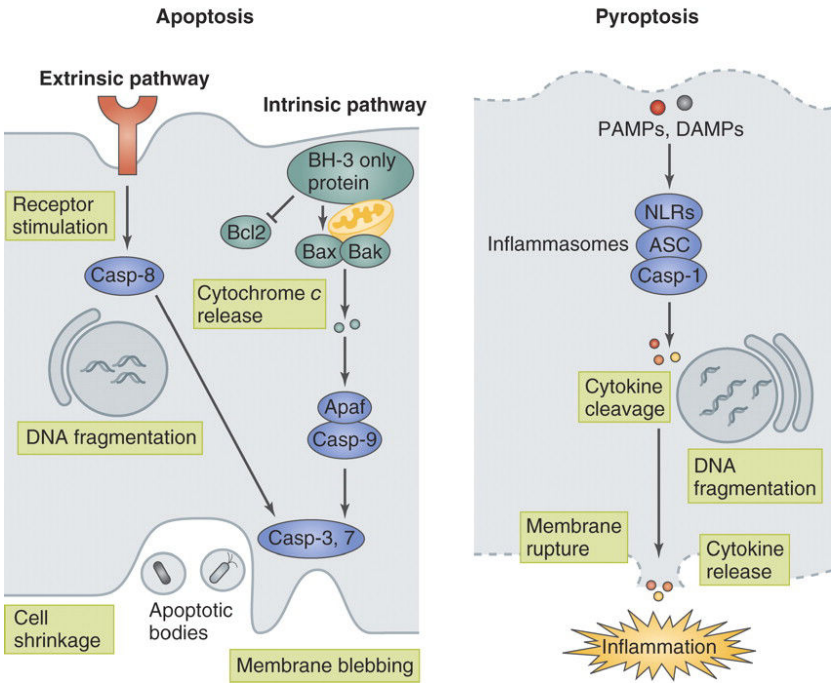

Figure 5 : Schéma de l'activation de la mort cellulaire par apoptose ou pyroptose lors de l'infection. A gauche, schéma de l'activation de l'apoptose par les voies extrinsèque et intrinsèque. A droite, schéma de l'activation de la pyroptose. Adapté de (Ashida et al., 2011).

Les bactéries intracellulaires ont développé des mécanismes leurs permettant de contrôler la mort de la cellule hôte, leur conférant un avantage de temps pour mener à bien leur cycle de réplication. Il existe autant de mécanismes d'activation ou d'inhibition de la mort cellulaire que de types bactériens différents. Par exemple, la bactérie *L. pneumophila* va être capable de décaler dans le temps la voie intrinsèque de l'apoptose. La bactérie va secréter, grâce à son système de sécrétion de type IV (SST6), les protéines SdhA et SidF qui vont venir fixer et neutraliser des protéines pro-apoptotiques tels que Bcl-2 et ainsi inhiber la mort cellulaire et favoriser la multiplication bactérienne (Banga et al., 2007; Laguna et al., 2006). A l'inverse, *S. typhimurium* va induire l'apoptose dans les macrophages. *Salmonella* va secréter, par l'intermédiaire de son SST3, la protéine SipB dans le cytosol. Cette protéine va directement se lier à la caspase-1 et l'activer. L'apoptose induite par *Salmonella* contribue à l'échappement des bactéries intracellulaires des cellules hôtes suite à l'épuisement des nutriments dans le milieu intracellulaire (Hersh et al., 1999).

4. Adaptation métabolique des bactéries intracellulaires

Pour survivre dans leur environnement intracellulaire, les bactéries doivent également posséder les machineries métaboliques nécessaires à l'exploitation optimale des nutriments disponibles. C'est particulièrement critique bactéries intracellulaires obligatoires qui dépendent exclusivement des nutriments obtenus à partir du milieu intracellulaire de la cellule hôte. Ces fonctions métaboliques sont souvent localisées dans des régions du génome acquises au cours de l'évolution de la bactérie, par des transferts horizontaux d'îlots de pathogénicité ou par l'insertion d'éléments génomiques mobiles (Rohmer et al., 2011). L'acquisition de nouvelles fonctions nutritionnelles ne se limite pas seulement à l'acquisition de nouveaux processus métaboliques mais aussi à l'acquisition de nouveaux facteurs de virulence plus proches des facteurs « traditionnels » comme par exemple des effecteurs bactériens, qui seront injectés dans la cellule hôte afin de manipuler les besoins en nutriments de la cellule ou des enzymes de dégradation des macromolécules (Niu et al., 2012; Price et al., 2011). On parle alors de « virulence nutritionnelle ».

4.1 Les macronutriments

- *Les acides aminés* : Les acides aminés peuvent être utilisés comme source d'énergie, de carbone, d'azote et de soufre pour maintenir le métabolisme microbien et constituent ainsi une source importante de nutriments pour certains pathogènes intracellulaires. Bien que certaines bactéries soient capables de synthétiser l'ensemble des acides aminés (*i.e.* prototrophes), certaines bactéries comme *L. pneumophila*, présentent de multiples auxotrophies et doivent donc trouver des solutions pour obtenir les acides aminés qu'elles sont incapables de biosynthétiser. L'une des principales sources d'énergie de *L. pneumophila* sont les acides aminés et notamment la cystéine, qui servent principalement à entretenir le cycle de Krebs (notamment la cystéine après sa conversion en pyruvate) et comme éléments constituants pour la synthèse des protéines.

L’utilisation des acides aminés permet à la bactérie de combler son absence de gènes codant pour des enzymes impliquées dans la voie de la glycolyse. Comme *L. pneumophila* est auxotrophe pour la cystéine, elle exploite le système de dégradation du protéasome de l'hôte pour augmenter le niveau intracellulaire de cystéine libre disponible (Price et al., 2011). Pour cela, *L. pneumophila* injecte dans le cytosol de la cellule hôte, grâce à son SST6, un effecteur protéique semblable à une protéine eucaryote, appelé Ankyrin B (AnkB). Cet effecteur va être ancré dans la double membrane phospholipidique de la LCV (Al-Quadan et al., 2012). L'effecteur AnkB fonctionne comme une plate-forme pour l'arrimage de protéines polyubiquitinées au LCV qui sont ensuite dégradées par le protéasome. Ce mécanisme génère une augmentation du pool d’acides aminés au niveau du LCV. Les acides aminés ainsi générés sont ensuite importés dans le LCV par l'intermédiaire de divers transporteurs d'acides aminés de type SLC (Al-Quadan et al., 2012). Pour les bactéries qui comme *L. penumophila* utilisent les acides aminés comme source principale de carbone et d’azote, la capacité de transporter efficacement les acides aminés disponibles est donc une condition essentielle pour mener à bien leur cycle de réplication intracellulaire (c’est également le cas pour *Francisella* que nous aborderons dans le chapitre suivant).

L'absorption des différents acides aminés par *L. pneumophila* dans les macrophages est assurée par la famille des transporteurs phagosomaux (Pht) (Schunder et al., 2014). Par exemple, le transport de la thréonine et de la valine sont exécutés par les protéines PhtA et PhtJ, respectivement, et sont nécessaires pour la différenciation dans la forme réplicative (Fonseca and Swanson, 2014; Sauer et al., 2005). Chez *M. tuberculosis*, l'absorption d'aspartate et d'asparagine dans les phagosomes des macrophages par les transporteurs AnsP1 et AnsP2 est importante pour l'assimilation de l'azote (Gouzy et al., 2013, 2014). L'utilisation de l'asparagine offre deux avantages importants pour *M. tuberculosis*. Cet acide aminé peut non seulement servir de source d'azote, mais peut également contribuer à réduire le stress acide dans le phagosome. Ce dernier est obtenu par clivage de l'asparagine en aspartate et en ammoniac, nécessaire au maintien du pH dans le phagosome (Gouzy et al., 2014).

La détection de la disponibilité des nutriments, et notamment des acides aminés,

dans les compartiments intracellulaires peut également induire une réponse «d'adaptation prédictive». Par exemple, toujours chez *L. pneumophila*, le répresseur d'arginine ArgR détecte les niveaux d'arginine dans le LCV et dé-réprime la transcription d'un ensemble de gènes impliqués dans la détoxification, l'adaptation au stress, le métabolisme des acides aminés et les substrats du système de sécrétion de type IV (Hovel-Miner et al., 2010).

- *Les carbohydrates* : pour la plupart des bactéries intracellulaires, la source de carbone la plus utilisée est le glucose. Le glucose est une source de nutriments facilement et rapidement assimilable, permettant d'alimenter de nombreuses voies métaboliques comme la glycolyse (ou Embden-Meyerhof-Parnas, EMP), la voie Entner-Doudoroff (ED), ou la voie des pentoses phosphates (PP), pour permettre la production d'énergie. Cependant, le glucose est souvent restreint dans les systèmes biologiques comme le milieux intracellulaires des macrophages. Les bactéries sont donc en concurrence avec leurs hôtes et ont développé des stratégies pour détecter, acquérir et métaboliser efficacement ce nutriment. Comme le glucose n'est pas une ressource toujours disponible dans les macrophages, les bactéries intracellulaires vont être capables d'utiliser des ressources alternatives en carbone et/ou simultanément plusieurs sources de carbone pour permettre leurs survie et leurs réplication (Abu Kwaik and Bumann, 2015). Par exemple, il a été montré que *L. monocytogenes* était capable d'utiliser deux autres substrats carbonés, le glycérol et le glucose-6P (Eisenreich et al., 2010; Grubmüller et al., 2014) dans le cytosol des cellules infectées. Pour les bactéries qui résident dans un compartiment vacuolaire, le glucose étant présent en très faible quantité, l'utilisation des sources de carbone alternatives est un prérequis (McKinney et al., 2000). Par exemple, certaines parties de la voie ED sont nécessaires à la croissance intracellulaire de *L. pneumophila* et la bactérie est capable d'utiliser des sources de carbone comme le polyol glycérol ou le myo-inositol pour sa réplication (Manske et al., 2016).

Enfin, certaines bactéries sont capables de contrôler le métabolisme des cellules hôtes et en tirer un avantage. Plusieurs études ont montré que les cellules eucaryotes infectées par des bactéries intracellulaires, telles que *M. tuberculosis*, *L. pneumophila* ou

Brucella abortus, ont un métabolisme altéré. Ces cellules présentent généralement une augmentation du transport du glucose et / ou une augmentation de l'activité de la glycolyse. Elles ont un programme métabolique très similaire a celui des cellules cancéreuses. Cet effet est connu sous le nom d '«effet Warburg». Prenons l'exemple de *M. tuberculosis*, on observe une reprogrammation métabolique des macrophages lors de l'infection par la bactérie, avec une augmentation du transport du glucose, une augmentation de l'activité glycolytique et une dérégulation des enzymes impliquées dans le cycle de Krebs (aussi appelé tricarboxilic acid cycle ou TCA cycle). On observe aussi une déviation des intermédiaires glycolytiques vers la synthèse de corps lipidiques, qui sont accumulés dans le macrophage et qui seront métabolisés par les bactéries intracellulaires. Le lactate produit par la glycolyse peut également être utilisé par la bactérie pour sa multiplication intracellulaire (Escoll and Buchrieser, 2018).

De son coté, *S. enterica* est capable de s'adapter à une grande variété de sources de carbone pour sa croissance intracellulaire. Equipée de toutes ses voies métaboliques totalement fonctionnelles, *S. enterica* s'adapte facilement à la disponibilité changeante en sources de carbone et d'énergie. En outre, ce pathogène peut synthétiser toutes les macromolécules cellulaires à partir de sources de carbone simples et va utiliser en parallèle plusieurs sources de carbones pour alimenter ces différentes voies métaboliques. Seules quelques mutations dans les voies cataboliques du carbone entraînent une diminution de la survie et de la réplication intracellulaire, démontrant la réussite de l'adaptation métabolique de ce pathogène (Steeb et al., 2013).

- *Les lipides* : Les lipides sont des éléments constitutifs fondamentaux des cellules et jouent un rôle central dans divers processus biologiques. Ce sont des composants structuraux cléfs pour les membranes cellulaires et peuvent servir de source de carbone pour certaines bactéries. Chez *M. tuberculosis*, il a été démontré que les gènes impliqués dans le métabolisme des lipides étaient régulés positivement et que les lipides sont importants pour sa virulence (McKinney et al., 2000). Les transporteurs Mce1 et Mce4 facilitent l'absorption du cholestérol et des acides gras présents dans le cytoplasme des macrophages infectés. La mutation du gène *mce4,* codant pour un transporteur de cholestérol, entraîne l'échec de la bactérie à maintenir une infection

chronique chez les souris tout en conservant une virulence complète pendant la phase aiguë de l'infection. Il semblerait que l'utilisation des lipides de l'hôte ne soit pas seulement essentielle pour la multiplication intracellulaire mais aussi pour la persistance de la bactérie (Brzostek et al., 2009; Lovewell et al., 2016; Pandey and Sassetti, 2008).

4.2 Les micronutriments

Pour se développer, les bactéries intracellulaires ont également besoin de micronutriments tels que le fer, qui est un élément essentiel mais rare sous forme libre dans la cellule, car il est généralement conservé ou stocké par les protéines. Les bactéries qui infectent les macrophages ont besoin de Fer pour leur croissance, et pendant l'infection, le Fer est requis à la fois par la cellule hôte et par le pathogène. Les macrophages ont besoin de Fer comme cofacteur pour les mécanismes antimicrobiens, comme la production de radicaux azotés catalysée par l'oxyde nitrique synthase ou certains effecteurs antimicrobiens (Leon-Sicairos et al., 2015). D'un autre côté, les bactéries intracellulaires telles que *L. pneumophila*, *Coxiella burnetii*, *S. typhimurium* et *M. tuberculosis* ont besoin de Fer pour leur croissance et leur survie dans les cellules hôtes (Leon-Sicairos et al., 2015)**.** Une privation de Fer *in vitro* et *in vivo* réduit généralement sévèrement la virulence des bactéries à multiplication intracellulaire.

Etant toxique pour les cellules sous forme libre, le Fer est sous forme complexée aux hèmes et représente 80% de fer présent dans les cellules (Jones and Niederweis, 2011). *M. tuberculosis* est capable d'utiliser des protéines membranaires, Mmpl3 et Mmpl11, qui sont des transporteurs d'hème (Tullius et al., 2011). La bactérie sécrète la protéine Rv0203 qui va capturer l'hème et permettre son entrée via le transporteur Mmpl3/Mmpl11. L'hème sera ensuite dégradé et permettre la libération du Fer dans le cytosol de la bactérie (Owens et al., 2013).

Comme nous vous l'avons présenté plus haut, de leur coté les macrophages mettent en place des mécanismes de restrictions en fer pour limiter la quantité de fer disponibilité pour les pathogènes. Pour contrer ces mécanismes, *M. tuberculosis* utilise

des sidérophores appelés carboxymycobactines qui vont être sécrétés et être capables de capturer le fer complexé aux protéines de l'hôte comme la ferritine, la transferrine ou la lactoferrine (Rodriguez, 2006). Des systèmes de transport dédiés vont permettre soit l'import (le transporteur ABC IrtAB) soit l'export (MmpS/L) de ces sidérophores (Rodriguez, 2006; Wells et al., 2013).

Partie II : Le cas particulier de *Francisella tularensis,* une bactérie à multiplication cytosolique.

1. Généralités

1.1 Histoire

Agent étiologique d'une zoonose appelée la tularémie, *F. tularensis* a été décrite pour la première fois au Japon en 1818 par Homma. Elle fut isolée la première fois en 1911 lors d'une épidémie d'une maladie proche de la peste chez les spermophiles dans le Comté de Tulare en Californie (origine de son nom). Le premier cas de tularémie chez l'Homme a été rapporté en 1914 en Ohio (Wherry and Lamb, 2004). Initialement appelée *Bacterium tularensis*, elle fut étudié jusqu'en 1924 par Edward Francis, McCoy, Chaplin, Lamb, Parker et Spencer. C'est en 1974, qu'elle fut rebaptisée *Francisella tularensis*, en l'honneur de son découvreur Edward Francis, un médecin americain qui a consacré sa vie à la recherche sur cette bactérie.

1.2 Taxonomie et sous espèces

Après de nombreuses modifications de sa taxonomie, c'est en 1947 que Dorofe'eva a proposé de créer le genre *Francisella* comportant comme unique espèce *F. tularensis* (Olsufjev, 1970). *Francisella* appartient à la classe des Gamma-Protéobactéries et ce n'est qu'en 1994, après des études des séquences de l'ARN

ribosomal 16S, que l'on a confirmé son appartenance taxonomique (**Figure 6**). Les organismes les plus apparentés aux *Francisella* sont des bactéries intracellulaires obligatoires telles que *Wolbachia persica*, un endosymbiote de la tique. Suite à des analyses de l'ADN et de la composition en acides gras, deux espèces ont été distinguées dans le genre *Francisella* : les espèces *tularensis* et *philomiragia*. Au sein de l'espèce *F. tularensis*, il existe quatre sous espèces principales (ssp.) : ssp. *tularensis* (Biovar tularensis ou type A), ssp. *holarctica* (type B), ssp. *Mediasitica* et ssp. *novicida*. (Forsman et al., 1994; Svensson et al., 2005). La ssp. *tularensis* (type A) est la bactérie la plus virulente pour l'Homme et peut engendrer un taux de mortalité pouvant aller jusqu'à 30 à 60% en absence de traitement antibiotique adéquate. La ssp. *holarctica* cause, quant à elle, des maladies aux symptômes sévères mais rarement fatales, avec un taux de mortalité de 5 à 15% en absence de traitement. Concernant les ssp*. novicida* et *mediasiatica*, elles sont très rarement virulentes pour l'homme sauf dans des cas particuliers d'immuno-dépression (Hollis et al., 1989).

En 2009, une autre espècede *Francisella* a été décrite : *F. noatunensis*. Cette espèce, découverte par l'Institut National Vétérinaire de Norvège dans des morues d'élevage et qui présentaient une maladie granulomateuse, constitue la quatrième espèce de genre *Francisella*. Elle fut dans un premier temps classée comme une sous-espèce de *F. philomiragia* puis reclassée au rang d'espèce, suite à l'étude des séquences ARN 16S et de neuf gènes domestiques (Ottem et al., 2009).

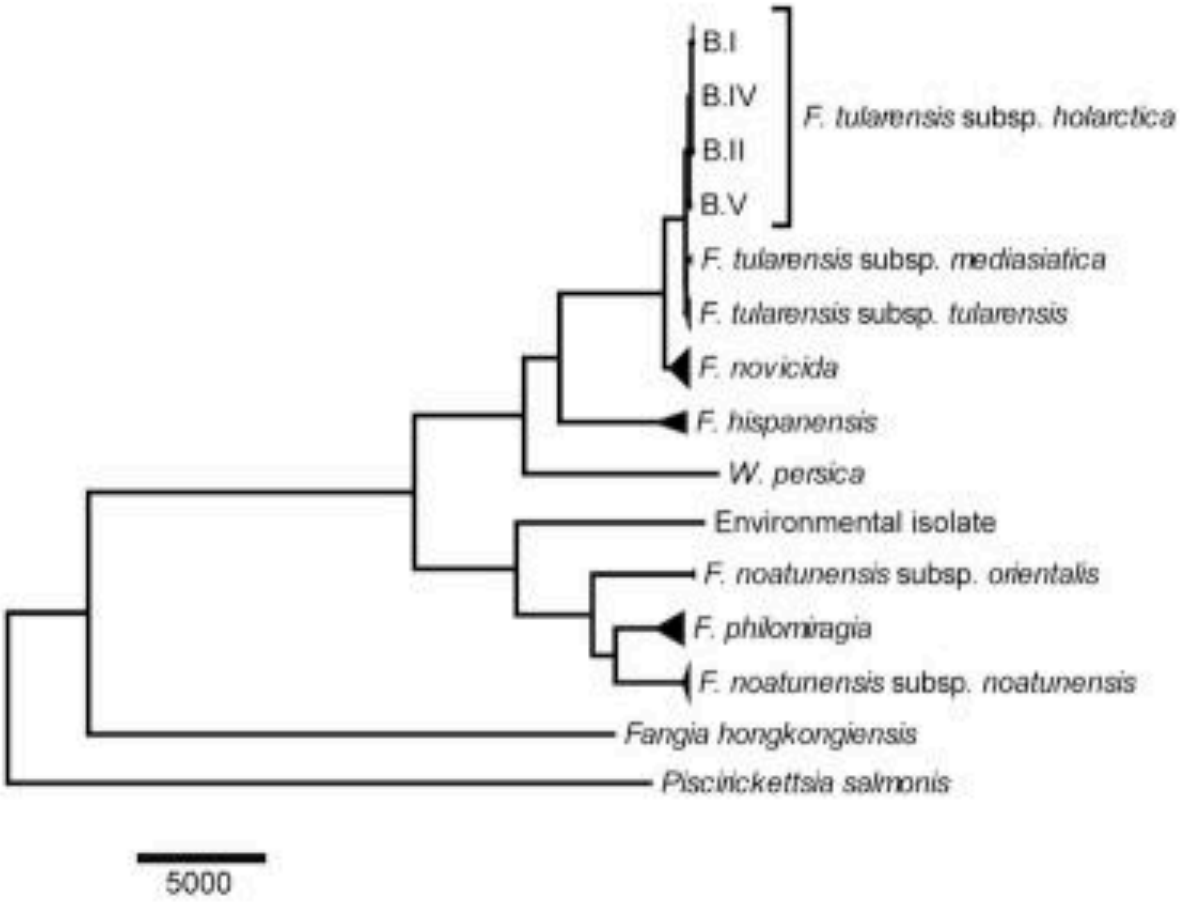

Figure 6 : Relations phylogénétiques entre les membres du genre *Francisella* basées sur les séquences de gènes complets de l'ARNr 16S. *Piscirickettsia salmonis* et *Fangia hongkongiensis* forment les bactéries des groupes extérieurs au genre *Francisella.* D'après (Coolen et al., 2013)**.**

1.3 Réservoir et Répartition Géographique

Une des principales caractéristiques de *F. tularensis* est sa capacité d'infecter une grande variété d'animaux, dont plus de 200 espèces différentes de mammifères sauvages et domestiques (Estavoyer et al., 1993). Initialement retrouvée chez les écureuils en 1911 par ses découvreurs, elle a ensuite été décrite chez d'autres rongeurs, les lagomorphes (lapin et lièvre), les ruminants (vaches et moutons), certains carnivores. En 2002, Hansson et al. ont mis en évidence que les oiseaux migrateurs étaient un vecteur important de la bactérie (Hansson and Ingvarsson, 2002). On la retrouve aussi

chez un certain nombre d'arthropode et notamment des tiques (*Ixodidae*, *Dermacentor*), de taons (*Tabanidae*) et de moustiques (*Aedes*, *Anopheles*) qui sont susceptibles d'être infectés et de jouer le rôle de vecteur de la maladie (Petersen and Schriefer, 2005).

Parmi tous les organismes cités, on pense que seuls les rongeurs et les tiques représentent le réservoir naturel de la bactérie. Les autres comme les lagomorphes ne sont que des vecteurs puisqu'ils ne peuvent pas maintenir la bactérie et permettre un cycle épidémiologique. Il existe toutefois un troisième grand réservoir à la bactérie, l'environnement. Etant donnée que la survie de la bactérie est dépendante de la temperature, *Francisella* est capable de survivre à des températures très basses (proche de 0°C) pendant plusieurs mois dans des cadavres d'animaux, de l'eau, de la terre, de la boue, de la paille ou des grains (Colquhoun and Duodu, 2011). L'environnement peut être contaminé par des déjections animales et en particulier de rongeurs. Il est clair aujourd'hui que la persistance de la bactérie dans l'environnement est en grande partie dûe à sa capacité de survivre au sein de petits protozoaires aquatiques tels que les amibes (*Acanthamoeba castellanii*) (Abd et al., 2003).

L'infection humaine peut se produire par des piqûres d'arthropodes infectés (habituellement des tiques), contact avec des tissus ou des fluides animaux infectés; contact direct avec ou ingestion d'eau, de nourriture ou de terre contaminée ou inhalation de bactéries aérosolisées. Elle a tendance à se produire principalement dans les zones rurales. La sous-espèce *tularensis* de *F. tularensis* est si contagieuse que le simple fait d'ouvrir une plaque de culture de laboratoire sans équipement de protection adéquat peut entraîner une infection. Cependant, aucune transmission interhumaine n'a été décrite.

En plus de leur virulence, les différentes ssp. de *F. tularensis* se distinguent aussi par leur répartition géographique (**Figure 7**; Titball et al., 2003). La ssp. *tularensis* est retrouvée principalement en Amérique du Nord et au Mexique ; la ssp. *holarctica,* sur la majorité de l'hémisphère Nord ; et la ssp. *mediasiatica,* au Kazakhstan et au Turkménistan. Quant à la ssp. *novicida*, elle est retrouvée principalement aux Etats-Unis et en Australie. Il s'agit d'ailleurs de la seule souche identifiée dans l'hémisphère Sud (Hollis et al., 1989).

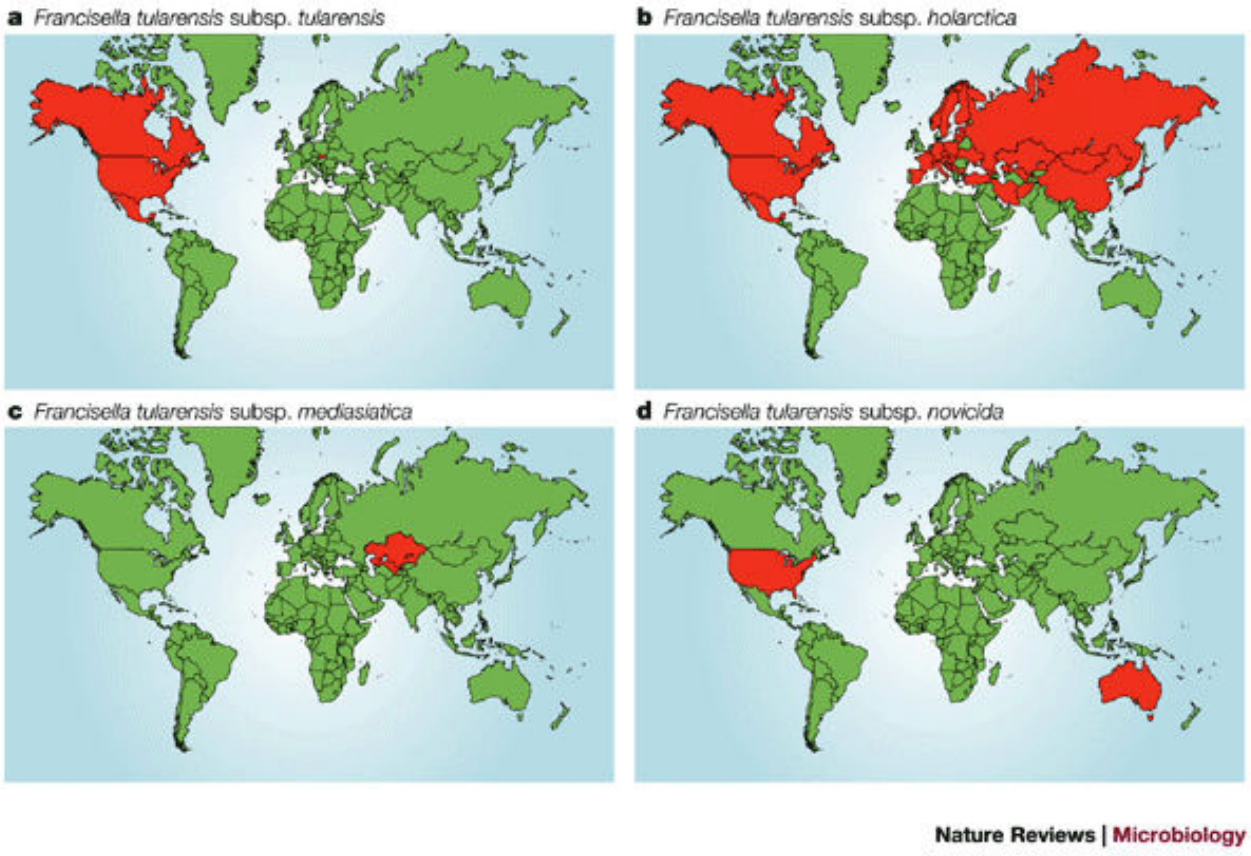

Figure 7 : Répartition géographique des différentes sous-espèce de *F. tularensis*. D'après (Oyston et al., 2004).

1.4 Le génome de *Francisella*

Le premier génome de *Francisella* séquencé est celui de la souche SCHU S4 de *F. tularensis* ssp. *tularensis* (isolée en 1941 d'un cas de tularémie humaine au USA)(Larsson et al., 2005). Les séquences des autres ssp. ont été réalisées peu de temps après. Depuis l'arrivée des nouvelles techniques de séquençage à haut débit de génome entier, le nombre de génomes disponibles de *Francisella* est en croissance exponentielle. La taille des génomes des différentes ssp. de *F. tularensis* varie entre 1,5 et 2 Mpb, avec un pourcentage en G+C très faible (entre 33 et 36%) caractéristique du genre *Francisella*.

Le séquençage du génome de SCHU S4 a montré l'existence de 1.804 séquences codantes, avec 302 gènes spécifiques au genre *Francisella*. L'étude de ce génome a

permis de mettre en évidence des mutations, par insertion ou délétion, dans plus de 10% des gènes, les rendant ainsi inactifs. La majorité de ces régions codantes déterminent des protéines impliquées dans le transport, dans le métabolisme de l'ADN ou dans la synthèse d'acides amines. L'analyse du génome a permis de montrer que 54% des voies métaboliques prédites de la bactérie sont interrompues, ce qui explique ses multiples exigences nutritionnelles. Par exemple, le besoin en cystéine pour la croissance de *Francisella* a pu être expliqué par la mutation dans la région codante d'un gène important d'une voie d'assimilation du sulfate (Alkhuder et al., 2009).

Le second génome à avoir été séquencé est celui de la ssp. *holartica* (de la souche OSU8 isolée en 1978). Cette séquence présente une identité de 99% avec la séquence de la ssp. *tularensis* SCHU S4 et possède un génome de 1,89 Mpb avec 1. 924 régions codante (Petrosino et al., 2006). Quant au génome de la ssp. *novicida*, il montre une identité de séquence de 97,8% avec la ssp. *holarctica* LVS (Live Vaccine Strain) et de 98,1% avec la ssp. *tularensis* SCHU S4 (Rohmer et al., 2007).

L'analyse comparée des génomes a également permis de montrer que les différentes ssp. de *F. tularensis* présentaient des réarrangements différents avec des régions répétées de type « séquences d'insertion » (IS), disposées à des endroits différents de leurs génomes. Ces régions répétées, qui favorisent des phénomènes de réarrangement génomique par recombinaison, sont particulièrement retrouvées chez la ssp. *tularensis* (Beckstrom-Sternberg et al., 2007). Des variations, dues à des inversions et des translocations de séquences, sont également observables chez différents isolats de ssp. *tularensis* originaires de différentes régions des Etats-Unis (Beckstrom-Sternberg et al., 2007). Il semblerait aussi que le génome de la ssp. *novicida* (souche U112) ait subit moins de réarrangements chromosomiques et moins d'insertions de séquence répétées que les ssp. *tularensis* et *holarctica*, expliquant en partie la culture plus rapide et le plus petit nombre d'auxotrophies de cette souche.

Les génomes de *Francisella* comprennent un îlot de pathogénicité (« *Fancisella* Pathogenicity Island » ou FPI) qui sera présenté en détail plus bas. Cet îlot est dupliqué chez les ssp. *tularensis* et *holarctica* mais présent en une seule copie chez la ssp. *novicida* (**Tableau 2**).

ssp.	SCHU S4	LVS	U112
Taille génome (pb)	1 892 819	1 895 998	1 910 031
GC %	32,25	32,15	32,47
Nombre de gènes total	1820	1924	1719
Nombre de pseudogènes	254	303	14
Nombre de protéines	1445	1380	1731
Copie du FPI	2	2	1

Tableau 2 : Comparaison du gènomes des trois sous-espèces de *Francisella.* Comparaison des ssp. *tularensis* (SCHU S4*), holarctica* (LVS) et *novicida* (U112). *D*'après (Kingry and Petersen, 2014; Larsson et al., 2005).

1.5 Caractéristique phénotypique

Francisella est un petit coccobacille à Gram négatif, aérobie stricte, non sporulé et immobile, catalase négative et oxydase positive. D'une longueur généralement comprise entre 0,2 mm et 1,7 µm et d'un diamètre entre 0,2 et 0,7 µm, la bactérie peut prendre dans les cellules différentes morphologies comme des formes allongées d'une taille plus importante (**Figure 8**)

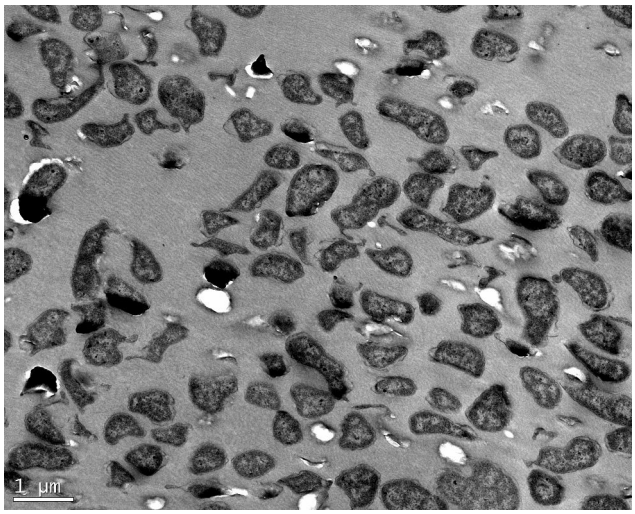

Figure 8 : *F. tularensis* ssp. *novicida* en microscopie electronique.

Les formes virulentes de *F. tularensis* sont entourées d'une capsule polysaccharidique dont la perte n'affecte pas la viabilité mais peut s'accompagner d'une perte de virulence. En plus de posséder un pourcentage assez élevé de lipide (70%) dans la composition de sa paroi, *Francisella* possède un lipopolysaccharide (LPS) plus long (16 à 18 carbones) par rapport aux autres bactéries à Gram négatif (Okan and Kasper, 2013) aux propriétés non-inflammatoires particulières (voir paragraphe dédié ci-dessous).

Du fait de la présence de nombreux pseudogènes (dans environ 10 % des gènes) ayant entrainé diverses pertes de fonctions métaboliques, *Francisella* est une bactérie qui reste difficile à cultiver, en particulier pour les ssp. *tularensis, holarctica* et *mediasiatica.* C'est pourquoi on les cultive de façon systématique dans des milieux riches. Les principaux milieux retrouvés dans la littérature sont, pour les milieux solides, des géloses « infusion cœur-cervelle » (Brain heart infusion agar) ou des géloses « chocolat » enrichies (PolyViteXTM ou IsoVitaleXTM). Pour les milieux liquides, on distingue le milieu défini de Chamberlain (Chamberlain, 1965), le bouillon Mueller-Hinton (il peut être supplémenté avec : 0.1% glucose, 2 % IsoVitalex, 0.025 % pyrophosphate de fer) et le milieu TSB pour Triptic Soy Broth (supplémenté avec 0.1% glucose et 0.4 % cystéine).

1.6 Les modèles d'études

Francisella est capable d'infecter un grand nombre de types cellulaires et d'organismes vivants différents. Ce qui facilite grandement l'étude de la virulence de cette bactérie (**Tableau 3**).

<table>
<tr><td rowspan="3">Modèle cellulaire</td><td rowspan="2">Lignées cellulaires</td><td>Phagocytaire</td><td>- J774.1 (Macrophage murin)
- THP1 (Monocyte humain)</td></tr>
<tr><td>Non phagocytaire</td><td>- A549 (cellule épithéliale alvéolaire de poumons)
- Hela (cellule épithéliale)
- HEK-293 (cellule épithéliale de rein)</td></tr>
<tr><td>Cellules primaires</td><td colspan="2">- Macrophage dérivé de moelle osseuse (BMM)
- Cellule dendritique</td></tr>
<tr><td rowspan="3">Modèle animal</td><td>Unicellulaires</td><td colspan="2">Amibe (Acanthamoeba castellanii)</td></tr>
<tr><td>Insectes</td><td colspan="2">Drosophile
Galleria mellonella</td></tr>
<tr><td>Mammifères</td><td colspan="2">- Souris (BALB/c ; C57BL/6)
- Rat (F344)
- Lapin (NZW)
- Singe (African Green Monkey ; Rhesus Monkey)</td></tr>
</table>

Tableau 3 : Exemples de quelques modèles cellulaires et animaux utilisés pour l'étude de la virulence de *Francisella*. D'après (Lo et al., 2013; Stundick et al., 2013).

1.7 Aspects Cliniques et formes de la maladie

De la fièvre et des symptômes aigus sont caractéristiques de la tularémie chez les individus en bonne santé. Après une période d'incubation de 3 à 5 jours, les aspects cliniques de la tularémie chez l'Homme dépendent essentiellement de la voie d'entrée du

pathogène. Les formes ganglionnaires et ulcéro-ganglionnaires sont les deux formes prédominantes de la tularémie en Europe, comprenant plus de 90% des cas. La tularémie ulcéro-ganglionnaire est normalement contractée par contact direct avec la chair d'animaux infectés ou, plus fréquemment, par transmission vectorielle. Au site de l'infection, une ulcération cutanée est observable. Cette ulcération est douloureuse, suintante et caractérisée par une inflammation localisée. L'ulcère est parfois discret et guérit généralement en une semaine. L'ulcère peut être confondu avec une piqûre de tique ou de moustique. Si l'ulcération ne se résorbe pas d'elle même, après plusieurs semaines, l'ulcère est accompagné d'une adénopathie. Si les antibiotiques ne sont pas administrés dans les 7-10 jours suivant l'infection initiale, une hypertrophie sévère des ganglions lymphatiques peut survenir et dans 30 à 40% des cas, la supuration finit par produire, une des complications les plus graves de la tularémie.

D'autres formes de tularémie comprennent la tularémie oculo-ganglionnaire, acquise par inoculation directe dans l'œil d'objets ou de gouttelettes contaminés ; la tularémie digestive ou oropharyngée (la forme la plus rare), acquise par ingestion d'eau ou d'aliments contaminés par des animaux infectés. La tularémie digestive prend la forme d'une gastro-entérite avec toxémie possible. Des lésions ulcéreuses du tube digestif, accompagnées d'adénites cervicales, pharyngées et mésentériques sont observables. Une autre forme très rare de la maladie est la tularémie typhoïdique ou fébrile pure : cette forme septicémique, s'accompagnant de symptômes systémiques sévères et ne comporte ni ulcérations cutanées, ni adénopathies.

Enfin la forme la plus grave est la tularémie pulmonaire (respiratoire), acquise par inhalation d'aérosols infectieux lors d'activités d'aménagement paysager, d'agriculture, de laboratoire ou inhalation de déjection de tiques contaminés. C'est la forme pneumonique qui est la plus préoccupante, et en particulier après un événement intentionnel d'aérosolisation (Dennis et al., 2001). Elle s'accompagne d'une fièvre très élevée, d'une toux sèche, de douleurs thoraciques, de difficultés respiratoires et une hémoptysie. Cette forme complique la forme ulcéro-ganglionnaire dans 1 à 15% des cas.

En France, l'incidence de la tularémie est suivie chaque année par l'Institut de Veille Sanitaire (InVS). Le nombre de cas déclarés oscille entre 40 et 100 par an depuis 2010 (voir ci-dessous)

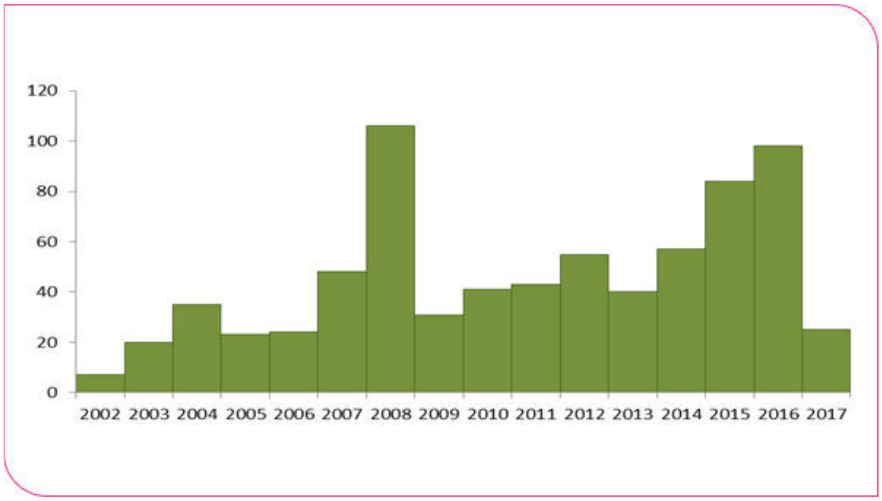

Figure 9 : Nombre de cas de tularémie déclarés en France de 2002 à 2017 par année de déclaration (Données InVS 2017).

1.8 *Francisella, l'A*gent de bioterrorisme

C'est en 1999, par le Centre de Contrôle et de Prévention des Maladie (CDC) basé au Etats-Unis, qu'a été établie la classification des agents biologiques. Cette classification s'organise en trois groupes : i) les agents de classe A, qui regroupe les agents pathogènes de haute priorité, dont l'utilisation aurait un impact majeur sur la santé publique et pourrait provoquer une désorganisation des structures économiques et sociales. Ils peuvent être produits et disséminés de façon aisée. Ces agents présentent une létalité importante et sont transmissibles par voie respiratoire. ii) Les agents de classes B, regroupent des agents faciles à disséminer mais présentant une létalité modérée et un impact moins important pour la santé humaine. Ils restent tout de même des agents sous surveillance. iii) Les agents de classes C, comprennent les pathogènes émergents qui pourraient être modifiés pour une diffusion massive en raison de leur disponibilité, leur facilité de production et de diffusion et pouvant avoir un impact majeur sur la santé.

Comme mentionné plus haut, la ssp. *tularensis* de *F. tularensis* est l'une des bactéries les plus infectieuses au monde. Des études effectuées aux États-Unis auprès de volontaires humains dans les années 1950 ont montré que l'inhalation de seulement

10 à 50 unités formant des colonies (UFC) de la ssp. *tularensis* causait la maladie (Christopher et al., 1997). C'est pour cette raison que *F. tularensis* ssp. *tularensis* à été classée comme agent de bioterrorisme de classe A par le CDC en 2004. Elle est considérée comme une arme biologique dangereuse en raison de sa capacité à infecter par aérosol, son infectivité sévère, la facilité avec laquelle on peut développer une arme biologique et sa capacité à entraîner des séquelles médicales importantes pouvant induire la mort.

2. Cycle Intracellulaire de *F. tularensis*

L'une des caractéristiques de *Francisella* est de pouvoir infecter un grand nombre de types cellulaires différents. En effet, *Francisella* est capable d'infecter des cellules phagocytaires comme les macrophages ou les cellules dendritiques mais aussi d'infecter des cellules non phagocytaires comme les hépatocytes ou les cellules épithéliale pulmonaires. Toutefois, la cellule de prédilection de *Francisella in vivo* reste le macrophage. Nous allons vous décrire dans cette partie le cycle intracellulaire de *Francisella* et ses principales particularités.

2.1 L'entrée de *Francisella*

L'entrée dans une cellule phagocytaire comme le macrophage se déroule en deux étapes : les étapes d'*adhésion* et d'*internalisation*. Les mécanismes d'entrée dans les cellules non phagocytaires sont encore mal définis (Law et al., 2011). Par contre, la phagocytose de *Francisella* par les macrophages a été largement étudiée (**Figure** 8). En fonction de l'état d'opsonisation de la bactérie, différents récepteurs phagocytaires vont intervenir. Le récepteur du mannose (MR) joue un rôle très important dans l'absorption de bactéries non opsonisées des ssp*. novicida* et *tularensis* dans des macrophages dérivés de moelle osseuse ou encore des macrophages en lignées (type J774A.1) (Balagopal et al., 2006; Geier and Celli, 2011; Schulert and Allen, 2006). L'opsonisation

de la bactérie améliore considérablement l'entrée de la bactérie et permet l'intervention d'autres récepteurs comme le récepteur du complément CR3, dans les macrophage murins et humain, les neutrophiles et les cellules dendritiques (Balagopal et al., 2006; Schulert and Allen, 2006). Le récepteur scavenger A (SR-A), les récepteurs Fcγ, la nucléoline et la protéine A du surfactant pulmonaire (SP-A) sont également impliqués dans la phagocytose de la bactérie opsonisée par le sérum, par des macrophages murins ou humains (Balagopal et al., 2006; Barel et al., 2008; Geier and Celli, 2011). Il n'est pas possible d'exclure que des protéines effectrices, impliquées dans le réarrangement du cytosquelette et la pénétration de la bactérie, soient également injectées par la bactérie dans la cellule, comme c'est le cas chez *S. typhimurium*, *S. flexneri* ou *L. pneumophila* (Hilbi, 2006).

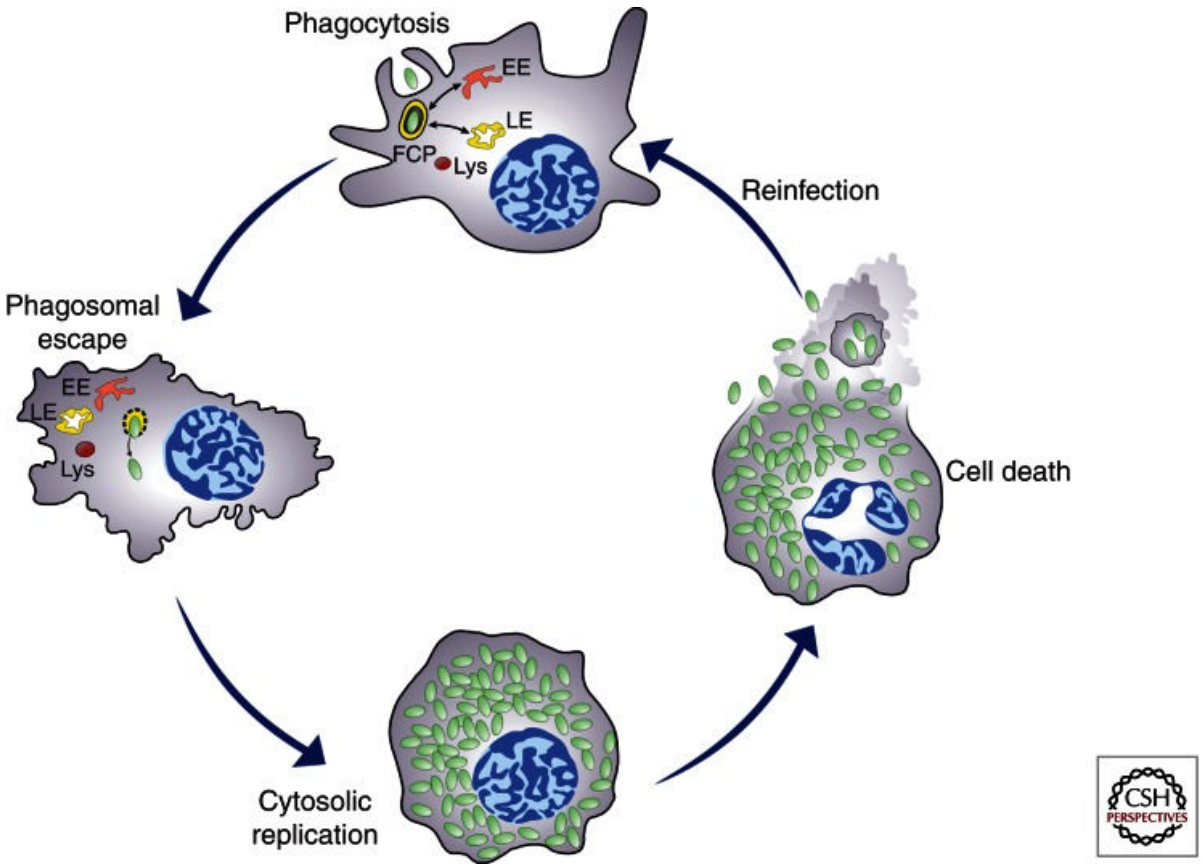

Figure 10 : Cycle de réplication de *Francisella tularensis* dans les macrophages. Le cycle démarre par l'internalisation de la bactérie par un processus dit « Looping », puis la bactérie va sortir du phagosome pour se multiplier dans le cytoplasme du macrophage. Après un certain nombre de cycle de réplication, la bactérie va provoquer la mort cellulaire pour lui permettre de réinfecter d'autres cellules. D'après (Celli and Zahrt, 2013).

L'étape d'internalisation a été notamment caractérisée par l'équipe d'Horwitz et collaborateurs. Leurs travaux ont démontré, par microscopie à fluorescence et microscopie électronique, que *F. tularensis* était internalisée par un mécanisme unique mettant en jeu de grandes boucles asymétriques de pseudopodes (**Figure 10**). La fusion de la boucle avec la membrane plasmique de la cellule permet l'internalisation de la bactérie dans de larges vacuoles à la surface du macrophage. Ce processus appelé "looping phagocytosis" implique un réarrangement de l'actine et une signalisation dépendante de la phosphatidylinositol 3-kinase (Clemens and Horwitz, 2007; Clemens et al., 2005). Comme chez certaines bactéries, il a été montré que la ssp. *holartica* (LVS) était capable de recruter au niveau de la membrane plasmique des radeaux lipidiques pour optimiser son internalisation. Les radeaux lipidiques sont des domaines particuliers de la membrane plasmique qui regroupent des glycosphingolipides (GSL) et des molécules de cholestérol (Tamilselvam and Daefler, 2008). *Francisella* utilise donc un mécanisme différent de ce que l'on peut observer chez les autres bactéries à multiplication intracellulaire.

2.2 L'étape phagosomale

Après l'internalisation, *Francisella* réside dans un phagosome (appelée « Francisella-containing phagosome » ou FCP), un compartiment vacuolaire initialement utilisé pour la dégradation endocytaire et qui est normalement soumis à une maturation progressive et devenir un phagolysosome bactéricide (**Figure 11**). Cette étape phagosomale est caractérisée par la capacité de *Francisella* a interférer avec les trois étapes du processus de phagocytose normal des macrophages: i) la maturation du phagosome, ii) l'acidification du phagosome et iii) le burst oxydatif. Les FCP nouvellement formés acquièrent séquentiellement des marqueurs endosomaux précoces et tardifs, tels que EEA-1, CD63, LAMP-1, LAMP-2 et Rab7 (Checroun et al., 2006; Clemens et al., 2004; Santic et al., 2005a), indiquant un processus de maturation normal. Cependant, les endosomes tardifs ne vont pas fusionner avec les lysosomes, car les

FCP ne semblent pas accumuler à leur surface des marqueurs lysosomaux comme la cathepsine D ou les traceurs lysosomaux (Anthony et al., 1991; Santic et al., 2005b). Il semblerait que cette inhibition de maturation du phagosome soit liée à différentes protéines eucaryotes. Par exemple, la protéine SHIP est phosphorylée en réponse à l'infection par *Francisella*. En conséquence, SHIP réprime la production de cytokines pro-inflammatoires, la maturation des phagosomes et la survie des macrophages (Parsa et al., 2006; Rajaram et al., 2009). Il a aussi été constaté que l'expression de SHIP était fortement diminuée lors de l'infection par la ssp. *novicida*, mais pas par la ssp. *tularensis* (Cremer et al., 2009). Ceci est probablement un facteur contribuant à l'absence de réponse inflammatoire au cours de l'infection par *F. tularensis* (Bosio et al., 2007; Cremer et al., 2009).

Une autre caractéristique importante de la maturation phagosomale est l'acidification progressive du phagosome, via le recrutement de la pompe à proton, l'ATPase vacuolaire (v-ATPase), qui est à la fois une exigence et une conséquence de la maturation phagosomale. Cette étape de maturation reste aujourd'hui très controversée dans la littérature pour l'infection de *Francisella.* En effet, certaines études ont montré que les FCP contenant les bactéries LVS et SCHU S4 (ssp. *holarctica* et *tularensis*) résistent à l'acidification et acquièrent des quantités limitées de v-ATPase (Clemens et al., 2004; Cremer et al., 2009), tandis que d'autres rapportent que les FCP contenant la souche U112 ou SCHU S4 (ssp. *novicida* et *tularensis*) s'acidifient en acquièrant la pompe à protons et montrant un rôle important de l'acidification dans l'échappement phagosomal (Chong et al., 2008; Santic et al., 2008). Il est important de noter que les FCP ne s'acidifient pas lorsque la bactérie est préalablement opsonisée (alors qu'ils sont acidifiés lorsque la bactérie est préalablement opsonisée), suggèrant donc que le mode d'internalisation peut affecter l'acidification du FCP et expliquer les divergences dans la littérature. Le pH acide du FCP permettrait l'induction de certains gènes de virulence et notamment ceux codés dans l'îlot de pathogénicité de *Francisella* (voir plus bas) (Chong et al., 2008; Nano et al., 2004).

Dans des conditions normales, le macrophage va générer un stress oxydant avec la production d'ions superoxydes dans le phagosome via l'assemblage à la membrane phagosomale de la « NADPH oxydase » comme nous l'avons vu précédemment.

Francisella est capable de résister à ce mécanisme de défense de l'hôte en bloquant le recrutement et l'activité de la NADPH oxydase, notamment grâce à l'activité de plusieurs phosphatases acides (comme AcpA) qui vont déphosphoryler les composants de la NADPH oxydase, empêchant l'assemblage de celle-ci et ainsi la production de ROS. Cependant, le blocage de l'assemblage de la NADPH oxydase n'étant pas toujours total, *Francisella* possède également toute une batterie d'enzymes de détoxification des ROS comme par exemple la catalase KatG, ou les superoxyde dismutases, SodB et SodC (Lindgren et al., 2007; Melillo et al., 2010).

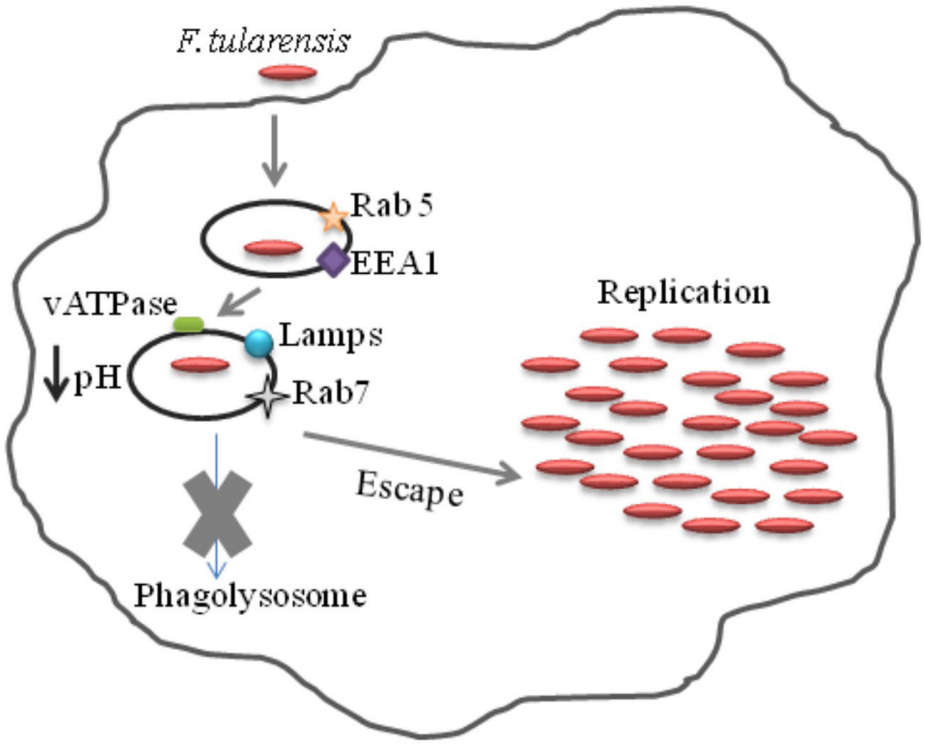

Figure 11 : Détail du contrôle phagosomal par *Francisella* dans les macrophages. D'après (Ozanic et al., 2015).

2.3 Multiplication cytosolique

Il semble très clair aujourd'hui que la sortie du phagosome est liée à l'utilisation d'un Système de sécrétion de type VI codé par le FPI. La structure et le fonctionnement de celui ci sera discuter plus bas. Lors de l'infection de macrophages murins de moelle

osseuse par *F. tularensis*, la moitié des bactéries se trouvent dans le cytosol en moins d'une heure et la totalité en 4 heures. La multiplication intracellulaire débute et atteint son maximum entre 8 heures et 12 heures d'infection puis atteint un plateau à 24 heures. Au total, les bactéries peuvent réaliser jusqu'à 8 à 9 cycles de division dans le cytosol des macrophages infectés. Le temps de doublement est différent selon les ssp. et selon les souches au sein d'une même ssp. Il est, par exemple, de 109 minutes pour la souche FSC200 et de 114 minutes pour la souche LVS, toutes deux appartenant à la ssp. *holarctica* (**Figure 10 et 11**).

2.4 Sortie et dissémination

A la fin de sa période de réplication, *Francisella* va induire la mort cellulaire par deux mécanismes différents : l'apoptose et la pyroptose, permettant ainsi le relargage de la bactérie dans le milieu extracellulaire et sa dissémination aux cellules adjacentes (Lai and Sjöstedt, 2003). Il a été montré que l'infection des macrophages de souris (J774.1) activait la voie intrinsèque de l'apoptose après 24 h d'infection. Les cellules infectées vont alors libérer du cytochrome c mitochondrial dans le cytosol et permettre l'activation de la procaspase-9 et de la procaspase-3. Le clivage de Procaspase-1 n'a pas été observé dans ces conditions, mais cela peut refléter une déficience dans la voie dépendant de la caspase-1 dans cette lignée cellulaire (Henry et al., 2007).

Le deuxième mécanisme de mort cellulaire activé par *Francisella* est la pyroptose. Pendant la réplication cytosolique de la bactérie, un certain nombre de PAMPs vont être relargués dans le cytosol des macrophages. Ces PAMPs, et en particulier l'ADN bactérien, vont être reconnus par le récepteur de l'inflammasome AIM2 (Absent In Melanoma 2). Cette reconnaissance va induire une activation de ce complexe par le recrutement de l'adaptateur ASC et de la pro-caspase 1. La procaspase 1 va être clivé en caspase 1 et permettre le clivage des cytokines pro-inflammatoire IL-1B et IL-18. La caspase 1 va alors induire la mort cellulaire du macrophage par pyroptose. Cette mort cellulaire permet alors à la bactérie d'être relarguée dans le milieu extracellulaire.

Cependant, ce mode de dissémination n'est pas le seul moyen utilisé par la bactérie. En effet, l'équipe de Tom Kawula a récemment mis en évidence chez *Francisella*, un moyen de dissémination par trogocytose (Steele et al., 2016). Les mécanismes cellulaires et moléculaires sous-jacents, mettant en évidence du transfert de cytoplasme d'une cellule infectée par *Francisella* vers une cellule non infectée, restent encore à être déterminés (**Figure 12**).

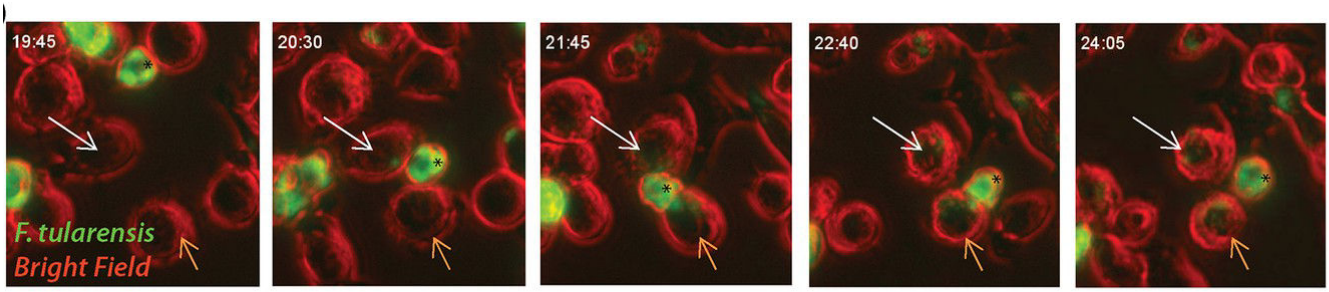

Figure 12 : Visualisation par Vidéo Microscopie du processus de trogocytose réalisé par des macrophages infectés par *Francisella*. Temps en heure après infection; Flèche blanche - premier événement de transfert bactérien; Flèche orange - deuxième événement de transfert bactérien ; * cellule initialement infectée. Adapté de (Steele et al., 2016).

3. Les facteurs de virulence

3.1 La capsule

La capsule a un rôle protection contre la lyse provoquée par le complément, la phagocytose et la reconnaissance immunitaire. Il existe deux types de capsules : i) les capsules polysaccharidiques, comme chez *Escherichia coli*, *Neisseria meningitidis* et *Streptococcus pneumoniae* (Preston and Dockrell, 2008; Willis and Whitfield, 2013) ; et ii) des capsules protéiques, comme chez *Bacillus antracis*. *Francisella* possède une capsule polysaccharidique d'une épaisseur de 0,02-0,04 µm (**Figure 13**) et qui a été décrite pour la première fois par Hood et s'est avérée jouer un rôle dans la virulence (Hood, 1977). En 2015, la composition, les gènes impliqués ainsi que le rôle de celle-ci, étaient encore sujet à controverse.

Cependant, les mutants non capsulés de la souche SCHU S4 (*F. tularensis* ssp.

tularensis) présentent une croissance cytosolique réduite dans les macrophages, en raison du déclenchement précoce de la mort cellulaire (apoptotique ou pyroptotique). Dans le modèle murin ces bactéries non capsulées présentent également une virulence atténuée (Hood, 1977; Lindemann et al., 2011).

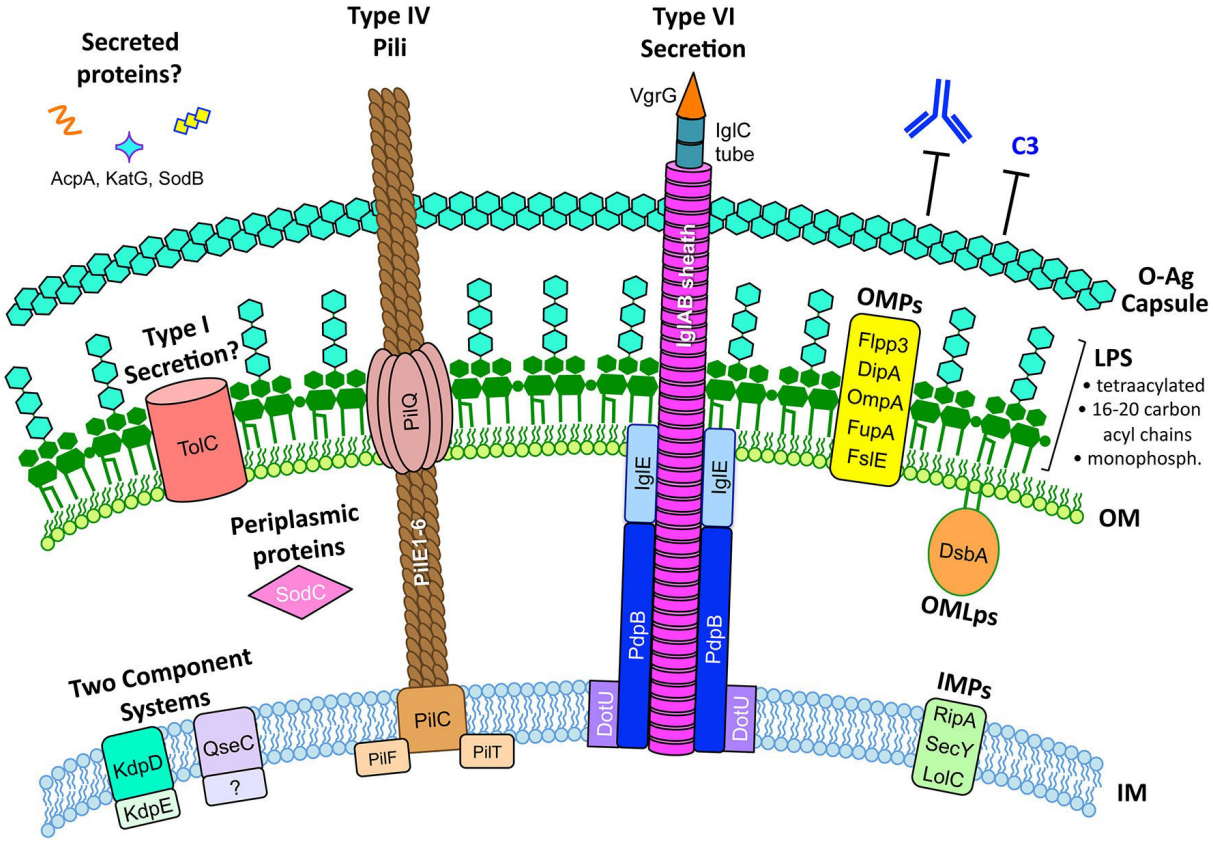

Figure 13 : Représentation des différentes structures membranaires de *Francisella*. D'après (Rowe and Huntley, 2015).

3.2 Le Lipopolysaccharide

Le lipopolysaccharide (LPS) est une endotoxine et un composant majeur de la membrane externe des bactéries à Gram négatif. Chez les autres espèces bactériennes à Gram-negatif, le LPS va être reconnu par le TLR4 du macrophage permettant son activation et ainsi induire la production de cytokine pro-inflammatoire. Le LPS est composé de trois parties : le lipide A, ancré dans la membrane externe, d'un complexe oligosaccharidique lié au lipide A et l'antigène O, sa partie libre dans le milieu extérieur.

Contrairement aux autres bactéries à Gram négatif, le LPS de *Francisella* est 1.000 fois moins endotoxique et n'active pas les cellules via les récepteurs TLR4 (Ancuta et al., 1996; Hajjar et al., 2006). Des différences structurales au niveau du lipide A ont été mises en évidence entre le LPS de *Francisella* et le LPS des autres bactéries, qui pourraient expliquer cette différence de reconnaissance par le TLR4 et ainsi permettre l'échappement à la réponse immunitaire de la cellule hôte (Miller et al., 2005). En effet, le lipide A de *Francisella* possède 4 chaines d'acides gras (au lieu de 6 pour *E. coli*) plus longues que celles des autres bactéries (16 à 18 carbones contre 12 à 14 carbones), et ne contenant qu'un seul groupement phosphate, au lieu de 2 classiquement (**Figure 13** ; Raetz et al., 2009).

3.3 Les pili de type IV

L'analyse de la séquence génomique de la souche SCHU S4 de *F. tularensis* a révélé la présence de gènes orthologues à des gènes codant pour la synthèse de pili de type IV (TFP). Les TFP sont des appendices filamenteux flexibles multifonctionnels importants pour la virulence de plusieurs pathogènes tels que *Pseudomonas aeruginosa*, *Neisseria spp*, *Vibrio cholerae* et *Moraxella catarrhalis*. Ils sont notamment requis pour l'adhérence, la motilité, la formation de biofilm et la compétence pour la transformation de l'ADN (Bergstrom et al., 1986; Sato et al., 1988; Taylor et al., 1987). Les génomes des différentes ssp. de *F. tularensis* codent tous pour plusieurs gènes dont un opéron comprenant six gènes de piline putatifs (Forsberg and Guina, 2007). Cependant, dans les souches virulentes de type B, les pilin pilE et pilV ne sont pas fonctionnels en raison de mutations non-sens, et $pilE_4$, héberge une mutation dans le codon stop entraînant un gène plus long. Certaines souches de type B hébergent un décalage dans le cadre de lecture supplémentaire dans le gène $pilE_4$. Les trois gènes de piline restants, sont identiques entre les souches de type A et de type B. En revanche, les six gènes de la piline sont intacts et fonctionnels chez les souches de type A et ssp. *novicida*. Le gène *pilA* chez ssp. *novicida* diffère à l'extrémité 3' par rapport à *pilA* chez les souches de type A et de type B (**Figure 13 et 14**) (Zogaj et al., 2008).

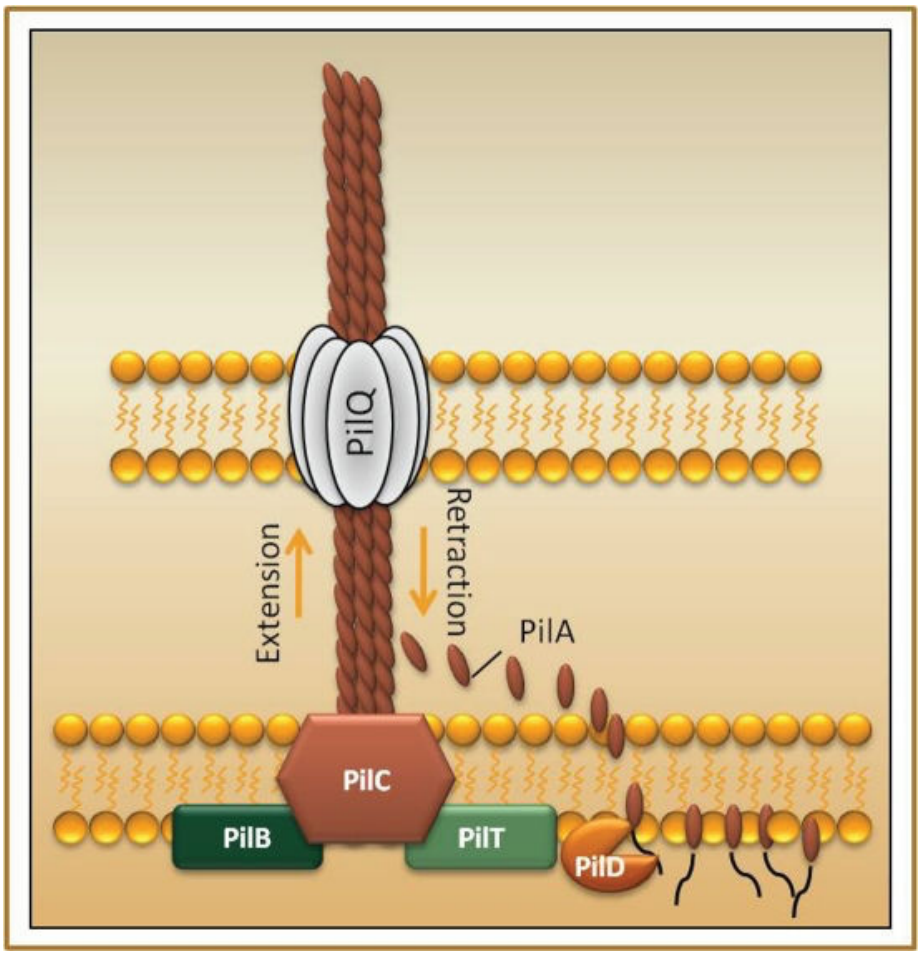

Figure 14 : Représentation schématique du pilus de type IV de *Francisella*. D'après (Salomonsson et al., 2011).

3.4 L'îlot de pathogénicité de *Francisella*

L'îlot de pathogénicité ou FPI (pour « *Francisella Pathogenicity Island* » est une région de 33 kb composé de 17 gènes (**Figure 15**). Ce FPI présente un pourcentage en G+C significativement différent du reste du génome de *Francisella* et est flanqué d'éléments de transposition (Nano et al., 2004). Le FPI détermine un Système de Sécrétion de type VI (abrégé ici SST6) (**Figure 13**) dont la structure, la fonction et les spécificités seront détaillées plus bas. Le FPI est très conservé chez toute les ssp. de *F. tularensis*, mais, alors qu'il est dupliqué chez la plupart des ssp, il est présent en une seule copie dans la ssp. *novicida*. Cette différence pourrait expliquer la virulence

amoindrie de la ssp. *novicida* chez l'Homme (Titball and Petrosino, 2007). Il est à noter que la ssp. *novicida* possède un second îlot « cryptique », désigné FNI (Rigard et al., 2016) codant pour certains gènes présentant des homologies protéiques avec les gènes du FPI (Larsson et al., 2009). Les seules différences notoires entre les FPI des différentes ssp. se trouve au niveau de deux gène : le gène *pdpD* qui est tronqué chez la ssp. *holarctica* et le gène *anmK* qui est absent chez ssp. *holarctica* et qui est plus court chez la ssp. *tularensis* (Nano and Schmerk, 2007).

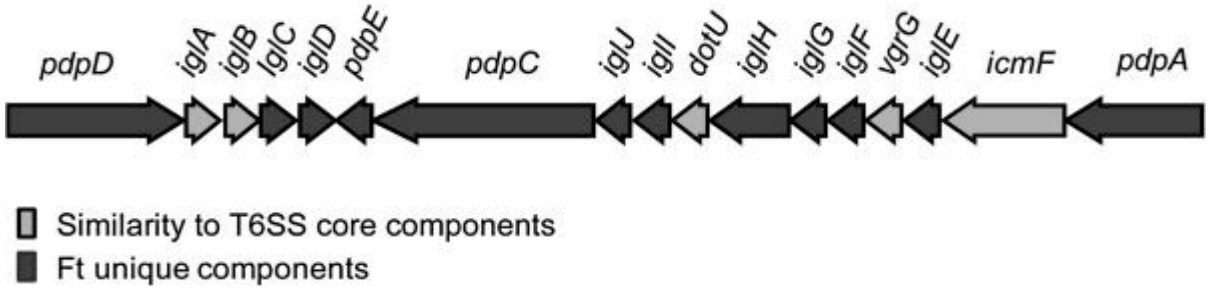

Figure 15 : Gènes de l'îlot de pathogénicité de *F. tularensis*. D'après (Lindgren et al., 2013).

Les gènes présents dans le FPI sont disposés en deux unités transcriptionnelles majeures et sont induits durant la croissance intracellulaire de *F. tularensis*. Il a également été démontré que les gènes du FPI sont régulés par d'autres conditions environnementales, notamment le fer, le peroxyde d'hydrogène, et par plusieurs régulateurs transcriptionnels, comme MglA, SspA, PmrA, FevR, MigR et Hfq. Le premier opéron regroupe les gènes *pdpD, iglA, iglB, iglC* et *iglD*. Le second qui est orienté dans le sens inverse, regroupe les autres gènes *pdpA, pdpB, iglE, vgrG, ilgF, iglG, iglH, dotU, igll, iglJ* et *pdpC* (Barker and Klose, 2007; Bröms et al., 2010a). L'intégralité des gènes de l'îlot a été mutée afin de mieux caractériser le rôle de chacun d'entre eux dans la virulence de *F. tularensis.* Ses analyses ont révélé une contribution de la plupart de ces gènes dans la sortie du phagosome (Bröms et al., 2010a, 2012).

3.5 Le système de sécrétion de type VI

a. Généralité

Les systèmes de sécrétion sont importants pour le transport ou la translocation de molécules (petites molécules, protéines ou d'ADN) de l'intérieur d'une bactérie vers l'extérieur. Ces molécules peuvent jouer des rôles clés dans l'adaptation et la survie d'une bactérie dans son environnement et également dans plusieurs processus physio-pathologiques. Selon le système de sécrétion, les substrats sécrétés ont trois destins possibles: i) ils restent associés à la membrane externe bactérienne (OM), ii) ils sont libérés dans l'espace extracellulaire, ou iii) ils sont injectés dans une cellule cible (cellule eucaryote ou bactérienne). Les systèmes de sécrétion sont des nanomachines macromoléculaires qui peuvent être utilisés par des bactéries pathogènes pour manipuler l'hôte et établir une niche réplicative. Ils peuvent aussi être utilisés pour de la compétition dans une niche environnementale, en sécrétant des protéines effectrices leur fournissant un avantage sélectif (ref générale).

Chez les bactéries à Gram négatif, il existe six principales classes de systèmes de sécrétion, désignés sous le nom de système de sécrétion de type I à VI (SST1 à SST6) (**Figure 16**). Nous allons nous intéresser dans cette partie au SST6.

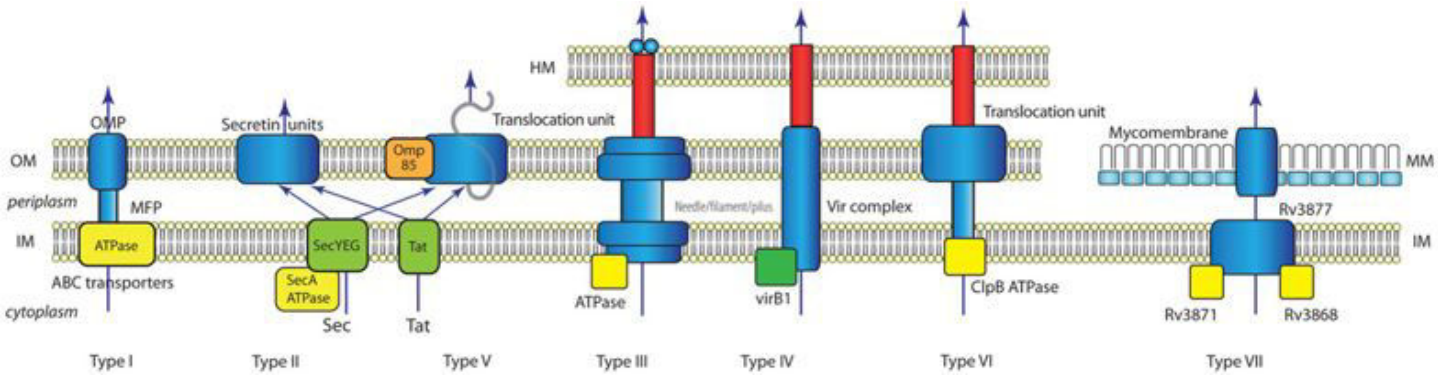

Figure 16 : Représentation schématique des différents systèmes de sécrétions connus chez les bactéries. Nommés de Type I à Type VII. D'après (Tseng et al., 2009).

Le SST6 est une seringue contractile permettant aux bactéries d'injecter des toxines directement dans les membranes ou dans le cytoplasme des cellules, soit pour tuer des bactéries voisines en compétition pour la même niche soit pour cibler des cellules eucaryotes lors d'une infection (MacIntyre et al., 2010; Schwarz et al., 2010). Très récemment, d'autres fonctions ont été attribuées au SST6 et notamment dans la réponse au stress chez *Vibrio anguillarum*, la reconnaissance de soi chez *Proteus mirabilis* et le transfert horizontal de gènes chez *V. cholerae* (Borgeaud et al., 2015; Weber et al.; Wenren et al., 2013).

Décrit pour la première fois en 2006, le SST6 est essentiel à la virulence de plusieurs bactéries pathogènes, par exemple chez *V. cholerae*, *Burkholderia thailandensis* et *P. aeruginosa* (Ma et al., 2009; Pukatzki et al., 2007; Schwarz et al., 2014). Des analyses bio-informatiques montrent que l'on peut classer les SST6 en trois sous-catégories bien distinctes phylogénétiquement (**Figure 17**) (SST6i-iii). La première sous-classe est la plus étudiée à l'heure actuelle puisqu'elle regroupe des SST6i de pathogènes comme *Pseudomonas*, les *E. coli* enteropathogènes ou *V. cholera* (qui est le premier système de sécrétion de type VI a avoir été découvert) (Pukatzki et al., 2006). *Francisella* est actuellement la seule bactérie à posséder un membre de la famille des SST6ii. Jusqu'à présent, il a été démontré que le SST6 de *Francisella* était exclusivement impliqué dans le cycle de vie intracellulaire, et principalement pour la sortie du phagosome (Nano et al., 2004). Enfin, les SST6iii comprennent les bactéries comme *B. fragilis* ou *Flavobacterium johnsoniae*.

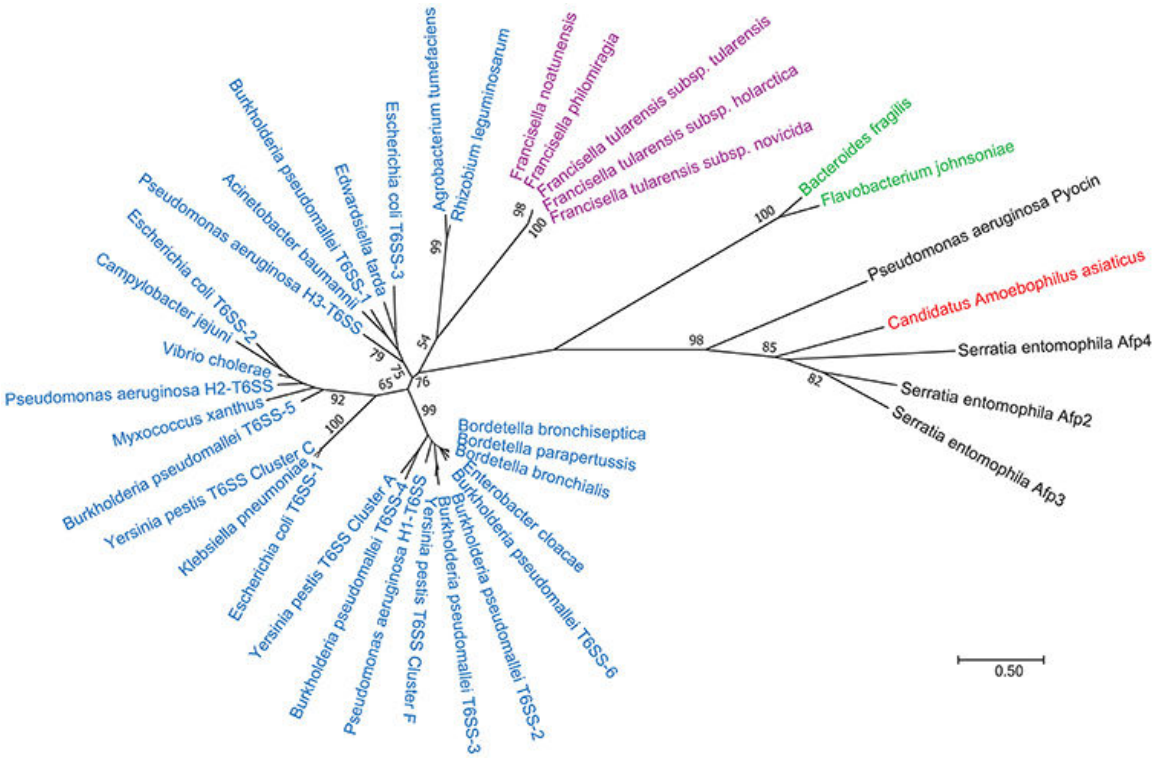

Figure 17 : Arbre phylogénétique représentant la répartition des différents types de SST6 d'après la comparaison d'une des sous unités du fourreau (IglB, VipB, TssC …). D'après (Clemens et al., 2018).

F. tularensis	*P. aeruginosa*	*V. cholerae*	Nom canonique
IcmF/PdpB	IcmF (TssM)	VasK	TssM
IglE	HsiJ (TssJ)	TssJ	TssJ
VgrG	VgrG	VgrG	VgrG
DotU	DotU	DotU	TssL
IglC	Hcp	HcP	Hcp
IglB	HsiC1(TssC)	VipB	TssC
IglA	HsiB1(TssB)	VipA	TssB

Tableau 4 : Protéines conservées du SST6 de *Francisella* avec d'autre bactéries à Gram négatif.

b. Structure

Tous les SST6 ont une structure très similaire et sont tous composés d'une *plateforme*, d'un long fourreau et d'un *tube interne* qui va transpercer la membrane lors de la contraction du fourreau (**Figure 18a**). Ces structures présentent des homologies avec la queue contractile du bactériophage T4 (**Figure 18b**). Le SST6 est constitué en général de 13 composants nommé Tss (pour «Type six secretion»).

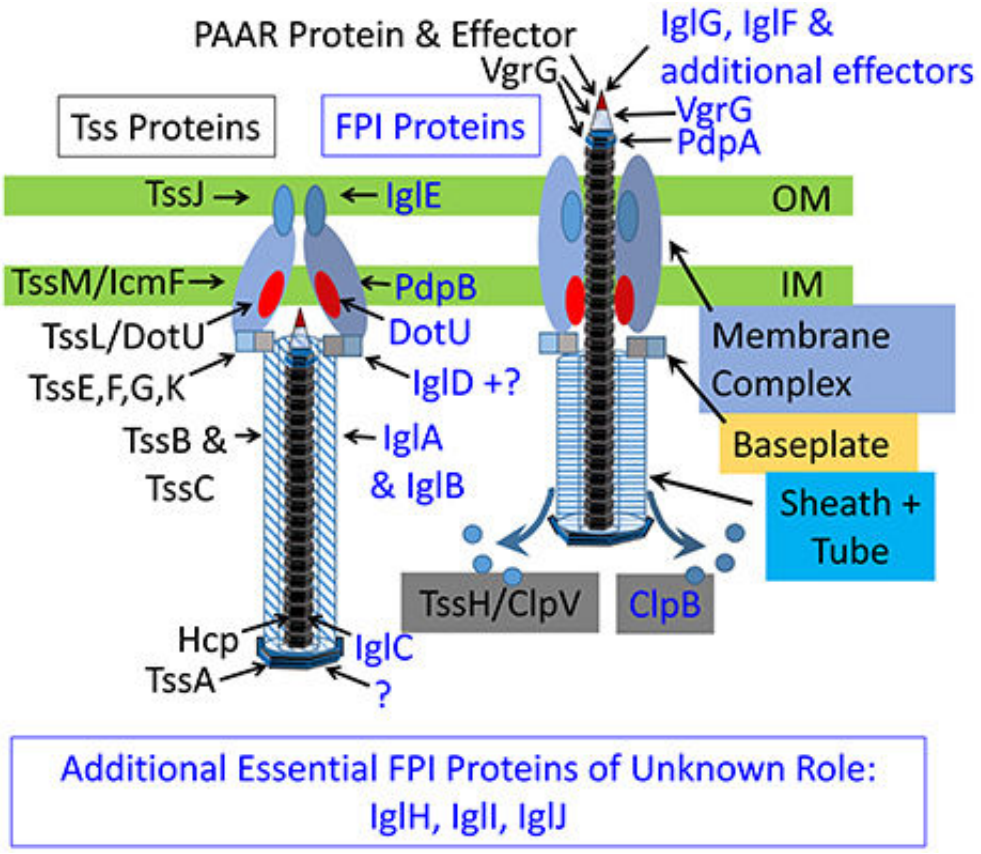

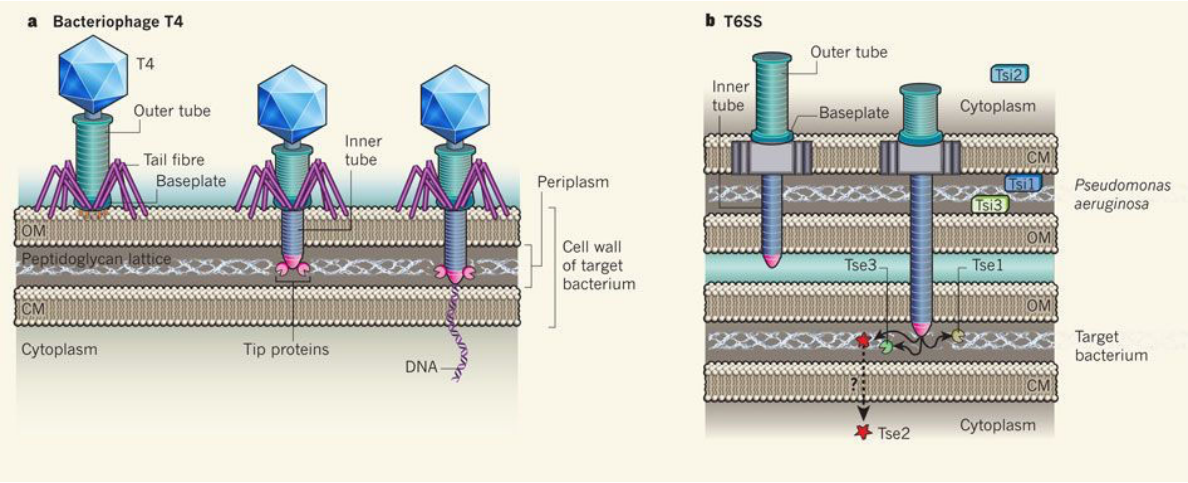

Figure 18 : a) Représentation schématiques du SST6 non contracté (gauche) et contractée (droite). Les sous-unités du SST6 canoniques sont marquées en noir et les sous-unités du SST6 de *Francisella* sont en bleu. D'après (Clemens et al., 2018) **b) Comparaison de la structure du bactériophage T4 et de SST6 de *P. aeruginosa*.** D'après (Cotter, 2011).

Le complexe membranaire (ou membrane core complex) : Chez les SST6 canonique, ce complexe est composé des protéines TssJ/L/M. Le complexe assemblé n'est pas intégralement inséré dans la membrane externe, mais ancré à celui-ci par le fragment lipidique N-terminal de TssJ (Durand et al., 2015). Chez *Francisella*, la plupart des protéines de ce complexe sont conservées et proches de celles des SST6 canoniques. On retrouve la lipoprotéines IglE (TssJ), localisée à la membrane externe et associée dans le périplasme à la partie C-terminale de la protéine PdpB (TssM ou IcmF), localisée dans la membrane interne et interagissant avec la protéine DotU (TssL) (**Tableau 4**). Ce complexe permet de former un canal traversant le périplasme qui facilite le passage du T6SS à travers la membrane (Felisberto-Rodrigues et al., 2011; Zheng and Leung, 2007).

*Plateforme (*ou *Baseplate)* : Chez les SST6 canonique, la *plateforme* est composée des protéines TssE,F,G et K. Ces protéines présentent de fortes homologies avec les protéines impliquées dans la formation la *plateforme* du bactériophage T4. En revanche, chez *Francisella*, les protéines formant la *plateforme* n'ont pas encore été identifiées.

Le fourreau (ou sheath) : Cette gaine contractile est composée de deux protéines, IglA

(équivalente à TssB ou VipA) et de la protéine IglB (équivalente à TssC ou VipB) qui sont associées pour former un « fourreau » externe qui contient un tube interne formé par la protéine IglC (équivalente à Hcp), homologue à la protéine gp19 du bactériophage T4 (Taylor et al., 2016). C'est la contraction de ce fourreau qui est à l'origine de la sécrétion des protéines. Ce fourreau forme une hélice cylindrique organisée autour d'un axe symétrique. Il est formé de six hétérodimères de protéine IglA et IglB qui vont s'empiler lors de la polymérisation du fourreau (**Figure 19**) (Clemens et al., 2015).

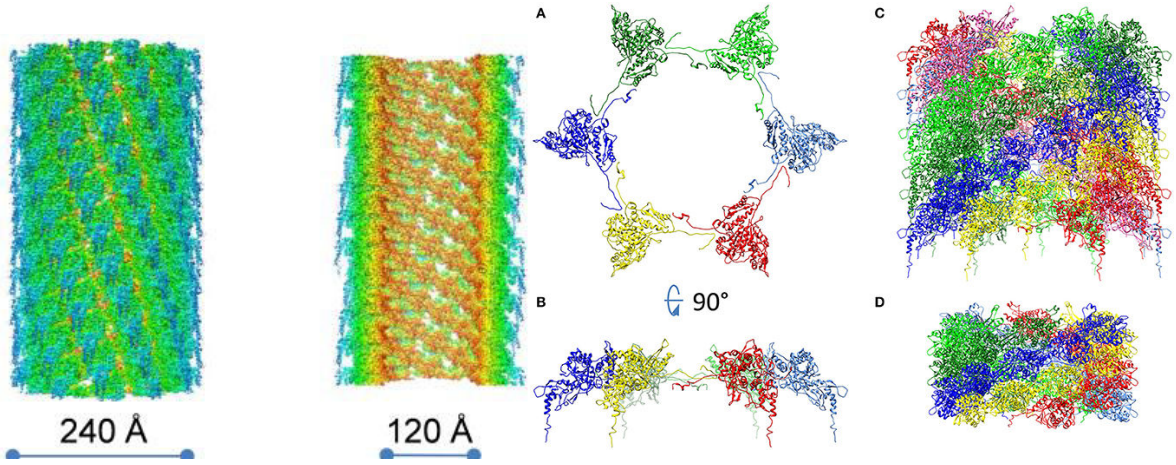

Figure 19 : Représentation structurale du fourreau et de l'anneau hexamérique du SST6 de la ssp*. novicida.* A gauche, representation de la gaine polymérisée ainsi que la taille de la structure. A droite, représentation des disques héxamériques. Adapté de (Clemens et al., 2015).

Le tube interne formé par la protéine IglC est sécrété dans le cytosol de la cellule hôte lors de la contraction du fourreau IglA/IglB. En 2007, la structure d'IglC a été publiée et a permis de montrer une similarité structurale entre la protéine IglC et la protéine Hcp de *P. aeroginosa*, ainsi qu'avec la protéine gp19 de la queue du bactériophage T4 (de Bruin et al., 2011; Taylor et al., 2016). L'analyse par cryo-electro-microscopie (CryoEM) révèle qu'il existe au niveau d'une hélice α (résidus 424-437), située à l'intérieur de la gaine près de l'extrémité C-terminale de IglB, une région avec des résidus qui ont des charges complémentaires à des résidus présents à la surface d'IglC (Clemens et al.,

2015). Il semblerait que ces résidus de IglB et IglC interagissent et stabilisent la conformation de la gaine avant sa contraction. Des situations similaires ont pu être observées chez certaines bactéries comme *Myxococcus xanthus* et *Vibrio cholerae* (Chang et al., 2017; Wang et al., 2017).

A la pointe de ce tube interne, on retrouve le complexe PdpA-VgrG-IglG qui va former l'aiguille moléculaire destinée à perforer la membrane. VgrG est présente aussi dans les autres SST6 mais présente une structure un peu différente des autres SST6. La protéine VgrG de *Francisella* présente une homologie de séquence avec d'autres protéines VgrG, mais elle est inhabituellement courte. En effet, alors que les protéines VgrG canoniques sont typiquement de 600 à 650 acides aminés, VgrG de *Francisella* comprend seulement 164 acides aminés. Chez les autres SST6, VgrG est très similaire à la pointe gp27 et gp5 du bactériophage T4, qui est le complexe utilisé par le phage pour rompre la membrane bactérienne. VgrG de *Francisella* n'a pas les extensions N-terminales de type gp27 et une partie du gp5 des autres VgrG, importantes pour lier le tube interne à la protéine VgrG. Eshraghi et al. ont montré que la protéine PdpA pourrait remplacer ces domaines N-terminaux manquants. Contrairement aux SST6 canoniques, il est probable que le tube IglC de *Francisella* interagisse avec PdpA plutôt qu'avec le VgrG tronqué (Eshraghi et al., 2016). Rigard et al. ont récemment proposé que IglG soit une protéine de type PAAR à la pointe du pic VgrG (Rigard et al., 2016).

La dynamique d'assemblage du SST6 est en cours d'étude chez de nombreux organismes modèles. Des données très récentes de l'équipe de Basler, suggèrent que la polymérisation de la gaine démarre à partir de la baseplate. L'analyse de l'assemblage de la gaine après photobleaching partiel montre que les sous-unités sont exclusivement ajoutées à la gaine à l'extrémité opposée de la baseplate et du complexe membranaire. Selon les auteurs, en raison de la conservation de la structure des sous unités de la gaine entre les différentes bactéries, ce mode d'assemblage est probablement commun à tous SST6 (Vettiger et al., 2017). Une fois la structure du SST6 assemblée, le complexe membranaire s'ouvre pour permettre le passage du tube Hcp / VgrG ou la force de contraction de la gaine induit des changements conformationnels du complexe TssJLM. Après le relargage du tube et des effecteurs, le complexe membranaire TssJLM

revient à l'état de repos, prêt à effectuer un autre cycle de sécrétion (Zoued et al., 2016).

Après la contraction du fourreau, celui ci va être recyclé par la protéine ClpV ATPase (Kudryashev et al., 2015). La protéine ClpV est seulement impliquée dans le désassemblage du fourreau après sa contraction puisque chez *V. cholerea*, en l'absence de la protéine, la bactérie est toujours capable de former un fourreau fonctionnel (Basler et al., 2012). Chez *Francisella*, le FPI ne code pour aucune protéine de type ClpV ATPase. Cependant, il a été très récemment démontré que la ssp*. novicida* utilise l'ATPase ClpB, codée en dehors du FPI, pour dépolymériser son SST6 contractée (Brodmann et al., 2017).

c. Fonctions du SST6 de *Francisella*

Comme mentionné plus haut, le FPI de *Francisella* code pour l'ensemble des protéines du SST6, et joue donc un rôle clef dans la sortie du phagosome qui permet à la bactérie d'avoir accès au compartiment cytosolique (Bröms et al., 2010b; Nano et al., 2004). En conséquence, toute mutation dans le FPI interférant avec la biogénèse normale du SST6 a un impact sur la capacité à sortir du phagosome (**Tableau 5**). Par exemple, des mutations dans les protéines IglA et IglB (protéines tronquées) du fourreau interfèrent avec la formation du SST6, l'échappement phagosomal et la réplication dans des macrophages humaines (Clemens et al., 2015).

Pour identifier des effecteurs sécrétés par le SST6 de *Francisella*, Bröms et al. ont systématiquement exprimé chacune des 17 protéines du FPI en fusion avec la β-lactamase, une molécule capable de cliver le CCF2, une sonde de transfert d'énergie par résonance de fluorescence (FRET) qui est retenu dans le cytosol suite à l'action des estérases de l'hôtes. Si les protéines sont transloquées dans le cytoplasme des cellules, le CCF2 est lysé et le spectre d'émission passe du vert au bleu. Chez *F. tularensis* LVS (ssp. *holarctica*), les auteurs ont détecté un signal fluorescent dans le cytosol de macrophages avec la β-lactamase fusionnée à IglE, IglC, VgrG, IglI, PdpE, PdpA, IglJ et IglF. Chez la ssp. *novicida,* le signal fluorescent dans le cytosol des macrophages a été

observée avec IglE, IglC, PdpA et PdpE, mais pas avec VgrG, IglJ, IglF ou IglI (contrairement à LVS). A noter cependant qu' en 2015, en stimulant les bactéries avec du KCl, Clemens et al. ont pu détecté la présence des protéines IglE, IglC, VgrG, IglI, PdpE, PdpA, IglJ et IglF dans les surnageants de cultures bacteriennes de la ssp. *novicida*, suggérant que ces protéines pourraient être toutes des effecteurs du SST6 (Clemens et al., 2015).

Eshraghi et al. ont très récemment identifié plusieurs autres protéines effectrices codées par des gènes en dehors du FPI, comme OpiA, OpiB-1, et OpiB-3. Ayant des fonctions structurales, les protéines IglC, VgrG et PdpA sont importantes pour la sécrétion des autres effecteurs et impacte la croissance de la ssp. *novicida* dans les macrophages et la virulence chez les animaux. Alors que la suppression des gènes codant pour PdpC, PdpD, OpiA ou OpiB ne bloque pas la sécrétion des autres protéines, puisqu'ils ne sont pas requis pour l'assemblage du SST6, la délétion combinée de pdpC, pdpD, OpiA et OpiB altère sérieusement la croissance intracellulaire sans affecter la fonction de sécrétion du SST6. Aucun de ces gènes ne se trouve chez les autres espèces et leur fonction reste inconnue (Eshraghi et al., 2016). La délétion des gènes PdpC ou pdpD a un effet intermédiaire, car ces gènes sont nécessaires pour la virulence chez les animaux, mais ils ne sont pas essentiels pour la croissance intracellulaire (Ludu et al., 2007). Dans la souche hautement virulente de *F. tularensis* SCHU S4 (ssp. *tularensis*), l'absence des deux copies de pdpC provoque un retard dans l'échappement du phagosome et une légère diminution de la croissance intracellulaire dans les macrophages de souris J774.1. Brodmann et al. ont confirmé que pdpC et pdpD ne sont pas requis pour l'assemblage de SST6 chez la ssp. *novicida*, mais que iglF, iglG, iglI et iglJ sont quant à eux importants pour l'assemblage. En revanche, la perturbation de pdpE n'a pas d'impact sur l'échappement des phagosomes dans les macrophages ou la virulence chez les souris chez les ssp. *novicida* et *holarctica* (Brodmann et al., 2017).

Chez *V. cholerae*, les effecteurs sont emballés dans une cavité de la plaque basale et ont une taille d'environs 450 kDa (Nazarov et al., 2018). Si on retire les protéines PdpA-VgrG-IglG et IglC qui sont des protéines structurales du SST6, les protéines IglF, PdpD, PdpC OpiA, OpiB, PdpE et IglI, ont une masse totale proche de

450 kDa. Si toutes ces protéines sont bien des effecteurs, il est possible que certaines soient emballées dans la plaque basale du SST6 comme c'est le cas chez *V. cholerae*. *Francisella* pourrait aussi empaqueter préférentiellement certains effecteurs en fonction des stimuli environnementaux (Clemens et al., 2018). De plus, comme c'est le cas chez certains SST6 canoniques, de petits effecteurs pourraient tenir dans le tube IglC et être sécrétés dans le cytoplasme de la cellule (Whitney et al., 2014).

	Croissance intracellulaire	Echappement phagosomal	Virulence dans la souris	Virulence dans la Drosophile
PdpA	+	+	+	+
IcmF/PdpB	+	NT	+	+
IglE	+	NT	+	+
VgrG	+	+	+	+
IglF	+	NT	+	+
IglG	+	-	+	+
IglH	+	NT	+	+
DotU	+	NT	+	+
IglI	+	+	+	+
IglJ	+	NT	+	+
PdpC	-	NT	+	-
PdpE	-	NT	-	-
IglD	+	NT	+	+
IglC	+	+	+	+
IglB	+	+	+	+
IglA	+	+	+	+
PdpD	-	NT	+	-
AnmK	-	NT	+	-

Tableau 5 : Rôle fonctionnel des gènes du FPI de *F. tularensis* ssp. *novicida*.

d. Régulation du SST6 de *Francisella*

L'expression des gènes du FPI est très sensible aux facteurs environnementaux et notamment ceux rencontrés par la bactérie dans les macrophages. Parmi ces facteurs environnementaux, on retrouve le stress oxydant, la carence en fer et la réponse stringente. A l'heure actuelle, on ne dénombre pas moins de six régulateurs transcriptionnels agissant directement sur le contrôle de l'expression du FPI.

MglA et *SspA* : Le rôle fondamental du régulateur *Mgla* pour la croissance intracellulaire et la virulence de *Francisella* a initialement été démontré chez les ssp. *novicida* et. *tularensis* (Baron and Nano, 1998). Le gène *mglA* est situé sur l'opéron *mglAB*, qui est exprimé en phase exponentielle de croissance. MglA présente 20% d'identité avec la protéine SspA (Stringent Stravation Protein A) d'*E. coli* (Baron and Nano, 1998; Charity et al., 2007), un régulateur transcriptionnel de gènes, associé à l'ARN polymérase, qui régule l'expression d'un groupe de gènes impliqués dans la réponse aux stress nutritionnel (Barker and Klose, 2007; Baron and Nano, 1998). Chez un mutant *mglA*, le niveau d'expression des gènes pdpD, iglA, iglC, iglD et pdpA est altéré, suggérant un rôle de régulateur sur les différents gènes du FPI (Lauriano et al., 2004). Des analyses transcriptionnelles ultérieures ont mis en évidence qu'une mutation du gène *mglA* provoquait la modification de l'expression de 102 gènes (Brotcke et al., 2006), dont tous les gènes du FPI. L'identification en 2007 de la protéine SspA dans les ssp. *tularensis* et *holarctica* (souches SCHU S4 et LVS), a permis de mettre en évidence la formation du complexe MglA-SspA-ARN polymérase, important pour initier la transcription de facteurs de virulence, dont les gènes du FPI (Charity et al., 2007).

FevR et le *ppGpp* : Ces études ont également mis en évidence que le complexe MglA-SspA-ARN polymérase était contrôlé par FevR (également appelé PigR) et l'alarmone ppGpp, deux facteurs dépendant de stress environnementaux. FevR a été montré comme étant essentiel pour la réplication dans le macrophage et dans le modèle animal (Charity et al., 2007). FevR régule à la fois l'expression des gènes du FPI et d'autres gènes du régulon mglA/sspA via le ppGpp (guanosine tétraphosphate) qui est

important pour favoriser cette interaction. En l'absence du ppGpp, l'interaction MglA / SspA avec FevR n'est pas stabilisée.

La réponse au stress intramacrophagique induit une production de ppGpp qui se lie spécifiquement à la face «ouverte» de MglA / SspA sans provoquer de changement conformationnel. En conséquence, le complexe MglA / SspA-ppGpp se lie au domaine C-terminal de FevR, qui renforce et stabilise de manière concomitante la machinerie transcriptionnelle au niveau de promoteurs spécifiques hébergeant un motif PRE. Par conséquent, FevR confère à la RNAP un second point ancrage sur l'ADN pour initier la transcription du FPI (**Figure 20**). Cependant, il n'a pas encore été prouvé que FevR interagisse directement avec l'ADN (Cuthbert et al., 2017).

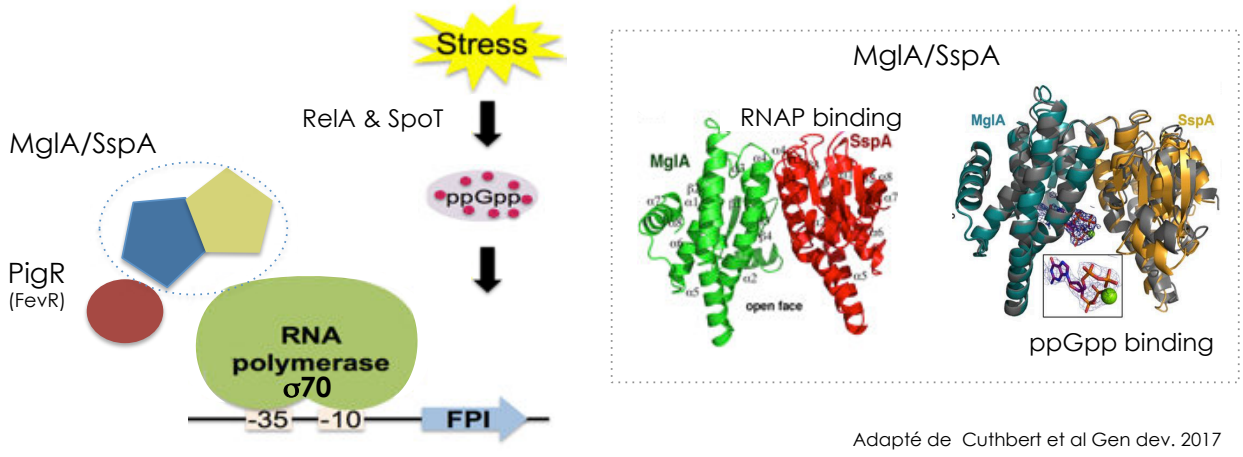

Figure 20 : Modèle de la régulation des gènes de l'îlot de pathogénicité de *Francisella* par le complexe FevR-ppGpp MglA/SspA/RNAP. Adapté de (Cuthbert et al., 2017).

PmrA : Ce régulateur est un des éléments d'un système à deux composants chez *Francisella*. Les systèmes à deux composants sont des systèmes mis en place par les bactéries pour répondre efficacement à des stimuli extérieurs comme la carence nutritionnelle. Chez *Francisella*, ce système à deux composant est dit orphelin puisqu'il ne présente pas de capteur. Chez la ssp. *novicida*, un mutant *pmrA* présente un défaut de multiplication intracellulaire ainsi qu'une virulence fortement atténuée chez les souris

lié à un défaut de sorti du phagosome. PmrA va être phosphorylé par une histidine kinase, KdpD. Suite à cette activation, PmrA va se fixer sur des régions précise de l'ADN et notamment sur son propre opéron pour s'autoréguler, mais il va aussi activer la transcription du FPI (Bell et al., 2010). Il a aussi été montré que PmrA se fixe au complexe MglA-SspA pour activer la transcription du FPI.

MigR : MigR (Macrophage Intracellular Growth Regulator) est un autre régulateur de l'opéron iglABCD. Un mutant dans ce régulateur présente un défaut de multiplication dans les macrophages dérivés de monocytes humains. La transcription de FevR est très affectée par une mutation de MigR, suggérant une action indirecte de MigR sur le FPI (Buchan et al., 2009). En réduisant l'expression de FevR, MigR permettrait une répression de l'opéron iglABCD. Il a été montré que suite à un signal environnemental (stress pH ou nutritionnel), MigR induisait la synthèse de l'alarmone ppGpp via RelA et SpoT. Le ppGpp va alors agir sur FevR et permettre l'induction du FPI (Buchan et al., 2009).

Hfq : Chez de nombreuse bactéries comme *V. cholerae ou E.* coli, Hfq est un régulateur post-transcriptionnel qui, sous la forme d'une protéine chaperonne permet l'interaction des petits ARN avec leurs ARN cible (Valentin-Hansen et al., 2004). Chez *Francisella*, Hfq régule négativement l'expression d'une partie des gènes du FPI. Elle va agir au niveau de l'opéron pdp, contenant les gènes pdpA, pdpB, pdpC, dotU, vgrG, iglE, iglF, iglG, iglH, iglI, iglJ et pdpE. Un mutant hfq, présente un défaut de multiplication intracellulaire dès les premières heures d'infection, une diminution de la virulence chez la souris ainsi qu'une diminution de la résistance aux stress (stress thermique, salin et dénaturant) (Meibom et al., 2009).

4. Besoin nutritionnel et Adaptation métabolique de *Francisella*

Un des défis majeurs de la survie intracellulaire de *Francisella* est la limitation en nutriments. En effet, le milieu intracellulaire est considéré comme étant un environnement riche en nutriment. Cependant, certains d'entre eux, nécessaires à la

multiplication bactérienne, sont présents en quantités limitantes (Fonseca and Swanson, 2014). *Francisella* a mis en place différentes stratégies d'adaptation à ce milieu carencé et pouvoir se multiplier efficacement. Des criblages génétiques à l'échelle du génome (criblage de banques de mutants par transposition), réalisés dans différents modèles cellulaires et / ou animaux, ont permis d'identifier un nombre important de gènes codant pour des voies métaboliques ou des protéines membranaires, soulignant l'importance de l'adaptation métabolique et de l'acquisition des nutriments dans la survie intracellulaire de *Francisella* (Meibom and Charbit, 2010).

4.1 Liens entre voies de biosynthèse et virulence chez *Francisella*

A la différence de certains pathogènes intracellulaires vacuolaires comme *L. pneunophila*, *Francisella* a un accès direct aux nutriments du cytoplasme de son hôte. Les acides aminés constituent une des sources de carbone et d'azote privilégiés par *Francisella* (Steele et al., 2013). Les hexoses, et plus précisément le glucose, sont aussi des sources majeures de carbones et d'énergie. Le métabolisme du carbone sert à produire de l'énergie et des précurseurs métaboliques essentiels tels le glucose 6-phosphate, le fructose 6-phosphate, le 3-phosphoglucérate, le phosphoénolpyruvate (PEP) ou l'acétyl-CoA. Cependant, à la différence des autres bactéries, toutes les voies du métabolisme du carbone ne sont pas actives chez *Francisella*. En effet, par des analyses de profils isotopique avec du glucose et du pyruvate marqué en C13, notre laboratoire a pu montrer que la voie Entner-Doudouroff et la branche oxydative de la voie des pentoses phosphate ne sont pas actives chez *Francisella* (Brissac et al., 2015).

Le cycle de Krebs (ou TCA cycle) est la source majeure de production d'énergie sous forme d'ATP (2 molécules par molécule de glucose) et de NADH (4 par molécule de pyruvate, qui seront converties en 3 molécules d'ATP chacune par la chaine respiratoire) (**Figure 21**). Cette voie vient à la suite de la glycolyse (qui produit 2 molécules d'ATP par molécule de glucose) et permet de transformer le PEP en oxaloacétate. Les acides aminés, constituants nutritionnels essentiels de *Francisella*, peuvent intégrer le cycle de Krebs à différents niveaux, comme le glutamate au niveau de l'oxoglutarate (via la

glutamate dehydrogenase) ou encore l'aspartate au niveau de l'oxaloacetate (via l'aspartate transaminase). Il est donc logique de penser que le cycle de Krebs joue un rôle important dans l'adaptation intracellulaire de *Francisella*. D'ailleurs, six enzymes du cycle de Krebs ont été identifiées comme étant importantes pour la virulence de *Francisella* : FumA, SdhC, SucA, SucB, SucC et SucD (Pechous et al., 2009).

La *Glycolyse / Gluconéogenèse* : Cette double voie métabolique est une suite de cascades enzymatiques qui aboutit soit à la production de pyruvate (glycolyse) afin d'alimenter la TCA, soit à la production de glucose (gluconéogenèse) à partir de composés non glucidiques (**Figure 21**). Des analyses transcriptomiques de la ssp. *tularensis* (souche SCHU S4) dans des macrophages de moelle osseuse de souris ont montré une augmentation significative des gènes impliqués dans la double voie glycolyse/néoglucogenèse (Wehrly et al., 2009). De plus, plusieurs gènes de cette voie jouent un rôle dans la virulence de la bactérie (Meibom and Charbit, 2010) et en particulier la Fructose-1,6-biphosphate aldolase (Fba) qui a fait l'objet d'une partie de mon travail de thèse (voir article 1).

La voie des *pentoses phosphates* : Cette voie importante dans métabolisme du carbone (**Figure** 21) débute au niveau du glucose-6-phosphate et permet la production d'un certain nombre de produit important comme le NADPH-H+, utilisé dans la réponse au stress oxydant, de ribose-5-phosphate nécessaire à la synthèse des nucléotides, d'érythrose-4-phosphate, un précurseur des acides aminés aromatiques et d'autres composants important pour la synthèse de la paroi bactérienne. Parmi les enzymes de la voie PP, on peut noter notamment l'importance de la transketolase (TktA) pour la multiplication cytosolique et la virulence de *Francisella*. Cette enzyme a été rapportée très récemment comme impliquée dans la sécrétion de vésicules de membrane externe (OMV) (Sampath et al., 2018). De telles vésicules pourraient fournir un système de communication de cellule à cellule et la délivrance de molécules effectrices telles que des facteurs de virulence.

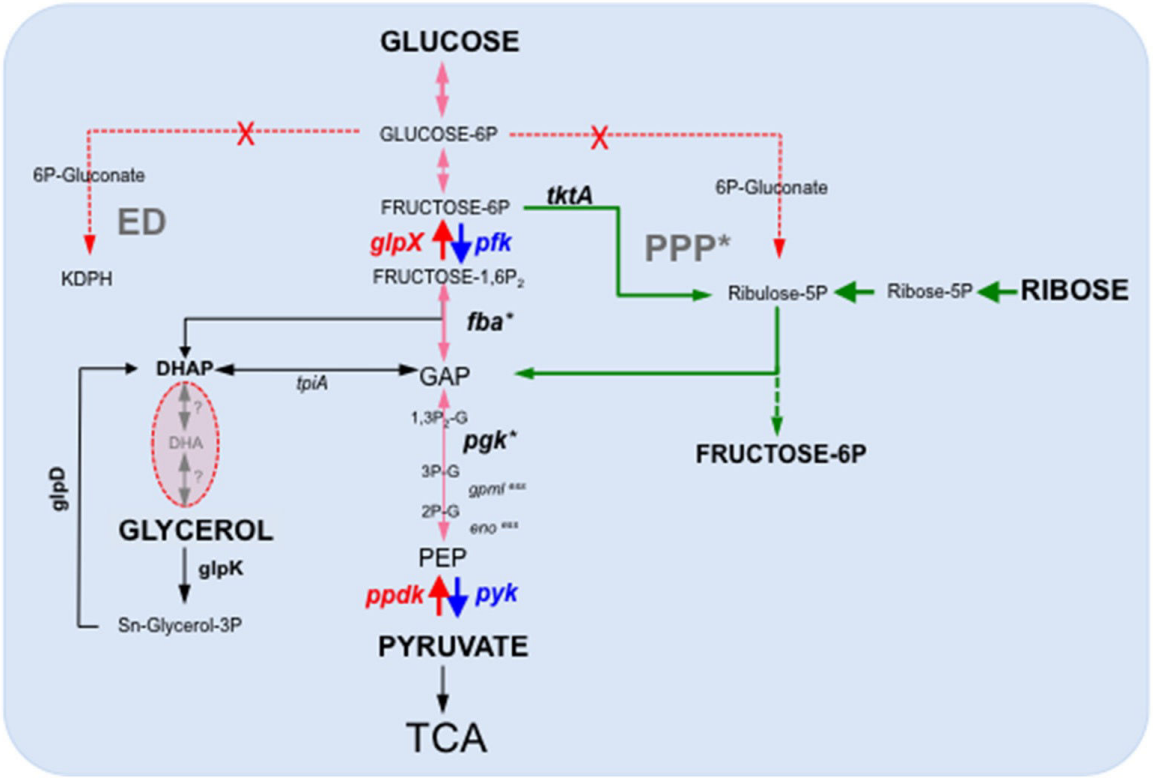

Figure 21 : Représentation schématique des voies la Glycolyse/ Gluconéogenèse de *Francisella*. Le TCA produit 2 ATP, plus les deux de la glycolyse, cela fait 4 ATP. Les 4 NADH contiennent également de l'énergie qui sera transformée en 3 ATP chacun lors de l'étape suivante (soit 24 ATP) et le FADH2 capable d'en produire 2 (4 au total). C'est donc un total de 32 ATP produit. D'après (Ziveri et al., 2017).

4.2 Relation Métabolique Hôte/Bactéries

a. Le transport des acides aminés

Francisella présente de nombreuses auxotrophies dont celles pour l'arginine, l'histidine, la lysine, la tyrosine, la méthionine ou la cystéine, résultant d'altérations génétiques dans leurs voies de biosynthèse respectives (Larsson et al., 2005). *Francisella* doit donc capter ces acides aminés directement dans la cellule hôtes. Pour cela, la bactérie possède des systèmes de transport dédiés de haute affinité. Des analyses du génome réalisées par notre équipe ont révélé que *Francisella* est principalement équipée de transporteurs secondaires (Meibom et Charbit, 2010). Cette famille de transporteurs regroupe plusieurs familles de transporteurs. On retrouve les

transporteurs d'acides aminés appelés les APC (« amino acid-polyamine-organocation transporters »), les transporteurs d'oligopeptide dépendant de proton (POT), les perméases d'acides aminés hydroxy / aromatiques (HAAAP), ainsi que les « major facilitator superfamily » (MFS), qui sont impliquées dans diverses fonctions de transport, y compris l'absorption des acides aminés. Parmi ces transporteurs on retrouve le transporteur du glutamate GadC, important pour la résistance au stress oxydant (**Figure 22**) (Ramond et al., 2014). La multiplication intracellulaire d'un mutant *gadC* est totalement abolie parce que les bactéries restent bloquées dans compartiment phagosomal. Le glutamate importé va alimenter le TCA (Tricarboxylique Acid) et peut être converti en divers composés comme la glutamine, le glutathion, le GABA ou l'oxoglutarate (OG), qui sont connus pour être des molécules antioxydantes (Mailloux et al., 2009).

Francisella possède également un transporteur à l'asparagine, une perméase appelée AnsP. Contrairement à un mutant *gadC*, un mutant *ansP* est capable de sortir du phagosome ; ce qui suggère que le transporteur AnsP est exclusivement requis pour la multiplication bactérienne cytosolique (**Figure 22**). Le défaut de croissance intracellulaire du mutant *ansP* de la ssp*. novicida* a pu être complètement supprimé par une supplémentation avec un excès d'asparagine, aussi bien in vitro qu'in vivo ; ce qui suggère que la bactérie utilise l'asparagine exogène pour sa multiplication intracellulaire (Gesbert et al., 2014). Fait intéressant, *Francisella* est prototrophe à la fois pour le glutamate et l'asparagine, impliquant donc que la bactérie devient "phénotypiquement" auxotrophe dans les cellules infectées. Le fait que l'absorption d'asparagine (dépendant de AnsP) est important pour la synthèse des protéines et que le transport de glutamate (dépendant de GadC) est quant à lui nécessaire pour la défense contre le stress oxydatif, il apparait que le transport des acides aminés contribue à de multiples aspects de l'adaptation bactérienne à la vie intracellulaire.

Un autre exemple que nous pouvons citer est celui de la perméase ArgP, un transporteur d'arginine de haute affinité (**Figure 22**) (Ramond et al., 2015). L'absorption de l'arginine par ArgP semble être cruciale pour une sortie phagosomale efficace. L'arginine est un acide aminé essentiel pour *Francisella* puisque les voies métaboliques

de biosynthèse de l'arginine sont prédites comme inactives. Une analyse protéomique globale a révélée que la limitation en arginine affectait la biogenèse de la majorité des protéines ribosomales. En effet, lorsque les bactéries sont cultivées dans des conditions limitantes en arginine, la majorité des protéines ribosomales identifiées (environ 80%) sont présentes en plus faible quantité chez le mutant *argP* que chez le sauvage, suggérant des liens possibles entre biogénèse du ribosome et l'échappement phagosomal (Ramond et al., 2015).

Enfin, pour compenser son auxotrophie pour la cystéine, *Francisella* est capable de capter le glutathion, un tripeptide contenant de la cystéine. Pour cela, *Francisella* va synthétiser une enzyme appelée la γ-glutamyl-transpeptidase (GGT). La GGT va hydrolyser le glutathion, ce qui libère un dipeptide cysteinyl-glycine, une source essentielle de cystéine pour la multiplication de *Francisella*. Un mutant pour le gène *ggt* est incapable de se multiplier dans les macrophages, en absence de d'apport supplémentaire de cystéine (Alkhuder et al., 2009) et est totalment avirulent dans le modèle murin. Le mécanisme par lequel le glutathion entre dans la bactérie n'est pas connu.

b. L'importance des carbohydrates

Durant sa phase de réplication intracellulaire, *Francisella* va préférentiellement utiliser le glucose comme source de carbone et d'énergie, plutôt que des acides aminés, si celui-ci est présent en excès. En absence de glucose (ou en conditions limitantes de glucose), la bactérie va être capable d'utiliser d'autre source de carbone comme le pyruvate, le glycérol ou glycérol-3-P. En effet, le génome de *Francisella* possède des transporteurs pour le glycérol (glycerol uptake transporter GlpF) ou des transporteurs pour le glycérol 3-P (glycerol-3 phosphate transporter GlpT). Il est à noter que *Francisella* ne possède pas de système PTS (PEP phosphotransférase), contrairement à *Listeria* qui possède un grand nombre de systèmes de ce type. Les systèmes PTS sont généralement impliqués dans le transport d'hexoses et autres carbohydrates. Les mécanismes par lesquels le glucose est capté par *Francisella* sont encore inconnus

(Meibom and Charbit, 2010).

Une étude très récente du laboratoire a permis de démontrer l'importance de la gluconéogenèse dans la virulence de la bactérie. En effet, l'inactivation du gène *glpX*, codant pour la Fructose biphosphatase de classe II, provoque une forte diminution de la multiplication intracellulaire, en présence de substrats gluconéogéniques et d'une virulence fortement atténuée chez la souris. L'enzyme GlpX strictement gluconéogénique est responsable de la conversion du fructose 1,6-bisphosphate en fructose 6-phosphate. Un défaut de multiplication intracellulaire important est observé chez un mutant *glpX* lorsque les cellules sont supplémentées avec un substrat gluconéogénique (par exemple pyruvate ou glycérol). En revanche, une multiplication normale est restaurée lorsque le milieu est supplémenté avec du glucose (Brissac et al., 2015). Cette étude a permis de montrer également une réduction de la concentration en glucose intracellulaire dans des macrophages (J774.1 et THP-1) infectés pendant 24 h avec la souche *F. tularensis* LVS (Brissac et al., 2015). Il est donc nécessaire pour *Francisella* d'avoir une gluconéogènese active et efficace pour compenser la réduction du pool de glucose cytosolique. Le contrôle de l'homéostasie du glucose intracellulaire est peut-être une réponse du macrophage à l'infection bactérienne. On peut imaginer que les cellules infectées pourraient réduire le pool intracellulaire de glucose disponible pour limiter la prolifération bactérienne.

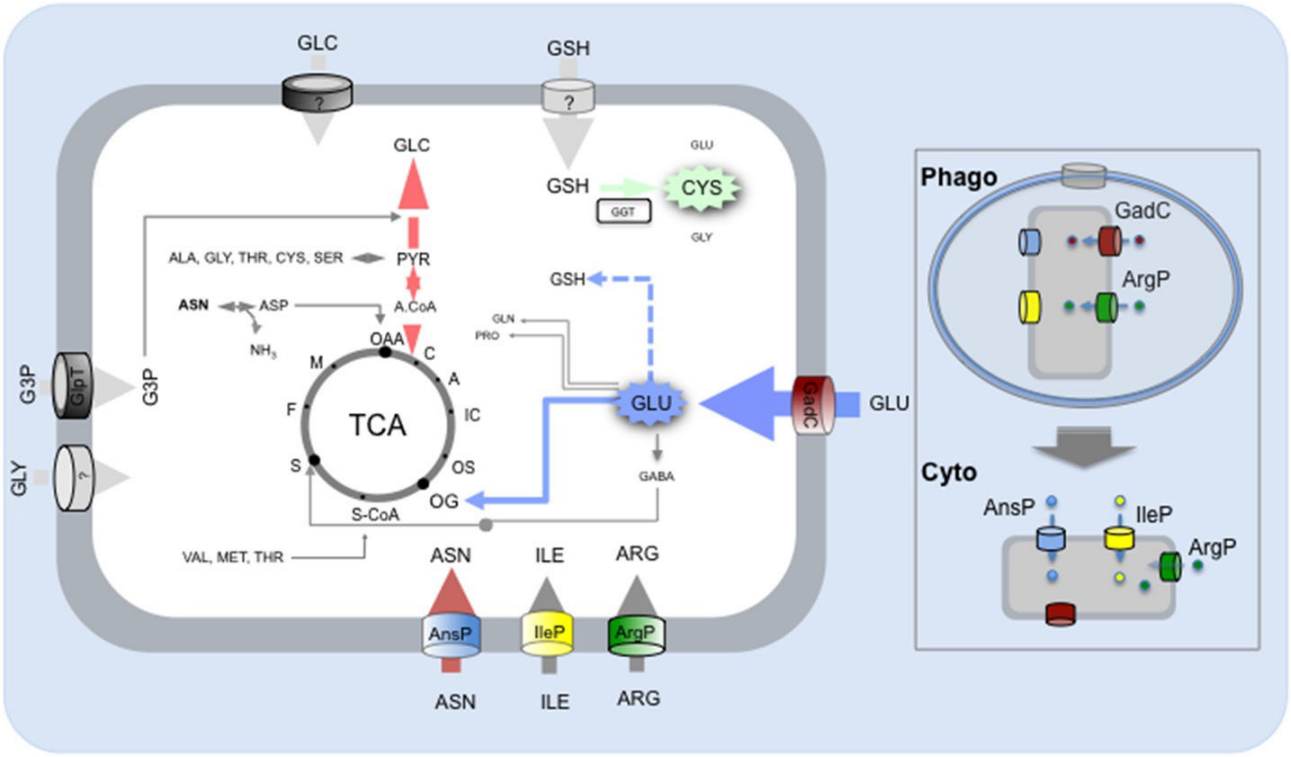

Figure 22 : Systèmes de transport d'acides aminés et de glucides impliqués dans la survie intracellulaire de *Francisella.* D'après (Ziveri et al., 2017).

OBJECTIFS

Ces travaux de thèse, centrés sur deux articles dont je suis le premier auteur (un publié en 2017 et un sur le point d'être soumis) ont porté sur deux aspects différents de l'adaptation à la vie intracellulaire de *F. tularensis*. Le premier aspect concerne l'importance de l'adaptation métabolique de la bactérie dans son pouvoir pathogène (Ziveri et al. Nat. Commun. 2017). Le second s'intéresse aux mécanismes moléculaires impliqués dans l'assemblage d'une machinerie de sécrétion très importante pour la virulence de la bactérie (Ziveri et al. En préparation).

Une étude précédente du laboratoire, à laquelle j'ai eu l'opportunité de participer activement, notamment pour la partie *in vitro* et *in vivo* (Brissac, Ziveri et al. Mol. Microbiol. 2015 ; présentée en annexe) a permis de démontrer l'importance de la gluconéogenèse dans la multiplication intracellulaire de la bactérie et sa virulence *in vivo*. En particulier, nos résultats ont montré que, dans le cytoplasme des cellules, *Francisella* utilisait principalement les acides aminés de l'hôte comme substrats gluconéogéniques. Je me suis donc intéressé à cette double voie de la Glycolyse / Gluconéogenèse et tout particulièrement à certaines de ces enzymes dont les gènes sont regroupés au sein d'un même opéron. L'une d'entre elle, décrite comme essentielle chez de nombreuses bactéries et pouvant jouer des fonctions accessoire a tout particulièrement attiré notre attention, la Fructose-1,6-biphosphate aldolase (FBA).

Nos analyses ont, dans un premier temps, confirmé le rôle clef de double voie de la Glycolyse / Gluconéogenèse dans la pathogénèse de *Francisella*. Puis, nous avons découvert que cette enzyme FBA jouait également un rôle de régulateur transcriptionnel. **De façon remarquable, cette activité régulatrice relie le métabolisme intracellulaire bactérien au contrôle de la réponse inflammatoire de l'hôte.**

Le deuxième projet développé dans ma thèse est parti d'un pari sur l'existence potentielle de mécanismes post-traductionnels de phosphorylation de protéines chez *Francisella* et contribuer à sa pathogenèse. En effet, les génomes de *Francisella* ne possèdent pas de gène codant pour des sérine / thréonine-protéine kinases ou tyrosine kinases putatives. En dépit de ce manque de kinases canoniques, une approche phosphoprotéomique globale de *Francisella*, nous a permis de confirmer l'existence de

nombreuses protéines phosphorylées. Une de ces protéines a tout particulièrement attiré notre attention, la protéine IglB, un composant clé de la gaine contractile du SST6 qui possédait un site de phosphorylation unique sur la tyrosine 139. Les résultats obtenus suggèrent que **cette modification post-traductionnelle intervient dans la dynamique d'assemblage du système de sécrétion de type VI de *Francisella*.**

Chapitre 2 :

Résultats

La Fructose-1,6-bisphosphate aldolase, une enzyme métabolique ubiquitaire aux fonctions régulatrices chez *Francisella*.

Jason Ziveri, Fabiola Tros, Ida Chiara Guerrera, Cerina Chhuon, Mathilde Audry, Marion Dupuis, Monique Barel, Sarantis Korniotis, Simon Fillatreau, Lara Gales, Edern Cahoreau, Alain Charbit.

La fructose-1,6-bisphosphate aldolase (FBA) occupe une place centrale dans les voies de glycolyse / gluconéogenèse. FBA est également considéré comme une protéine « moonlight », avec plusieurs fonctions différentes dans plusieurs bactéries pathogènes, et une cible potentielle pour les études de développement de médicaments.

Le gène fba est non essentiel chez *Francisella* puisque son inactivation n'a eu qu'un impact mineur sur la croissance bactérienne, aussi bien en culture synthétique que dans les macrophages infectés, en présence de glucose ou d'autres substrats glycolytiques. En revanche, un mutant Δ*fba* a montré un défaut de croissance sévère lorsque des substrats gluconéogéniques ont été utilisés comme sources de carbone, indiquant que FBA contribue de manière préférentielle à la gluconéogenèse chez *Francisella*. La virulence du mutant Δ*fba* a également été sévèrement atténuée chez la souris, suggérant que la bactérie rencontre des concentrations limites de substrats glycolytiques in vivo. Des analyses métabolomiques des macrophages primaires ont révélé que l'infection bactérienne affectait de multiples métabolites de l'hôte et conduisait notamment à une réduction importante du glucose intracellulaire.

Des tests de stress bactérien ont révélé que l'inactivation de *fba* augmentait spécifiquement la résistance bactérienne au stress oxydatif. Les analyses protéomiques comparatives de la souche sauvage, du Δ*fba* et de la souche surproductrices ont permis l'identification de 26 protéines dont la quantité différait significativement entre les trois souches. Parmi ces protéines, nous avons retrouvé l'enzyme katG, une catalase impliquée dans la détoxification du stress oxydant dont la quantité était aumentées dans

le mutant. A l'inverse nous avons retrouvé aussi une des sous unités de l'ARN polymérase (RpoA2) dont les quantités sont diminuées dans le mutant.

Des analyses de qRT-PCR et de Co-Immunoprécipitation de la Chromatine (ChIP) ont révélé la liaison directe de FBA à la région promotrice des gènes katG et ropA2. Cette étude a ainsi dévoilé un nouveau rôle de FBA dans la régulation transcriptionnelle chez une bactérie pathogène et notamment en reliant le métabolisme à la régulation de l'homéostasie redox de la bactérie.

nature COMMUNICATIONS

ARTICLE

DOI: 10.1038/s41467-017-00889-7 OPEN

The metabolic enzyme fructose-1,6-bisphosphate aldolase acts as a transcriptional regulator in pathogenic *Francisella*

Jason Ziveri[1,2], Fabiola Tros[1,2], Ida Chiara Guerrera[1,3], Cerina Chhuon[1,3], Mathilde Audry[1,2], Marion Dupuis[1,2], Monique Barel[1,2], Sarantis Korniotis[1,4], Simon Fillatreau[1,4], Lara Gales[5], Edern Cahoreau[5] & Alain Charbit[1,2]

The enzyme fructose-bisphosphate aldolase occupies a central position in glycolysis and gluconeogenesis pathways. Beyond its housekeeping role in metabolism, fructose-bisphosphate aldolase has been involved in additional functions and is considered as a potential target for drug development against pathogenic bacteria. Here, we address the role of fructose-bisphosphate aldolase in the bacterial pathogen *Francisella novicida*. We demonstrate that fructose-bisphosphate aldolase is important for bacterial multiplication in macrophages in the presence of gluconeogenic substrates. In addition, we unravel a direct role of this metabolic enzyme in transcription regulation of genes *katG* and *rpoA*, encoding catalase and an RNA polymerase subunit, respectively. We propose a model in which fructose-bisphosphate aldolase participates in the control of host redox homeostasis and the inflammatory immune response.

[1] Université Paris Descartes, Sorbonne Paris Cité, Bâtiment Leriche, Paris 75993, France. [2] INSERM U1151 - CNRS UMR 8253, Institut Necker-Enfants Malades, Team 11: Pathogenesis of Systemic Infections, Paris 75993, France. [3] Plateforme Protéomique 3P5-Necker, Structure Fédérative de Recherche Necker and Université Paris Descartes, INSERM US24/CNRS UMS3633, Paris 75993, France. [4] INSERM U1151 - CNRS UMR 8253, Institut Necker-Enfants Malades, Team 16: Immunity in Health and Disease, Paris 75993, France. [5] Metatoul Platform, LISBP, Université de Toulouse, CNRS, INRA, INSA, Toulouse 31077, France. Correspondence and requests for materials should be addressed to A.C. (email: alain.charbit@inserm.fr)

Francisella tularensis is the causative agent of the zoonotic disease tularemia[1]. This Gram-negative facultative intracellular pathogen can infect humans by different means including direct contact with sick animals, inhalation, insect bites, or ingestion of contaminated water or food. *F. tularensis* is able to infect numerous cell types, including dendritic cells, neutrophils, macrophages as well as hepatocytes, or endothelial cells but is thought to replicate in vivo mainly in macrophages[2]. Four major subspecies of *F. tularensis* are currently listed: subsp *tularensis* (also designated Type A), subsp *holarctica* (also designated Type B), and *F. tularensis* subsp *novicida*[3]. These subspecies differ in virulence and geographical origin but all cause a fulminant disease in mice that is similar to tularemia in humans[4]. Although *F. novicida* is rarely pathogenic in humans, it is highly infectious in mice and its genome shares a high degree of nucleotide sequence conservation with the human pathogenic species. *F. novicida* is thus widely used as a model to study highly virulent subspecies[5–7].

Francisella virulence is tightly linked to its capacity to multiply in the cytosolic compartment of infected cells, and in particular of macrophages in vivo. The ability of *Francisella* to replicate within macrophages necessitates the coordinate control of three master transcription regulators, called MglA, SspA, and PigR[8, 9], which integrate the nutritional status of the pathogen to virulence gene expression in the host[10]. *Francisella* belongs to the limited group of intracellular bacteria, notably with *Listeria monocytogenes* and *Shigella flexneri*, that can gain access to -and proliferate within- the host cell cytosol[11]. Cytosolic bacterial multiplication often requires the utilization of multiple host-derived nutrients[12–15] and hexoses such as glucose are generally the preferred carbon and energy sources. In mammalian cells, glycolysis and the oxidative branch of the pentose-phosphate pathway occur in the cytosol, whereas the tricarboxylic acid (TCA) cycle, glutaminolysis, and β-oxidation take place in the mitochondria. In contrast, the anabolic reactions (gluconeogenesis and amino acid, nucleotide, and fatty acids biosynthesis) occur mainly in the cytosol. Hence, the bacterial enzymes responsible for glucose metabolism (catabolism and anabolism) are likely to play a key role in intracellular bacterial adaptation.

In the present study, we decided to address the role of the unique class II fructose-1,6-bisphosphate aldolase (FBA) of *Francisella*, a ubiquitous metabolic enzyme occupying a central position in glycolysis and gluconeogenesis pathways. Remarkably, FBA has been recently reported to play a role in the pathogenesis of two important human pathogens, highlighting the importance of metabolism in pathogenesis. In *M. tuberculosis*, FBA was shown to be required for growth in the acute phase and for survival in the chronic phase of mouse infections[16]. FBA was also shown to be essential for replication and virulence of the obligate intracellular parasite *Toxoplasma gondii*[17].

Two different classes of FBAs, with different catalytic mechanisms, have been described according to their amino acid sequences and designated Class I- and Class-II FBAs, respectively[18–20]. These aldolases have also been implicated in many "moonlighting" or non-catalytic functions, based upon their binding affinity for multiple other proteins, in both prokaryotic and eukaryotic organisms[21]. Class I FBAs are usually found in higher eukaryotic organisms (animals and plants). They utilize an active site lysine residue to stabilize a reaction intermediate via Schiff-base formation. Class I FBAs have been shown to interact with proteins displaying different functions predominantly involved in cellular structure, including notably F-actin, WASP, phospholipase D, and V-ATPase[22]. Class II FBAs are commonly found in bacteria, archae and lower eukaryotes, including fungi and some green algae. Some bacterial species, including *Escherichia coli*[23, 24], have been reported to express both types of the enzyme. Class II FBAs have been further subdivided into type A and type B[25] on the basis of the amino acid sequence. Of note, type A enzymes have been found mostly involved in glycolysis and gluconeogenesis, while diverse metabolic roles and substrate specificities have been reported for type B aldolases[21].

Several attempts to disrupt the Class II fructose biphosphate aldolase genes from different bacterial species, including *Escherichia coli*, *Bacillus subtilis*, and *Pseudomonas aeruginosa*, have been unsuccessful, thereby suggesting that the Class II FBP aldolases were essential for the viability of these organisms. In *M. tuberculosis*, FBA was indeed demonstrated to be essential[16, 26].

Here we show that the gene *fba* is dispensable for *Francisella* survival and growth under defined conditions, and appears to play a regulatory role in pathogenesis. This enzyme appears to lie at the crossroad between carbon metabolism and the control of host redox homeostasis.

Results

Metabolomics reveal high glucose consumption in infected BMMs. To assess the impact of bacterial infection and multiplication on the metabolism of infected macrophages, we first analyzed the metabolome of mouse bone marrow-derived macrophages (BMMs) and compared the concentration of a series of metabolites recorded in non-infected (NI) cells to those recorded in infected cells. We used for infection, either wild-type (WT) *F. novicida* (WT) or a *F. novicida* mutant with a deletion of the entire *Francisella* pathogenicity Island (designated Δ*FPI* mutant strain[27] unable to escape from phagosomes and, hence, to grow in macrophages. Values were recorded 1 and 24 h after infection (Fig. 1a). We analyzed, in parallel, the corresponding exometabolomes of these cells to get further insight into metabolite exchanges (consumption/production) between cells and medium (Fig. 1b).

The quantitative metabolomics analysis of intracellular metabolites was performed by ion chromatography and tandem mass spectrometry (IC-MS/MS)[28]. This approach allowed us to quantify central and intermediary metabolites from a number of metabolic pathways occurring in BMMs (i.e., glycolysis/gluconeogenesis, pentose-phosphate pathway, TCA cycle, nucleotides biosynthesis, and activated sugars biosynthesis). Whereas at 1 h, overall only minor modifications were observed (Supplementary Fig. 2A), at 24 h, infection affected the central metabolite pools (Fig. 1 and Supplementary Fig. 2B). Remarkably, the concentrations of Glucose-6P, Glycerol-3P and P5P were higher in BMMs infected with WT *F. novicida* than the other two conditions (NI cells or cells infected with the Δ*FPI* mutant), suggesting that cytosolic multiplication of WT *F. novicida* could be responsible for their increased intracellular concentration (Fig. 1). Of note, a reduction of all the quantified metabolites of the TCA and of most of the metabolites from the Glycolysis/Gluconeogenesis pathways was recorded with both the WT and the Δ*FPI* mutant (Fig. 1). The intracellular concentrations of fructose-1,6P, PEP, 2PG, and 3PG were also decreased, in both WT- and Δ*FPI*-infected BMMs, suggesting that the infection itself was sufficient to trigger these changes. Concomitantly, the concentrations of UDP-glucose and pentose-5P both increased in BMMs infected with WT *F. novicida*.

Of note, the changes observed in macrophages infected by *Francisella* may not strictly reflect the adaptation of the host cell metabolism and might correspond to the combined activity of bacterial and host metabolisms. However, the bacterial contribution to the metabolome should be -if not marginal- at least minor since: (i) approximately only 10% of macrophages cells are generally infected, in the infection conditions used; (ii) each infected cell generally do not contain more than a hundred

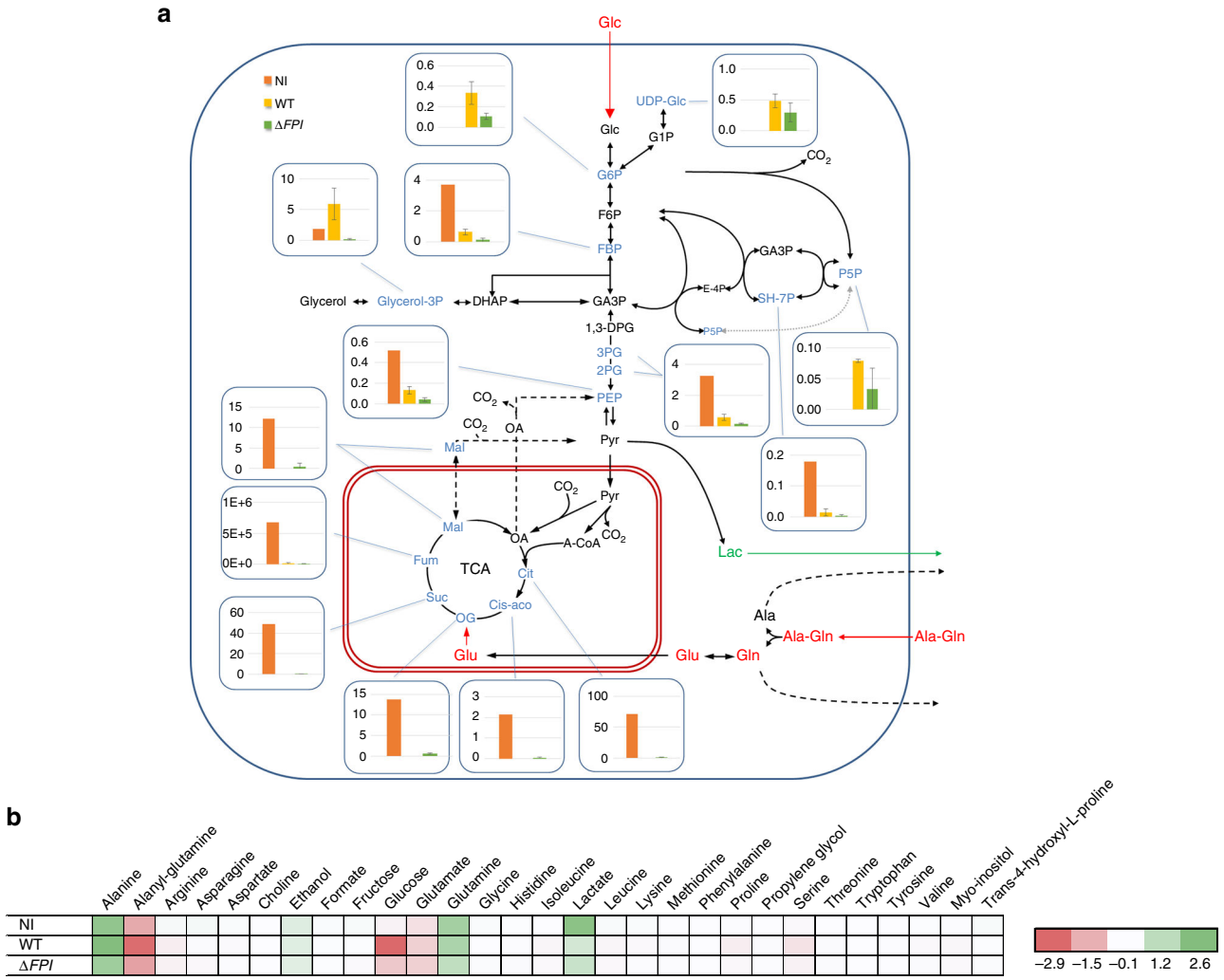

Fig. 1 Carbon isotopologue distribution of central metabolites in BMMs. **a** Absolute concentrations of central metabolites in intracellular cell extracts (in μmol L^{-1}) after 24 h of cultivation of BMM macrophages: NI ($n = 1$); or infected either with wild-type *F. novicida* (WT) ($n = 3$) or Δ*FPI* (ΔFPI) strain ($n = 3$). Fumarate measurements (Fum) represent MS peak area instead of absolute concentrations. **b** Consumed and produced metabolites, measured in extracellular media in the different infection conditions, profiled by NMR. Mean concentration changes, presented here by substracting concentration measured at 24 h to those measured at 1 h. Absolute concentrations changes are expressed in mM. *Positive/green values* correspond to metabolites accumulated in the media, *negative/red values* correspond to metabolites consumed by cells from the media between 1 and 24 h of incubation. Analyses were performed on biological triplicates and each sample was run in technical triplicates (mean and SD of metabolite concentrations were calculated using R 3.2.3, R Foundation for Statistical Computing, Vienna, Austria. URL http://www.R-project.org/)

bacteria; and (iii) the average volume of a bacterial cell is much lower than that of a macrophage, in the range of $1–2 \times 10^{-12}$ cm^3 per bacterium or $1–4 \times 10^{-9}$ cm^3 per macrophage cell[29]. Thus, it is reasonable to assume that the amount of metabolites contained in bacterial cells, in the samples analyzed, do not significantly contribute to the overall amounts measured.

We next performed the quantitative metabolomics analysis of the cell culture supernatants by nuclear magnetic resonance (NMR) to follow the evolution of the exometabolome during growth. This allowed us, by subtraction of concentrations measured at 24 and 1 h, to gain information on the substrates that were consumed from the medium and/or produced by the cells. The main substrates consumed in NI macrophages were alanyl-glutamine, glutamate, and glucose. In infected cells, the same substrates seemed to be consumed but a clear increase of glucose consumption was observed, especially for WT *F. novicida*. The main metabolites which accumulated in the media were alanine, glutamine, and lactate, in NI as well as in infected cells (Fig. 1b).

The metabolic modifications recorded in infected macrophages, and especially the glucose consumption, highlighted the importance of metabolic adaptation of *Francisella* for its intracellular survival and multiplication. We focused here on the role of the FBA in *Francisella* pathogenesis. This central enzyme of glycolysis and gluconeogenesis pathways (Supplementary Fig. 1) is at the crossroad of several other metabolic pathways that involve metabolites derived from glycolysis.

FBA is required for growth on gluconeogenic substrates. The FBA protein of *F. novicida* (FTN_1329) shows 99.2–99.4% amino acid sequence identity with its orthologues in other *F. tularensis* subspecies (Supplementary Fig. 3). FBA is also highly conserved in multiple other bacterial pathogens. For example, it shares 81.6% identity with *Pseudomonas aerugionosa* (PAO555) FBA, one of its closest homologs, and 74.3% with *Neisseria meningitidis* (NMA0587) FBA. However, it has only modest homology with FBAs of *Mycobacterium tuberculosis* (TBMG_00367) and *E. coli*

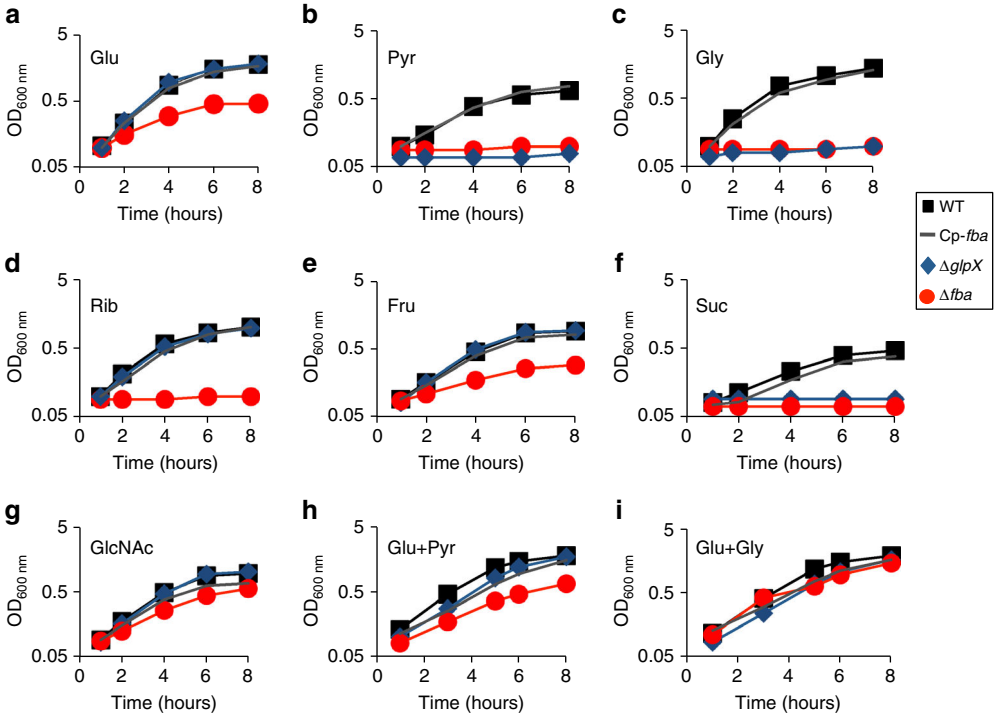

Fig. 2 FBA inactivation inhibits growth of *Francisella* in the presence of various carbon sources. Wild-type *F. novicida* (WT, close *black squares*), isogenic Δ*fba* mutant (Δ*fba*, *red circles*), and complemented *fba* strain (Δ*fba* Cp-*fba*, *gray line*), and isogenic Δ*glpX* mutant (Δ*glpX*, *blue diamond*), were grown in chemically defined medium (CDM) lacking glucose and supplemented with different carbon source at a final concentration of 25 mM. **a** Glucose (Glc); **b** Pyruvate (Pyr); **c** Glycerol (Gly); **d** Ribose (Rib); **e** Fructose (Fru); **f** Succinate (Suc); **g** N-Acetylglucosamine (GlcNAc); **h** Glucose + Pyruvate (Glc + Pyr); **i** Glucose + Glycerol (Glc + Gly)

K12 (eco: b2925), with 27 and 25.6% amino acid identity, respectively. The FBA protein sequence does not contain any secretion-export signal and is predicted to be cytosolic. The *Francisella* proteins possess two signature motifs of FBA II according to Prosite database (PS00602 and PS00806) and bear a conserved C-terminal lysine like the FBA of *N. meningitidis*, suggesting that they are genuine IIB FBA (Supplementary Fig. 3).

We constructed an isogenic deletion mutant of *fba* in *F. novicida* by allelic replacement (Methods section) and first evaluated the impact of *fba* inactivation on bacterial growth in chemically defined medium (CDM[30], supplemented with various carbohydrates (Fig. 2). We included in these assays a Δ*glpX* mutant[31] lacking the strickly gluconeogenic enzyme fructose biphosphatase (FBPase; Supplementary Fig. 1). The Δ*fba* mutant (like the Δ*glpX* mutant) was unable to grow in media supplemented with gluconeogenic substrates such as pyruvate, glycerol, or succinate, a metabolite of the TCA cycle. In contrast, the Δ*fba* mutant showed only moderate growth defect in the presence of the glycolytic substrates glucose and fructose, as well as in the presence of N-acetylglucosamine (an amino sugar used for the synthesis of cell surface structures and entering the glycolytic pathway after its conversion into fructose-6P). WT growth was restored in the presence of both glucose and glycerol, confirming that FBA is required for growth of *F. novicida* in culture, mainly when gluconeogenic substrates are used as carbon sources.

It is likely that glycolytic substrates can use alternate route in the Δ*fba* mutant, and in particular the pentose-phosphate pathway (PPP). Indeed, we have recently demonstrated, using ^{13}C-labeled glucose, the recycling of carbons through the PPP in WT *F. novicida*. In contrast, when ^{13}C-labeled pyruvate was used, compounds of the PPP were not detected[31].

Of note, whereas the Δ*fba* mutant was unable to grow on ribose (a product of the PPP), the Δ*glpX* mutant showed WT growth on this sugar. WT growth was always restored in the Δ*fba*-complemented strain, confirming quantitative reverse transcription PCR (qRT-PCR) analyses, which demonstrated the absence of polar effect of the mutation (Supplementary Fig. 4). Since ribose cannot be converted into glucose-6P because the oxidative branch of the PPP is irreversible, FBA seems to be the only way for ribose to feed gluconeogenesis.

***fba* inactivation impairs virulence**. We next evaluated the impact of *fba* inactivation in vitro, on intracellular multiplication; and in vivo, on virulence in the mouse model. The ability of wild-type *F. novicida* (WT) and Δ*fba* strains to survive and multiply in murine macrophage-like J774.1 cells was determined in cell culture medium supplemented either with glucose or glycerol or supplemented with both glucose and glycerol (Fig. 3a–c). We used a Δ*FPI* mutant strain as a negative control. In standard Dulbecco's modified eagle's medium (DMEM; i.e, supplemented with glucose), the intracellular multiplication of the Δ*fba* mutant was moderately affected (8–10-fold reduction of bacterial counts at 10 and 24 h, as compared to WT; Fig. 3a). In contrast, when glucose was substituted by glycerol, multiplication of the Δ*fba* mutant was severely impaired (Fig. 3b). The Δ*fba* mutant already showed a 10-fold reduction of intracellular bacteria compared to cells infected with the WT strain at 10 h; and a 1000-fold reduction of bacterial counts were recorded at 24 h (comparable to the Δ*FPI* mutant). Remarkably, when the medium was simultaneously supplemented with glucose and glycerol, the Δ*fba* mutant multiplied like the WT strain (Fig. 3c). Functional complementation (i.e, introduction of a plasmid-born WT *fba* allele into the Δ*fba* mutant strain) always restored WT growth.

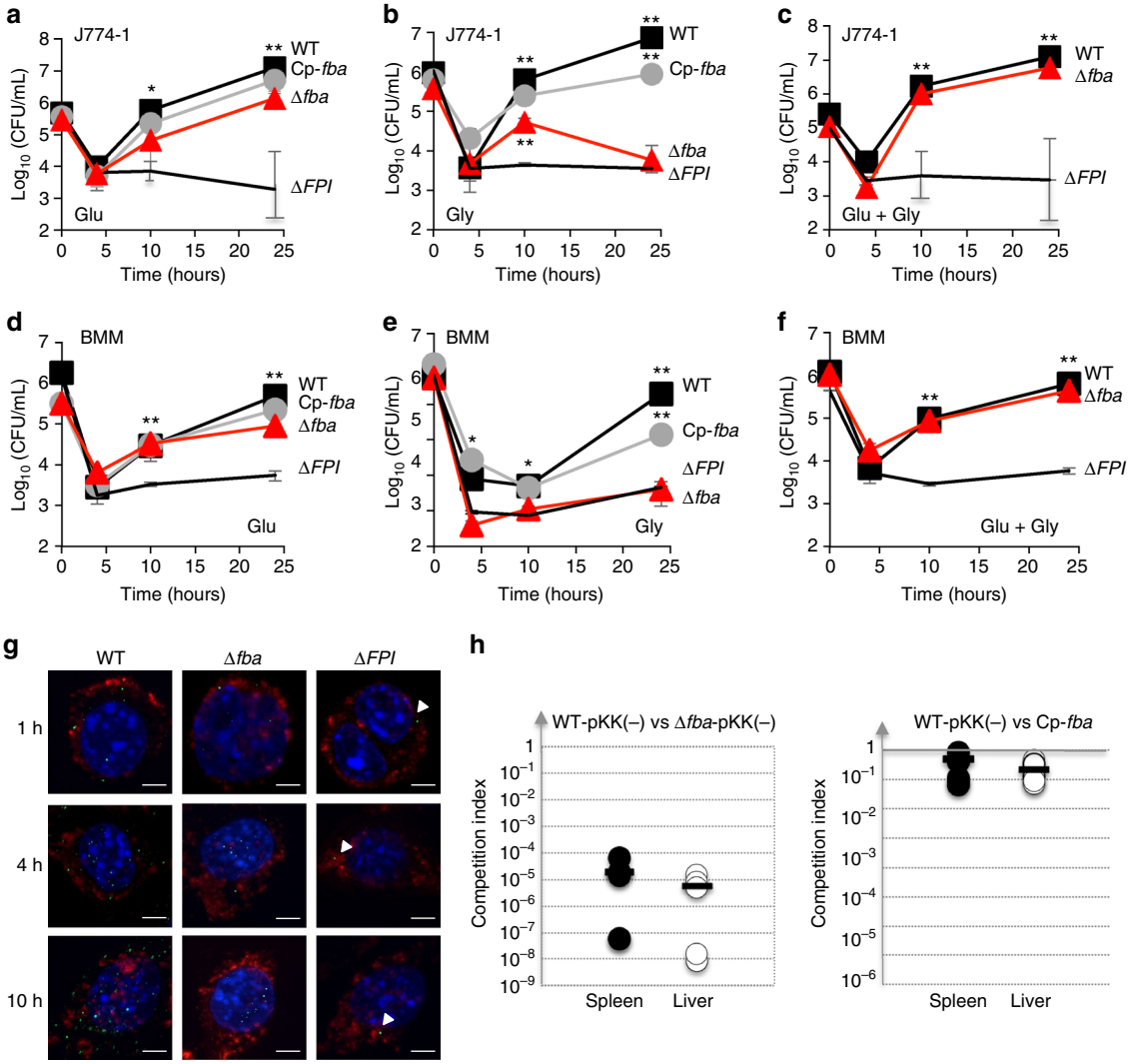

Fig. 3 *fba* inactivation affects intracellular survival. Intracellular bacterial multiplication of wild-type *F. novicida* (WT, *black squares*), isogenic Δ*fba* mutant (Δ*FBA*, *red triangles*), and complemented Δ*fba* strain (Cp-*fba*, *gray circles*), and the Δ*FPI* negative control (*black lines*), was monitored during 24 h in J774A.1 macrophage cells and bone marrow-derived macrophages (BMM) from 6 to 8-week-old female BALB/c mice. DMEM (Dulbecco's modified eagle medium) was supplemented either with glucose **a**, **d**, glycerol **b**, **e**, or an equimolar concentration of glucose and glycerol **c**, **f**. **a**–**f** mean and SD of triplicate wells are shown. Each sugar was added to the cell culture medium at a final concentration of 5 mM. $*p < 0.01$; $**p < 0.001$ (determined by two-tailed unpaired Student's *t*-test). **g** Glycerol-grown J774.1 were infected for 30 min with wild-type *F. novicida* (WT), Δ*fba*, or Δ*FPI* strains and their co-localization with the phagosomal marker LAMP-1 was observed by confocal microscopy 1, 4, and 10 h, after beginning of the experiment. *Scale bars* at the *bottom right* of each panel correspond to 5 µM. J774.1 were stained for *F. tularensis* (*green*), LAMP-1 (*red*), and host DNA (*blue*, DAPI stained). **h** Group of five BALB/c mice were infected intraperitoneally with 100 CFU of wild-type *F. novicida* and 100 CFU of Δ*fba* mutant strain. Bacterial burden was realized in liver (*open circles*, *right column*) and spleen (*black circles*, *left column*) of mice. The data represent the competitive index (CI) value (in ordinate) for CFU of mutant/wild-type of each mouse, after 48 h infection, divided by CFU of mutant/wild-type in the inoculum. *Bars* represent the geometric mean CI value

The intracellular behavior of the Δ*fba* mutant was also tested in BMMs from BALB/c mice. Comforting the observations in J774-1 cells, growth of the Δ*fba* mutant was identical to that of the WT at 10 h and only slightly impaired (fivefold less bacterial counts) at 24 h (Fig. 3d) when BMMs were supplemented with glucose. In contrast, intracellular multiplication of the Δ*fba* mutant was severely impaired (Fig. 3e) when the culture medium was supplemented with glycerol. In medium supplemented with both glucose and glycerol, the multiplication defect of the Δ*fba* mutant was completely eliminated (Fig. 3f). Functional complementation restored normal intracellular bacterial replication in both cell types, in the presence of glucose. In the presence glycerol, complementation was fully restored up to 10 h and only partially at 24 h. Altogether these assays demonstrate that the Δ*fba* mutant is unable to multiply intracellularly when gluconeogenic substrates are used as carbon sources (Figs. 2–3). In contrast, when glycolytic substrates are used, the growth defect of the Δ*fba* mutant is essentially suppressed.

We confirmed that the presence of the empty vector (pKK214) in WT and Δ*fba* mutant strains used in these experiments had no impact on the phenotypes observed (Supplementary Fig. 5).

Interestingly, it has been recently shown that macrophages stimulated with the PPARβ/∂ agonist GW0742 increased their intracellular concentration of glucose[32]. This prompted us to test whether the addition of GW0742 to cell culture medium would result in increased intracellular bacterial multiplication of the Δ*fba* mutant. Addition of GW0742 had no visible effect on the multiplication of the Δ*fba* mutant in glycerol-grown J774-1 cells, during the first 10 h. However, a 15-fold increase in the number of intracellular Δ*fba* mutant bacteria was recorded at 24 h,

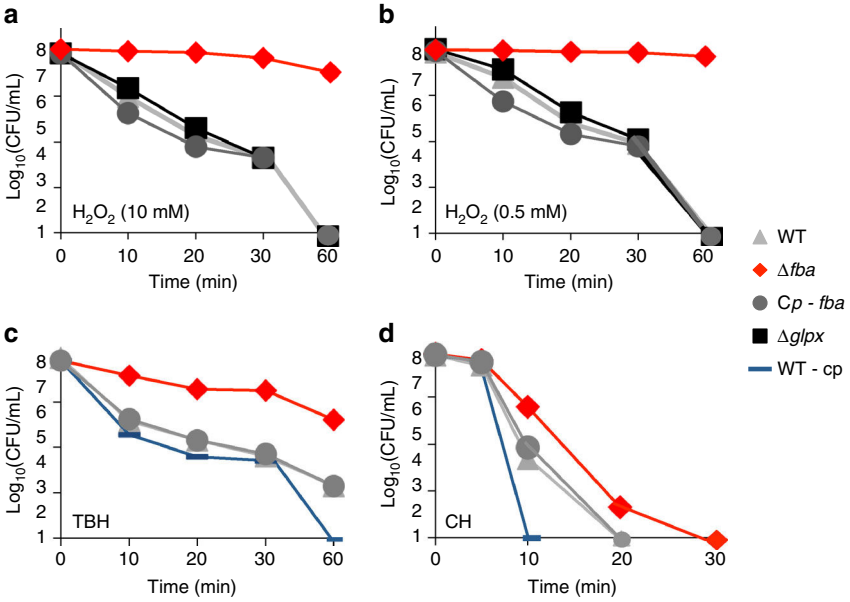

Fig. 4 Oxidative stress survival. After an overnight culture in CDM supplemented with glucose and glycerol, bacteria were diluted in PBS and were subjected to oxidative stress **a** 10 mM H_2O_2, **b** 500 µM H_2O_2, **c** Tert-butyl hydroperoxide 10 mM (TBH), and **d** Cumene hydroperoxide 10 mM (CH). Bacteria were plated on chocolate agar plates at different time points and viable bacteria were numerated 2 days after. Experiments were realized three times

compatible with a GW0742-dependent stimulation of glucose production by these cells (Supplementary Fig. 6).

In order to determine whether the multiplication defect of the Δ*fba* mutant could be due to impaired phagosomal escape, we used confocal immunofluorescence microscopy. J774.1 macrophages were infected with either WT *F. novicida* or Δ*fba* mutant strain (the isogenic Δ*FPI* mutant was used as a negative control). Bacteria and the late phagosomal marker LAMP-1 were labeled with specific antibodies and their co-localization was monitored at three time points (1, 4, and 10 h). In glycerol-supplemented cells (Fig. 3g, Supplementary Fig. 7A), after 1 h, most of Δ*fba* mutant bacteria no were no longer associated with LAMP-1 (~13 and 21% of co-localization recorded with WT *F. novicida* and Δ*fba* mutant, respectively) and co-localization of the Δ*fba* mutant remained low after 4 h (~14%) and after 10 h (~15%). In glucose-grown cells (Supplementary Fig. 7B), after 1 h of infection, only 14 and 22% of co-localization was recorded with WT *F. novicida* and Δ*fba* mutant, respectively, indicating that the Δ*fba* mutant was able to escape phagosomes as fast as WT *F. novicida*. Co-localization of the Δ*fba* mutant remained still very low after 4 h (~10%) and after 10 h (~12%). In contrast, the Δ*FPI* mutant strain remained trapped into phagosomes, as illustrated by high co-localization with LAMP-1 at all time points tested (80, 85, and 88%, after 1, 4, and 10 h, respectively). Altogether, these results indicate that the intracellular growth defect of the Δ*fba* mutant, observed in glycerol-grown conditions, was not due to altered phagosomal escape but to impaired cytosolic multiplication.

Finally, to estimate the impact of *fba* inactivation on bacterial virulence, we performed an in vivo competition assay between WT and Δ*fba* mutant bacteria, in 7-week-old female BALB/c mice and monitored the bacterial burden in spleen and livers 2.5 days after infection by the ip route (Fig. 3h). The competition index recorded for the Δ*fba* mutant was very low in both target organs (between 10^{-3} and 10^{-4}), demonstrating the importance of FBA in *Francisella* virulence in the mouse model.

***fba* inactivation increases resistance to oxidative stress**. Upon entry into cells, *Francisella* transiently resides in a phagosomal compartment that acquires bactericidal reactive oxygen species (ROS). We therefore examined the ability of WT *F. novicida* and Δ*fba* mutant strains to survive under oxidative stress conditions. We included in these assays a Δ*glpX* mutant as a control to evaluate the contribution of gluconeogenesis to oxidative stress. Bacteria were first grown in CDM supplemented with glucose + glycerol and then exposed to either to H_2O_2 (Fig. 4a, b), the organic hydroperoxides tert-butyl hydroperoxide (TBH, 10 mM) or cumene hydroperoxide (CH, 10 mM) (Fig. 4c, d) for 1 h. In the two H_2O_2 conditions tested (10 or 0.5 mM), the viability of both WT, Δ*glpX* and Δ*fba*-complemented strains was equally affected and behaved like the WT strain (Fig. 4a, b). In contrast, the Δ*fba* mutant was systematically more resistant to these stresses than the other strains. Indeed, after 30 min of exposure to H_2O_2, the viability of the Δ*fba* mutant was essentially unaffected whereas that of the other strains showed a 4 logs decrease in the number of viable bacteria. The Δ*fba* mutant showed also a greater resistance to organic hydroperoxides (CH and TBH), especially to TBH compared to WT. Of note, the FBA overproducing strain (WT strain bearing a plasmid carrying the WT *fba* gene) showed greater susceptibility to TBH and CH than WT. The fact that the Δ*glpX* mutant was as susceptible to oxidative stress as the WT strain was indicative of a role of FBA in oxidative stress resistance beyond its role in gluconeogenesis. We next examined the resistance of the mutant to other stresses: acidic, SDS, or upon incubation in the presence of 10% human serum. Under all the conditions tested, the viability of Δ*fba* mutant strain was undistinguishable from that of the parental strain (Supplementary Fig. 8).

The bactericidal activity of macrophages, and notably ROS production, is increased in the presence of IFNγ[33]. We therefore tested the intracellular multiplication of the Δ*fba* mutant compared to WT bacteria, in IFNγ-stimulated J774.1 macrophages. The Δ*fba* mutant showed improved survival and/or intracellular multiplication in the presence of IFNγ compared to WT (up to 20-fold increase in bacterial counts after 24 h), supporting the notion that *fba* inactivation confers to *Francisella*

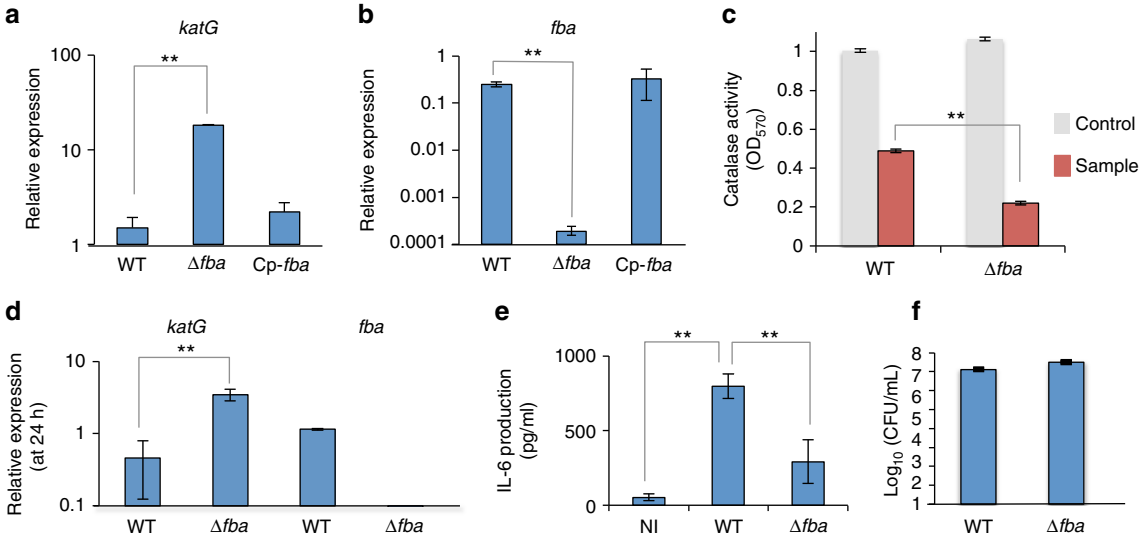

Fig. 5 Quantitative real-time RT-PCR analysis. **a**, **b** Bacteria were grown overnight in TSB and qRT-PCR analyses were performed on selected genes, **a** *katG* gene or **b** *fba* gene in wild-type *F. novicida*, Δ*fba* mutant, and *fba*-complemented (Cp-*fba*) strains. For each gene, the transcripts were normalized to helicase rates (*FTN_1594*). **c** Catalase activity assay was realized at 570 nm, using the Catalase Assay Kit (ab83464; Abcam). The assay was performed according to manufacturer's recommendation. Each assay was performed on two independent protein lysates. The average of $OD_{570} \pm SD$ was recorded for wild-type *F. novicida* and the Δ*fba* mutant. The catalase activity recorded in the Δ*fba* mutant was significantly lower than that recorded in the wild-type strain (**$p <$ 0.01). **d** J774.1 cells were infected for 24 h with wild-type *F. novicida* (*WT*) and Δ*fba* mutant. Total RNA was analyzed by quantitative RT-PCR with *katG* and *fba* gene. For each gene, the transcripts were normalized to helicase rates (*FTN_1594*) (**$p < 0.01$). **e** J774.1 cells were infected for 24 h with wild-type *F. novicida* (*WT*) and Δ*fba* mutant in DMEM supplemented with glucose and glycerol (25 mM). The supernatants were analyzed by ELISA to detect the amounts of IL-6 produced at 24 h in pg mL^{-1}. **f** Intracellular bacterial multiplication of wild-type *F. novicida* (WT) and Δ*fba* mutant was determined at 24 h, in the infected J774.1 cells used for the IL-6 dosage, as a control. (**$p < 0.01$). **a**–**c** mean and SD of three independent experiments are shown; **d**–**f** each assay was repeated at least three times. Mean and SD of three wells of one typical experiment are shown. *p*-values were determined by the two-tailed unpaired Student's *t*-test

an increased resistance to the ROS stress induced upon IFNγ treatment (Supplementary Fig. 9).

A role for FBA in transcription. The apparent specific impact of *fba* inactivation on oxidative stress resistance prompted us to first test the expression of the unique gene, *katG*, encoding the catalase responsible for the detoxification of H_2O_2 into H_2O and O_2. The transcription of *katG* was quantified in WT and Δ*fba* mutant strains, in broth as well as in infected macrophages (Fig. 5). qRT-PCR analyses revealed that *fba* inactivation provoked a 12-fold increase of *katG* gene transcription in tryptic soya broth (TSB) (Fig. 5a) and complete inactivation of *fba* in the Δ*fba* mutant was confirmed (Fig. 5b). Catalase activity was also measured in whole-cell lysates from bacteria grown in the same TSB medium (Fig. 5c). Supporting the qRT-PCR data, increased catalase activity (twofold) was recorded in the Δ*fba* mutant compared to WT. We next quantified, by qRT-PCR, *katG* expression in infected J774-1 macrophages. We found that *fba* inactivation induced a sevenfold increase of *katG* transcription (Fig. 5d). As expected, we did not detect any *fba* transcript in macrophages infected with the Δ*fba* mutant.

It has been shown that a Δ*katG* mutant of *Francisella* provoked the rapid cytosolic accumulation of H_2O_2, triggering an inflammatory reaction via Ca^{2+} signaling[34–36]. This *katG*-dependent control on the available intracellular H_2O_2 pool was proposed to control the production of pro-inflammatory cytokine and increased IL-6 production. We therefore thought to monitor the amount of IL-6 secreted in the supernatant of J774-1 macrophages, infected either with WT or with the Δ*fba* mutant (Fig. 5e). Supernatant from NI cells was used as negative control. As expected, IL-6 secretion, measured by ELISA[37], was significantly higher in the supernatant of WT-infected cells compared to NI cells. Remarkably, IL-6 secretion was also significantly higher in the supernatant of WT-infected cells than in the supernatant of Δ*fba*-infected cells.

Intracellular bacterial counts, performed on the same cells as controls (Fig. 5f), confirmed that comparable numbers of intracellular bacteria were present in WT and Δ*fba* mutant at 24 h. These data are in agreement with a direct correlation between FBA-mediated *katG* repression and increased inflammatory response.

We next compared the amount of ROS in WT-infected cells to that in Δ*fba*-infected cells, 10 and 24 h after infection. For this, we used the 2′,7′-dichlorofluorescin diacetate (DCFDA) Cellular ROS Detection Assay Kit (Abcam, Cambridge, UK). The ROS content was ~20% lower with the Δ*fba* mutant compared to WT, at both time points (Supplementary Fig. 10A). As positive control, NI cells were stimulated with 5 μg mL^{-1} of lipopolysaccharide from E. coli K12 (LPS-EK) Standard. LPS stimulation provoked an increase of ROS production that was up to 1.5-fold higher than that in WT-infected cells, at both time points tested. DCFDA levels were also visualized using fluorescence microscopy. The percentage of fluorescent cells was significantly higher in WT-infected cells (33%) or LPS-stimulated NI cells (63.5%) than in Δ*fba*-infected cells (8.5%) (Supplementary Fig. 10B). Altogether, these assays further supported a direct correlation between the FBA⁻mediated repression of KatG expression and cellular ROS production.

These data led us to hypothesize that FBA functions might extend beyond metabolic functions. To check whether *fba* inactivation could have a broader impact on protein expression than solely affecting KatG expression, we next performed a whole-cell comparative nanoLC-MS/MS proteomic analysis of WT, Δ*fba*, and FBA-overproducing (WT-cp), strains.

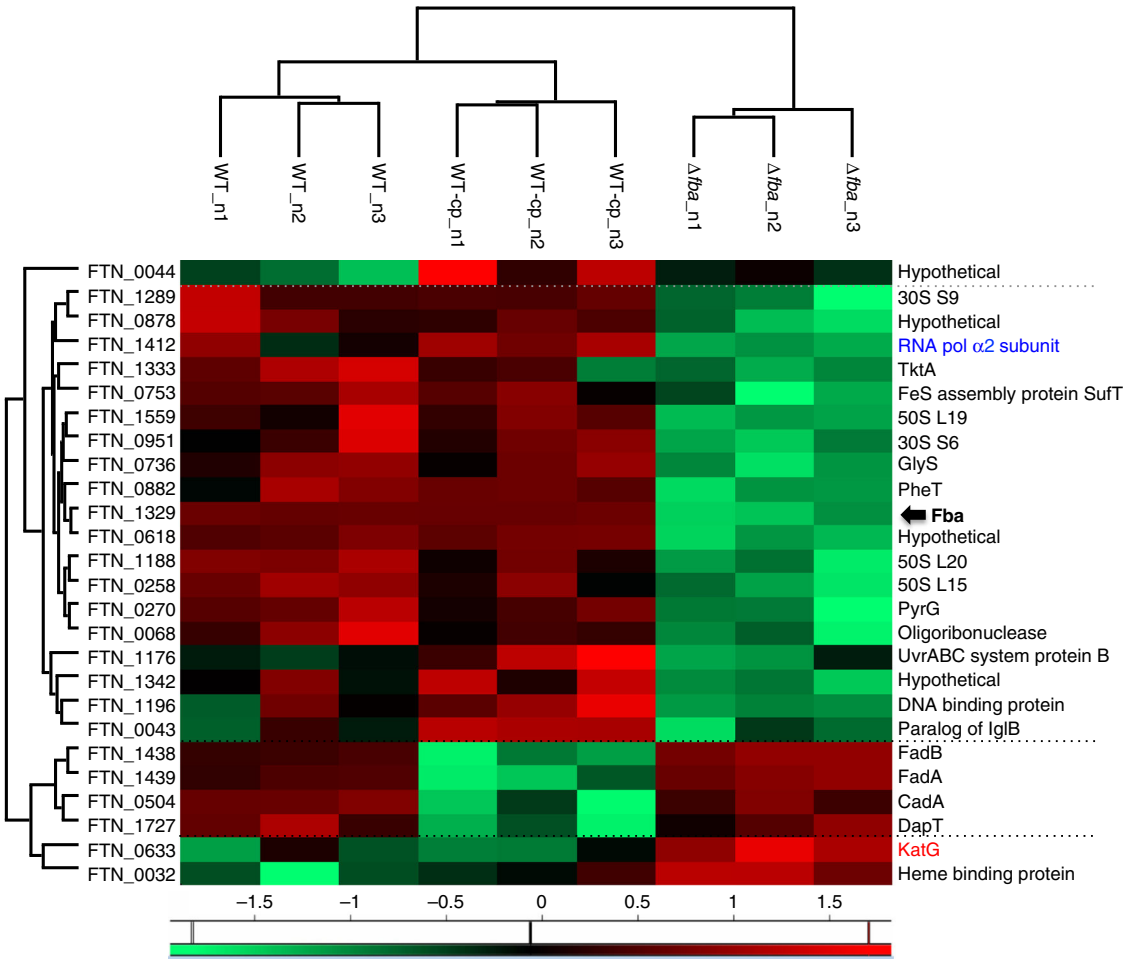

Fig. 6 Biclustering and heat map of differential proteins. Heat map and biclustering were obtained by comparing the 26 differentially expressed proteins identified from label-free MS analysis of WT, Δ*fba*, and WT-complemented (WT-Cp) strains. To the *left*, FTN protein numbers; to the *right*, corresponding predicted functions. FBA, *in bold*, is indicated by a *black arrow*; RNA polymerase α2 subunit (down-regulated in Δ*fba*) is highlighted in *blue*, and KatG (up-regulated in Δ*fba*) in *red*

We could identify 1372 proteins across the 9 samples analyzed, which represent 80% of the predicted *F. tularensis* proteome. For statistical analysis, we kept 1154 proteins robustly quantified (data are available via ProteomeXchange with identifier PXD006908). An ANOVA test identified 26 proteins whose amount significantly differed between the three strains. Of note, most of them were conserved in the subspecies *holarctica* and *tularensis*. These 26 proteins were submitted to biclustering analysis and represented in the heatmap (Fig. 6). The column tree revealed that the protein profiles of the WT and the WT-cp strains were different from the Δ*fba* mutant.

Two opposite patterns could be distinguished: (i) a group of 19 proteins were expressed in lower amount only in the Δ*fba* mutant strain, suggesting that they are (directly or indirectly) positively regulated by FBA; and (ii) two proteins were in higher amount only in the Δ*fba* mutant strain, suggesting that they are (directly or indirectly) negatively regulated by FBA. The largest group of proteins under-represented or absent in the proteome of the Δ*fba* mutant strain comprised (in addition to FBA itself) proteins belonging to various functional categories, such as ribosomal proteins, a putative DNA binding protein and RpoA2, one of the two α subunits of RNA polymerase. Remarkably, fully supporting the transcriptional data, the catalase KatG was one of the two proteins expressed in higher amounts only in the Δ*fba* mutant strain (together with a putative Heme binding protein). Of note, the only down-regulated proteins in the FBA overproducing strain comprised two proteins of the same operon (FadA and FadB) involved in fatty acid degradation, and two proteins linked to lysine metabolism. The fact that these pathways might also be affected by the over-production of FBA, suggest that FBA functions might extend beyond the proteins analyzed in this study.

In order to directly probe a role of FBA in transcription regulation, we constructed a His-tagged version of FBA, by fusing the His tag to its C-terminus (FBA-HA). The FBA-HA protein expressed in Δ*fba* was used to detect the in vivo binding of FBA to the promoters of genes corresponding to proteins whose expression varied over twofold in the proteomic comparison between WT and Δ*fba* mutant strains (Fig. 7). We performed chromatin immunoprecipitation (ChIP) followed by qRT-PCR analysis on two sets of genes: (i) two genes corresponding to proteins expressed in higher amounts in the Δ*fba* mutant (*katG* and *hemeBP*); and (ii) three genes corresponding to proteins expressed in lower amounts in the Δ*fba* mutant (*rpoA*, *uvrB*, and *fadA*) (Fig. 7a). We observed a nearly 30-fold enrichment of the *katG* promoter region and a fivefold enrichment of *hemeBP* promoter region. A nearly 10-fold enrichment of the *rpoA* promoter region was observed but no–or only very modest–enrichment was observed with the two other promoter regions (i.e., *uvrB* and *fadA*) (Fig. 7a). Transcription *of rpoA* was also significantly higher in the WT (>80-fold) and *fba*-complemented strains compared to the Δ*fba* mutant, suggesting

a direct role of FBA on *rpoA* transcription activation (Supplementary Fig. 11).

Transcription of seven additional genes, corresponding to proteins positively controlled by FBA, was also tested by qRT-PCR. Corroborating the proteomic analyses, transcription of these genes was higher in the WT and *fba*-complemented strains than in the Δ*fba* mutant. In particular, transcription of four of them (*pyrG*, *30S S9*, *glyS*, and *pheT*) was 50-fold to 200-fold higher in the WT strain than in the Δ*fba* mutant (Supplementary Fig. 11). We also monitored qRT-PCR, *katG* and *rpoA* gene expression in a Δ*glpX* mutant compared to WT *F. novicida*. Comparable expression of these two genes was recorded in the two strains, confirming that GlpX was not involved in their transcriptional control (Supplementary Fig. 11).

Electrophoretic mobility shift assays (EMSAs) were then performed to confirm direct binding of FBA to *katG* and *rpoA* promoter regions (Fig. 7b). For this, DIG-labeled double-stranded DNA fragments, corresponding to the regions immediately preceding each coding sequence (designated p*KatG* and p*rpoA*, respectively) were incubated in the presence of purified his-tagged FBA (FBA-HA) recombinant protein. With p*KatG*, a single band was detected with the labeled probe alone. Upon incubation with FBA-HA, a fraction of the probe was shifted and this shift was almost completely suppressed when a 125-fold excess of competing unlabeled specific p*KatG* oligonucleotide was added to the reaction (in addition to the labeled specific probe). With p*rpoA*, two bands were detected with the labeled probe alone, possibly corresponding to different conformations of the probe. A major shifted additional band was detected upon incubation with FBA-HA as well as faint upper bands. The shifted bands disappeared when a 125-fold excess of competing unlabeled specific oligonucleotide was added to the reaction (Fig. 7b).

Finally, transcriptional p*katG-lacZ* and p*rpoA-lacZ* fusion were constructed and expressed in WT *F. novicida* or in Δ*fba* isogenic mutant strain (Fig. 7c). As expected, the β-galactosidase activity recorded with the p*katG-lacZ* construct was 3.5-fold higher in the Δ*fba* mutant background compared to WT. Conversely, the β-galactosidase activity recorded with the p*rpoA-lacZ* construct was 2.2-fold lower in the Δfba mutant background compared to WT.

Altogether, these assays confirmed the specificity of the interaction between FBA and *katG*, and *rpoA* promoter regions and supported that FBA specifically binds to different promoter regions, contributing either to transcriptional activation or repression.

Discussion

Recent studies have shown that amino acids are likely to represent major carbon sources for intracellular *Francisella* and serve as gluconeogenic substrates[31, 38–44]. We show here that FBA is not involved in phagosomal escape but is critical for cytosolic multiplication in the presence of gluconeogenic substrates. Our metabolomics analysis performed on BMMs revealed that the infection by *Francisella* triggered numerous variations of intracellular metabolites, translating a complex metabolic response of the host to infection. Remarkably, a strong reduction of glucose present in the cell culture supernatant, with a concomitant increase of intracellular glucose-6P, was recorded after 24 h in infected BMMs, reflecting an increase of glucose consumption by

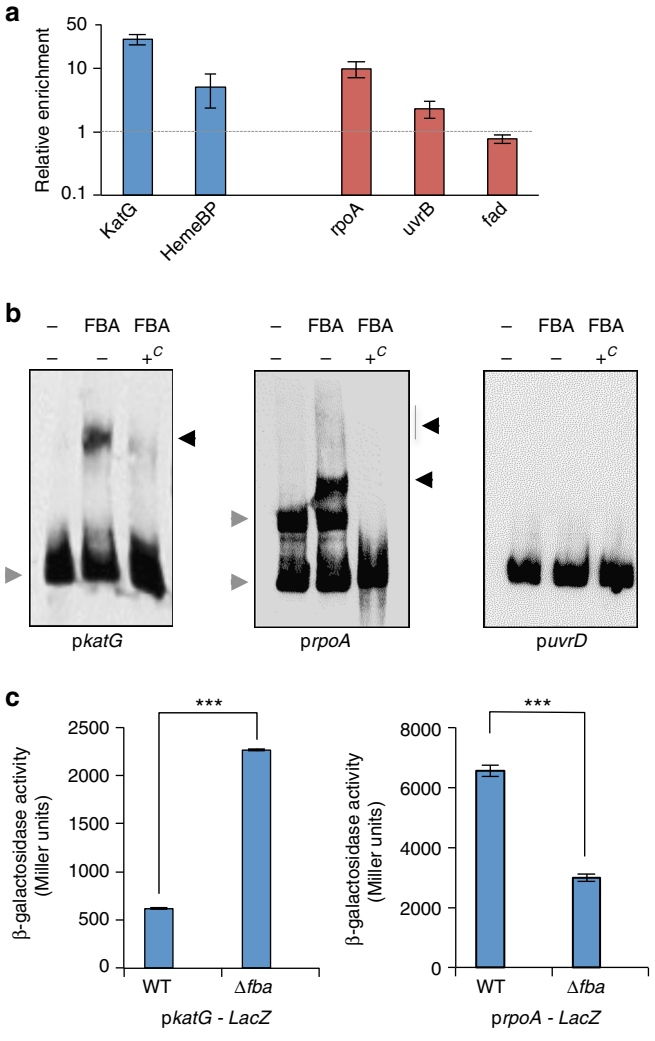

Fig. 7 ChIP-qPCR, EMSA, and β-galactosidase assays. **a** ChIP-qPCR experiments were performed with Δ*fba* strain expressing a His-tagged version of FBA (Δ*fba*/cpFBA-HA) and with wild-type *F. novicida* (WT, negative control). The results are expressed as relative enrichment of the detected fragments. Mean and SD of three independent experiments are shown. Five promoter regions were tested: two (*blue* columns) corresponding to down-regulated proteins (according to the proteomic analysis) i.e., *katG* (KatG) and *hemeBP* (FTN_0032 or Heme Binding Protein); and three (*red* columns) to up-regulated proteins i.e., *rpoA* (RNA polymerase α subunit), *uvrB* (Endonuclease ABC subunit B), and *fadA* (Fatty acid degragation). **b** Electrophoretic mobility shift assays (EMSA) analysis of FBA—p*KatG* (*left*) and FBA—p*rpoA* (*right*) promoter interactions. EMSA assays were performed with DIG-labeled *katG* and *rpoA* promoter regions (p*katG*, 200 bp; p*rpoA*, 220 bp) and purified his-tagged FBA (FBA-HA) recombinant protein. Lane 1: labeled probe alone; lane 2, labeled probe incubated with 0.8 µg purified FBA-HA; lanes 3: probe incubated with 0.8 µg purified FBA-HA in the presence of 125-fold excess of corresponding unlabeled probe. The *gray arrows* (to the *left* of each panel) indicate the migration of the probe alone and the *black arrows* (to the *right*), the shifted bands. As negative control (*right panel*), EMSA assays were performed with DIG-labeled *uvrD* promoter region (p*uvrD*, 188 bp). Lane 1: labeled probe alone; lane 2, labeled probe incubated with 0.8 µg purified FBA-HA; lanes 3: probe incubated with 0.8 µg purified FBA-HA in the presence of 125-fold excess of corresponding unlabeled probe. As expected, no specific shifted bands were observed with this promoter region in presence of purified FBA-HA. **c** Quantification of *lacZ* expression in *F. novicida* wild type (WT) and Δ*fba* mutant strains containing either p*katG* (*left*) or p*rpoA* (*right*) promoter regions by β-galactosidase assay, as measured in Miller units. Each assay was repeated at least three times. Mean and SD of three wells of one typical experiment are shown. (*p*-values were determined by the two-tailed unpaired Student's *t*-test, $***p < 0.0001$)

these cells. In contrast to *L. monocytogenes*, which possesses a specific hexose phosphate transporter (Hpt)[45] required for virulence, *Francisella* cannot use the cytosolic pool of glucose-6P directly as a glycolytic substrate since its lacks a dedicated transporter. In this glucose-restricted context, a fully functional gluconeogenic pathway is thus likely to be critical for the bacterium to allow the utilization of alternative available nutrients (such as amino acids, glycerol, or other carbohydrates). The intracellular concentrations of all the measured TCA cycle metabolites decreased in infected BMMs. This could be due to their increased consumption by the cell in response to the infection and contributed by the multiplying bacteria themselves. In spite of that, the level of intracellular ATP appeared to have increased by at least twofold in WT-infected BMMs whereas it remained unchanged in Δ*FPI*-infected BMMs compared to NI macrophages. Other sources of ATP generation have been very recently described[46] which would account for the maintenance of a sufficient ATP pool in these cells. For comparison, infection with *L. monocytogenes* has been shown to increase glycolytic activity, enhance flux of pyruvate into the TCA cycle in infected BMM[47], and favor glucose uptake by infected cell and the production of compounds, such as glucose-6P, serine, and glycerol[48]. Altogether, these observations are compatible with the notion that cytosolic multiplying bacteria may take advantage of the glycolytic activity of the host to obtain a valuable source of metabolites for their own intracellular nutrition. The requirement of a functional FBA enzyme, for growth in the presence of gluconeogenic substrates and for virulence in the mouse, suggests that in vivo *Francisella* does not encounter the proper combination of carbon sources that could compensate for the lack of FBA.

Francisella produces several antioxidant enzymes such as the superoxide dismutases SodB and SodC, and the catalase KatG. In addition to these primary antioxidant enzymes, other proteins have also been shown to contribute (directly or indirectly) to oxidative stress defense, such as the alkyl-hydro-peroxide reductase AhpC, proteins with sequence similarities to the Organic hydroperoxide resistance protein (Ohr)[49] as well as the MoxR-like ATPase[38, 50]. The pleiotropic regulator OxyR is a primary regulator of oxidative stress in many bacteria[51] that responds to peroxides (H_20_2). In *Francisella*, inactivation of *oxyR* confers high sensitivity to oxidants, deficient intramacrophage growth, and attenuated virulence in mice[52]. OxyR was also shown to bind to the upstream promoter regions of *katG* [53], indicating that *katG* expression is under the control of multiple regulatory mechanisms.

An earlier transcriptomic study, carried out in BMMs infected with *F. tularensis* Schu S4 strain, has shown that *katG* transcription was expressed during the first two hours after bacterial entry[42] and was later shut down for the rest of the infectious cycle whereas that of *fba* was induced after 4 h of infection and remained high up to 24 h. In agreement with this report, and further supporting the notion that FBA negatively regulates the expression of *katG* in infected cells, our qRT-PCR analysis (Fig. 5d) showed that *katG* expression was 7-fold up-regulated in the Δ*fba* mutant compared to WT, at 24 h of infection, in J774-1 macrophages supplemented with glucose and glycerol. These data suggest that the up-regulation of *katG* in the Δ*fba* mutant is not critical for intracellular multiplication in these conditions (in which the Δ*fba* metabolic defect is fully bypassed by appropriate carbohydrate supplementation). A role at later stages of the infectious cycle (such as cell to cell dissemination) and in other cell types is however possible.

ROS generated by macrophages upon infection have been shown to act as microbicidal effector molecules as well as secondary signaling messengers that regulate the expression of various inflammatory mediators. Of interest, the antioxidant action of the *katG*-encoded catalase of *Francisella* contributes to maintain the redox homeostasis in infected macrophages[34, 35]. The rapid cytosolic accumulation of H_2O_2, recorded in macrophages infected with a Δ*katG* mutant (i.e., lacking catalase activity), triggers a strong inflammatory reaction mediated by Ca^{2+} entry via the transient receptor potential melastatin 2 (TRPM2)[36]. Indeed, TRPM2 channels are gated by H_2O_2 through cysteine oxidation[54–56].

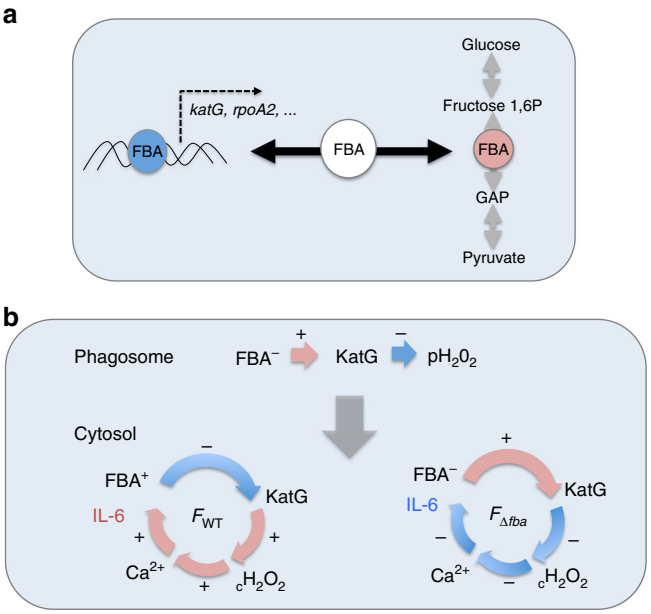

Fig. 8 Proposed model of FBA regulation. **a** Schematic depiction of the dual role played by FBA: as a fructose biphosphate aldolase in glucose metabolism (*right*); and as transcription regulator (*left*). **b** Proposed *fba*-dependent regulation of *katG*. In the phagosomal compartment (*upper* part), *fba* is not expressed (FBA^-), and *katG* expression is up-regulated (+) by H_2O_2 generated by phagosomal NADPH oxidase (pH_2O_2). In the cytosol (*lower* part), with the wild-type strain, *fba* expression is up-regulated (FBA^+), which leads to *katG* down-regulation (−). Cytosolic H_2O_2 (cH_2O_2) then progressively accumulates which activates the Ca^{2+} transporter TRPM2. Increased intracellular Ca^{2+} ultimately activates inflammatory reactions and notably the production of IL-6. In contrast, with the Δ*fba* mutant (FBA^-), *katG* expression is not repressed and cytosolic H_2O_2 is low. Consequently, the TRPM2-dependent Ca^{2+} accumulation is limited and IL-6 production remains low

The control of *katG* expression, mediated by FBA in the host cytosol, might constitute a mean of fine-tuning the redox status of the infected cell, leading to the control of pro-inflammatory cytokine and IL-6 production. Supporting this notion, we found that the total amount of ROS produced in cells infected with the Δ*fba* mutant (in which KatG expression is not repressed) was lower than in cells infected with the WT strain (Supplementary Fig. 10). Interestingly, previous studies have shown that *Francisella* also secreted KatG into the macrophage cytosol upon infection[57] as well as in the supernatant of bacterial cultures[58, 59]. Thus, KatG-dependent H_2O_2 detoxification might occur not only upon bacterial adsorption but might also be due to the direct action of the enzyme released in the host cytosol.

Altogether, these data are compatible with a sequential model of regulation (Fig. 8): (i) in the phagosomal compartment, *katG* expression is up-regulated due to the accumulation of H_2O_2 (designated pH_2O_2, derived from ROS produced by the NADPH oxidase) and FBA is not or poorly expressed; (ii) upon cytosolic escape, WT *Francisella* initially scavenges cytosolic H_2O_2, limiting

the activation of the calcium channel TRMP2 and delaying the Ca^{2+} dependent inflammatory response[34]; (iii) the progressive increase of *fba* expression in actively multiplying bacteria leads to the concommittant reduction of *katG* expression; (iv) the accumulation of cytosolic H_2O_2 then stimulates the TRMP2-dependent entry of Ca^{2+},[36]; and (v) ultimately leads to an increased production of IL-6, as described in this paper.

In contrast, in a Δ*fba* mutant strain, KatG production is not inhibited. In this context, the cytosolic concentration of H_2O_2 remains low and ultimately triggers only reduced IL-6 production in infected cells compared to WT bacteria.

Hence, FBA-mediated control of KatG expression should not be seen as a specific pathophysiologic role to render *Francisella* more vulnerable to a pro-inflammatory response but rather as a mean for the bacterium to combine metabolism and transcriptional regulation to optimally modulate the redox status of the infected cell. Indeed, one should bear in mind that intracellular survival and dissemination of the pathogen relies on its capacity to counteract both nutritional and innate immunity through an adaptation to the available nutritional resources and a tight and temporally-controlled dampening of cytokine production[60], ultimately leading to inflammasome activation and pyropsosis, allowing bacterial release and dissemination to adjacent cells.

Proteins that perform two or more distinct biological functions have been designated moonlighting proteins[61] and FBA can certainly be considered as a member of this family[21]. However, the only moonlight activity of FBA described thus far in pathogenic bacteria was a role as a secondary adhesin. For example, FBA is an essential enzyme in *M. tuberculosis* and also binds human plasminogen. Pneumococcal FBA is involved in the binding to human lung epithelial A549 cells via an interaction with a receptor belonging to the cadherin family. In *N. meningitidis*, FBA is not essential but is required for optimal adhesion to both human epithelial and endothelial cells[62, 63]. The recent detection of FBA in the cell wall fraction of *Coxiella burnetii*[64] and the identification of FBA orthologues in other pathogenic Gram-negative bacterial species, suggest that translocation of FBA to the Gram-negative cell envelope might constitute a more generalized phenomenon.

A putative role of metabolic enzymes in transcription regulation has been already suggested in bacteria, yeast as well as in eukaryotic cells. For example, in pathogenic *Streptococcus pyogenes*, the tagatose-1,6- bisphosphate aldolase LacD.1 acts as a negative regulator of the gene encoding the secreted cysteine protease SpeB[65]. This led to suggest that it might be a mechanism used by the bacterium to couple essential transcription programs to the sensing of its nutritional environment. In the yeast *Saccharomyces cerevisiae*, The class II FBA, in addition to its function in glycolysis, interacts physically with RNA polymerase III and plays a role in the control of its transcription[66]. In mammalian tissues, several enzymes involved in the glycolytic pathway display various non-glycolytic functions such as DNA repair and transcription, and are thus involved in important cellular functions including apoptosis, cell cycle control, and signaling pathways[67].

Our proteomic analyses showed that FBA exerted a specific repressive effect on only two proteins, including the catalase KatG. FBA appeared to be also involved in the up-regulation of multiple proteins including the α2 subunit of RNA polymerase (RNAP). Since the α subunit is a common site of interaction of RNAP with transcription activator proteins[68], affecting its expression is likely to alter transcription. Intriguingly, the *Francisella* genomes have the unique property to encode two different α subunits of RNAP with different regions predicted to be critical for dimer formation, promoter recognition, and activator interaction, suggesting possible distinct roles for the two α subunit in transcription regulation. Beyond this, our data also suggest that FBA might be involved in other pathways such as fatty acid metabolism. The role of metabolic enzymes in the regulation of non-metabolic functions in pathogenic microorganism should deserve renewed attention.

Methods

Ethics statement. All experimental procedures involving animals were conducted in accordance with guidelines established by the French and European regulations for the care and use of laboratory animals (Decree 87–848, 2001–464, 2001–486 and 2001–131, and European Directive 2010/63/UE) and approved by the INSERM Ethics Committee (Authorization Number: 75-906).

Strains and culture conditions. All strains used in this study are derivative from *F. tularensis* subsp. *novicida* U112 (*F. novicida* WT) and are described in Supplementary Table 1. Strains were grown at 37 °C on pre-made chocolate agar PolyViteX plates (BioMerieux), TSB or CDM supplemented with the appropriate carbon source at a final concentration of 25 mM. The CDM used for *F. tularensis* subsp *novicida* corresponds to standard CDM[30] without threonine and valine[39]. For growth condition determination, bacterial strains were inoculated in the appropriate medium at an initial OD_{600} of 0.05 from an overnight culture in TSB.

Stress assays. Stationary-phase bacterial cultures were diluted at a final OD_{600} of 0.1 in TSB broth. Exponential-phase bacterial cultures were diluted to a final concentration of 10^8 bacteria per mL and subjected to either 500 µM H_2O_2, 10 mM H_2O_2, 10 mM Tertbutyl hydroperoxide, 10 mM Cumene hydroperoxide (1 h); pH 5.5 (1 h); 0.05% SDS (4 h); or 10% human serum (1 h). The number of viable bacteria was determined by plating appropriate dilutions of bacterial cultures on Chocolate Polyvitex plates at the start of the experiment and after the indicated durations. Cultures (5 mL) were incubated at 37 °C with rotation (100 rpm) and aliquots were removed at indicated times, serially diluted and plated immediately. Bacteria were enumerated after 48 h incubation at 37 °C. Experiments were repeated independently at least twice and data represent the average of all experiments.

Construction of chromosomal deletion mutants. We inactivated the gene *fba* in *F. novicida* (*FTN_1329*) by allelic replacement resulting in the deletion of the entire gene (start and three last codons were conserved). We constructed a recombinant PCR product containing the upstream region of the gene *fba* (*FBA*-UP), a kanamycin resistance cassette (*nptII* gene fused with *pGro* promoter) and the downstream region of the gene *fba* (*FBA*-DN) by overlap PCR. Primers (Supplementary Table 2) *FBA* upstream FW (p1) and *FBA* upstream (spl_K7) RV (p2) amplified the 505 bp region upstream of position + 1 of the *FBA*coding sequence (*FBA*-UP), primers *pGro* FW (p3) and *nptII* RV (p4) amplified the 1091 bp kanamycin resistance cassette (*nptII* gene fused with *pGro* promoter); and primers *FBA* downstream (spl_K7) FW (p5) and *FBA* downstream RV (p6) amplified the 559 bp region downstream of the position + 1057 of the *FBA* gene coding sequence (*FBA*-DN). Primers p2 and p5 have an overlapping sequence of 12 and 12 nucleotides with primers p3 and p4, respectively, resulting in fusion of *FBA*-UP and *FBA*-DN with the cassette after crossing-over PCR. All single-fragment PCR reactions were realized using Phusion High-Fidelity DNA Polymerase (ThermoScientific) and PCR products were purified using NucleoSpin® Gel and PCR Clean-up kit (Macherey-Nagel). Overlap PCRs were realized using 100 ng of each purified PCR products and the resulting fragment of interest was purified from agarose gel. This fragment was then directly used to transform wild type *F. novicida* by electroporation[69]. Recombinant bacteria were isolated by spreading onto Chocolate agar plates containing kanamycin (5 µg mL^{-1}). The mutant strains were checked for loss of the wild type gene by PCR product direct sequencing (GATC-biotech) using appropriate primers.

Functional complementation. The plasmid used for complementation of the *F. novicida* Δ*fba* mutant (Δ*fba*), pKK-FBA_{cp}, is described below. Primers pGro FW and pGro RV amplified the 328 bp of the *pGro* promoter and primers *FBA*FW/*FBA* [PstI] RV amplified the 1064 bp *FBA* gene from U112. PCR products were purified and SmaI (*pGro* promoter) or PstI (*FBA*) restricted in presence of FastAP Thermosensitive Alkaline Phosphatase (ThermoScientific) to avoid self-ligation. A mixture of *pGro* promoter and interest gene fragments was then incubated in T4 Polynucleotide Kinase to allow blunt end ligation and fragments were then cloned in pKK214 vector after SmaI/PstI double restriction and transformed in *E. coli* TOP10. Recombinant plasmid pKK-FBA_{cp} (designated Cp-*fba*) was purified and directly used for chemical transformation in *F. novicida* U112[38] by electroporation. Recombinant colonies were selected on Chocolate agar plates containing tetracycline (5 µg mL^{-1}) and kanamycin (5 µg mL^{-1}).

As controls, WT *F. novicida* and Δ*fba* mutant strains, carrying the empty vector pKK214, designated WT(−) and Δ*fba*(−), respectively, were also constructed and tested.

Catalase assay. Catalase enzyme activity was analyzed with a Catalase Assay Kit (Abcam, Cambridge, UK). WT *F. novicida* and Δ*fba* strains were grown overnight

in TSB supplemented with glucose and cysteine. 2×10^6 bacteria were harvested and used for the enzyme assay according to the manufacturer's instructions. After 30 min incubation time the reaction was stopped and the optical density was measured at OD_{570} with a microplate reader. The assay was repeated twice, with similar results.

Transcriptional analyses. Isolation of total RNA and reverse transcription: For transcriptional analyses of bacteria grown in TSB, cultures were centrifuged for 2 min in a microcentrifuge at room temperature and the pellet was quickly resuspended in Trizol solution (Invitrogen, Carlsbad, CA, USA). For transcriptional analyses of bacteria in infected cells, J774-1 cells grown in standard DMEM were infected with either WT *F. novicida* (WT) or Δ*fba* mutant strain for 24 h. NI cells, incubated in the same conditons, were used a negative control. Cells were then collected by scratching, centrifuged at max speed in a microcentrifuge at room temperature and the pellet was quickly resuspended in Trizol solution.

Samples were either processed immediately or frozen and stored at −80 °C. Samples were treated with chloroform and the aqueous phase was used in the RNeasy Clean-up protocol (Qiagen, Valencia, CA, USA) with an on-column DNase digestion of 30 min. RNA RT-PCR experiments were carried out with 500 ng of RNA and 2 pmol of specific reverse primers. After denaturation at 70 °C for 5 min, 15 µL of the mixture containing 4 µL GoScript 5 × reaction buffer, 1 µL of 0.5 mM PCR Nucleotide Mix, 0.5 µL of RNasin Ribonuclease Inhibitor, and 1 µL GoScript Reverse Transcriptase (Promega) were added. Samples were incubated 5 min at 25 °C and then, 60 min at 42 °C, heated at 72 °C for 15 min and chilled on ice. Samples were stored at −20 °C. Different pairs of primers were used in PCR to amplify the messenger RNA corresponding to the transcript of operon FTN_1333 to FTN_1329 (see Supplementary Table 2).

Quantitative real-time RT-PCR: WT *F. novicida* and mutant strains were grown overnight at 37 °C. Then, samples were harvested and RNA was isolated and reverse trancript in cDNA. The 25 µL reaction consisted of 5 µL cDNA template, 12.5 µL Fastart SYBR Green Master (Roche Diagnostics), and 2 µL 10 µM of each primer and 3.5 µL water. qRT-PCR was performed according to manufacturer's protocol on Applied Biosystems—ABI PRISM 7700 instrument (Applied Biosystems, Foster City, CA, USA). To calculate the amount of gene-specific transcript, a standard curve was plotted for each primer set using a series of diluted genomic DNA from WT *F. novicida*. The amounts of each transcript were normalized to helicase rates (*FTN_1594*).

Chromatin immunoprecipitation-qPCR assay. Chromatin immunoprecipation (ChIP) was performed with wild-type *F. novicida* (WT) and a *Δfba* strain expressing a His-tagged version of FBA (FBA-HA) (Δ*fba*/cpFBA-HA) bearing the 6x-His epitope fused at the C-terminal end of the protein). Bacteria were grown at 37 °C in 100 mL TSB supplemented to mid-log (OD_{600} 0.3–0.4). Then bacteria were incubated in a final concentration of 1% formaldehyde (Sigma) for 30 min, after which glycine (Sigma) was added to a final concentration of 250 mM. Then, the bacteria were lysed by sonication (Branson Sonifier 250) to obtain a chromatin size of <500 pb. Aliquots were stored as input controls.

Immunoprecipitations were performed after an overnight incubation with the anti-HA antibody (6x-His Epitope Tag Antibody, Life Technologie), and with Dynabeads protein G (ThermoFisher Scientific). The beads were then washed and DNA was reverse-crosslinked and purified. Following ChIP, DNA was analyzed by qPCR. All ChIP-qPCRs were performed in triplicate from at least three independent experiments.

Briefly, the qPCR values were first normalized as follows: (i) qPCR values of the target promoter sequences (derived from ChIP and input samples) were divided by the qPCR values of the coding region of house keeping gene *uvrD* (Helicase) as internal control; (ii) the values obtained for *fba*/cpFBA-HA were next normalized by dividing them by their corresponding background values (derived from ChIP and input from WT). Then, the normalized signals from *fba*/cpFBA-HA derived from ChIP were divided by the normalized signals of *fba*/cpFBA-HA derived from input samples.

The results were expressed as relative enrichment of the detected fragments.

Electrophoretic mobility shift assay. We evaluated the ability of purified his-tagged FBA (FBA-HA) recombinant protein to bind to the *katG* or *rpoA* promoter regions (designated p*katG* and p*rpoA*, respectively), using EMSA. EMSAs were carried out using a DIG gel shift kit (Roche Diagnostic Corporation, Indianapolis, IN, USA), according to the manufacturer's instructions. Briefly, p*katG* (the 200 bp region immediately upstream of the ATG start codon of *katG*) was amplified with the pair of primers: Fw, 5′-GATATCGCTGGTGGATTATAAATAAATCG-3′ and Rv, 5′-GGTGATTTCCTCGCTATAAAGTTGA-3′; and p*rpoA* (the 220 bp region immediately upstream of the ATG start codon of *rpoA*) was amplified with the pair of primers: Fw, 5′-TCCAAACTCATATGTTATCCAGCAATAT-3′ and Rv, 5′-AGCAGTTTAAAACCTAGTTATATTTTATAG-3′), PCR products were resuspended in TEN buffer (10 mmol L^{-1} Tris-HCl, 1 mmol L^{-1} ethylene diamine tetraacetic acid (EDTA), 100 mmol L^{-1} NaCl; pH 8.0) and labeled with DIG-ddUTP (Roche, Indianapolis, IN, USA) by the terminal transferase (Feng and Cronan, 2011). After 15 min of incubation of the DIG-labeled DNA probes (0.2 pmol) with 0.8 µg FBA-HA in binding buffer (Roche) at room temperature, the DNA-protein complexes were separated using a native 5% polyacrylamide gel electrophoresis at 4 °C, transferred onto an equilibrated, positively charged nylon membrane (Amersham) followed by UV cross-linking (120 mJ for 180 s). Finally, the signals were captured by exposure to the high-performance chemiluminescence film (Amersham Hyperfilm ECL). As controls, we used the labeled probe without FBA-HA and the labeled probe incubated 30 min with the purified FBA-HA and with a 125-fold excess of unlabeled probe.

As a negative control, we used the promoter region of *uvrD*, a gene that is not regulated by FBA. p*uvrD* (corresponding to the 188 bp region immediately upstream of the ATG start codon of *uvrD*) was amplified with the pair of primers: Fw, 5′-TGCGACAAACTAATTTGTGAAACTTAG-3′ and Rv, 5′-CTGCCAGCACCAGCGAGA-3′. The labeled probe was incubated for 30 min: without FBA-HA, in the presence of FBA-HA, or in the presence of FBA-HA and with a 125-fold excess of unlabeled probe.

β-galactosidase assays. Reporter fusion construction: Two *lacZ* transcriptional fusion were constructed by cloning either p*katG* or p*rpoA* promoter region upstream of the *E. coli lacZ* gene. The p*katG* and p*rpoA* promoter regions were amplified using the primer pairs used in the EMSA and *E. coli s17-1 λpir* was the source of chromosomal DNA for amplification of the native *lacZ* gene. A 3075 bp region encompassing the entire coding sequence and its preceeding Shine-Dalgarno sequence was amplified with the pair of primers: Fw, 5′-TTAAT-TAAAGGAGGAACAGCTATG-3′ and Rv, 5′-TTATTTTTGACACCA-GACCAACTGG-3′). PCR amplifications were performed using Phusion High-Fidelity DNA Polymerase (ThermoScientific). The p*katG-LacZ* and p*rpoA2-LacZ* amplicons were then generated by overlap PCR. The purified products (3300 bp for *pkatG-LacZ* and 3295 bp for *prpoA2-LacZ*, respectively), flanked by *Sma*I and *Pst*I sites were further digested with *Sma*I and *Pst*I restriction enzymes, in presence of FastAP Thermosensitive Alkaline Phosphatase (ThermoScientific) to avoid self-ligation. Fragments were then cloned into pKK214 plasmid vector after *Sma*I/*Pst*I double restriction and transformed into *E. coli* TOP10. The recombinant plasmids pKK-p*katG-LacZ* and pKK-p*rpoA2* were purified and directly used for cryo-transformation into *F. novicida* WT of Δ*fba* mutant strains. Recombinant colonies were selected on Chocolate agar plates containing tetracycline (5 µg mL^{-1}).

β-galactosidase assay: The assays were performed essentially as described previously[10]. Briefly, overnight cultures of reporter fusion construction strains were diluted in TS media and grown until mid exponential phase (0.2–0.8 OD_{600}). Bacteria were then harvested by centrifugation, resuspended in 1 mL of Z buffer with β-mercaptoethanol (60 mM Na_2HPO_4, 40 mM NaH_2PO_4, 10 mM KCl, 1 mM $MgSO_4$, pH 7.0, and 50 mM mercaptoethanol). SDS 0.2% and Chloroform was added and the samples were vigorously vortexed 15 sec and kept 5 min at room temperature. Then, 200 ul of ONPG (4 mg mL^{-1} in Z Buffer) were added to the samples and incubated at 30 °C. The reactions were stopped by the addition of 1 M Na_2CO3. The absorbance at 420_{nm} and 550_{nm} was measured and the data converted in Miller units, using the classical formula $[(OD_{420} - 1.75 \times OD_{550})/(OD_{600} \times \text{Volume} \times \text{Time})] \times 1000$.

Cell culture and cell infection experiments. J774A.1 (ATCC TIB-67) cells were propagated in DMEM (PAA), containing 10% fetal bovine serum (FBS, PAA) unless otherwise stated. BMM from 6 to 8-week-old female BALB/c mice were grown in Roswell Park Memorial Institute (RPMI-1640) or DMEM, containing 10% FBS. The day before infection, ~2×10^5 eukaryotic cells (i.e., J774A.1 and BMM) per well were seeded in 12-well cell tissue plates (in appropriate cellular culture medium supplemented with the appropriate carbon source) and bacterial strains were grown overnight in 5 mL of TSB at 37 °C.

Infections were realized at a multiplicity of infection (MOI) of 100 and incubated for 1 h at 37 °C in culture medium supplemented with the appropriate carbon source (glucose, glycerol, or pyruvate). We used in our assays DMEM without glucose supplemented either with glucose at 5 mM or with other carbon sources at the same molarity. After 3 washes with cellular culture medium, plates were incubated for 4, 10, and 24 h in fresh medium supplemented with gentamycin (10 µg mL^{-1}). At each kinetic point, cells were washed 3 times with culture medium and lysed by addition of 1 mL of distilled water for 10 min at 4 °C. The titer of viable bacteria was determined by spreading preparations on chocolate plates. Each experiment was conducted at least twice in triplicates.

IL-6 production. Supernatants from J774-1 infected with either wild-type *F. novicida* (WT) or Δ*fba* mutant (MOI of 100) were harvested at 24 h. NI cells were tested as negative control. Cytokine were quantified by ELISA (BD) as previously described[37], using commercially available anti- IL-6 antibody in accordance with the manufacturer's instructions.

ROS detection assay. Intracellular ROS were detected by using the oxidation-sensitive fluorescent probe dye, DCFDA as recommended by the manufacturer (DCFDA Cellular ROS Detection Assay Kit, Abcam, Cambridge, UK). J774.1 cells were seeded at 4×10^4 cells per well. Cells were infected with bacteria for 10 or 24 h (MOI of 1000:1), washed three times with PBS and incubated with DCFDA diluted in PBS (15 µM). DCF fluorescence was measured with a multiplate reader Berthold TriStar (Berthold France SAS, Thoiry, France) with the use of excitation and

emission wavelengths of 480 and 525 nm, respectively. Values were normalized by protein concentration in each well (Bradford). Samples were tested in triplicates in two experiments.

Determination of ROS generation via fluorescence microscopy. J774.1 cells were seeded at 4×10^4 cells per well. Cells were infected with bacteria for 10 h (MOI of 1000:1), washed three times with PBS and incubated with DCFDA diluted in PBS for 1 h (15 µM). Images of the cells were captured with an Olympus CKX41 microscope and treated with Image J software. Cell counts were performed over 5 images of approx. 50 cells.

Confocal experiments. J774.1 macrophage cells were infected (MOI of 1,000) with wild-type *F. novicida* U112 (WT), the Δ*fba* isogenic mutant (Δ*fba*), or an isogenic strain deleted for the "*Francisella* Pathogenicity Island" (Δ*FPI*) in standard DMEM (DMEM-glucose) or DMEM without glucose and supplemented with either glucose or glycerol (5 mM each) for 30 min at 37 °C. Cells were then washed three times with PBS and maintained in fresh DMEM supplemented with gentamycin (10 µg mL^{-1}) until the end of the experiment. Three kinetic points (i.e., 1, 4, and 10 h) were sampled. For each point cells were washed with 1X PBS, fixed 15 min with 4% Paraformaldheyde, and incubated 10 min in 50 mM NH_4Cl in 1X PBS to quench free aldehydes. Cells were then blocked and permeabilized with PBS containing 0.1% saponin and 5% goat serum for 10 min at room temperature. Cells were then incubated for 30 min with anti-*F. novicida* mouse monoclonal antibody (1/500 final dilution, Creative Diagnostics) and anti-LAMP-1 rabbit polyclonal antibody (1/100 final dilution, ABCAM). After washing, cells were incubated for 30 min with Alexa488-conjugated goat anti mouse and Alexa546 conjugated donkey anti rabbit secondary antibodies (1/400 final dilution, AbCam). After washing, DAPI was added (1/1000 final dilution) for 1 min and glass coverslips were mounted in Mowiol (Cityfluor Ltd.). Cells were examined using an × 63 oil-immersion objective on a LeicaTSP SP5 confocal microscope. Co-localization tests were quantified by using Image J software; and mean numbers were calculated on more than 500 cells for each condition. Confocal microscopy analyses were performed at the Cell Imaging Facility (Faculté de Médecine Necker-Enfants Malades).

Mouse infection. WT *F. novicida* and Δ*fba* mutant strains were grown in TSB to exponential growth phase and diluted to the appropriate concentrations. Six to 8-week-old female BALB/c mice (Janvier, Le Genest St Isle, France) were intraperitoneally inoculated with 200 µl of bacterial suspension. The actual number of viable bacteria in the inoculum was determined by plating dilutions of the bacterial suspension on chocolate plates. For competitive infections, WT *F. novicida* and Δ*fba* mutant bacteria were mixed in 1:1 ratio and a total of 100 bacteria were used for infection of each of five mice. After 2 days, mice were killed. Homogenized spleen and liver tissue from the five mice in one experiment were mixed, diluted, and spread on to chocolate agar plates. Kanamycin selection to distinguish WT and mutant bacteria was performed. Competitive index (CI) [(mutant output/WT output)/(mutant input/WT input)]. Statistical analysis for CI experiments was as described[40] using the Student's unpaired *t*-test.

Proteomic analyses. Protein digestion: FASP (Filter-aided sample preparation) procedure for protein digestion was performed as previously described[70], using 30 kDa MWCO centrifugal filter units (Microcon, Millipore, Cat No MRCF0R030). Briefly, sodium dodecyl sulfate (SDS, 2% final) was added to 30 µg of each lysate to increase solubility of the proteins, in a final volume of 120 µL. Proteins were reduced with 0.1 M dithiotreitol (DTT) for 30 min at 60 °C, then applied to the filters, mixed with 200 µL of 8 M urea, 100 mM Tris-HCl pH 8.8 (UA buffer), and finally centrifuged for 15 min at 15,000 x *g*. In order to remove detergents and DTT, the filters were washed twice with 200 µl of UA buffer. Alkylation was carried out by incubation for 20 min in the dark with 50 mM iodoacetamide. Filters were then washed twice with 100 µl of UA buffer (15,000 x *g* for 15 min), followed by two washes with 100 µl of ABC buffer (15,000 x *g* for 10 min), to remove urea. All centrifugation steps were performed at room temperature. Finally, trypsin was added in 1:30 ratio and digestion was achieved by overnight incubation at 37 °C.

NanoLC-MS/MS protein identification and quantification: Samples were vacuum dried, and resuspended in 30 µL of 10% acetonitrile, 0.1% trifluoroacetic acid for LC-MS/MS. For each run, 1 µL was injected in a nanoRSLC-Q Exactive PLUS (RSLC Ultimate 3000, ThermoScientific, Waltham, MA, USA). Peptides were separated on a 50 cm reversed-phase liquid chromatographic column (Pepmap C18, Thermo Scienfitic). Chromatography solvents were (A) 0.1% formic acid in water, and (B) 80% acetonitrile, 0.08% formic acid. Peptides were eluted from the column with the following gradient 5 to 40% B (120 min), 40 to 80% (10 min). At 131 min, the gradient returned to 5% to re-equilibrate the column for 30 min before the next injection. Two blanks were run between triplicates to prevent sample carryover. Peptides eluting from the column were analyzed by data dependent MS/MS, using top-10 acquisition method. Briefly, the instrument settings were as follows: resolution was set to 70,000 for MS scans and 17,500 for the data dependent MS/MS scans in order to increase speed. The MS AGC target was set to 3×10^6 counts, while MS/MS AGC target was set to 1×10^5. The MS scan range was from 400 to 2000 *m/z*. MS and MS/MS scans were recorded in profile mode. Dynamic exclusion was set to 30 s duration. Three replicates of each sample were analyzed by nanoLC-MS/MS.

Data processing following nanoLC-MS/MS acquisition: The MS files were processed with the MaxQuant software version 1.5.3.30 and searched with Andromeda search engine against the NCBI *F. tularensis* subsp. *novicida* database (release 28-04-2014, 1719 entries). To search parent mass and fragment ions, we set a mass deviation of 3 and 20 ppm respectively. The minimum peptide length was set to 7 amino acids and strict specificity for trypsin cleavage was required, allowing up to two missed cleavage sites. Carbamidomethylation (Cys) was set as fixed modification, whereas oxidation (Met) and N-term acetylation were set as variable modifications. The false discovery rates at the protein and peptide level were set to 1%. Scores were calculated in MaxQuant as described previously[71]. The reverse and common contaminants hits were removed from MaxQuant output. Proteins were quantified according to the MaxQuant label-free algorithm using LFQ intensities[71, 72]; protein quantification was obtained using at least 2 peptides per protein.

Statistical and bioinformatic analysis, including heatmaps, profile plots, and clustering, were performed with Perseus software (version 1.5.0.31) freely available at www.perseus-framework.org[73]. For statistical comparison, we set three groups, each containing biological triplicate. Each sample was run in technical triplicates as well. We then filtered the data to keep only proteins with at least 2 valid values out 3 in at least one group. Next, the data were imputed to fill missing data points by creating a Gaussian distribution of random numbers with a SD of 33% relative to the SD of the measured values and 1.8 SD downshift of the mean to simulate the distribution of low signal values. We performed an ANOVA test, $p < 0.01$, S0 = 1. Hierarchical clustering of proteins that survived the test was performed in Perseus on logarithmic scaled LFQ intensities after z-score normalization of the data, using Euclidean distances.

Metabolomic analyses. Central metabolite profiling by IC-MS/MS: Metabolome profiling of bone marrow-derived macrophages cells was performed in NI condition, in cells infected either with the wild-type *F. novicida* strain (WT) or with a Δ*FPI* isogenic mutant. Central metabolites of cells were harvested and quantified 1 and 24 h after infection. After elimination of cultivation medium by aspiration, adherent cells were washed with 3 ml of PBS buffer, also eliminated by aspiration. Cells were then rapidly quenched in cultivation plates with liquid nitrogen at −196 °C and extracted with 5 ml of a solvent mixture of ACN/Methanol/H_2O (2:2:1) at −20 °C. Samples were then evaporated and resuspended in 120 µL of ultrapure H_2O before analysis. The metabolites quantified were: Glucose-1-P (G1P), Glucose-6P (G6P), UDP-glucose (UDP-Glc) Fructose-6-P (F6P), Fructose-Bis-P (FBP), Pentoses-5-P = Ribose-5P + Ribulose-5P + Xylulose-5P (P5P), Ribose-1-P (R1P), Sedoheptulose-7-P (SH-7P), glycerol-3P (gly-3P), 2 and 3-PhosphoGlycerate (2/3-PG), Phospho-Enol-Pyruvate (PEP), Citrate (Cit), cis-aconitate (cis-aco), Oxoglutarate (OG), Succinate (Suc), Fumarate (Fum), Malate (Mal), Adenosine Mono, Di and Tri-phosphate (AMP, ADP, ATP), Cytidine Mono, Di and Tri-phosphate (CMP, CDP, CTP), Uridine Mono, Di and Tri-phosphate (UMP, UDP, UTP), Guanidine Mono and Di-phosphate (GMP, GDP), UDP-Acetylglucosamine (UDP-AcGluN), Shikimate-3-phosphate (Shikimate-3P), and Phosphor-Serine (P-Serine). Metabolite separation was performed by ionic chromatography (Dionex ICS 2500 ion chromatograph). Measurement of metabolite concentrations was performed by mass spectrometry with an Applied Biosystems 4000 Qtrap mass Spectrometer (ElectroSpray Ionisation in Negative mode; Detection mode: Multiple Reaction Monitoring). Quantification of metabolites from MS signals was made by external calibration with standards compounds mixture.

Exometabolome profiling by nuclear magnetic resonance: To estimate metabolites consumed and produced by the cells, samples of culture medium were harvested for each condition (NI, infected cells with WT and Δ*FPI F. novicida* strain) for each time point 1 and 24 h after infection. Extracellular samples were harvested by filtration of medium with a 0.45 µm diameter syringe filter. A 540 µL volume of extracellular sample was mixed with 40 µL Trimethyl-Sillyl-Propionic Acid 10 mM in D_2O. Measurement of exometabolome was performed by 1D 1H NMR with presaturation on a 500 Mhz NMR spectrometer equipped with a 5 mm TXI cryoprobe. NMR spectra were processed with Bruker Topspin 3.2, profiling and quantification of metabolites was performed with the Chenomx NMR suite 8.1. From spectra profiling, 29 metabolites (Supplementary Fig. 4) coming from original medium or produced by cells were unambiguously identified and quantified. We compared measured concentrations at 1 and at 24 h to evaluate substrates consumption in extracellular medium and metabolites production by cells.

Data availability. The mass spectrometry proteomics data have been deposited to the ProteomeXchange Consortium via the PRIDE partner repository with the dataset identifier PXD006908. The authors declare that all other data supporting the findings of this study are available within the paper and its Supplementary Information files.

Received: 2 January 2017 Accepted: 2 August 2017
Published online: 11 October 2017

References

1. Sjostedt, A. Tularemia: history, epidemiology, pathogen physiology, and clinical manifestations. *Ann. N. Y. Acad. Sci.* **1105**, 1–29 (2007).
2. Santic, M., Molmeret, M., Klose, K. E. & Abu Kwaik, Y. *Francisella tularensis* travels a novel, twisted road within macrophages. *Trends Microbiol.* **14**, 37–44 (2006).
3. McLendon, M. K., Apicella, M. A. & Allen, L. A. *Francisella tularensis:* taxonomy, genetics, and Immunopathogenesis of a potential agent of biowarfare. *Annu. Rev. Microbiol.* **60**, 167–185 (2006).
4. Kingry, L. C. & Petersen, J. M. Comparative review of *Francisella tularensis* and *Francisella novicida*. *Front. Cell. Infect. Microbiol.* **4**, 35 (2014).
5. Eshraghi, A. et al. Secreted effectors encoded within and outside of the *Francisella* pathogenicity island promote intramacrophage growth. *Cell Host Microbe* **20**, 573–583 (2016).
6. Eisenreich, W. & Heuner, K. The life stage-specific pathometabolism of *Legionella pneumophila*. *FEBS Lett.* **590**, 3868–3886 (2016).
7. Qin, A. et al. Components of the type six secretion system are substrates of *Francisella tularensis* Schu S4 DsbA-like FipB protein. *Virulence* **7**, 882–894 (2016).
8. Charity, J. C. et al. Polymerase-associated proteins control virulence gene expression in *Francisella tularensis*. *PLoS Pathog.* **3**, e84 (2007).
9. Ramsey, K. M. et al. Ubiquitous promoter-localization of essential virulence regulators in *Francisella tularensis*. *PLoS Pathog.* **11**, e1004793 (2015).
10. Charity, J. C., Blalock, L. T., Costante-Hamm, M. M., Kasper, D. L. & Dove, S. L. Small molecule control of virulence gene expression in *Francisella tularensis*. *PLoS Pathog.* **5**, e1000641 (2009).
11. Pizarro-Cerda, J., Charbit, A., Enninga, J., Lafont, F. & Cossart, P. Manipulation of host membranes by the bacterial pathogens *Listeria*, *Francisella*, *Shigella* and *Yersinia*. *Semin. Cell Dev. Biol.* **60**, 155–167 (2016).
12. Eisenreich, W., Dandekar, T., Heesemann, J. & Goebel, W. Carbon metabolism of intracellular bacterial pathogens and possible links to virulence. *Nat. Rev. Microbiol.* **8**, 401–412 (2010).
13. Eisenreich, W., Heesemann, J., Rudel, T. & Goebel, W. Metabolic host responses to infection by intracellular bacterial pathogens. *Front. Cell. Infect. Microbiol.* **3**, 24 (2013).
14. Eisenreich W., Heesemann J., Rudel T. & Goebel W. Metabolic adaptations of intracellullar bacterial pathogens and their Mammalian host cells during infection ("pathometabolism"). *Microbiol. Spectr.* **3**, MBP-0002-2014 (2015).
15. Fuchs, T. M., Eisenreich, W., Heesemann, J. & Goebel, W. Metabolic adaptation of human pathogenic and related nonpathogenic bacteria to extra- and intracellular habitats. *FEMS Microbiol. Rev.* **36**, 435–462 (2012).
16. Puckett, S. et al. Inactivation of fructose-1,6-bisphosphate aldolase prevents optimal co-catabolism of glycolytic and gluconeogenic carbon substrates in *Mycobacterium tuberculosis*. *PLoS Pathog.* **10**, e1004144 (2014).
17. Blume, M. et al. A *toxoplasma gondii* gluconeogenic enzyme contributes to Robust central carbon metabolism and is essential for replication and virulence. *Cell Host Microbe* **18**, 210–220 (2015).
18. Marsh, J. J. & Lebherz, H. G. Fructose-bisphosphate aldolases: an evolutionary history. *Trends Biochem. Sci.* **17**, 110–113 (1992).
19. Nagano, N., Orengo, C. A. & Thornton, J. M. One fold with many functions: the evolutionary relationships between TIM barrel families based on their sequences, structures and functions. *J. Mol. Biol.* **321**, 741–765 (2002).
20. Katebi, A. R. & Jernigan, R. L. Aldolases utilize different oligomeric states to preserve their functional dynamics. *Biochemistry* **54**, 3543–3554 (2015).
21. Shams, F., Oldfield, N. J., Wooldridge, K. G. & Turner, D. P. Fructose-1,6-bisphosphate aldolase (FBA)-a conserved glycolytic enzyme with virulence functions in bacteria: 'ill met by moonlight'. *Biochem. Soc. Trans.* **42**, 1792–1795 (2014).
22. Ritterson Lew, C. & Tolan, D. R. Aldolase sequesters WASP and affects WASP/Arp2/3-stimulated actin dynamics. *J. Cell. Biochem.* **114**, 1928–1939 (2013).
23. Alefounder, P. R. & Perham, R. N. Identification, molecular cloning and sequence analysis of a gene cluster encoding the class II fructose 1,6-bisphosphate aldolase, 3-phosphoglycerate kinase and a putative second glyceraldehyde 3-phosphate dehydrogenase of *Escherichia coli*. *Mol. Microbiol.* **3**, 723–732 (1989).
24. Thomson, G. J., Howlett, G. J., Ashcroft, A. E. & Berry, A. The dhnA gene of *Escherichia coli* encodes a class I fructose bisphosphate aldolase. *Biochem. J.* **331** (Pt 2), 437–445 (1998).
25. Plaumann, M., Pelzer-Reith, B., Martin, W. F. & Schnarrenberger, C. Multiple recruitment of class-I aldolase to chloroplasts and eubacterial origin of eukaryotic class-II aldolases revealed by cDNAs from Euglena gracilis. *Curr. Genet.* **31**, 430–438 (1997).
26. de la Paz Santangelo, M. et al. Glycolytic and non-glycolytic functions of *Mycobacterium tuberculosis* fructose-1,6-bisphosphate aldolase, an essential enzyme produced by replicating and non-replicating bacilli. *J. Biol. Chem.* **286**, 40219–40231 (2011).
27. Weiss, D. S. et al. In vivo negative selection screen identifies genes required for *Francisella* virulence. *Proc. Natl Acad. Sci. USA* **104**, 6037–6042 (2007).
28. Gika, H. G., Theodoridis, G. A., Plumb, R. S. & Wilson, I. D. Current practice of liquid chromatography-mass spectrometry in metabolomics and metabonomics. *J. Pharm. Biomed. Anal.* **87**, 12–25 (2014).
29. Krombach, F. et al. Cell size of alveolar macrophages: an interspecies comparison. *Environ. Health Perspect.* **105**(Suppl 5): 1261–1263 (1997).
30. Chamberlain, R. E. Evaluation of live tularemia vaccine prepared in a chemically defined medium. *Appl. Microbiol.* **13**, 232–235 (1965).
31. Brissac, T. et al. Gluconeogenesis, an essential metabolic pathway for pathogenic *Francisella*. *Mol. Microbiol.* **98**, 518–534 (2015).
32. Eisele, N. A. et al. Salmonella require the fatty acid regulator PPARdelta for the establishment of a metabolic environment essential for long-term persistence. *Cell Host Microbe* **14**, 171–182 (2013).
33. McNab, F., Mayer-Barber, K., Sher, A., Wack, A. & O'Garra, A. Type I interferons in infectious disease. *Nat. Rev. Immunol.* **15**, 87–103 (2015).
34. Ma, Z. et al. Elucidation of a mechanism of oxidative stress regulation in *Francisella tularensis* live vaccine strain. *Mol. Microbiol.* **101**, 856–878 (2016).
35. Franchini, A. M., Hunt, D., Melendez, J. A. & Drake, J. R. FcgammaR-driven release of IL-6 by macrophages requires NOX2-dependent production of reactive oxygen species. *J. Biol. Chem.* **288**, 25098–25108 (2013).
36. Shakerley, N. L., Chandrasekaran, A., Trebak, M., Miller, B. A. & Melendez, J. A. *Francisella tularensis* catalase restricts immune function by impairing TRPM2 channel activity. *J. Biol. Chem.* **291**, 3871–3881 (2016).
37. Barr, T. A. et al. B cell depletion therapy ameliorates autoimmune disease through ablation of IL-6-producing B cells. *J. Exp. Med.* **209**, 1001–1010 (2012).
38. Dieppedale, J. et al. Possible links between stress defense and the tricarboxylic acid (TCA) cycle in *Francisella* pathogenesis. *Mol. Cell. Proteomics* **12**, 2278–2292 (2013).
39. Gesbert, G. et al. Importance of branched-chain amino acid utilization in *Francisella* intracellular adaptation. *Infect. Immun.* **83**, 173–183 (2015).
40. Ramond, E. et al. Glutamate utilization couples oxidative stress defense and the tricarboxylic acid cycle in Francisella phagosomal escape. *PLoS Pathog.* **10**, e1003893 (2014).
41. Gesbert, G. et al. Asparagine assimilation is critical for intracellular replication and dissemination of *Francisella*. *Cell. Microbiol.* **16**, 434–449 (2014).
42. Wehrly, T. D. et al. Intracellular biology and virulence determinants of *Francisella tularensis* revealed by transcriptional profiling inside macrophages. *Cell. Microbiol.* **11**, 1128–1150 (2009).
43. Raghunathan, A., Shin, S. & Daefler, S. Systems approach to investigating host-pathogen interactions in infections with the biothreat agent *Francisella*. Constraints-based model of Francisella tularensis. *BMC Syst. Biol.* **4**, 118 (2010).
44. Steele, S. et al. *Francisella tularensis* harvests nutrients derived via ATG5-independent autophagy to support intracellular growth. *PLoS Pathog.* **9**, e1003562 (2013).
45. Chico-Calero, I. et al. Hpt, a bacterial homolog of the microsomal glucose- 6-phosphate translocase, mediates rapid intracellular proliferation in *Listeria*. *Proc. Natl Acad. Sci. USA* **99**, 431–436 (2002).
46. Wright, R. H. et al. ADP-ribose-derived nuclear ATP synthesis by NUDIX5 is required for chromatin remodeling. *Science* **352**, 1221–1225 (2016).
47. Gillmaier, N., Gotz, A., Schulz, A., Eisenreich, W. & Goebel, W. Metabolic responses of primary and transformed cells to intracellular *Listeria monocytogenes*. *PLoS ONE* **7**, e52378 (2012).
48. Grubmuller, S., Schauer, K., Goebel, W., Fuchs, T. M. & Eisenreich, W. Analysis of carbon substrates used by *Listeria monocytogenes* during growth in J774A.1 macrophages suggests a bipartite intracellular metabolism. *Front. Cell. Infect. Microbiol.* **4**, 156 (2014).
49. Meireles Dde, A., Alegria, T. G., Alves, S. V., Arantes, C. R. & Netto, L. E. A 14.7 kDa protein from *Francisella tularensis* subsp. *novicida* (named FTN_1133), involved in the response to oxidative stress induced by organic peroxides, is not endowed with thiol-dependent peroxidase activity. *PLoS ONE* **9**, e99492 (2014).
50. Dieppedale, J. et al. Identification of a putative chaperone involved in stress resistance and virulence in *Francisella tularensis*. *Infect. Immun.* **79**, 1428–1439 (2011).
51. Imlay, J. A. Transcription factors that defend bacteria against reactive oxygen Species. *Annu. Rev. Microbiol.* **69**, 93–108 (2015).
52. Binesse, J., Lindgren, H., Lindgren, L., Conlan, W. & Sjostedt, A. Roles of reactive oxygen species-degrading enzymes of *Francisella tularensis* SCHU S4. *Infect. Immun.* **83**, 2255–2263 (2015).
53. Barker, J. H., Kaufman, J. W., Apicella, M. A. & Weiss, J. P. Evidence suggesting that *Francisella tularensis* O-antigen capsule contains a lipid A-like molecule that is structurally distinct from the more abundant free lipid A. *PLoS ONE* **11**, e0157842 (2016).
54. Akimana, C. & Kwaik, Y. A. *Francisella*-arthropod vector interaction and its role in patho-adaptation to infect mammals. *Front. Microbiol.* **2**, 34 (2011).

55. Knowles, H., Li, Y. & Perraud, A. L. The TRPM2 ion channel, an oxidative stress and metabolic sensor regulating innate immunity and inflammation. *Immunol. Res.* **55**, 241–248 (2013).
56. Knowles, H. et al. Transient receptor potential melastatin 2 (TRPM2) ion channel is required for innate immunity against *Listeria monocytogenes*. *Proc. Natl Acad. Sci. USA* **108**, 11578–11583 (2011).
57. Lee, B. Y., Horwitz, M. A. & Clemens, D. L. Identification, recombinant expression, immunolocalization in macrophages, and T-cell responsiveness of the major extracellular proteins of *Francisella tularensis*. *Infect. Immun.* **74**, 4002–4013 (2006).
58. McCaig, W. D., Koller, A. & Thanassi, D. G. Production of outer membrane vesicles and outer membrane tubes by *Francisella novicid*a. *J. Bacteriol.* **195**, 1120–1132 (2013).
59. Bandyopadhyay, S., Long, M. E. & Allen, L. A. Differential expression of microRNAs in *Francisella tularensis*-infected human macrophages: miR-155-dependent downregulation of MyD88 inhibits the inflammatory response. *PLoS ONE* **9**, e109525 (2014).
60. Broz, P. & Monack, D. M. Molecular mechanisms of inflammasome activation during microbial infections. *Immunol. Rev.* **243**, 174–190 (2011).
61. Henderson, B. An overview of protein moonlighting in bacterial infection. *Biochem. Soc. Trans.* **42**, 1720–1727 (2014).
62. Tunio, S. A. et al. The moonlighting protein fructose-1, 6-bisphosphate aldolase of *Neisseria meningitidis*: surface localization and role in host cell adhesion. *Mol. Microbiol.* **76**, 605–615 (2010).
63. Shams, F. et al. Fructose-1,6-bisphosphate aldolase of *Neisseria meningitidis* binds human plasminogen via its C-terminal lysine residue. *Microbiologyopen* **5**, 340–350 (2016).
64. Flores-Ramirez, G., Jankovicova, B., Bilkova, Z., Miernyk, J. A. & Skultety, L. Identification of *Coxiella burnetii* surface-exposed and cell envelope associated proteins using a combined bioinformatics plus proteomics strategy. *Proteomics* **14**, 1868–1881 (2014).
65. Loughman, J. A. & Caparon, M. Regulation of SpeB in *Streptococcus pyogenes* by pH and NaCl: a model for in vivo gene expression. *J. Bacteriol.* **188**, 399–408 (2006).
66. Ciesla, M., Mierzejewska, J., Adamczyk, M., Farrants, A. K. & Boguta, M. Fructose bisphosphate aldolase is involved in the control of RNA polymerase III-directed transcription. *Biochim. Biophys. Acta* **1843**, 1103–1110 (2014).
67. Lincet, H. & Icard, P. How do glycolytic enzymes favour cancer cell proliferation by nonmetabolic functions? *Oncogene* **34**, 3751–3759 (2015).
68. Ishihama, A. Role of the RNA polymerase alpha subunit in transcription activation. *Mol. Microbiol.* **6**, 3283–3288 (1992).
69. Anthony, L. D., Burke, R. D. & Nano, F. E. Growth of *Francisella* spp. in rodent macrophages. *Infect. Immun.* **59**, 3291–3296 (1991).
70. Lipecka, J. et al. Sensitivity of mass spectrometry analysis depends on the shape of the filtration unit used for filter aided sample preparation (FASP). *Proteomics* **16**, 1852–1857 (2016).
71. Cox, J. & Mann, M. MaxQuant enables high peptide identification rates, individualized p.p.b.-range mass accuracies and proteome-wide protein quantification. *Nat. Biotechnol.* **26**, 1367–1372 (2008).
72. Cox, J. et al. Accurate proteome-wide label-free quantification by delayed normalization and maximal peptide ratio extraction, termed MaxLFQ. *Mol. Cell. Proteomics* **13**, 2513–2526 (2014).
73. Tyanova, S. et al. The perseus computational platform for comprehensive analysis of (prote)omics data. *Nat. Methods* **13**, 731–740 (2016).

Acknowledgements

These studies were supported by INSERM, CNRS, and Université Paris Descartes Paris Cité Sorbonne. J.Z. was funded by a fellowship from the French "Délégation Générale à l'Armement" (DGA).

Author contributions

J.Z. performed most of the in vitro experiments; F.T. performed murine in vivo experiments and some immunofluorescence experiments; I.C.G. and C.C. performed the proteomic analyses and I.C.G. analyzed and compiled the data; E.C. and L.G. performed metabolomic analyses and E.C. analyzed and compiled the data; M.A., M.D., and S.K. performed some in vitro experiments; M.B. analyzed the data; A.C. designed the experiments, and J.Z. and A.C. analyzed the data and wrote the paper. The funders had no role in study design, data collection and analysis, decision to publish, or preparation of the manuscript.

Additional information

Supplementary Information accompanies this paper at doi:10.1038/s41467-017-00889-7.

Competing interests: The authors declare no competing financial interests.

La phosphorylation de la gaine du système de sécrétion de type VI contrôle la virulence de *Francisella*.

Jason Ziveri, Cerina Chhuon, Anne Jamet, Guénolé Prigent, Fabiola Tros, Monique Barel, Claire Lays, Thomas Henry, Nicholas H Keep, Ida Chiara Guerrera, Alain Charbit.

Les systèmes de sécrétion de type VI (SST6) sont utilisés par de nombreuses bactéries à Gram négatif pour transloquer des protéines effectrices dans des cellules eucaryotes ou procaryotes. *Francisella* possède un T6SS non canonique codé sur un l'îlot de pathogénicité (FPI).

Une analyse phosphoprotéomique globale et spécifique au site de la sous-espèce de *novicida* a permis l'identification de protéines avec des sites de phosphorylation uniques et conservés. Nous nous sommes concentrés dans cette étude sur la protéine IglB, qui constitue avec IglA la gaine extérieure du SST6 de *Francisella*.

En utilisant de la mutagenèse dirigée contre le site phosphorylé, nous avons démontré que la tyrosine phosphorylée unique (Y139) de la protéine IglB était cruciale pour le processus d'assemblage et de désassemblage du SST6. La substitution de ce résidu par l'alanine ou à la phénylalanine (analogue non phosphorylable) empêche la formation de la gaine et entrave l'échappement phagosomal bactérien.

L'analyse phosphoprotéomique des fractions sous-cellulaires de cultures bactériennes stimulées au KCl a révélé que seules les formes solubles de IglB étaient phosphorylées, ce qui suggère que la phosphorylation de IglB est impliquée dans le désassemblage de la gaine. Nous proposons que la modulation de l'état de phosphorylation de l'IglB constitue un mécanisme par lequel la bactérie contrôle l’assemblage / désassemblage de son SST6 pour répondre rapidement et de manière réversible à son environnement.

Phosphorylation of the Type VI secretion system sheath controls *Francisella* virulence

Jason Ziveri[1], Cerina Chhuon[2], Anne Jamet[1], Guénolé Prigent[1], Fabiola Tros[1], Monique Barel[1], Claire Lays[4], Thomas Henry[4], Nicholas H Keep[3], Ida Chiara Guerrera[2]*, Alain Charbit[1]*

[1] Université Paris Descartes, Sorbonne Paris Cité, Bâtiment Leriche, Paris, INSERM U1151 - CNRS UMR 8253, Institut Necker-Enfants Malades. Team 11: Pathogenesis of Systemic Infections, Paris, France

[2] Plateforme protéomique 3P5-Necker, Université Paris Descartes - Structure Fédérative de Recherche Necker, INSERM US24/CNRS UMS3633, Paris 75014, France

[3] Crystallography, Institute for Structural and Molecular Biology, Department of Biological Sciences Birkbeck, University of London, United Kingdom

[4] CIRI, Centre International de Recherche en Infectiologie, Université Lyon, Inserm, U1111, University Claude Bernard Lyon 1, CNRS, UMR5308, École Normale Supérieure de Lyon, Labex Ecofect, Eco-evolutionary dynamics of infectious diseases, F-69007, LYON, France

Running title: Phosphorylation of IglB is critical for *Francisella* sheath assembly

Keywords: Type 6 secretion system, Phosphoproteome, *Francisella tularensis*, IglB.

Bâtiment Leriche. 14 Rue Maria Helena Vieira Da Silva CS 61431 - 75993 PARIS – FRANCE

*Corresponding authors: Ida Chiara Guerrera, Alain Charbit.

e-mail: alain.charbit@inserm.fr; chiara.guerrera@inserm.fr

Tel: 33 1 – 72 60 65 11 — Fax: 33 1 - 72 60 65 13

Abstract

Many Gram-negative bacteria use type VI secretion systems (T6SS) to translocate effector proteins into eukaryotic or prokaryotic cells. *Francisella novicida* possesses a non-canonical T6SS encoded on the *Francisella* pathogenicity island (FPI) that is essential for efficient phagosomal escape and access to the cytosol of infected host cells. Using a global and site-specific phosphoproteomic analysis of *F. novicida*, we identified a unique phosphorylation site on IglB, the TssC homologue and a key component of the T6SS contractile sheath. We demonstrate here that phosphorylation status of IglB plays a critical role in the assembly of a functional T6SS. We propose that this post-translational modification of the sheath may constitute a previously unrecognized mechanism to modulate the dynamics of assembly-disassembly of the T6SS.

Introduction

Francisella tularensis is the causative agent of the zoonotic disease tularemia[1, 2, 3, 4]. This facultative intracellular pathogen is able to infect a variety of different cell types but, *in vivo*, is thought to replicate and disseminate mainly in phagocytes[5]. The four major subspecies (subsp) of *F. tularensis* currently listed are the subsps: *tularensis*, *holarctica, mediasiatica* and *novicida* (the latter is also called *F. novicida*). These subspecies differ in their virulence and geographical origin[6] but all cause a fulminant disease in mice that is similar to tularemia in humans[7]. Although *F. novicida* is rarely pathogenic in humans, its genome shares a high degree of nucleotide sequence conservation with the human pathogenic species and is thus widely used as a model to study highly virulent subspecies[8, 9, 10]. The efficiency of *Francisella* systemic dissemination is tightly linked to its capacity to multiply in the cytosolic compartment of infected macrophages. The transcriptional and post-transcriptional regulatory processes, controlling phagosomal escape and cytosolic bacterial multiplication, have been already well-characterized[11, 12, 13, 14, 15, 16, 17]. In contrast, the contribution of post-translational protein modifications (PTMs) has remained largely underestimated. For example, protein glycosylation has been only very recently identified in *Francisella*[18, 19] and the importance of protein phosphorylation in *Francisella* pathogenesis is still largely unknown[20], although it constitutes one of the most prevalent PTM involved in controlling protein activity.

Two major systems of protein phosphorylation exist in Gram-negative bacteria: i) two-component systems (TCSs), composed of a membrane-bound sensor kinase that auto-phosphorylates at a conserved histidine residue and a cognate response regulator that is phosphorylated at a conserved aspartate residue; and ii) serine/threonine or tyrosine protein kinases (Ser/Thr/Tyr-K) and their associated phosphatases[21, 22, 23 and references therein]. In addition, many Gram-negative bacteria also possess a phospho-relay system, designated phosphoenol pyruvate:carbohydrate phosphotransferase system (or PTS), that is more

specifically devoted to sugar transport[24, 25 and references therein]. *Francisella* genomes, do not encode any PTS[26] but encode elements of two-component regulatory systems (TCS). Whereas most *Francisella* strains possess only incomplete TCS pairs[27], *F. novicida* has two complete and two incomplete TCS pairs[28,29].

Our careful inspection of the *Francisella* genomes did not identify any gene encoding for a putative serine/threonine-protein kinase or tyrosine kinase. In spite of this lack of canonical kinases, we hypothesized that such post-translational protein modifications might occur in *Francisella* and contribute to pathogenesis. By using state-of-the art mass spectrometry analyses, we identified and quantified 82 peptides bearing phosphorylated residues in the proteome of *F. novicida.* One peptide, corresponding to a phosphorylation of IglB on tyrosine 139 (Tyr139), particularly attracted our attention. Indeed, IglB is analogous to the TssC protein in canonical T6SS and oligomerizes with IglA (TssB homologue) to form the contractile sheath[30] of its type six secretion apparatus (T6SS).

T6SS have been described as contractile syringes used by bacterial species either to kill neighboring bacteria competing for the same niche or to target eukaryotic cells upon infection. Bioinformatic analyses have divided bacterial T6SS in three phylogenetically distinct subtypes (designated T6SSi-iii)[31]. Whereas most of the well-characterized T6SS belong to the T6SSi (including in *P. areruginosa* and *V. cholerae*), *Francisella* is currently the only bacterium to possess a T6SSii family member[32]. *Francisella* T6SS has been shown, thus far, to be exclusively involved in the intracellular life cycle of the pathogen. Phagosomal escape occurs as early as 30 minutes post-infection[33] and critically depends on the T6SS that is encoded by a 33 kb locus named *Francisella* pathogenicity island (FPI)[34, 35, 36, 37, 38]. The FPI (**Supplementary Fig. 1**) also encodes a number of proteins of unknown functions, some of which (such as IglF,PdpC or PdpD) have been proposed to be T6SS effectors[9]. Remarkably, the FPI does not encode any homologue of the unfoldase ClpV, present in all the canonical T6SS, involved in the recycling of the contracted sheaths. However, it has been recently shown that, in *F. novicida*, the general chaperone ClpB[39] could fulfill ClpV

function[8] by specifically colocalizing with the contracted sheath and promoting its disassembly. Of note, the FPI is duplicated in all the subspecies of *F. tularensis* except in *F. novicida*, in which it is present in a single copy.

Our current knowledge of the structure and functional assembly of the *Francisella* T6SSii are mainly based on recent cryo-electron microscopy data[30] and structural homologies with other members of the T6SSi. It has been proposed that the tube comprised of IglC subunits (Hcp homologue) that form hexameric rings, fits within the cavity of the IglA/IglB sheath (TssB/C in *Pseudomonas*, VipA/B in *Vibrio*). Contraction of the sheath results in the ejection of the Hcp tube, together with effector proteins located within the tube and on top of the tip of the tube [40]. By analogy with other T6SS structural data, it has been suggested but not formally proven that, in *Francisella*, the sheath assembles on a preassembled IglC tube[30]. This assumption awaits additional structural information on the different conformations of the *Francisella* T6SS (from fully elongated to fully contracted stages).

The data presented here reveal that the phosphorylation status of a single tyrosine residue of IglB is essential for the proper activity of the T6SS and, hence, *Francisella* pathogenicity. We propose that, upon infection, this post-translational mechanism may participate in the control of T6SS dynamics, for a rapid and reversible response to its different intracellular environments.

Results

The phosphoproteome of *Francisella.*

We carried out a global and site-specific phosphoproteomic analysis of *F. novicida* (strain U112), based on phosphopeptide enrichment and high-resolution LC-MS/MS determination of whole cell lysates (see Methods). This analysis detected 82 phosphopeptides (68 with high probability for site attribution). The majority of the phosphosites (53 out of 82) were found on serine residues (S), while similar lower number of sites, 13 and 16, were found on threonine (T) and tyrosine (Y), respectively (**Fig. 1A and Supplementary Tables 1, 2**). In order to highlight possible consensus sequences, we aligned the sequences of the phosphoserine / threonine / tyrosine peptides. Although the number of peptides is perhaps too low to be conclusive, we could observe the recurrence of some amino acids in specific positions, like lysine (K) in position n-1 of phosphothreonines (pT) or apolar amino acids valine and phenylalanine (V, F) in n-1 of phosphotyrosines (pY) (**Fig. 1B**). These phosphosites corresponded to 49 proteins, of which 13 presented multiple phosphorylation sites. The 49 proteins belonged to various functional categories and the most represented classes were carbohydrate metabolism, energy production and conversion and translation (**Fig. 1C**).

Remarkably, the two proteins that constitute the T6SS sheath[30, 41, 42] (IglA and IglB, **Supplementary Fig. 1**) appeared to bear a unique phosphorylation site (at Ser173 for IglA, and Tyr139 for IglB). This somewhat unexpected observation prompted us to determine whether the phosphorylated forms of the two proteins were incorporated into the sheath upon its assembly. For this, we first monitored sheath formation using the procedure previously described in [30]. Briefly, lysates of wild-type *F. novicida,* grown in the presence of 5% KCl in order to trigger sheath formation, were layered onto 15%-55% sucrose gradients (**Fig. 2A**) and the different fractions were tested by western blotting with anti-Igl (A,B or C) antibodies. IglA and IglB were detected in all the fraction of the gradient, although with variable

intensities (**Fig. 2B**). In contrast, IglC was only detected in the upper fractions of the gradient (in the 15% and in part of the 35% fractions). The fractions sedimenting in equilibrium at 55% sucrose and below (55% Optiprep, grey arrow, **Fig.2A**) were further dialyzed and used for negative staining TEM imaging. Confirming earlier reports, we observed rod-shaped particles of variable length in this fraction by electron microscopy, corresponding to assembled sheath-like structures (**Fig. 2A**). We then compared by mass spectrometry the fractions at the bottom of the gradient (sucrose 55%-Optiprep 55% density zone) that contained these sheath-like particles, to the fractions at the top of the gradient (15-35% sucrose density zone), presumably containing non-polymerized forms of the IglA and IglB proteins (hereafter called “heavy fraction”, H or “light fraction”, L, respectively). The mass spectrometry analysis of the H and L fractions identified over 1,145 proteins (**Supplementary Table 3**). Of note, proteins exclusively identified in the H fraction included several Type IV pili assembly proteins (fimT, PilE, PilF) that might interact with the sheath. IglA and IglB were detected in both H and L fractions. In order to estimate the proportion of the Igl proteins in the two fractions, we calculated the ratio of the intensity of the protein, proportional to the amount of protein in the fraction. Fully supporting the western blotting analyses, IglA and B were more abundant in the L fraction than in the H fraction and only 2% of IglC was detected in the H fraction (**Fig. 2C**).

As illustrated in **Fig. 2D**, the peptide bearing the phosphorylated tyrosine residue (pY139) of IglB was exclusively detected in the L fraction of the gradient, suggesting that only the soluble forms of IglB are phosphorylated (**Supplementary Table 3**). Unmodified peptides containing Tyr139 were however detected in both H and L fractions, indicating that soluble IglB include both phosphorylated and unphosphorylated forms of the protein. The phosphopeptide, bearing the phosphorylated serine residue of IglA, identified in the whole cell lysate, was not detected in either of the two samples analyzed. This lack of detection could be due either to an insufficient amounts (below the threshold of detection), to its localization in other fractions of the gradient that were not tested or to the fact that KCl treatment might have triggered its dephosphorylation.

We decided to focus here on IglB and evaluate the importance of the phosphorylation on Tyr139 on T6SS functionality and *Francisella* pathogenicity.

Comparative sequence analyses on 33 IglB proteins from 19 genomes of the *Francisella* genus were performed to evaluate the conservation of residue Tyr139 (**Supplementary Fig. 2**). All, but 5 genomes, encode two IglB proteins (due to the duplication of the FPI in these genomes). Sequences were highly conserved between 31 IglB proteins sharing 93 to 100% amino acid identity. In contrast, the proteins encoded by *FTN_0043,* encoded in another genomic island termed the *F. novicida* island or FNI[42]) and *F7308_1917* (Fsp_TX077308) exhibit only 48% amino acid identity with the 31 other IglB proteins whereas they both share 85% identity. Excluding these 2 outliers, among 506 sites, 458 were without polymorphism (91%), with Tyr139 conserved in all IglB sequences (**Supplementary Fig. 2**). Of note, since IglB is among the most conserved components of T6SS[30, 41] (**Supplementary Fig. 1**) we were able to retrieve orthologues of IglB encoded outside of *Francisella* genus. Out of 535 non-redundant IglB orthologues (also named VipB, TssC or EvpB/VC_A0108), we found 90 sequences with a tyrosine in the vicinity of Tyr139 site outside of *Francisella* genus. In 82 sequences, the predicted location of the tyrosine residue was similar to that of Tyr139 (in a turn region between two helices) (**Supplementary Fig. 2**).

3D analysis.

Inspection of the 3.7 Å EM reconstruction of the *F. novicida* sheath[32] (PDB 3j9o) does not show any atoms close enough to form a hydrogen bond with the hydroxyl of Tyr139. However, the carboxylates of Asp114 from IglB, and Asp63 of IglA in the next dimer, are around 5 Å away. At the resolution of the reconstruction, side chain positions are not clearly defined and so these may approach close enough to Tyr139 OH to form hydrogen bond interactions stabilizing the assembly.

There is space for a phosphate group on this atom as the OH is pointing into a pocket in the structure (**Fig. 3**). This was modeled by adding a phosphate group (using ccp4mg to

position a phosphate and then editing the PDB file to generate a PTR residue) onto the hydroxyl and showing there were no steric clashes. However, the negatively charged phosphate would induce charge repulsion with the nearby Asps from the next dimer most likely preventing assembly of the strands when Tyr139 is phosphorylated.

Hence, the charge repulsion provoked by addition of the phosphogroup (when Y139 is phosphorylated) is likely to weaken the stability of the assembled sheath.

Role of IglB phosphorylation on IglA/IglB interaction and sheath formation.

We evaluated the importance of the phosphorylation site in IglB on T6SS assembly and bacterial virulence by constructing two IglB variants in which Tyr139 was substituted either by an alanine (Ala) or by the non-phosphorylatable aromatic analogue phenylalanine (Phe). These IglB mutated proteins (designated Y139A and Y139F, respectively) were expressed *in trans* in a Δ*iglB* mutant of *F. novicida* carrying a chromosomal deletion of the entire *iglB* gene, (see Methods). A *F. novicida* mutant with a deletion of the entire *FPI*, unable to escape from phagosomes and hence to grow in macrophages[43], was used as a negative control.

The mutations Y139A and Y139F had no effect on bacterial growth in broth (**Supplementary Fig. 3**). The impact of Y139A and Y139F substitutions was first tested by Western blotting on whole cell lysates. As expected (**Fig. 4A**), IglB was detected in wild-type and complemented strains but not in the Δ*iglB* and Δ*FPI* strains. IglA was detected in all the strains, except the ΔFPI mutant, but in clearly lower amounts in the Δ*iglB* strain. This observation is in agreement with earlier observations[44], suggesting that the presence of IglB increases the stability of the IglA protein.

A classical measure of basal T6SS function is the export of an Hcp-related protein. Therefore, we examined IglB-dependent IglC export in the different *F. novicida* mutant strains by Western-blot on bacteria grown in the presence -or absence- of 5% KCl. In agreement with previous reports, IglC was detected in the culture supernatant in the presence, but not in the absence, of KCl, in the wild-type and $iglB_{WT}$ complemented strains.

In contrast, deletion of *iglB* as well as the two single amino acid substitutions in IglB abolished the secretion of IglC into the culture medium (**Fig. 4B**), revealing that a wild-type form of IglB is required for IglC secretion. KCl treatment did not modify the amounts of IglA, IglB and IglC proteins detected by western blotting on whole cells (bacterial pellet fractions).

To test if any of the two substitutions at Tyr139 would impair IglA/IglB heterodimer formation, we performed co-immunoprecipitation assays (**Fig. 4C**), using either anti-IglA to precipitate the complex, followed by western blotting with anti-IglB (upper panel) or anti-IglB, followed by western blotting with anti-IglA (lower panel). In both assays, the two IglB mutant alleles (Y139A and Y139F) were able to interact with IglA like wild-type IglB.

Since the presence of sheath-like structures correlated with the presence of non-phosphorylated forms of IglB (**Fig. 2**), we anticipated that the non-phosphorylatable Y139F mutant might permanently produce oligomerized sheath-like structures. To test this possibility, we performed sucrose gradient fractionation followed by western blotting (as described previously) on the Y139F mutant strain. In contradiction of the above hypothesis, the proteins IglA and IglB were detected in the L fractions of the gradient but not in the H fraction corresponding to the sheath (**Fig. 3D**) and no sheath-like structure could be visualized by TEM in the H fraction of the Y139F mutant. Mass spectrometry analysis of the fractions confirmed that only a very low portion of the IglA, B and C is present in the H fractions compared to the L (**Fig. 4E**). Since the only difference between the non-phosphorylated form of Tyr139 and its non-phosphorylatable Phe analogue is the presence of an additional hydroxyl moiety, it is likely that this hydroxyl contributes to sheath formation/stability.

Critical role of IglB residue Y139 in *Francisella* pathogenesis.

We next evaluated the impact of the Y139A and Y139F mutations on bacterial virulence by studying their behavior in macrophages and in the mouse model. The ability of wild-type *F. novicida* (WT), Δ*iglB* and complemented strains (CpWT, Y139A and Y139F) to survive and

multiply in murine macrophage-like J774.1 cells was monitored over a 24 h-period (**Fig. 5A**). Confirming earlier reports[45], intracellular multiplication of the Δ*iglB* mutant was essentially abolished and comparable to that of the Δ*FPI* mutant. The single amino acid substitution of Tyr139 by Ala (Y139A) was also sufficient to abolish intracellular bacterial multiplication. A severe intracellular growth defect was also recorded when Tyr139 was substituted by Phe (Y139F), until 10 h after infection (almost fifty-fold less bacterial counts). However, at 24 h, the Y139F mutant strain multiplied and showed a ten-fold reduction of bacterial counts compared to wild-type, suggesting that a late phagosomal escape had occurred in the Y139F mutant, therefore promoting some cytosolic bacteria multiplication. As expected, functional complementation (*i.e.,* introduction of a plasmid-born wild-type *iglB* allele into the Δ*iglB* mutant strain (CpWT)) restored wild-type growth.

We next tested the intracellular behavior of the Δ*iglB* mutant and complemented strains in primary bone marrow-derived macrophages (BMMs). Growth of the Δ*iglB* deletion mutant as well as that of the two Y139A or Y139F was identical to that of the Δ*FPI* mutant (**Fig. 5B**) at all time points tested. The fact that no multiplication of Y139F was recorded at 24 h is most likely due to the higher bactericidal activity of primary macrophages compared to the J774-1 cell line. Functional complementation restored normal intracellular bacterial replication (in CpWT).

The impact of the mutations in *iglB* on bacterial virulence was evaluated in an *in vivo* competition assay between wild-type (WT) and Δ*iglB* mutant bacteria. For this, we monitored the bacterial burden in spleen and livers 2.5 days after infection of 7-week-old female BALB/c mice by the intra-peritoneal route (**Fig. 5C**). The competition index recorded for the *iglB* mutants (Y139A and Y139F) was very low ($\leq 10^{-6}$ in both target organs for Y139F; $\leq 10^{-5}$ in livers and $\leq 10^{-6}$ in spleens for Y139A), demonstrating the importance of residue Tyr139 in *Francisella* virulence in the mouse model. As a control, we also performed an *in vivo* competition assay between wild-type and the Δ*iglB* complemented strain (WT and CpWT). The competition index recorded close to 1 for CpWT ($\leq 10^{-1}$ in both target organs), confirmed almost complete functional complementation.

To determine whether this lack of intracellular multiplication, associated with reduced virulence, was due to impaired access to the host cytosol or aborted cytosolic multiplication, we compared the ability of the Δ*iglB* mutants to escape from the phagosomal compartment to that of the wild-type strain. For this, we first monitored co-localization of intracellular bacteria with LAMP-1, in J774-1 macrophages (**Fig. 5D**), using specific antibodies and automated quantification (**Fig. 5E**). The frequency of bacteria co-localizing with LAMP-1 at all 3 time points was elevated (between 60% and 90%), with Δ*iglB* and the two complemented strains expressing mutated *iglB* alleles (designated Y139A and Y139F; respectively). In contrast, co-localization of the wild-type strain with LAMP-1 was below 20% after 1 h and remained in the same range throughout the infection. These results strongly suggest that the Δ*iglB* mutant as well as the two complemented strains expressing mutated *iglB* alleles, are still trapped in the phagosomal compartment after 10 h, whereas the wild-type strain has already escaped into the cytosol after 1 h.

The ability of the Δ*iglB* mutants to induce phagosomal membrane rupture was further tested by using a CCF4 assay in BMMs, essentially as previously described[42, 46]. Briefly, bacteria were added to the macrophages at multiplicity of infection (MOI) of 100. After 1 h of infection, cells were loaded for 1 h with CCF4. *F. novicida* naturally secretes β-lactamase that is able to cleave the cytosolic CCF4 substrate. Once CCF4 is lysed, its emission spectrum changes from 535 nm (green) to 450 nm (blue). Wild-type *F. novicida* and CpWT strains showed similar amount of cleaved CCF4 at the three time-points tested (1 h, 3 h and 6 h) whereas there was no (or marginal) loss of FRET signal with Δ*iglB* (**Fig. 5F**), Y139A, Y139F, and in the two negative control strains Δ*FPI* and Δ*bla,* carrying a deletion of the functional copy of the β-lactamase-encoding gene. These data confirmed that the two *iglB* mutant strains (Y139A, Y139F) remained confined into intact phagosomes at least up to 6 h after infection.

Cytosolic escape of wild-type *F. novicida* is associated with the release of DNA that is sensed by the host macrophage and triggers innate immune responses, namely secretion of type I interferon (IFN), and activation of the AIM2 inflammasome[47, 48, 49]. In contrast, mutants

that remain trapped in the phagosomal compartment generally fail to induce type I IFN secretion[42]. To check whether in spite of their phagosomal confinement, the *iglB* mutants could still promote some cytosolic immune response, we quantified Type I IFN secretion triggered upon infection with the *iglB* mutant strains, in supernatants of BMMs infected for different time points (1 h, 3 h and 6 h; **Fig. 6A**) by an ISRE-luciferase bioassay[50]. IFN secretion reached between 25 and 30 U/mL after 6 h, for both WT and CpWT complemented strains whereas it remained below 5 U/mL for the other mutant strains tested, further demonstrating that the *iglB* mutants remained trapped in phagosomes during the time course of these assays.

Finally, cell death kinetics were determined to monitor possible cytotoxicity in infected BMMs (measured by real time propidium iodide incorporation). Indeed, host cell death could be an alternate explanation for the lack of bacterial intracellular multiplication. As expected, delayed cell death (starting five hours after infection) was observed in BMM infected with wild-type *F. novicida* (**Fig. 6B**) as a result of normal intracellular bacterial multiplication and activation of the AIM2 inflammasome. The Δ*iglB* complemented strain (CpWT) showed similar cell death kinetics to the WT strain. In contrast, none of the other strains tested had any substantial effect on BMM death, demonstrating that the intracellular multiplication defects of the Y139A, Y139F mutant strains were not due to increased cytotoxicity and further demonstrating that these mutants are likely to be stuck in intact phagosomes.

These data demonstrated that residue Y139 of IglB is critical for functional T6SS assembly, phagosomal escape and bacterial virulence and suggested that only the unphosphorylated form of the protein was incorporated into sheath structures.

To verify that a residue possibly mimicking the phosphorylated state of Tyr139 would be deleterious for functional T6SS assembly, we replaced Tyr139 by two phosphomimetics *i.e.* the negatively charged amino acids Aspartate and Glutamate. We first evaluated the impact of these amino acid substitutions (Y139D and Y139E) on intracellular multiplication in J774-1 cells (**Supplementary Fig. 4A**). The two mutants led to severe defects in intracellular multiplication and, at all time points tested, the replication defect was comparable to that of

the Y139A or Δ*FPI* mutant. We next evaluated the capacity of the Y139D and Y139E mutants to form sheath-like structure by using the sucrose gradient assay. In the two mutants, the IglB protein was exclusively detected by Western blot in the L fractions of the sucrose gradient (**Supplementary Fig. 4B**), strongly suggesting that the two amino acid substitutions at Tyr139 also prevented sheath-like assembly.

Altogether, the data presented support the notion that dephosphorylated Tyr139 is required for functional sheath assembly. Furthermore, they suggest that the free hydroxyl group, present on the aromatic ring of the dephosphorylated form of Tyr139 (absent in the Y139F mutant; **Supplementary Table 4**), plays an important role in the assembly of IglA/IglB oligomers.

Discussion

We show here that phosphorylation status of IglB critically influences T6SS functional assembly, bacterial phagosomal escape and virulence. This post-translational modification of the sheath could constitute a mechanism controlling the dynamics of T6SS assembly.

Phosphorylation of the sheath, a novel player in control of the T6SS

Cryo-electron microscopy analyses [30] have demonstrated that the FPI of *F. novicida* encodes a genuine T6SS and proposed a model in which the sheath of the T6SS is composed of discs of heterodimers of inter-digitated IglA/IglB proteins. The dynamics of T6SS sheaths have also been studied by live imaging approaches[8, 51 and references therein]. However, the molecular mechanisms associated with T6SS sheath contraction remain speculative. Interestingly, the recently published structure of the sheath of one of T6SS of *P. aeruginosa* (TssB1C1 from H1-T6SS)[52] suggests that the sheath shifts from an extended state to a contracted state using a spring-like motion that might be conserved in other T6SS.

Formation of the *Francisella* T6SS is believed to occur in the phagosome before cytosolic escape of the bacterium. Nevertheless, T6SS elements are also likely to be required during the cytosolic stage of the infectious cycle. Indeed, most FPI genes are induced during late intra-macrophage growth[53] and IglC has been shown to be required for intracellular growth of *F. novicida* that are microinjected directly into the cytosol of HeLa cells[54]. IglC-export in *F. novicida* depends on the T6SS core components IglA and IglB[55]. Of note, Clemens *et al*.[30] reported that some split-GFP fusions with truncated IglA proteins, although still able to form IglA/IglB-heterodimers, had lost their IglC secretory function, which suggests that heterodimer formation is not sufficient to generate a functional sheath.

Mass spectrometry analyses revealed that IglB contained a phosphorylated residue (Tyr139). Remarkably, this residue was found in a phosphorylated form exclusively in non-oligomerized IglB proteins, suggesting that the phosphorylation status of IglB residue Tyr139 could be instrumental in the biogenesis of a functional T6SS. The substitution of Tyr139

either by an alanine or by the non-phosphorylatable aromatic analogue phenylalanine still allowed the interaction of IglA and IglB in co-immunoprecipitation assays. However, both substitutions prevented secretion of IglC in the culture supernatant, revealing impaired T6SS expression in these mutants. Fully supporting the notion that phosphorylation of Tyr139 impairs sheath assembly, replacement of this residue by a phosphomimetic (Y139D or Y139E) led to a severe intracellular multiplication defect and prevented sheath-like structure formation.

Our 3D predictions suggest that the OH of tyrosine, that is absent in the aromatic ring of phenylalanine (**Fig. 3 and Supplementary Table 4**), might be important for sheath formation. Upon addition of a phosphoryl moiety at this position, charge repulsion between the phosphate group and nearby aspartate residues would lead to the interaction between IglA and IglB being destabilized. Therefore, phosphorylation is unfavorable for the formation of stable hexameric rings and sheath-like structures. The fact that a late phagosomal escape of the Y139F mutant apparently occurred in J774-1 macrophages (translated by some bacterial multiplication at 24 h) tends to suggest that a partially active T6SS could still assemble in the Y139F mutant.

Possible regulatory mechanisms involved in tyrosine phosphorylation

Protein phosphorylation on tyrosine is catalyzed by autophosphorylation of ATP-dependent protein-tyrosine kinases[56]. Bacterial tyrosine kinases do not share sequence homology with eukaryotic tyrosine kinases (also called Hanks-type kinases) and, hence, have been named BY-kinases. To date, the best-characterized function of BY-kinases is related to capsular polysaccharide synthesis[57]. Two main classes of bacterial tyrosine phosphatases catalyze the reverse reaction: conventional eukaryotic-like phosphatases and low molecular weight acidic phosphatases. *M. tuberculosis* possesses only one tyrosine kinase (PtkA), but encodes two tyrosine phosphatases (PtpA and PtpB); the latter being also active against phospho-Ser and phospho-Thr residues). These two tyrosine phosphatases have been shown to act on host tyrosine signaling pathways. *S. aureus* also encodes one PtpA

orthologue (designated PtpA, sharing 32% amino acid identity with PtpA of *M. tuberculosis*) that is phosphorylated by the tyrosine kinase CapA1B2 and secreted by the bacterium [57], suggesting that, like in *M. tuberculosis*, the *S. aureus* PtpA protein could act as a host cell signaling molecule[58].

As mentioned earlier, the *Francisella* genomes do not encode a canonical tyrosine kinase. However, we identified a unique gene encoding a highly conserved protein (97.5% amino acid identity between the different *F. tularensis* subsps), that is predicted be a low molecular weight phosphotyrosine protein phosphatase (FTN_1046 in *F. novicida*). This protein, designated PtpA, is composed of 161 amino acids and shares 40.1% amino acid identity with its orthologue in *Staphylococcus aureus* (SAAG_02400), 29.2% with PtpA of *M. tuberculosis* (TMBG_01746) and less than 28% amino acid identity with the tyrosine phosphatase of *Escherichia coli* (Wzb and Etp[59]; **Supplementary Fig. 5**).

This prompted us to evaluate the impact of *ptpA* inactivation on *F. novicida* virulence, using a *ptpA* transposon insertion mutant (from the *F. novicida* Tn insertion library[60]). We evaluated the capacity of the *ptpA* mutant to survive and multiply in J774.1 cells, over a 24 h-period. We assumed that if PtpA served to dephosphorylate IglB, its inactivation would lead to a constitutive production of sheath-like structures in this mutant that might affect normal intracellular bacterial multiplication. The *ptpA* mutant multiplied in these cells like the wild-type strain (**Supplementary Fig. 5**). We also evaluated the functionality of the T6SS in this mutant by monitoring IglC secretion in the supernatant of KCl-induced bacterial cultures and on the formation of sheath-like structures by sucrose fractionation and western blotting. Confirming the kinetics of intracellular multiplication, iglC secretion and T6SS assembly were similar in the *ptpA* mutant to that of the wild-type strain. Altogether, these data strongly indicate that, in Francisella, the protein PtpA does not play a role in T6SS assembly. At this stage, it cannot be excluded that this putative phosphatase could play a similar function to its secreted orthologues in *S. aureus* or *M. tuberculosis* that act on host proteins.

Thanks to the recent improvements in phosphoproteomic approaches, novel families of protein kinases with a Ser/Thr/Tyr kinase activity have been identified[23]. It is likely that

Francisella expresses non-canonical Ser/Thr/Tyr kinase-like activities that still await authentication and characterisation.

Structural and functional implications of IglB phosphorylation

Tyrosine phosphorylation can regulate protein activity in multiple ways, including causing electrostatic effects and allosteric transitions, but the most important function of phosphotyrosine is to serve as a docking site for specific interaction with a target protein that contains a phosphotyrosine binding domain. The Src homology 2 (SH2) domains represent the largest class of known phosphotyrosine recognition domains in eukaryotic proteins[61] and tyrosine phosphorylation serves to recruit SH2-containing targets.

Remarkably, no specific phosphotyrosine binding proteins have been found in bacteria. Since the phosphate on Tyr is linked to the O^4 position of the phenolic ring, and therefore lies much further away from the peptide backbone than the phosphate on the β-OH groups of Ser and Thr, the effects of Tyr phosphorylation in bacteria may be exerted primarily through allosteric/electrostatic effects. Looking at the full helical reconstruction, one can see that Y139 is close to both D63 of IglA and D114 of IglB. These are from two different symmetry-related chains (**Fig. 3**). Putting a phosphate on Y139 is likely to repel the aspartate residues and to disassemble the structure. Although, Aspartates and a Glutamate are not a likely environment for a Phosphate, there is a quite large pocket which may be able to accommodate the phosphate.

Since both Y139A and Y139F substitutions in IglB impaired secretion of IglC in the supernatant of KCl-stimulated bacterial cultures (**Fig. 6B**) and prevented normal phagosomal escape in BMDM macrophages (**Fig. 4, Fig. 5**), it is clear that Tyr139 of IglB plays a critical role in the functional assembly of the T6SS. Moreover, the fact that Y139F substitution also prevented the formation of a sheath-like structure in KCl-stimulated bacteria, further indicates that the presence of the non-phosphorylated OH moiety on the C4 of the phenol ring is also important for proper assembly of the T6SS. The absence of phosphorylated IglB peptide

(carrying Y139p) in sheath like structures (**Fig. 2C,** and **Supplementary Table 2**), suggests that phosphorylation of IglB is not favorable for sheath assembly (**Fig. 7)**. Hence, it is tempting to propose that modulating the phosphorylation status of IglB could represent a simple and rapid mean for *Francisella* to regulate T6SS assembly/disassembly process (**Fig. 7)**. Upon entry into the host cell phagosome, induced expression of IglB generated by induction of the FPI (dephosphorylated form due to a reduced phosphorylation and/or increased dephosphorylation) would promote T6SS assembly. Once in the cytosol, phosphorylation of IglB (due to a reduced dephosphorylation and/or and increased dephosphorylation) would then favor disassembly the contracted T6SS in concert with the general stress chaperone ClpB[39] and allow active cytosolic bacterial multiplication. In the Tyr139 mutant, bacteria remain trapped in the phagosome because of their inability to promote efficient sheath assembly.

The post-translational phosphorylation of protein is a rapid and reversible mechanism. Hence, yet unidentified phosphorylation-dependent mechanisms controlling the dynamics of T6SS assembly might exist in other pathogens and should be carefully re-examined.

Methods

Ethics Statement. All experimental procedures involving animals were conducted in accordance with guidelines established by the French and European regulations for the care and use of laboratory animals (Decree 87–848, 2001–464, 2001–486 and 2001–131 and European Directive 2010/63/UE) and approved by the INSERM Ethics Committee (Authorization Number: 75-906).

Strains and culture conditions

All strains used in this study are derived from *F. tularensis* subsp. *novicida* U112 (*F. novicida*) as described in **Supplementary Table 5**. Strains were grown at 37°C on pre-made chocolate agar PolyViteX plates (BioMerieux), Schaedler K3 or Chemically Defined Medium (CDM). The CDM used for *F. novicida* corresponds to standard CDM [62] without threonine and valine[63]. For growth condition determination, bacterial strains were inoculated in the appropriate medium at an initial OD_{600} of 0.05 from an overnight culture in Schaedler K3 medium.

Construction of a Δ*iglB* deletion mutant

We inactivated the gene *iglB* in *F. novicida* (*FTN_1323*) by allelic replacement resulting in the deletion of the entire gene (4 first codons and 7 last codons were conserved). We constructed a recombinant PCR product containing the upstream region of the gene *iglB* (*iglB*-UP), a kanamycin resistance cassette (*nptII* gene fused with *pGro* promoter) and the downstream region of the gene *iglB* (*iglB*-DN) by overlap PCR. Primers *iglB* upstream FW (p1) and *iglB* upstream (spl_K7) RV (p2) amplified the 689 bp region upstream of position +3 of the *iglB* coding sequence (*iglB*-UP), primers *pGro* FW (p3) and *nptII* RV (p4) amplified the 1091 bp kanamycin resistance cassette (*nptII* gene fused with *pGro* promoter); and primers

iglB downstream (spl_K7) FW (p5) and *iglB* downstream RV (p6) amplified the 622 bp region downstream of the position +1520 of the *iglB* gene coding sequence (*iglB*-DN). Primers p2 and p5 have an overlapping sequence of 12 nucleotides with primers p3 and p4 respectively resulting in fusion of *iglB*-UP and *iglB*-DN with the cassette after cross-over PCR. All single fragment PCR reactions were realized using Phusion High-Fidelity DNA Polymerase (ThermoScientific) and PCR products were purified using NucleoSpin® Gel and PCR Clean-up kit (Macherey-Nagel). Overlap PCRs were carried out using 100 ng of each purified PCR products and the resulting fragment of interest was purified from agarose gel. This fragment was then directly used to transform wild type *F. novicida* by chemical transformation [64]. Recombinant bacteria were isolated on Chocolate agar plates containing kanamycin (10 µg mL^{-1}). The mutant strains were checked for loss of the wild type gene by PCR product direct sequencing (GATC-biotech) using appropriate primers.

Functional complementation

The Δ*iglB* mutant strain was transformed with the recombinant pKK214-derived plasmids (pKK-*iglBY139A*$_{cp}$, pKK-*iglBY139F*$_{cp}$, pKK-*iglBY139D*$_{cp}$ and pKK-*iglBY139E*$_{cp}$) described below (**Supplementary Table 5**). Primers pGro[65] FW and pGro RV amplified the 328 bp of the *pGro* promoter and primers *iglB* FW / *iglB*[PstI] RV amplified the 1,534 bp *iglB* gene from U112. PCR products were purified and SmaI (*pGro* promoter) or PstI (*iglB*) digested in presence of FastAP Thermosensitive Alkaline Phosphatase (ThermoScientific) to avoid self-ligation. Mixtures of *pGro* promoter and fragments of the genes of interest were then incubated with T4 DNA Ligase (New England Biolabs) to allow blunt end ligation and fragments were then cloned in pKK214 vector after SmaI/PstI double digest and transformed in *E. coli* TOP10. Recombinant plasmid pKK-*iglB*$_{cp}$ was purified and directly used for chemical transformation in *F. novicida* Δ*iglB* [64]. Recombinant colonies were selected on Chocolate agar plates containing tetracycline (5 µg mL^{-1}) and kanamycin (10 µg mL^{-1}).

For site-directed mutagenesis of *iglB* gene, we used plasmid pKK-*iglB*$_{cp.}$ The recombinant plasmids pKK-*iglBY139A*$_{cp}$, pKK-*iglBY139F*$_{cp}$, pKK-*iglBY139D*$_{cp}$ and pKK-*iglBY139E*$_{cp}$ were constructed using the primer pairs iglB (Y/A, Y/F,Y/D, or Y/E) FW and iglB RV (**Supplementary Table 6**). The three first bases of primers iglB FW were modified to change Tyr139 to Ala, Phe, Asp or Glu

PCR products were purified, phosphorylated by the T4 Polynucleotide Kinase and then incubated with T4 DNA Ligase (New England Biolabs) and transformed in *E. coli* TOP10. Recombinant plasmids were purified and directly used for chemical transformation in *F. novicida* Δ*iglB*, as described previously[64]. Recombinant colonies were selected on Chocolate agar plates containing tetracycline (5 µg mL^{-1}) and kanamycin (10 µg mL^{-1}).

Immunodetection

Antibodies to IglA, IglB and IglC were obtained through the NIH Biodefense and Emerging Infections (BEI) Research Resources Repository, NIAID, NIH.

Immunoblotting analysis. Protein lysates for immunoblotting were prepared by using Laemmli sample buffer. Protein lysates corresponding to equal OD_{600} were loaded on 12% Bis/Tris gels (Invitrogen), and run in TGS buffer. Primary antibodies (anti-IglA or anti-IglB) were used at final dilution of 1:2,000. Secondary horseradish peroxidase (HRP)-conjugated goat anti-mouse antibody (Santa Cruz Biotechnology, CA, USA) or (HRP)-conjugated goat anti-rabbit antibody and the enhanced Chemiluminescence system (ECL) (Amersham Biosciences, Uppsala, Sweden) were used as previously described [66].

Co-immunoprecipitations. Wild-type *F. novicida* was grown to late exponential phase in Schaedler K3; collected by centrifugation and lysed with lysozyme and 1% TritonX-100 detergent in 20 mM Tris HCl, (pH 7.8) with 1 mM EDTA, protease inhibitor cocktail and benzonase nuclease. The lysate was centrifuged at 15,000 g for 15 min at 4°C to pellet bacterial debris. Monoclonal anti-IglB antibody was incubated 40 min with Dynabeads protein G (Invitrogen) and the complex was incubated at room temperature with the bacterial lysate

for 1 hour. After washing, the complex was loaded on 12% Bis/Tris gels (Invitrogen), and run in TGS buffer.

Purification of T6SS

T6SS were prepared essentially as described in [30]. Briefly, wild-type *F. novicida* was grown to late exponential phase in Schaedler K3 containing 5% KCl; pelleted by centrifugation and lysed with lysozyme and 1% TritonX-100 detergent in 20 mM Tris HCl, (pH 7.8) with 1 mM EDTA, protease inhibitor cocktail and benzonase nuclease. The lysate was centrifuged 3 times at 15,000 g for 30 min at 4°C to pellet bacterial debris, and the supernatant was layered onto a 10%–55% sucrose gradient overlying a 55% Optiprep cushion and centrifuged at 100,000 g for 18 hr. Fractions were collected and examined by TEM negative staining using 2% uranyl acetate. The sheath-like structures sedimented to just below the 55% sucrose/Optiprep interface.

Phosphoproteomic analyses

Reagents and chemicals. For protein digestion, dithiothreitol, iodoacetamide and ammonium bicarbonate were purchased from Sigma-Aldrich (St Louis, MO, USA). For phosphopeptide enrichment and LC-MS/MS analysis, trifluoroacetic acid (TFA), formic acid, acetonitrile and HPLC-grade water were purchased from Fisher Scientific (Pittsburgh, PA, USA) at the highest purity grade.

Protein digestion. For proteomic analysis, *F. novicida* was analysed in three independent biological replicates. Protein concentration was determined by DC assay (Biorad, CA, USA) according to the manufacturer's instructions. An estimated 1.2 mg of proteins for each biological replicates were digested following a FASP protocol[67] slightly modified. Briefly, proteins were reduced using 100 mM dithiothreitol in 50 mM ammonium bicarbonate for 1h at 60°C. Proteins were then split into four samples of 300 µg and applied on 30 kDa MWCO centrifugal filter units (Microcon, Millipore, Germany, Cat No MRCF0R030). Samples were

mixed with 200 µL of 8M urea in 50 mM ammonium bicarbonate (UA buffer) and centrifuged for 20 min at 15,000 x g. Filters were washed with 200 µL of UA buffer. Proteins were alkylated for 30min by incubation in the dark at room temperature with 100 µL of 50 mM iodoacetamide in UA buffer. Filters were then washed twice with 100 µL of UA buffer (15,000 x g for 15 min) followed by two washes with 100 µL of 50 mM ammonium bicarbonate (15,000 x g for 10 min). Finally, sequencing grade modified trypsin (Promega, WI, USA) was added to digest the proteins in 1:50 ratio for 16 h at 37°C. Peptides were collected by centrifugation at 15,000 x g for 10min followed by one wash with 50mM ammonium bicarbonate and vacuum dried.

Phosphopeptides enrichment by titanium dioxide (TiO_2) and phosphopeptides purification by graphite carbon (GC). Phosphopeptide enrichment was carried out using a Titansphere TiO_2 Spin tip (3 mg/200 µL, Titansphere PHOS-TiO, GL Sciences Inc, Japan) an estimated 1.2 mg of digested proteins for each biological replicate. Briefly, the TiO_2 Spin tips were conditioned with 20 µL of solution A (80% acetonitrile, 0,1% TFA), centrifuged at 3,000 x g for 2min and equilibrated with 20µL of solution B (75% acetonitrile, 0,075% TFA, 25% lactic acid) followed by centrifugation at 3,000 x g for 2 min. Peptides were resuspended in 10 µL of 2% TFA, mixed with 100 µL of solution B and centrifuged at 1,000 x g for 10min. Sample was applied back to the TiO_2 Spin tips two more times in order to increase the adsorption of the phosphopeptides to the TiO_2. Spin tips were washed with, sequentially, 20 µL of solution B and two times with 20 µL of solution A. Phosphopeptides were eluted by the sequential addition of 50 µL of 5% NH_4OH and 50 µL of 5% pyrrolidine. Centrifugation was carried out at 1,000 x g for 5 min.

Phosphopeptides were further purified using GC Spin tips (GL-Tip, Titansphere, GL Sciences Inc, Japan). Briefly, the GC Spin tips were conditioned with 20 µL of solution A, centrifuged at 3,000 x g for 2 min and equilibrated with 20 µL of solution C (0,1% TFA in HPLC-grade water) followed by centrifugation at 3,000 x g for 2 min. Eluted phosphopeptides from the TiO_2 Spin tips were added to the GC Spin tips and centrifuged at 1,000 x g for 5 min. GC

Spin tips were washed with 20 µL of solution C. Phosphopeptides were eluted with 70 µL of solution A (1,000 x g for 3 min) and vacuum dried.

nanoLC-MS/MS protein identification and quantification. Samples were resuspended in 12 µL of 0.1% TFA in HPLC-grade water. For each run, 5 µL was injected in a nanoRSLC-Q Exactive PLUS (RSLC Ultimate 3000, Thermo Scientific, MA, USA). Phosphopeptides were loaded onto a µ-precolumn (Acclaim PepMap 100 C18, cartridge, 300 µm i.d.×5 mm, 5 µm, Thermo Scientific, MA, USA) and were separated on a 50 cm reversed-phase liquid chromatographic column (0.075 mm ID, Acclaim PepMap 100, C18, 2 µm, Thermo Scientific, MA, USA). Chromatography solvents were (A) 0.1% formic acid in water, and (B) 80% acetonitrile, 0.08% formic acid. Phosphopeptides were eluted from the column with the following gradient 5% to 40% B (180 min), 40% to 80% (6 min). At 181 min, the gradient returned to 5% to re-equilibrate the column for 20 minutes before the next injection. Two blanks were run between each sample to prevent sample carryover. Phosphopeptides eluting from the column were analyzed by data dependent MS/MS, using top-8 acquisition method. Phosphopeptides were fragmented using higher-energy collisional dissociation (HCD). Briefly, the instrument settings were as follows: resolution was set to 70,000 for MS scans and 17,500 for the data dependent MS/MS scans in order to increase speed. The MS AGC target was set to 1 x 10^6 counts with maximum injection time set to 250 ms, while MS/MS AGC target was set to 2 x 10^5 with maximum injection time set to 250 ms. The MS scan range was from 400 to 1.800 m/z. MS and MS/MS scans were recorded in profile mode. Dynamic exclusion was set to 30 seconds.

Data Processing Following nanoLC-MS/MS acquisition. The MS files were processed with the MaxQuant software version 1.5.3.30 and searched with Andromeda search engine against the UniProtKB/Swiss-Prot *F. tularensis* subsp. *novicida* database (release 28-04-2014, 1719 entries). To search parent mass and fragment ions, we set an initial mass deviation of 4.5 ppm and 0.5 Da respectively. The minimum peptide length was set to 7 amino acids and strict specificity for trypsin cleavage was required, allowing up to two missed

cleavage sites. Carbamidomethylation (Cys) was set as fixed modification, whereas oxidation (Met), N-term acetylation and phosphorylation (Ser, Thr, Tyr) were set as variable modifications. The match between runs option was enabled with a match time window of 0.7 min and an alignment time window of 20 min. The false discovery rates (FDRs) at the protein and peptide level were set to 1%. Scores were calculated in MaxQuant as described previously[68]. The reverse and common contaminants hits were removed from MaxQuant output.

The phosphopeptides output table and the corresponding logarithmic intensities were used for phosphopeptide analysis. The phosphopeptide table was expanded to separate individual phosphosites, and we kept all sites identified at least once in the three independent replicates of the analysis of *F. novicida*.

All data analysis of mass spectrometry data was performed in Perseus 1.6.0.7. For functional class annotation, we also integrated COG and EggNog databases in Perseus 1.6.0.7, freely available at www.perseus-framework.org. Data are available via ProteomeXchange with identifier PXD009225.

Cell cultures and cell infection experiments

J774A.1 (ATCC® TIB-67™) cells were propagated in Dulbecco's Modified Eagle's Medium (DMEM, PAA), containing 10% fetal bovine serum (FBS, PAA) unless otherwise stated. The day before infection, approximately $2x10^5$ eukaryotic cells per well were seeded in 12-well cell tissue plates and bacterial strains were grown overnight in 5 mL of Schaedler K3 at 37°C. Infections were realized at a multiplicity of infection (MOI) of 100 and incubated for 1 h at 37°C in culture medium. After 3 washes with cellular culture medium, plates were incubated for 4, 10 and 24 h in fresh medium supplemented with gentamycin (10 µg mL^{-1}). At each kinetic point, cells were washed 3 times with culture medium and lysed by addition of 1 mL of distilled water for 10 min at 4°C. The titre of viable bacteria was determined by

spreading preparations on chocolate plates. Each experiment was conducted at least twice in triplicates.

Confocal experiments

J774.1 macrophage cells were infected (MOI of 1,000) with wild-type *F. novicida* U112, the isogenic Δ*iglB* mutant, the Δ*iglB* complemented either with wild-type *iglB* (CpWT) Y139A, Y139F mutants or an isogenic Δ*FPI* strain, in standard DMEM (DMEM-glucose) for 30 min at 37°C. Cells were then washed three times with PBS and maintained in fresh DMEM supplemented with gentamycin (10 μg mL^{-1}) until the end of the experiment. Three kinetic points (*i.e.* 1 h, 4 h and 10 h) were sampled. For each time point, cells were washed with 1X PBS, fixed 15 min with 4% paraformaldheyde, and incubated 10 min in 50 mM NH_4Cl in 1X PBS to quench free aldehydes. Cells were then blocked and permeabilised with PBS containing 0.1% saponin and 5% goat serum for 10 min at room temperature. Cells were then incubated for 30 min with anti-*F. novicida* mouse monoclonal antibody (1/500e final dilution, Creative Diagnostics) and anti-LAMP1 rabbit polyclonal antibody (1/100e, ABCAM). After washing, cells were incubated for 30 min with Alexa488-conjugated goat anti mouse and Alexa546 conjugated donkey anti rabbit secondary antibodies (1/400e, AbCam). After washing, DAPI was added (1/1,000) for 1 min and glass coverslips were mounted in Mowiol (Cityfluor Ltd.). Cells were examined using an X63 oil-immersion objective on a Zeiss Apotome 2 microscope. Co-localisation tests were quantified by using Image J software; and mean numbers were calculated on more than 500 cells for each condition. Confocal microscopy analyses were performed at the Cell Imaging Facility (Faculté de Médecine Necker Enfants-Malades).

BMDMs Infections

Infection of WT or *ASC*$^{-/-}$ BMDMs was performed as described previously [42]. Briefly, BMDMs were differentiated in DMEM (Invitrogen) with 10% v/v FCS (Thermo Fisher Scientific), 15%

MCSF (L929 cell supernatant), 10 mM HEPES (Invitrogen), and non-essential amino acids (Invitrogen). One day before infection, macrophages were seeded into 12- 48- or 96-well plates at a density of 2 x10^5, 1.5 x10^5 or 5 x10^4 cells per well, respectively and incubated at 37°C, 5% CO_2. The overnight culture of bacteria was added to the macrophages at multiplicity of infection (MOI) of 100. The plates were centrifuged for 15 min at 500 g to ensure comparable adhesion of the bacteria to the cells and placed at 37°C for 1h. After 3 washes with PBS, fresh medium with 5 µg mL^{-1} gentamycin (Invitrogen) was added to kill extracellular bacteria and plates were incubated for the desired time.

Phagosomal rupture assay

Quantification of vacuolar escape using the β-lactamase/CCF4 assay (Life technologies) was performed as previously described[49]. *ASC*$^{-/-}$ BMDMs seeded onto non-treated plates were infected as described above for 2 h, washed and incubated in CCF4 for 1 h at room temperature in the presence of 2.5 mM probenicid (Sigma). Propidium iodide negative cells were considered for the quantification of cells containing cytosolic *F. novicida* using excitation at 405 nm and detection at 450 nm (cleaved CCF4) or 510 nm (intact CCF4).

Type I IFN secretion

Type I IFN secretion was determined in *ASC*$^{-/-}$ BMDMs by an ISRE-luciferase bioassay[50]. L929 ISRE-luciferase cells were plated at 5x10^4 cells per well in a 96 wells-plate and incubated 24 h at 37°C with 5% CO_2. 50 µl of supernatants from infected BMDMs were added for 4 h onto the ISRE-luciferase cells. Luciferase luminescence was detected using Bright Glo Assay (Promega) following the manufacturer's instructions. Mouse rINF-β was used as standard to determine the concentration of type I IFN in each sample.

Cell death assays

After infection 1h at MOI=100, WT BMMs were washed 3 times and incubated with Propidium Iodide (PI; 5 µg mL^{-1}) in CO_2-independent medium (ThermoFisher Scientific). PI incorporation was determined by measuring the fluorescence emission at 635 nm every 15 min on a microplate fluorescent reader (Tecan).

Mouse infection

Wild-type *F. novicida*, the Δ*iglB* mutant and the Δ*iglB* mutant complemented either with wild-type *iglB* (CpWT) or with Y139A and Y139F mutants, were grown in Schaedler K3 to exponential growth phase and diluted to the appropriate concentrations. 6 to 8-week-old female BALB/c mice (Janvier, Le Genest St Isle, France) were intraperitoneally (i.p.) inoculated with 200 µL of bacterial suspension. The actual number of viable bacteria in the inoculum was determined by plating dilutions of the bacterial suspension on chocolate plates. For competitive infections, wild-type *F. novicida* and mutant bacteria were mixed in 1:1 ratio and a total of 100 bacteria were used for infection of each of five mice. After two days, mice were sacrificed. Homogenized spleen and liver tissue from the five mice in one experiment were mixed, diluted and spread on to chocolate agar plates. Kanamycin selection to distinguish wild-type and mutant bacteria was performed. Competitive index (CI) [(mutant output/WT output)/(mutant input/WT input)]. Statistical analysis for CI experiments was as described in [69]. Macrophage experiments were analyzed by using the Student's unpaired t test.

Sequence analyses

To retrieve IglB homologous proteins, we used the Hidden Markov Model (HMM) profile "T6SSii_iglB.hmm" from reference[32]. We scanned a dataset of 2,462 predicted proteomes of complete bacterial genomes retrieved from GenBank Refseq (last accessed September 2016)[70] using *hmmsearch* program of HMMER v.3.1b2 (gathering threshold = 25).

Our dataset included 19 genomes of the *Francisella* genus. All IglB sequences encoded by *Francisella* genomes were aligned with MUSCLE v.3.8.31[71]. Due to differences in the annotation of the first methionine codon, we used the sequence of FTN_1323 as a reference for the multiple sequence alignment.

Redundancy of the sequence set retrieved from *hmmsearch* was reduced using cd-hit-v4.6.7[72] with a 90% identity threshold. The longest representative sequence of each cluster was then aligned with MUSCLE v.3.8.31[71]. Outliers that were very divergent in sequence length were removed. PROMALS3D and ESPript3.0[73] servers were used to visualize multiple sequence and structure alignment using 3J9O.B PDB structure reference file[30]. To determine the conservation of the phosphotyrosine site identified in *Francisella* genus (Tyr139 or Y139) we focused on the 12 amino acids surrounding the *Francisella* Tyr139 residue in the 535 aligned sequences.

To determine the conservation of the phosphotyrosine site identified in *Francisella* genus (Tyr139) we focused on the 12 amino acids surrounding the *Francisella* Y139 residue in the 535 aligned sequences. Out of the 535 aligned sequences, we found 90 sequences with a tyrosine residue in the vicinity of *Francisella* Tyr139 residue. For illustrative purpose, we selected 12 representative sequences out of 90 as shown in **Fig. 2D**.

Data Availability

The mass spectrometry proteomics data have been deposited in the ProteomeXchange Consortium via the PRIDE [74] partner repository with the dataset identifier PXD009225.

The authors declare that all other data supporting the findings of this study are available within the paper and its Supplementary Information files.

Author Contributions

J.Z. performed most of the in vitro experiments; F.T. performed murine in vivo experiments and some immunofluorescence experiments; I.C.G and C.C. performed the proteomic analyses and I.C.G analyzed and compiled the data; N. K. performed the 3D analysis; A.J. performed the sequence alignments and analyzed the data; C.L. and G.P. performed some in vitro experiments; M.B. and T.H. analyzed the data ; A.C. designed the experiments and J.Z. and A.C. analyzed the data, and wrote the paper.

The funders had no role in study design, data collection and analysis, decision to publish, or preparation of the manuscript.

Acknowledgements

We thank Dr A. Sjostedt for providing the *Francisella* strain U112 and its *ptpA* transposon insertion derivative (*FTN_1046*) and Alain Schmitt (Cochin Institute Electron Microscopy Facility) for excellent technical support. These studies were supported by INSERM, CNRS and Université Paris Descartes Paris Cité Sorbonne. Jason Ziveri was funded by a fellowship from the “Délégation Générale à l’Armement”. Claire Lays was funded by a fellowship from the LABEX ECOFECT (ANR-11-LABX-0048) of Université de Lyon, within the program "Investissement d'Avenir" (ANR-11-IDEX-0007) operated by the French National Research Agency (ANR). The funders had no role in study design, data collection and analysis, decision to publish, or preparation of the manuscript.

Competing financial interests

The authors declare no competing financial interests.

References

1. Sjostedt A. Tularemia: history, epidemiology, pathogen physiology, and clinical manifestations. *Ann N Y Acad Sci* **1105**, 1-29 (2007).
2. Sjostedt A. Francisella tularensis and tularemia. In: *Fontiers Research Topic Ebooks* (eds). Fontiers Media SA (2011).
3. Luque-Larena JJ*, et al.* Irruptive mammal host populations shape tularemia epidemiology. *PLoS Pathog* **13**, e1006622 (2017).
4. Maurin M, Gyuranecz M. Tularaemia: clinical aspects in Europe. *Lancet Infect Dis* **16**, 113-124 (2016).
5. Santic M, Molmeret M, Klose KE, Abu Kwaik Y. Francisella tularensis travels a novel, twisted road within macrophages. *Trends Microbiol* **14**, 37-44 (2006).
6. McLendon MK, Apicella MA, Allen LA. Francisella tularensis: taxonomy, genetics, and Immunopathogenesis of a potential agent of biowarfare. *Annu Rev Microbiol* **60**, 167-185 (2006).
7. Kingry LC, Petersen JM. Comparative review of Francisella tularensis and Francisella novicida. *Front Cell Infect Microbiol* **4**, 35 (2014).
8. Brodmann M, Dreier RF, Broz P, Basler M. Francisella requires dynamic type VI secretion system and ClpB to deliver effectors for phagosomal escape. *Nat Commun* **8**, 15853 (2017).
9. Eshraghi A*, et al.* Secreted Effectors Encoded within and outside of the Francisella Pathogenicity Island Promote Intramacrophage Growth. *Cell Host Microbe* **20**, 573-583 (2016).
10. Lagrange B*, et al.* Human caspase-4 detects tetra-acylated LPS and cytosolic Francisella and functions differently from murine caspase-11. *Nat Commun* **9**, 242 (2018).

11. Charity JC, Blalock LT, Costante-Hamm MM, Kasper DL, Dove SL. Small molecule control of virulence gene expression in Francisella tularensis. *PLoS Pathog* **5**, e1000641 (2009).
12. Charity JC, Costante-Hamm MM, Balon EL, Boyd DH, Rubin EJ, Dove SL. Twin RNA polymerase-associated proteins control virulence gene expression in Francisella tularensis. *PLoS Pathog* **3**, e84 (2007).
13. Cuthbert BJ*, et al.* Dissection of the molecular circuitry controlling virulence in Francisella tularensis. *Genes Dev* **31**, 1549-1560 (2017).
14. Meibom KL*, et al.* Hfq, a novel pleiotropic regulator of virulence-associated genes in Francisella tularensis. *Infect Immun* **77**, 1866-1880 (2009).
15. Meibom KL, Barel M, Charbit A. Loops and networks in control of Francisella tularensis virulence. *Future Microbiol* **4**, 713-729 (2009).
16. Celli J, Zahrt TC. Mechanisms of Francisella tularensis intracellular pathogenesis. *Cold Spring Harb Perspect Med* **3**, a010314 (2013).
17. Ziveri J, Barel M, Charbit A. Importance of Metabolic Adaptations in Francisella Pathogenesis. *Front Cell Infect Microbiol* **7**, 96 (2017).
18. Balonova L*, et al.* Characterization of protein glycosylation in Francisella tularensis subsp. holarctica; identification of a novel glycosylated lipoprotein required for virulence. *Mol Cell Proteomics* **11**, M111.015016. (2012).
19. Dankova V, Balonova L, Link M, Straskova A, Sheshko V, Stulik J. Inactivation of Francisella tularensis Gene Encoding Putative ABC Transporter Has a Pleiotropic Effect upon Production of Various Glycoconjugates. *J Proteome Res* **15**, 510-524 (2016).
20. Barel M, Charbit A. Role of Glycosylation/Deglycolysation Processes in Francisella tularensis Pathogenesis. *Front Cell Infect Microbiol* **7**, 71 (2017).
21. Canova MJ, Molle V. Bacterial serine/threonine protein kinases in host-pathogen interactions. *J Biol Chem* **289**, 9473-9479 (2014).

22. Shi L*, et al.* Cross-phosphorylation of bacterial serine/threonine and tyrosine protein kinases on key regulatory residues. *Front Microbiol* **5**, 495 (2014).
23. Nguyen HA*, et al.* Expanding the Kinome World: A New Protein Kinase Family Widely Conserved in Bacteria. *J Mol Biol* **429**, 3056-3074 (2017).
24. Deutscher J*, et al.* The bacterial phosphoenolpyruvate:carbohydrate phosphotransferase system: regulation by protein phosphorylation and phosphorylation-dependent protein-protein interactions. *Microbiol Mol Biol Rev* **78**, 231-256 (2014).
25. Rodionova IA*, et al.* The phosphocarrier protein HPr of the bacterial phosphotransferase system globally regulates energy metabolism by directly interacting with multiple enzymes in Escherichia coli. *J Biol Chem* **292**, 14250-14257 (2017).
26. Meibom KL, Charbit A. Francisella tularensis metabolism and its relation to virulence. *Front Microbiol* **1**, 140 (2010).
27. Dai S, Mohapatra NP, Schlesinger LS, Gunn JS. Regulation of Francisella tularensis virulence. *Frontiers in Microbiology* **2**, (2011).
28. Alkhuder K, Meibom KL, Dubail I, Dupuis M, Charbit A. Identification of trkH, Encoding a Potassium Uptake Protein Required for Francisella tularensis Systemic Dissemination in Mice. *PLoS One* **5**, e8966 (2010).
29. Bell BL, Mohapatra NP, Gunn JS. Regulation of virulence gene transcripts by the Francisella novicida orphan response regulator PmrA: role of phosphorylation and evidence of MglA/SspA interaction. *Infect Immun* **78**, 2189-2198 (2010).
30. Clemens DL, Ge P, Lee BY, Horwitz MA, Zhou ZH. Atomic structure of T6SS reveals interlaced array essential to function. *Cell* **160**, 940-951 (2015).
31. Russell AB*, et al.* A type VI secretion-related pathway in Bacteroidetes mediates interbacterial antagonism. *Cell Host Microbe* **16**, 227-236 (2014).
32. Abby SS, Cury J, Guglielmini J, Neron B, Touchon M, Rocha EP. Identification of protein secretion systems in bacterial genomes. *Sci Rep* **6**, 23080 (2016).

33. Pizarro-Cerda J, Charbit A, Enninga J, Lafont F, Cossart P. Manipulation of host membranes by the bacterial pathogens Listeria, Francisella, Shigella and Yersinia. *Semin Cell Dev Biol*, (2016).
34. Lindgren H, Golovliov I, Baranov V, Ernst RK, Telepnev M, Sjostedt A. Factors affecting the escape of Francisella tularensis from the phagolysosome. *J Med Microbiol* **53**, 953-958 (2004).
35. Nano FE*, et al.* A Francisella tularensis pathogenicity island required for intramacrophage growth. *J Bacteriol* **186**, 6430-6436 (2004).
36. Lauriano CM*, et al.* MglA regulates transcription of virulence factors necessary for Francisella tularensis intraamoebae and intramacrophage survival. *Proc Natl Acad Sci U S A* **101**, 4246-4249 (2004).
37. Nano FE, Schmerk C. The Francisella pathogenicity island. *Ann N Y Acad Sci* **1105**, 122-137 (2007).
38. Broms JE, Sjostedt A, Lavander M. The Role of the Francisella Tularensis Pathogenicity Island in Type VI Secretion, Intracellular Survival, and Modulation of Host Cell Signaling. *Front Microbiol* **1**, 136 (2010).
39. Meibom KL*, et al.* The heat-shock protein ClpB of Francisella tularensis is involved in stress tolerance and is required for multiplication in target organs of infected mice. *Mol Microbiol* **67**, 1384-1401 (2008).
40. Vettiger A, Basler M. Type VI Secretion System Substrates Are Transferred and Reused among Sister Cells. *Cell* **167**, 99-110 e112 (2016).
41. Bröms JE, Sjöstedt A, Lavander M. The Role of the Francisella Tularensis Pathogenicity Island in Type VI Secretion, Intracellular Survival, and Modulation of Host Cell Signaling. *Front Microbiol* **1**, 136. (2010).
42. Rigard M*, et al.* Francisella tularensis IglG Belongs to a Novel Family of PAAR-Like T6SS Proteins and Harbors a Unique N-terminal Extension Required for Virulence. *PLoS Pathog* **12**, e1005821 (2016).

43. Weiss DS, Brotcke A, Henry T, Margolis JJ, Chan K, Monack DM. In vivo negative selection screen identifies genes required for Francisella virulence. *Proc Natl Acad Sci U S A* **104**, 6037-6042 (2007).
44. Broms JE, Lavander M, Sjostedt A. A conserved alpha-helix essential for a type VI secretion-like system of Francisella tularensis. *J Bacteriol* **191**, 2431-2446 (2009).
45. Spidlova P, Stulik J. Francisella tularensis type VI secretion system comes of age. *Virulence* **8**, 628-631 (2017).
46. Ramond E*, et al.* Importance of host cell arginine uptake in Francisella phagosomal escape and ribosomal protein amounts. *Mol Cell Proteomics* **14**, 870-881 (2015).
47. Henry T, Brotcke A, Weiss DS, Thompson LJ, Monack DM. Type I interferon signaling is required for activation of the inflammasome during Francisella infection. *J Exp Med* **204**, 987-994 (2007).
48. Jones JW*, et al.* Absent in melanoma 2 is required for innate immune recognition of Francisella tularensis. *Proc Natl Acad Sci U S A* **107**, 9771-9776 (2010).
49. Meunier E*, et al.* Guanylate-binding proteins promote activation of the AIM2 inflammasome during infection with Francisella novicida. *Nat Immunol* **16**, 476-484 (2015).
50. Jiang Z*, et al.* CD14 is required for MyD88-independent LPS signaling. *Nat Immunol* **6**, 565-570 (2005).
51. Vettiger A, Winter J, Lin L, Basler M. The type VI secretion system sheath assembles at the end distal from the membrane anchor. *Nat Commun* **8**, 16088 (2017).
52. Salih O*, et al.* Atomic Structure of Type VI Contractile Sheath from Pseudomonas aeruginosa. *Structure* **26**, 329-336 e323 (2018).
53. Wehrly TD*, et al.* Intracellular biology and virulence determinants of Francisella tularensis revealed by transcriptional profiling inside macrophages. *Cell Microbiol* **11**, 1128-1150 (2009).

54. Meyer L, Broms JE, Liu X, Rottenberg ME, Sjostedt A. Microinjection of Francisella tularensis and Listeria monocytogenes reveals the importance of bacterial and host factors for successful replication. *Infect Immun* **83**, 3233-3242 (2015).

55. Ludu JS*, et al.* The Francisella pathogenicity island protein PdpD is required for full virulence and associates with homologues of the type VI secretion system. *J Bacteriol* **190**, 4584-4595 (2008).

56. Grangeasse C, Nessler S, Mijakovic I. Bacterial tyrosine kinases: evolution, biological function and structural insights. *Philos Trans R Soc Lond B Biol Sci* **367**, 2640-2655 (2012).

57. Brelle S*, et al.* Phosphorylation-mediated regulation of the Staphylococcus aureus secreted tyrosine phosphatase PtpA. *Biochem Biophys Res Commun* **469**, 619-625 (2016).

58. Pereira SF, Goss L, Dworkin J. Eukaryote-like serine/threonine kinases and phosphatases in bacteria. *Microbiol Mol Biol Rev* **75**, 192-212 (2011).

59. Vincent C*, et al.* Relationship between exopolysaccharide production and protein-tyrosine phosphorylation in gram-negative bacteria. *J Mol Biol* **304**, 311-321 (2000).

60. Gallagher LA, Ramage E, Jacobs MA, Kaul R, Brittnacher M, Manoil C. A comprehensive transposon mutant library of Francisella novicida, a bioweapon surrogate. *Proc Natl Acad Sci U S A* **104**, 1009-1014 (2007).

61. Hunter T. The genesis of tyrosine phosphorylation. *Cold Spring Harb Perspect Biol* **6**, a020644 (2014).

62. Chamberlain RE. Evaluation of Live Tularemia Vaccine Prepared in a Chemically Defined Medium. *Appl Microbiol* **13**, 232-235 (1965).

63. Gesbert G*, et al.* Asparagine assimilation is critical for intracellular replication and dissemination of Francisella. *Cell Microbiol* **16**, 434-449 (2014).

64. Gesbert G*, et al.* Importance of branched-chain amino acid utilization in Francisella intracellular adaptation. *Infect Immun* **83**, 173-183 (2015).

65. Klionsky DJ*, et al.* Guidelines for the use and interpretation of assays for monitoring autophagy (3rd edition). *Autophagy* **12**, 1-222 (2016).
66. Ziveri J*, et al.* The metabolic enzyme fructose-1,6-bisphosphate aldolase acts as a transcriptional regulator in pathogenic Francisella. *Nat Commun* **8**, 853 (2017).
67. Lipecka J*, et al.* Sensitivity of mass spectrometry analysis depends on the shape of the filtration unit used for filter aided sample preparation (FASP). *Proteomics* **16**, 1852-1857 (2016).
68. Cox J, Mann M. MaxQuant enables high peptide identification rates, individualized p.p.b.-range mass accuracies and proteome-wide protein quantification. *Nat Biotechnol* **26**, 1367-1372 (2008).
69. Brotcke A*, et al.* Identification of MglA-regulated genes reveals novel virulence factors in Francisella tularensis. *Infect Immun* **74**, 6642-6655 (2006).
70. Coordinators NR. Database Resources of the National Center for Biotechnology Information. *Nucleic acids research* **45**, D12-D17 (2017).
71. Edgar RC. MUSCLE: multiple sequence alignment with high accuracy and high throughput. *Nucleic acids research* **32**, 1792-1797 (2004).
72. Fu L, Niu B, Zhu Z, Wu S, Li W. CD-HIT: accelerated for clustering the next-generation sequencing data. *Bioinformatics* **28**, 3150-3152 (2012).
73. Robert X, Gouet P. Deciphering key features in protein structures with the new ENDscript server. *Nucleic acids research* **42**, W320-324 (2014).
74. Vizcaino JA*, et al.* 2016 update of the PRIDE database and its related tools. *Nucleic Acids Res* **44**, 11033 (2016).

Figure Legends

Figure 1. The phosphoproteome of *F. novicida*

(**A**) Distribution of phosphosites according to the modified amino acid (tyrosine,Y; threonine, T and serine, S). (**B**) Logos of phosphopeptide amino acid sequences; (**C**) Histograms of the most represented classes of protein. The values correspond to the number of proteins bearing phosphosites in each category.

Figure 2. Importance of IglB amino acid Y139 in sheath formation

(**A**) Sucrose gradient. Lysates of bacteria grown in Schaedler K3 medium in the presence of KCl were laid on top of a discontinuous sucrose gradient 15%-55%/Optiprep 55%. Left panel, composition of the gradient; Right panel, transmission electron microscopy (TEM) of the "heavy" fraction (grey arrow, topping the Optiprep cushion). The assembled sheath-like structure, sedimenting at equilibrium to below 55% sucrose, showed rod-shaped particles of variable length (100 - 600 nm). (**B**) Western blotting analysis of the different fractions, using anti-Igl (A, B or C) antibodies. (**C**) Mass spectrometry analysis of the H and L fractions. Ratio of the intensities of the proteins IglA, B and C detected in the H and the L fractions (H / L %). (**D**) Proteome and phosphoproteome of cellular fractions. Intensities (in log2) of the non phosphorylated (left) and phosphorylated (right) Tyr139-containing peptide in the "heavy" (H) and "light" (L) fractions. The signal of the phosphopeptide was only detectable after phosphoenrichment. nd, not detectable.

Figure 3. Predicted role of Y139 of IglB in sheath assembly

(**A**) Overview of the sheath that consists of 12 helical strands based on EM reconstruction at 3.7 Å. Each unit consists of a IglA/IglB dimer. The same colors were used in the further

pictures. The chains near Tyr139 of IglB consist of 2 IglA/IglB dimers from the same strand (pink/grey and coral/sky blue). The N-terminal tail of an IglA (blue) from an adjacent strand wraps round to close to Y139 of this strand. (**B**) A closer view of just the selected chains. (**C**) Close up of the region of Tyr139. The hydroxyl is pointing into a pocket and not obviously making a Hydrogen bond. However, the carboxylates of Asp114 from IglB and Asp63 of IglA in the next dimer are around 5 Å away. At the resolution of the reconstruction side chain density is not well defined and these could in fact be close enough to H bond. (**D**) Surface of the assembly clipped to show Tyr139. There is enough space for a Phospho group on the Tyr. The two Asps will however be close to the phosphogroup and so there is likely to be charge repulsion impairing the sheath assembly or weakening the sheath stability when Y139 is phosphorylated.

Figure 4. Immunodetection

(**A**) Western Blots (WB) of whole cell protein extracts. Upper gel: WB with anti-IglB; lower gel: WB with anti-IglA. (**B**) Western Blots (WB) with anti-IglC on bacteria / culture filtrates. Bacteria were grown in Schaedler-K3 supplemented or not with 5% KCl until late log phase and then harvested by centrifugation. Culture supernatants were collected after filtration on 0.2 µM Millipore filters and concentrated using Amicon 3 kDa membranes. The equivalent of 200 µg of total protein were loaded onto each well. Upper gel, bacterial cultures grown without KCl; lower gel, bacterial cultures supplemented with 5% KCl. (**C**) Co-immunoprecipitations (Co-IP). Upper gel: IP-anti-IglA, followed by WB with anti-IglB; lower gel: IP-anti-IglB, followed by WB with anti-IglA. (**D**) WBs of sucrose gradient fractions of the Y139F mutant strain. Upper gel, WB with anti-IglB; Middle gel, WB with anti-IglA; lower gel, WB with anti-IglC. (**E**) Mass spectrometry analysis of the H and L fractions of the Y139F mutant strain. Ratio of the intensities of the proteins IglA, B and C detected in the H and the L fractions (H / L %).

Figure 5. IglB mutants show impaired intracellular survival and attenuated virulence

(**A, B**) Intracellular bacterial multiplication of wild-type *F. novicida* (WT, Grey squares), isogenic Δ*iglB* mutant (Δ*iglB*, blue triangles) and complemented Δ*iglB* strain (Cp-WT, grey circles; Y139A, blue square; Y139F, red squares) and the Δ*FPI* control (black lines), was monitored during 24 h in J774A.1 macrophage cells (**A**) and bone marrow-derived macrophages (BMDM) from BALB/c mice (**B**). In J774.1, the values recorded for Y139F, at 24 h, were significantly different from those of Δ*FPI*, Δ*iglB* or Y139A. In both cell types, the values recorded for WT or CpWT, at 10 h and 24 h, were significantly different from those of Δ*FPI*, Δ*iglB,* Y139A or Y139F. **p<0.001 (determined by student's t-test). (**C**) Groups of five BALB/c mice were infected intraperitoneally with 100 CFU of wild-type *F. novicida* and 100 CFU of Δ*iglB* mutant strain or complemented strain (Cp-WT, Y139A, Y139F). Bacterial burden was quantified in liver (L) and spleen (S) of mice. The data represent the competitive index (CI) value (in ordinate) for CFU of mutant/wild-type of each mouse, after 48 h infection, divided by CFU of mutant/wild-type in the inoculum. Bars represent the geometric mean CI value. (**D, E**) Confocal microscopy of intracellular bacteria with J774-1 infected with wild-type *F. novicida* (WT), Δ*iglB* or complemented strains and their co-localization with the phagosomal marker LAMP1 observed at 1 h, 4 h and 10 h. J774.1 were stained for *F. novicida* (green), LAMP-1 (red) and host DNA (blue, DAPI stained) (**D**). Analysis was performed with ImageJ software (**E**). (**F**) CCF4 assay. Infection of *ASC*$^{-/-}$ BMDM were performed at MOI of 100 and the cytosol of BMDMs was loaded with CCF4, as described previously[46]. *F. novicida* naturally expresses a β-lactamase able to cleave the CCF4. Bacterial escape into the host cytosol is thus associated with a shift of the CCF4 probe fluorescence emission from 535 nm to 450 nm. The number of cells demonstrating CCF4 cleavage, determined at different time points (1 h, 3 h and 6 h) by flow cytometry, reached above 50% at 6 h for both WT and CpWT complemented strains whereas it was below 1% for the other mutant strains tested. *p<0.01 (determined by student's t-test).

Figure 6. Type I IFN secretion and cell death assays

(**A**) Type I IFN secretion in the culture supernatant of BMDMs infected with the indicated strains at an MOI of 1 was determined by the ISRE-luciferase bioassay and normalized using rIFNβ. The supernatants of infections (50 µL) collected at different time points (1 h, 3 h and 6 h) were analyzed. Type I IFN secretion reached between 25 and 30 U/mL after 6 h, for both WT and CpWT complemented strains whereas it remained below 5 U/mL for the other mutant strains tested. (**B**) Cell death of BMDMs infected with the indicated strains at an MOI of 1 was monitored in real time by monitoring propidium iodide fluorescence (expressed in arbitrary units -AU) every 15 min. Mean and SD of triplicates from one experiment representative of two independent experiments are shown in panels A, B. Unpaired t-tests were performed, two-tailed P-values were $P \leq 0.001$.

Figure 7. Proposed model of phosphorylation-dependent TSS6 assembly-disassembly

(**Left**) Upon bacterial entry into the phagosomal compartment, phosphorylation of IglB may decrease and non-phosphorylated IglB can form stable heterodimers with IglA. Sheath assembly initiates at the bacterial pole. (**Right**) Within 30 min, T6SS sheath contraction triggers the secretion of effectors and the rupture of the phagosomal membrane. Once in the cytosol, the T6SS sheath disassembles, thanks to the concerted action of the ClpB unfoldase and of the phosphorylation of IglB residue Y139.

A

B

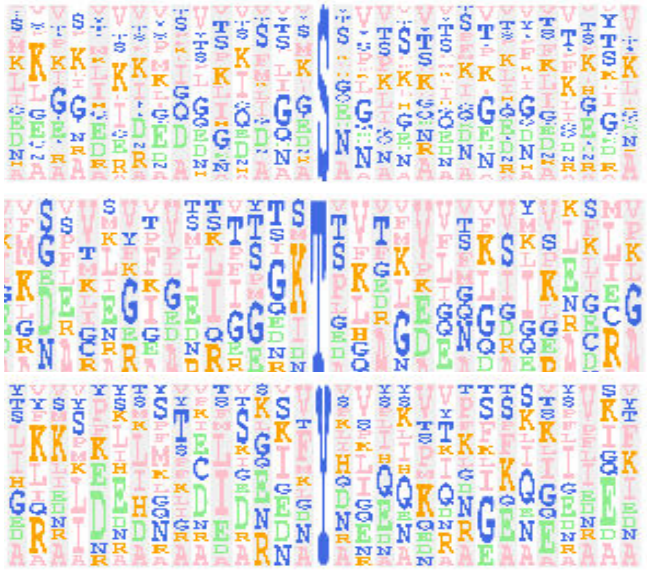

C

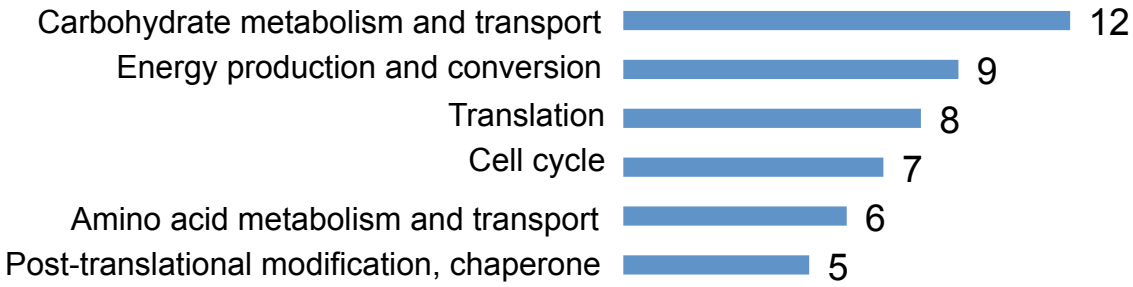

Fig. 1. Ziveri et al.

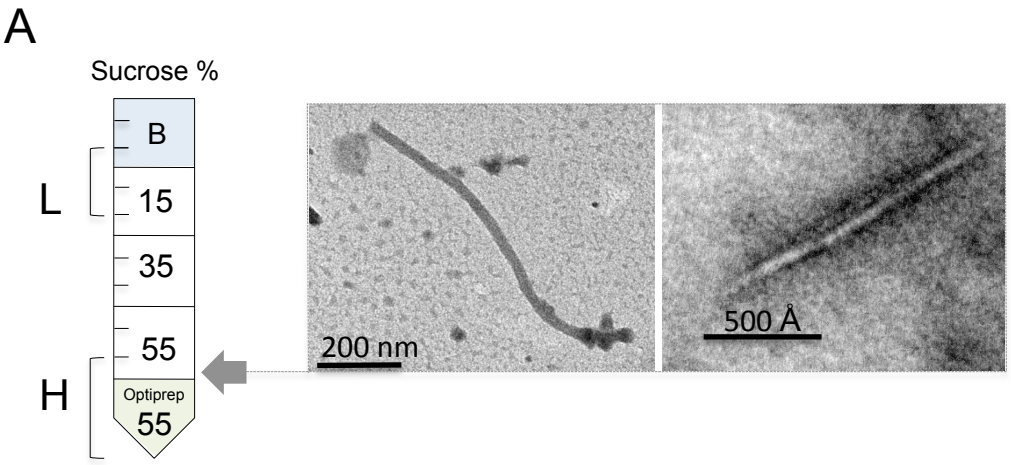

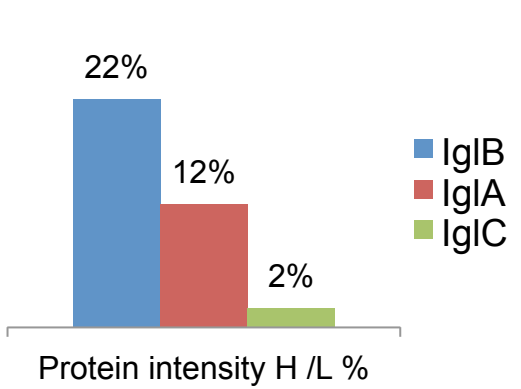

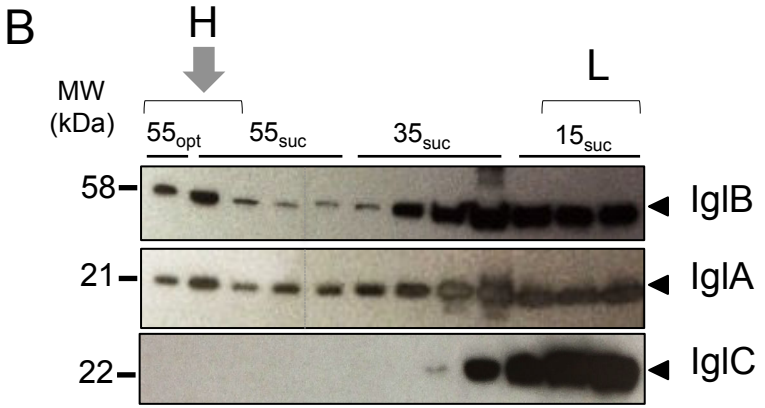

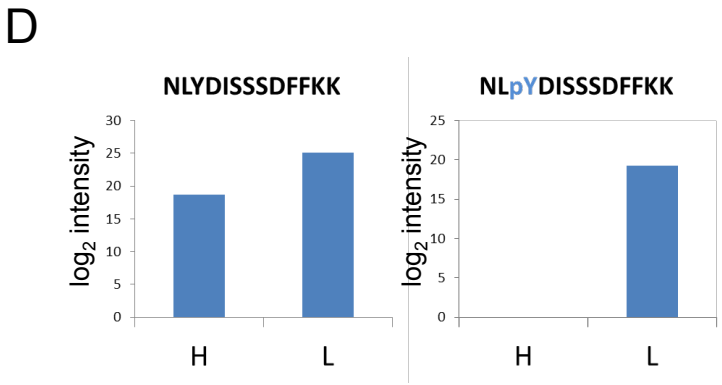

Fig. 2. Ziveri et al.

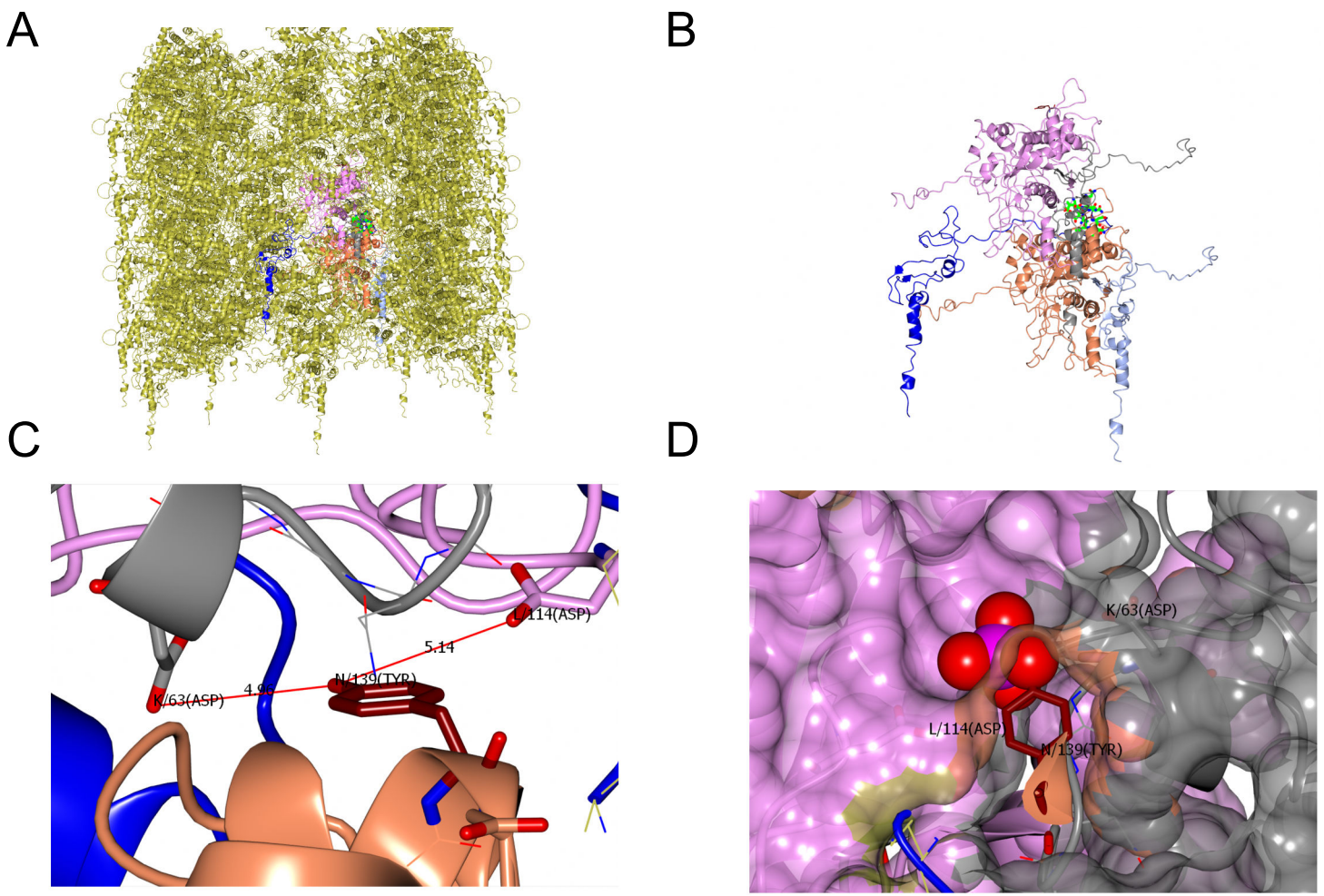

Fig. 3. Ziveri et al.

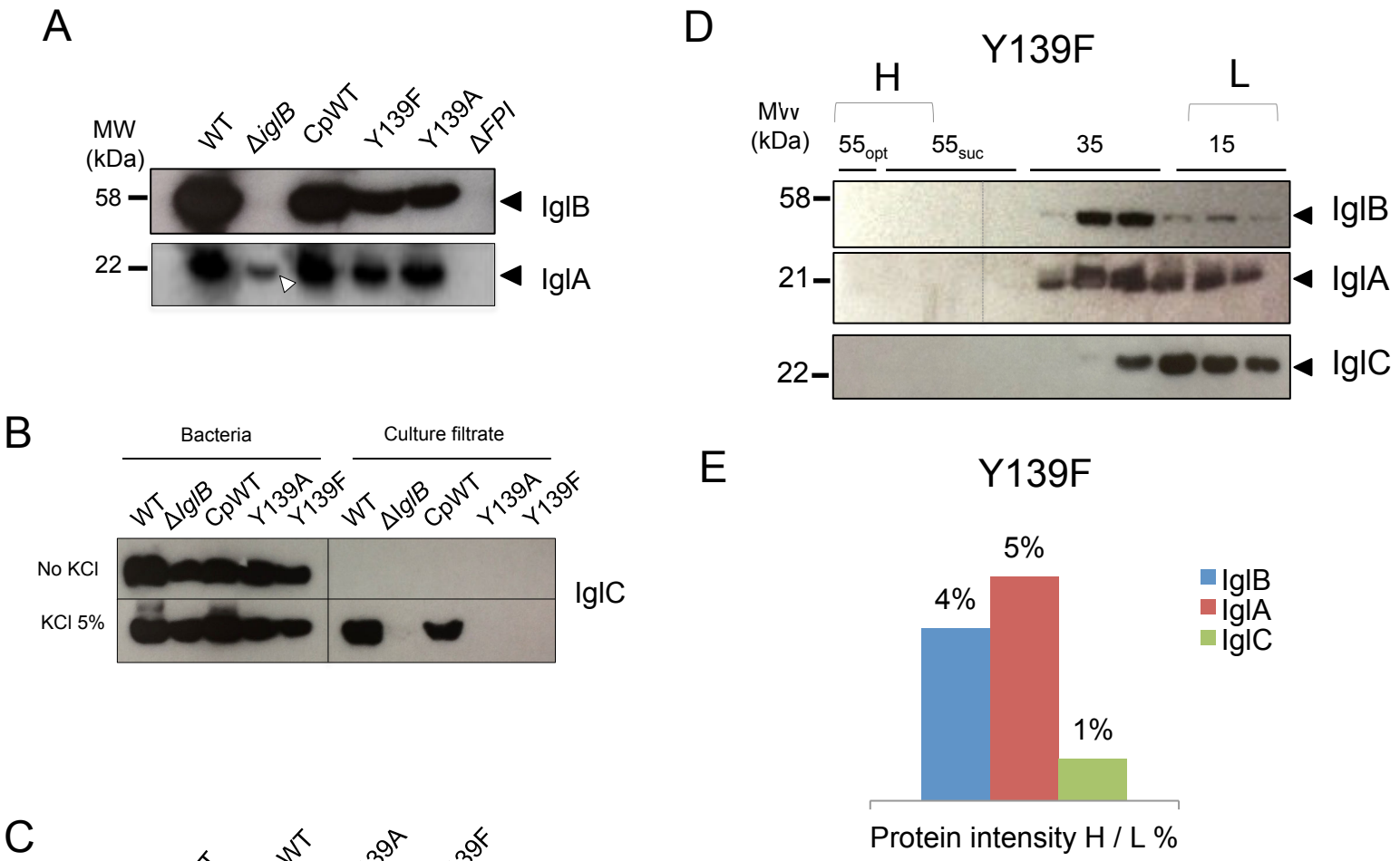

Fig. 4. Ziveri et al.

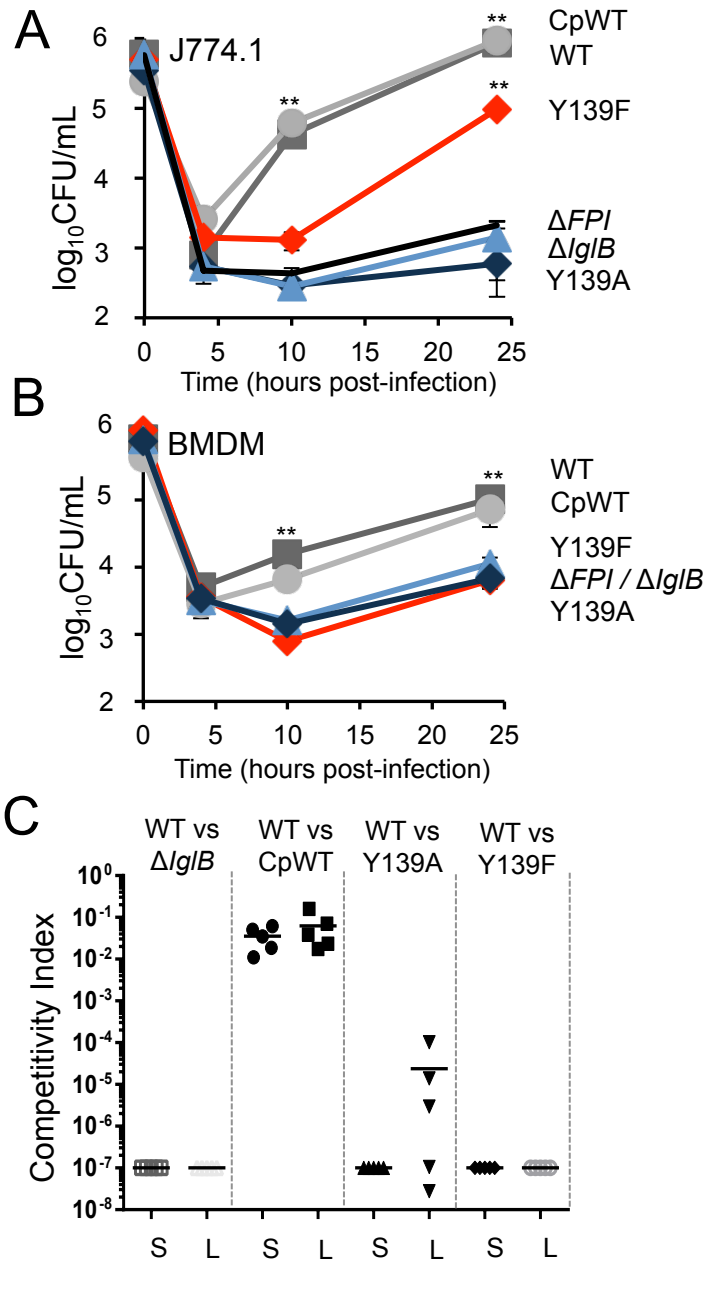

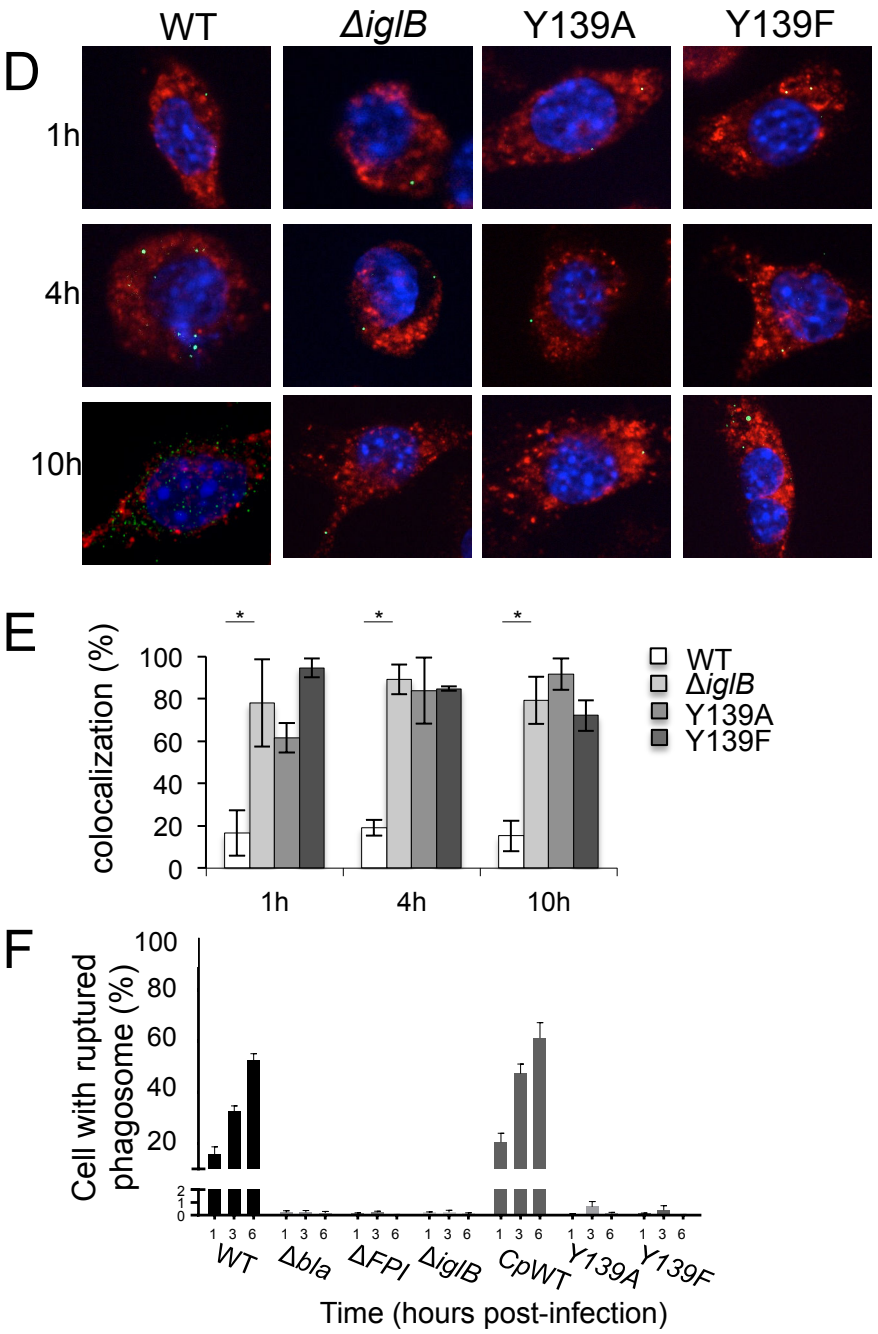

Ziveri *et al.* Fig. 5

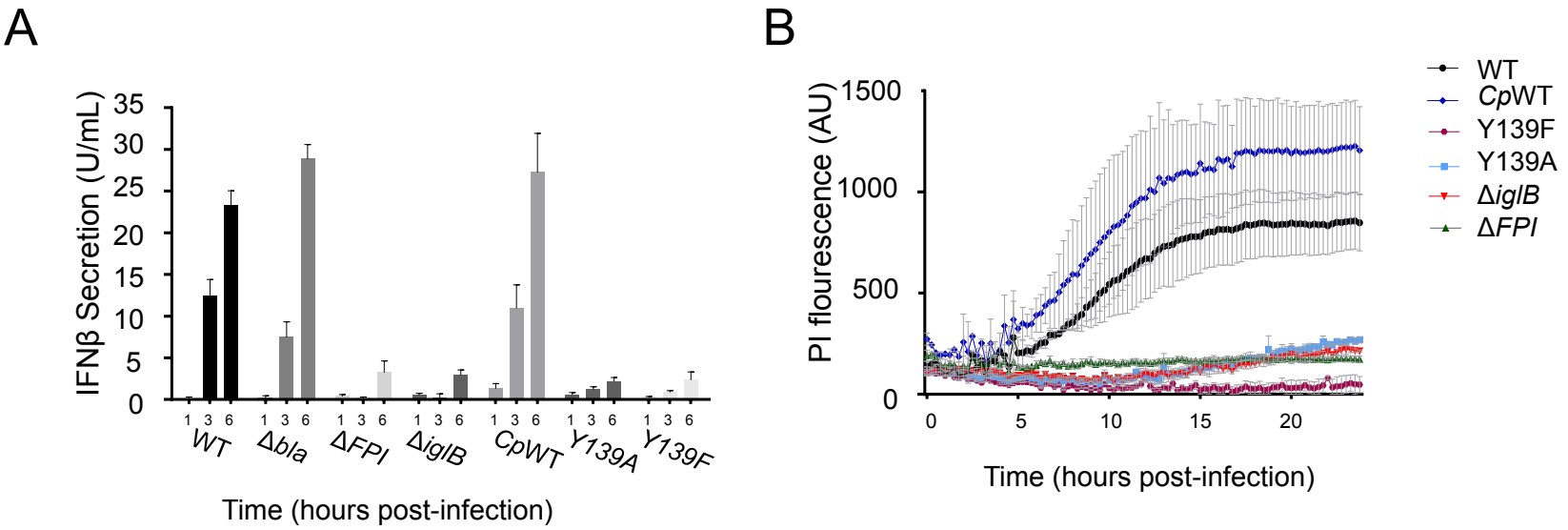

Fig. 6. Ziveri et al.

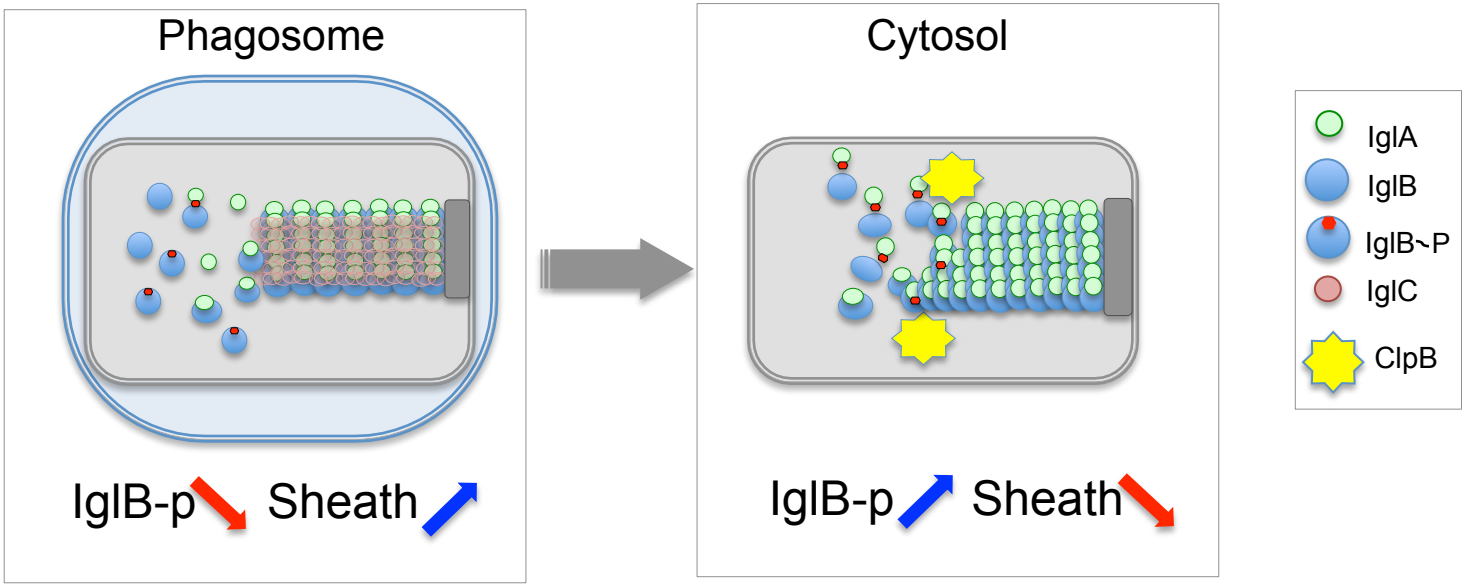

Fig. 7. Ziveri et al.

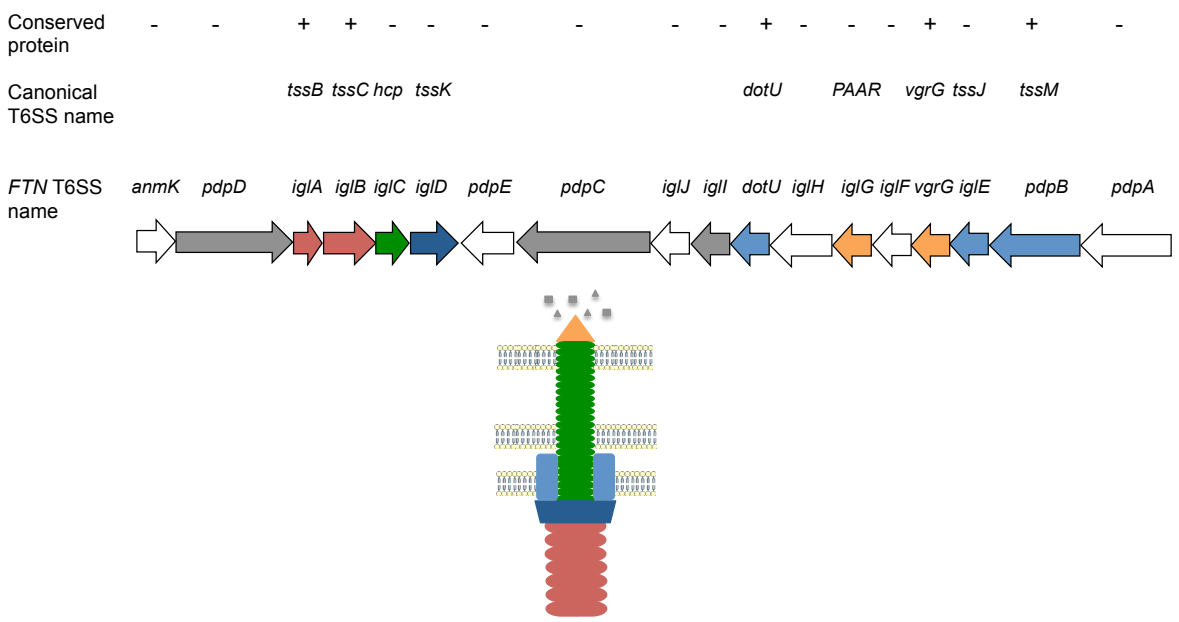

Supplementary Figure 1: Schematic representation of the FPI locus and overview of the T6SS structure of *Francisella*. The *Francisella* FPI locus representation (*anmK* to *pdpA* gene) with nomenclature of the canonical T6SS and the *F. novicida* T6SS. A color was assigned for each gene function and applied on the overview of the T6SS structure. Red/Green/Blue/Orange, structural protein; Grey, secreted protein; White, hypothetical protein

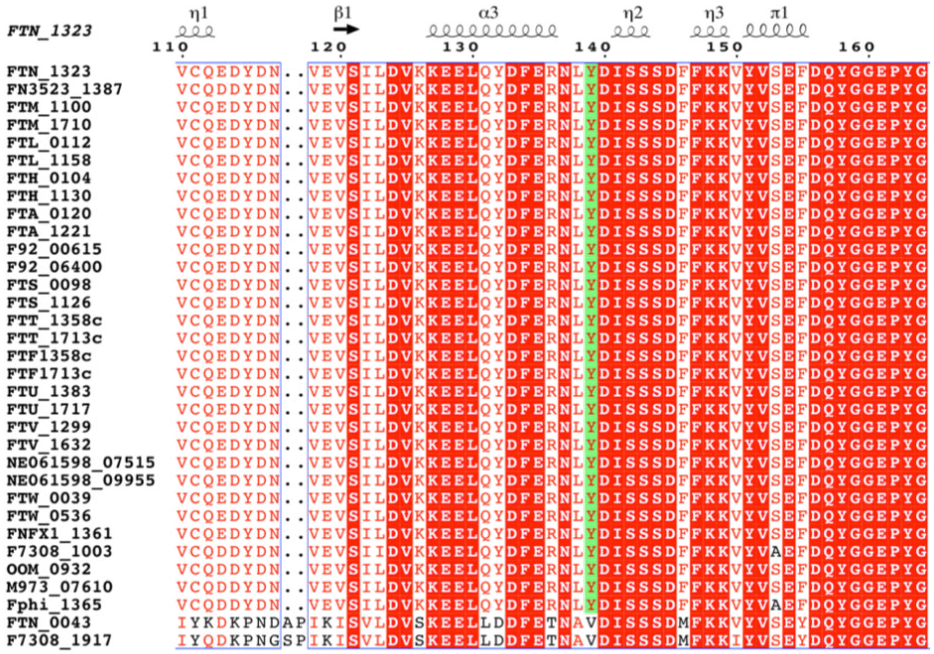

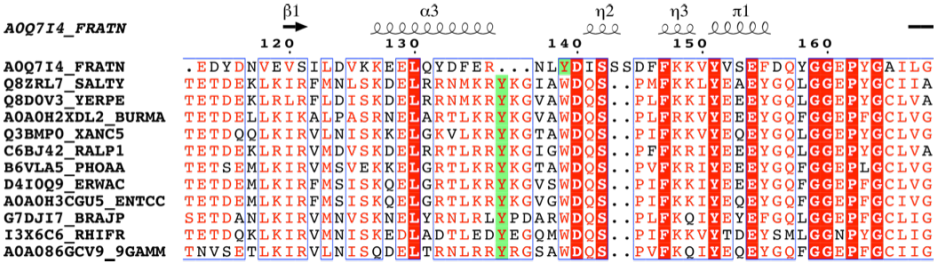

Supplementary Figure 2: Alignments of orthologous IglBs proteins. Related to Figure 2. (**A**) Alignments of orthologous IglBs proteins showing conservation of Y139 in *Francisellae*. The IglB sequences retrieved from 19 *Francisella* genomes were aligned using MUSCLE [71] and rendered using ESPript3.0 [73]. Secondary structure elements information is extracted from 3J9O PDB file [32] and is displayed at the top of the alignment. Sequences are identified by corresponding species name followed by strain name and locus tag. Species names are abbreviated as follow: Fn, *Francisella tularensis* subsp. *novicida*; Ftm, *Francisella tularensis* subsp. *mediasiatica*; Fth, *Francisella tularensis* subsp. *holarctica*; Ftt, *Francisella tularensis* subsp. *tularensis*; Ft, *Francisella tularensis*; Fno, *Francisella noatunensis*; Fsp, *Francisella* sp. (**B**) Alignments of orthologous IglBs in other genera showing conservation of

a tyrosine residue. Sequences of 11 representative IglB orthologs with a tyrosine residue in the vicinity of Y139 were aligned using MUSCLE [71] and rendered using ESPript3.0 [73]. Secondary structure elements information is extracted from 3J9O PDB file [32] and is displayed at the top of the alignment. Sequences are identified by corresponding Uniprot accession number. Species names are abbreviated as follow: FRATN, *Francisella tularensis* subsp. *novicida*; SALTY, *Salmonella* Typhimurium; YERPE, *Yersinia pestis*; BURMA, *Burkholderia mallei;* XANC5, *Xanthomonas campestris*; RALP1, *Ralstonia pickettii*; PHOAA, *Photorhabdus asymbiotica*; ERWAC, *Erwinia amylovora*; ENTCC, *Enterobacter cloacae*; BRAJP, *Bradyrhizobium japonicum*; RHIFR, *Rhizobium fredii*; 9GAMM, *Serratia nematodiphila.*

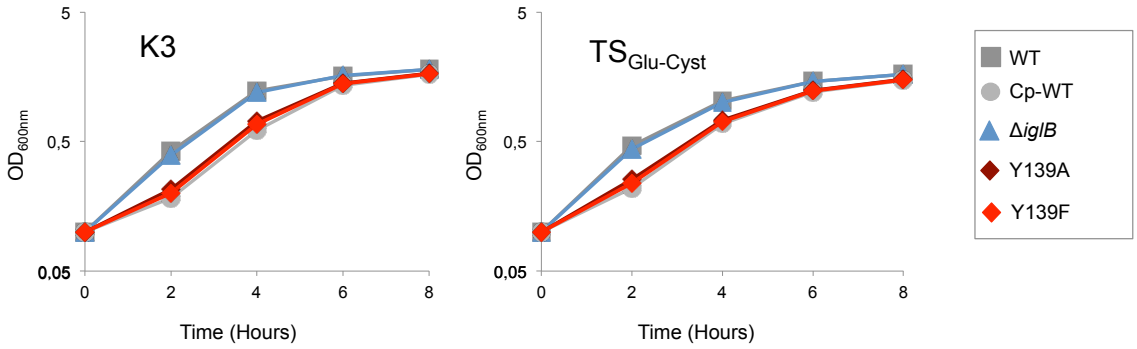

Supplementary Figure 3: Effect of IglB mutations on growth in broth. Wild-type *F. novicida* (WT, Grey squares), isogenic Δ*iglB* mutant (Δ*iglB*, blue triangles), and complemented *iglB* strain (Cp-WT, grey circles; Y139A, purple square; Y139F, red square), were grown in Schaedler K3 (left panel) or in Tryptic Soy broth (TSB) supplemented with 0,2% cysteine (right panel).

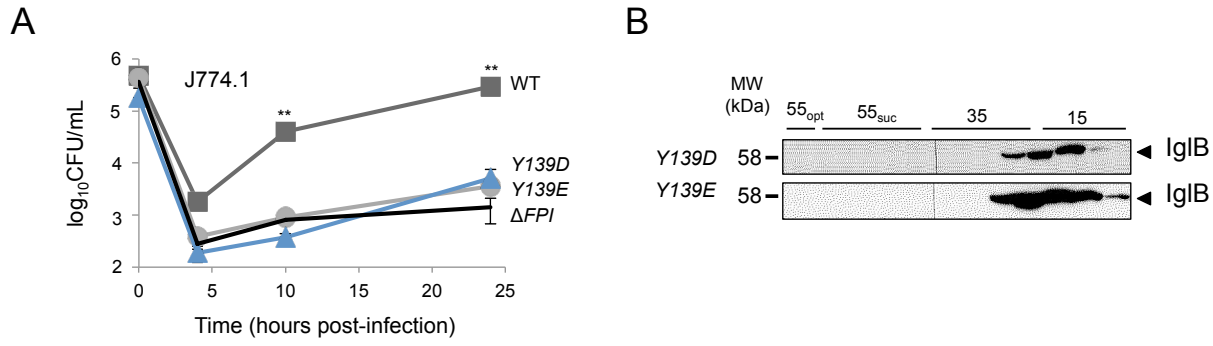

Supplementary Figure 4: Impact of substitution of Tyr139 by phosphomimetics (Glu or Asp) on *Francisella* intracellular multiplication and T6SS assembly. (**A**) J774.1 macrophage-like cells were infected in DMEM with 100 MOI of wild-type *F. novicida* (WT) and mutated strains (Y139E, Y139D, Δ*FPI*) for 24 h. Results are shown as the average of $\log_{10}$ cfu mL^{-1} ± standard deviation. Each experiment was performed in triplicate. **, $p<0.001$ (as determined by two-tailed unpaired Student's *t*-test). (**B**) WB with anti-IglB of sucrose gradient fractions.

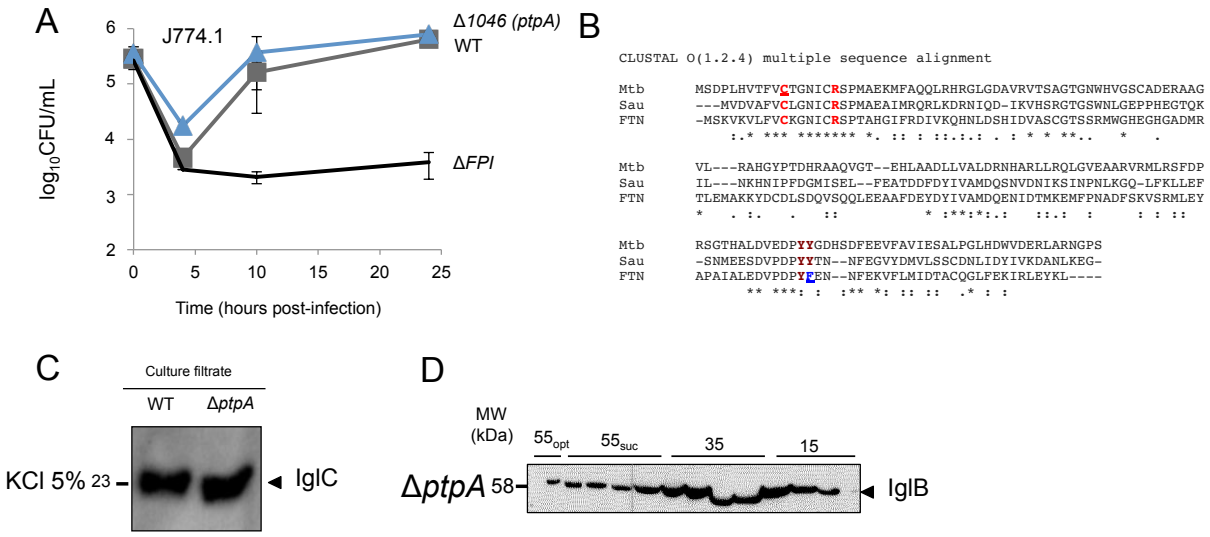

Supplementary Figure 5: Impact of *ptpA* inactivation on *Francisella* intracellular multiplication and T6SS assembly. (**A**) J774.1 macrophage-like cells were infected in DMEM with 100 MOI of wild-type *F. novicida* (WT), Δ*iglB* mutant, Δ*ptpA* mutant and Δ*FPI* mutant, for 24 h. Results are shown as the average of log10 cfu mL^{-1} ± standard deviation. Each experiment was performed in triplicate. **, $p<0.001$ (as determined by two-tailed unpaired Student's *t*-test). (**B**) Alignments of orthologous PtpAs proteins from different species (FTN, *Francisella* novicida; Wtb, *Mycobacterium tuberculosis*; *Sau*, *Staphylococcus aureus*). The PtpAs sequences were aligned using CLUSTALW. (**C**) WBs on bacteria / culture filtrates. Bacteria were grown in Schaedler-K3 supplemented with 5% KCl until late log phase and then harvested by centrifugation. Culture supernatants were collected after filtration on 0.2 µM Millipore filters and concentrated on Amicon 3 kDa. The equivalent of 200 µg of total protein were loaded onto each well. Left gel, WB with anti-IglC for the culture pellets; right gel, WB with anti-IglC for the culture supernatants. (**D**) WB with anti-IglB of sucrose gradient fractions.

Supplementary Table 1 (separate file). **Detailed list of phosphosites identified in *F. novicida.*** In this table, we report: i) the average of the log2 (intensity) of the phosphosites identified from three independent replicates; ii) the amino acid carrying the phosphorylation ("Amino Acid"); iii) its position on the protein (Position); iv) the "localization probability" of the phosphosite (1 being 100%); v) the number of replicates the phosphosite has been identified in ("identified"); vi) the "sequence window" of 15 amino acids before and after the amino acid phosphorylated; vii) the probability and score of identification and localization (PEP, score, score for localization); viii) the "charge" of the peptide; and ix) the annotation according to COG and EggNOG.

Supplementary Table 2 (separate file). **Table of intensities for IglB peptide carrying Y139 phosphorylation.**

Supplementary Table 3 (separate file). **List of proteins identified in the "Heavy" (H) and "Light" (L) Fraction in WT and in the Y139F mutant.** WT_H, WT_L, Y139_H, Y139F_L report the log2 (intensity) of the proteins identified in the fractions. Peptides and sequence coverage indicates the number of total peptides identified and the primary sequence coverage for that protein across samples. The Q value and the score refer to the quality of the identification.

AA	Backbone	Side Chain	Sheath assembly
Tyr	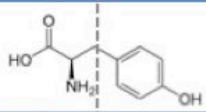		+
Tyr-P	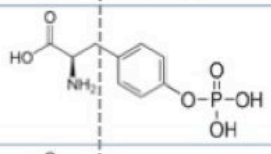		-
Phe	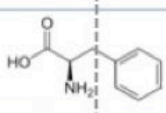		-
Ala	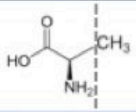		-
Glu	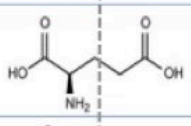		-
Asp	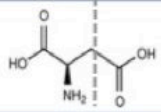		-

Supplementary Table 4. Impact of amino acid substitutions at site 139 of IglB on sheath assembly. Related to Figure 6 and Supplementary Fig. 5.

Strain	Relevant Genotype	Antibiotic resistance [a]	Relevant Features	Ref [b]
***F. novicida* U112**				
WT			*F. tularensis* subsp. *novicida* strain U112	1
U112 Δ*iglB*	Δ*iglB*::pGro-*nptII*	Km	Replacement of *iglB* by *nptII* under control of pGro promoter	2
Δ*iglB-Cp iglB*	Δ*iglB*::pGro-*nptII* pKK214::pGro-*iglB*	Km,Tet	U112 Δ*iglB* transformed with pKK214 vector containing *iglB* under control of pGro promoter	2
Δ*iglB-Cp iglB Y139A*	Δ*iglB*::pGro-*nptII* pKK214::pGro-$iglBY139A_{cp}$	Km,Tet	U112 Δ*iglB* transformed with pKK214 vector containing *iglB Y139A* under control of pGro promoter	2
Δ*iglB-Cp iglB Y139F*	Δ*iglB*::pGro-*nptII* pKK214::pGro-$iglBY139F_{cp}$	Km, Tet	U112 Δ*iglB* transformed with pKK214 vector containing *iglB Y139F* under control of pGro promoter	2
Δ*iglB-Cp iglB Y139E*	Δ*iglB*::pGro-*nptII* pKK214::pGro-$iglBY139E_{cp}$	Km, Tet	U112 Δ*iglB* transformed with pKK214 vector containing *iglB Y139E* under control of pGro promoter	2
Δ*iglB-Cp iglB Y139D*	Δ*iglB*::pGro-*nptII* pKK214::pGro-$iglBY139D_{cp}$	Km, Tet	U112 Δ*iglB* transformed with pKK214 vector containing *iglB Y139D* under control of pGro promoter	2
E. coli				
E. coli TOP10			Chemically competent cell used for routine cloning	3
Ec pKK	pKK214	Tet	*Escherichia coli* TOP10 transformed with pKK214 vector	1
Ec pKK-$iglB_{cp}$	pKK214::pGro-*iglB*	Km, Tet	*Escherichia coli* TOP10 transformed with pKK214 vector containing *iglB* under control of pGro promoter	2
Ec pKK-*iglB Y139A*$_{cp}$	pKK214::pGro-*iglB Y139A*	Km, Tet	*Escherichia coli* TOP10 transformed with pKK214 vector containing *iglB Y139A* under control of pGro promoter	2
Ec pKK-*iglB Y139F*$_{cp}$	pKK214::pGro-*iglB Y139F*	Km, Tet	*Escherichia coli* TOP10 transformed with pKK214 vector containing *iglB Y139F* under control of pGro promoter	2

[a] Km: Kanamycin (10 µg.mL^{-1}), Tet: Tetracyclin (5 µg.mL^{-1})
[b] [1] lab collection, [2] this study, [3] Life Technology

Supplementary Table 5: Strains and plasmids.

Primer code	Name	Sequence (5'-3')[a]	Relevant Features
p1	*iglB* upstream FW	TGTGTTATTGGCGTTGTTAAGGT	Construction of the *F. novicida* U112 Δ*iglB* mutant (Δ*FTN_1323*)
p2	*iglB* upstream(spl_K7) RV	TAATCCATACAATGTCATAACAAAATCCTCTCT	
p3	*iglB* downstream(spl_K7) FW	GAGTTCTTCTGATTCGGTACAAATAATAACTAAAAA	
p4	*iglB* downstream RV	CTAGCTGCGCAACATACTGG	
p5	*pGro* FW	TTGTATGGATTAGTCGAGC	Amplification of the Km^r cassette
	pGro(spl_*nptII*) RV	TTCAATCATAACAATCTTACTCCTTTGTTAAAT	
	nptII(spl_*pGro*) FW	AAGATTGTTATGATTGAACAAGATGGATTG	
p6	*nptII* RV	TCAGAAGAACTCGTCAAGAAGGCG	
	pGro[SmaI] FW	TGCACCCGGGCGACGAACTAATACTCATCTTGTAATG	Amplification of pGro promoter *from F. novicida* strain U112 used for functional complementation
	pGro RV	TATTGTCATAACAAAATCCTCTCTACTTATTATCTTTTGTATGGATTAGTCGAGCTAAAAAGCTCA	
	iglB FW	TGAGCTTTTTAGCTCGACTAATCCATACAATAAGTAGAGAGGATTTTGTTATGACAATA	Amplification of *iglB* gene from *F. novicida* strain U112 used for functional complementation
	iglB[PstI] RV	CTACTGCAGTTAGTTATTATTTGTACCGAATAATTCTGGT	
	iglB Y/A FW	GCTGATATATCTAGTAGTGACTTTTTCAAA	Mutagenesis of Tyrosine 139 by Alanine
	iglB Y/F FW	TTCGATATATCTAGTAGTGACTTTTTCAAA	Mutagenesis of Tyrosine 139 by Phenylalanine
	iglB Y/E FW	GAAGATATATCTAGTAGTGACTTTTTCAAA	Mutagenesis of Tyrosine 139 by Phenylalanine
	iglB Y/D FW	GATGATATATCTAGTAGTGACTTTTTCAAA	Mutagenesis of Tyrosine 139 by Glutamic acid
	iglB RV	TAAATTTCTCTCGAAATCATATTGTAGCTC	Mutagenesis of Tyrosine 139

[a] restriction sites are underlined

Supplementary Table 6: Primers.

DISCUSSIONS et PERSPECTIVES

De part son exceptionnelle capacité à échapper au compartiment phagosomal et sa flexibilité métabolique, *Francisella tularensis* représente aujourd'hui un modèle particulièrement intéressant pour l'étude des mécanismes moléculaires mis en jeu par les bactéries à multiplication intracellulaire lors de leur cycle infectieux.

Je me suis intéressé durant cette thèse à deux angles très différents de la pathogénèse de la bactérie. D'une part au métabolisme, avec l'étude d'une enzyme présente à un véritable carrefour métabolique et possédant de façon étonnante, une fonction « accessoire » dans la régulation transcriptionnelle d'un certains nombres de gènes. Et d'autre part, à cette fabuleuse machinerie de sécrétion qu'est le système de sécrétion de type VI et l'importance potentielle d'une modification post traductionnelle pour la dynamique d'assemblage de sa structure.

Dans un premier article, à travers l'étude de la fructose-1,6-biphosphatase (GlpX), nous démontrons l'importance de la gluconéogenèse pour la virulence *Francisella* et le rôle clef de cette voie dans le métabolisme des acides aminés récupérés de la cellule hôte. Dans un second article, nous confirmons dans un premiers temps le rôle essentiel de la gluconéogenèse dans la multiplication intracellulaire de la bactérie, avec l'étude de la fructose-1,6-bisphosphate aldolase (FBA). Nous démontrons l'importance de cette enzyme pour la multiplication cytosolique de *Francisella* en présence de substrats gluconéogéniques et dans la virulence dans le modèle animal. Le fait qu'un mutant délété du gène *fba* ne présente pas défaut de multiplication cytosolique *in vitro*, lorsqu'il est cultivé en présence de substrats glycolytiques indique que, bien que FBA soit une enzyme impliquée dans les voies glycolytiques et gluconéogéniques, la bactérie est capable d'utiliser des voies annexes à la glycolyse pour contourner l'absence de l'enzyme et métaboliser ces substrats. Inversement, l'incapacité du mutant *fba* à pousser en présence de substrats gluconéogéniques démontre que ces substrats doivent être métabolisés principalement (ou exclusivement) par la gluconéogenèse dépendante de FBA. Il est vraisemblable, qu'*in vivo*, *Francisella* ne rencontre pas la bonne combinaison de sources de carbone lui permettant de compenser l'absence de FBA.

De façon intéressante, chez de nombreuses bactéries, FBA est considérée comme une protéine « moonlight », c'est à dire possédant au moins deux fonctions biologiques distinctes dont une classique et une ou plusieurs annexe. Actuellement, on dénombre pas moins de 90 espèces bactériennes employant une ou plusieurs familles de protéines de ce type pour faciliter leurs cycles infectieux. Ces protéines peuvent avoir des fonctions très différentes et être impliquées dans des processus variés comme le métabolisme (voie de la glycolyse, le cycle TCA, le cycle glyoxylate et une gamme d'autres enzymes métaboliques), des fonctions des protéases, des activités de transporteurs mais aussi des fonctions de chaperones. Les protéines moonlight peuvent être divisées en deux catégories : celles qui n'ont qu'une seule fonction annexe et celles qui ont plusieurs actions biologiques supplémentaires (Henderson, 2014). La seule activité moonlight de FBA décrite dans la littérature jusqu'à présent chez les bactéries pathogènes était un rôle d'adhésine secondaire. Chez *Neisseiria meningitidis*, FBA n'est pas essentielle mais importante pour l'adhésion aux cellules épithéliales et endothéliales humaines. A l'inverse, FBA est essentielle chez *M. tuberculosis* et elle est importante pour la liaison au plasminogène humain. FBA n'est pas la seule enzyme de la glycolyse à posséder une fonction accessoire. En effet, la glyceraldehyde-3-phosphate dehydrogenase (GAPDH) est décrite comme étant une protéine moonlight chez *Streptococcus pyogenes* et *S. aureus*. La GAPDH de ces deux bactéries est retrouvée à la surface bactérienne et semblerait jouer un rôle dans la liaison à la fibronectine pour *S. pyogenes* et de liaison à la transferrine pour *S. aureus* (Tunio et al., 2010).

De façon remarquable, nous démontrons dans notre étude une fonction tout à fait nouvelle de FBA chez *Francisella*, en tant que régulateur transcriptionnel. En effet, nous montrons que l'enzyme est capable de se lier directement sur les séquences promotrices de certains gènes pour réguler leur transcription. Parmi ces gènes régulés par FBA, on retrouve le gène codant pour KatG, une catalase importante pour la détoxification des espèces réactives de l'oxygène. En combinant l'ensemble de ces résultats avec les données de la littérature, nous proposons un modèle dans lequel FBA participerait au

contrôle de l'homéostasie redox de la cellule et la mise en place d'une réponse immunitaire inflammatoire.

Nous savons aujourd'hui qu'une partie non négligeable (peut être encore sous estimée) d'enzymes métaboliques possède des fonctions accessoires qui n'ont rien à voir avec leurs fonctions initiales. D'un point de vue survie et adaptation, cette stratégie qui consiste à coupler son métabolisme avec d'autre fonction utile pour la pathogénèse de la bactérie s'avère être payante. Il est tentant de penser que les bactéries peuvent se servir de leurs métabolismes comme senseur pour adapter leurs stratégies d'adaptation à la vie intracellulaire lorsqu'elles rencontrent des conditions favorables ou défavorables à leurs multiplications.

Nous attribuons pour la première fois une fonction régulatrice à une protéine moonlight chez les bactéries. Il serait maintenant intéressant de déterminer si d'autres protéines de ce type (enzymes ou autres protéines structurales) pourraient avoir des fonctions de régulation chez *Francisella*. Dans ce cadre, nous travaillons actuellement sur une autre enzyme du métabolisme, la transketolase (TktA), une enzyme essentielle de la voie des Pentoses Phosphates. Une mutation dans le gène codant pour cette enzyme provoque un défaut majeur de virulence, ainsi qu'une modification non négligeable du protéome de la bactérie. Nous ne savons pas encore si les effets de la mutation sont directs ou indirects. Des premières analyses transcriptomiques par qRT-PCR suggèrent que la transketolase pourrait elle aussi posséder une fonction accessoire régulatrice. Ces données devront être complétées par des expériences de liaison directe à l'ARNm des cibles déjà identifiées.

Les modifications post traductionnelles constituent des stratégies efficaces pour répondre rapidement à des stress venant de l'extérieur. Ces modifications transitoires permettent de s'affranchir d'une réponse transcriptionnelle plus longue à mettre en place. Malgré l'absence de gènes codant pour des systèmes S/TK-P prédits dans les génomes de *Francisella* et l'absence de données dans la littérature sur ce type de modification de protéines chez *Francisella*, nous avons décidé de réaliser une analyse phosphoprotéomique globale de *Francisella*. Cette première étude phosphoprotéomique

a révélé l'existence d'une cinquantaine de protéines phosphorylées sur serine, thréonine ou tyrosine (dont certains polyphosphorylées).

Nous avons été particulièrement intrigués, dans cette analyse, par l'identification d'une des protéines majeures du fourreau du système de sécrétion de type VI de *Francisella*, la protéine IglB (l'homologue de TssC, VipB). Cette protéine présente un site de phosphorylation unique sur la tyrosine 139. La question a alors été de savoir si la forme phosphorylée était associée au fourreau (suggérant que la phosphorylation d'IglB pourrait être favorable à son assemblage) ou aux formes non-polymérisées de la protéines (suggérant alors que la phosphorylation serait défavorable à l'assemblage). La modélisation de la région du site Y139 suggère que l'ajout d'un phosphate sur l'hydroxyl du noyau aromatique de la tyrosine entrainerait une répulsion de l'interaction avec les résidus aspartate avoisinants (d'IglA et IglB). De façon remarquable, nous retrouvons cette protéine IglB phosphorylée exclusivement dans la forme non-polymérisée du fourreau, confirmant les données de modélisation et suggérant que la phosphorylation de la Tyrosine139 pourrait jouer un rôle dans la biogenèse d'un SST6 fonctionnel.

La substitution de ce résidu par des résidus non phosphorylables (alanine et phénylalanine) ou par des résidus mimant la phosphorylation (aspartate et glutamate) affecte sévèrement la formation du fourreau.

L'ensemble de ces données nous ont conduit à proposer un mécanisme par lequel la phosphorylation d'IglB pourrait être un nouvel acteur dans la régulation la dynamique d'assemblage / désassemblage du SST6 de *Francisella*.

A ce stade du projet, il serait vraiment intéressant de caractériser les partenaires impliqués dans ce mécanisme de régulation. L'absence de Tyrosine Kinase ou Phosphatase canonique dans le génome de la bactérie rend difficile cette identification. Grâce aux récentes améliorations des approches phosphoprotéomiques, de nouvelles familles de protéines kinases ayant une activité Ser / Thr / Tyr kinase non-canoniques ont été identifiées. Il est probable que *Francisella* possède ce type de protéines qui attendent encore d'être identifiées et caractérisées. Une approche aléatoire pourrait être utilisée pour permettre l'identification de ces enzymes. En se basant sur la banque de mutants, testée sur les macrophage U937 et les cellules S2 dérivées de la Drosophile (Asare and Kwaik, 2010), nous pourrions nous focaliser sur les mutant

bloqués dans le phagosome (91 mutants identifiés sur 3.050 mutants d'insertion de transposon criblés). Parmi ces 91 mutants, une analyse par phosphoprotéomique sur les mutants présentant une altération dans la formation de la gaine pourrait être réalisée. Une telle approche nous permettrait d'identifier la phosphatase. En effet, l'inactivation de la phosphatase devrait conduire à une phosphorlyation stitutive d'IglB et donc inhiber la formation du fourreau. Le phénotype d'un mutant dans la kinase est moins prédictible dans la mesure où il pourrait ne pas présenter de défaut d'assemblage ni de défaut sortie du phagosome. La limitation majeure de cette approche aléatoire serait l'existence de fonctions redondantes par d'autre enzyme rendant ce criblage impossible. Dans ce cas, une approche ciblée serait alors plus envisageable. Chez *P. aeruginosa*, l'enzyme impliquée dans la phosphorylation (PpkA) sur un résidu thréonine de la protéine Fha du SST6 (HSI-I) est codée par un des gènes de l'îlot de pathogénicité (Mougous et al., 2007). Nous pourrions donc cibler dans un premier temps, l'ensemble des gènes du FPI (dont plusieurs sont de fonction totalement inconnue) et tester s'ils présentent des fonctions tyrosine kinase et/ou phosphatase. Il serait également envisageable de cibler les kinases des systèmes à deux composants connus chez *Francisella*, dans la mesure où il pourrait exister des fonctions croisées de ces enzymes.

L'ensemble de ces travaux de thèse ont permis d'en savoir davantage sur les mécanismes moléculaires importants pour l'adaptation de *Francisella* à la vie intracellulaire. De tels mécanismes pourraient être conservés chez d'autres intracellulaires pathogènes et mériteraient d'être soigneusement réexaminés.

ANNEXES

Molecular Microbiology (2015) 98(3), 518–534 ■
doi:10.1111/mmi.13139
First published online 10 September 2015

Gluconeogenesis, an essential metabolic pathway for pathogenic *Francisella*

Terry Brissac,[1,2] Jason Ziveri,[1,2] Elodie Ramond,[1,2] Fabiola Tros,[1,2] Stephanie Kock,[1,2] Marion Dupuis,[1,2] Magali Brillet,[1,2] Monique Barel,[1,2] Lindsay Peyriga,[3,4,5] Edern Cahoreau[3,4,5] and Alain Charbit[1,2]*

[1]*Université Paris Descartes, Sorbonne Paris Cité, Bâtiment Leriche, Paris, France.*
[2]*INSERM U1151 – CNRS UMR 8253, Institut Necker-Enfants Malades, Equipe 11: Pathogénie des Infections Systémiques, Paris, France.*
[3]*Université de Toulouse, INSA, UPS, INP, LISBP, 135 Avenue de Rangueil, Toulouse 31077, France.*
[4]*INRA, UMR792, Ingénierie des Systèmes Biologiques et des Procédés, Toulouse 31400, France.*
[5]*CNRS, UMR5504, Toulouse 31400, France.*

Summary

Intracellular multiplication and dissemination of the infectious bacterial pathogen *Francisella tularensis* implies the utilization of multiple host-derived nutrients. Here, we demonstrate that gluconeogenesis constitutes an essential metabolic pathway in *Francisella* pathogenesis. Indeed, inactivation of gene *glpX*, encoding the unique fructose 1,6-bisphosphatase of *Francisella*, severely impaired bacterial intracellular multiplication when cells were supplemented by gluconeogenic substrates such as glycerol or pyruvate. The Δ*glpX* mutant also showed a severe virulence defect in the mouse model, confirming the importance of this pathway during the *in vivo* life cycle of the pathogen. Isotopic profiling revealed the major role of the Embden–Meyerhof (glycolysis) pathway in glucose catabolism in *Francisella* and confirmed the importance of *glpX* in gluconeogenesis. Altogether, the data presented suggest that gluconeogenesis allows *Francisella* to cope with the limiting glucose availability it encounters during its infectious cycle by relying on host amino acids. Hence, targeting the gluconeogenic pathway might constitute an interesting therapeutic approach against this pathogen.

Accepted 16 July, 2015. *For correspondence. E-mail alain.charbit@inserm.fr; Tel. 331 7260 6511; Fax 331 7260 6513.

Introduction

For intracellular microbial pathogens, acquisition of nutrients from their host and the capacity to adapt to any modification of the available nutrient pools are both required to establish a successful infection. While many intracellular bacterial pathogens mainly rely on glucose as a preferred carbon source for their intracellular metabolism, others simultaneously use multiple carbon sources (Abu Kwaik and Bumann, 2013; 2015; Zhang and Rubin, 2013; Fonseca and Swanson, 2014). For example, *Listeria monocytogenes* has been shown to rely on two major carbon substrates, glycerol (for energy supply) and glucose-6P (to fuel the pentose phosphate shunt and to provide components essential for cell envelope and nucleotides biosynthesis) (Eisenreich *et al.*, 2010; Grubmüller *et al.*, 2014), but preferentially uses glycerol during its intracellular replication. In contrast, *Shigella flexneri*, which also exclusively replicates in the cytosol of infected host cells, was shown to require glycerol-3-phosphate as a carbon source (Lucchini *et al.*, 2005). *Mycobacterium tuberculosis*, which replicates within a vacuolar compartment, utilizes fatty acids in addition to glycerol or glycerol-3-phosphate as carbon sources in macrophages (Schnappinger *et al.*, 2003). *Salmonella enterica* serovar *Typhimurium*, which also replicates within a vacuolar compartment, requires glucose import, glycolysis and the tricarboxylic acid (TCA) cycle to replicate within host phagocytes (Tchawa Yimga *et al.*, 2006; Mercado-Lubo *et al.*, 2008; 2009; Bowden *et al.*, 2009).

As an alternative to glucose uptake, gluconeogenesis permits glucose synthesis from non-sugar compounds such as amino acids or TCA cycle intermediates. This anabolic pathway has been shown to be involved in virulence of several intracellular bacterial pathogens, including notably *Mycobacterium tuberculosis* (Marrero *et al.*, 2010; Puckett *et al.*, 2014), but appeared to be dispensable for *Salmonella enterica* serovar *Typhimurium* (Tchawa Yimga *et al.*, 2006) as well as for *Brucella abortus* (Zuniga-Ripa *et al.*, 2014).

Francisella tularensis, a small Gram-negative facultative intracellular pathogen, is the causative agent of the zoonotic disease tularemia (Sjostedt, 2007; 2011). Humans can be infected by this highly infectious pathogen by different means, including direct contact with sick

animals, inhalation, insect bites or ingestion of contaminated water or food. *F. tularensis* is able to infect numerous cell types, including dendritic cells, neutrophils, macrophages as well as hepatocytes or endothelial cells but is thought to replicate *in vivo* mainly in macrophages (Santic *et al*., 2006). Four subspecies (ssp or biovars) of *F. tularensis* are currently listed: *F. tularensis* ssp *tularensis*, *F. tularensis* ssp *holarctica*, *F. tularensis* ssp *mediasiatica* and *F. tularensis* ssp *novicida* (McLendon *et al*., 2006). The four subspecies differ in their virulence and geographical origin, but all cause a fulminant disease in mice that is similar to tularemia in humans (Kingry and Petersen, 2014). Although *F. novicida* is rarely pathogenic in humans, its genome shares approximately 97% nucleotide sequence identity with the human pathogenic species and is thus widely used as a model to study highly virulent subspecies. *Francisella* virulence is tightly linked to its capacity to multiply in the cytosolic compartment of infected macrophages. The importance of sugar metabolism in the bacterial adaptation to this niche is currently totally unknown.

The aim of the present study was to understand the importance of the gluconeogenic pathway in *Francisella* pathogenesis, focusing on *glpX*, encoding a key enzyme of this anabolic pathway, converting fructose 1,6-bisphosphate (F-1,6P) into fructose 6-phosphate (F-6P). This reaction is catalyzed by the fructose 1,6-bisphosphatase (FBPase), one of the two steps in gluconeogenesis that is uncoupled from enzymes involved in glycolysis. Indeed, two different enzymes are also required for the phosphoenolpyruvate (PEP) and pyruvate interconversion, encoded by genes *pyk* and *ppdk* respectively. Hence, Ppdk and FBPase represent two enzymatic steps specifically acting in the gluconeogenic direction and which are not depending on the reversibility of a glycolytic enzyme.

Five different classes of FBPases have been described according to their amino acid sequences (Donahue *et al*., 2000). Types I–III are primarily found in bacteria, type IV in archaea and type V in thermophilic prokaryotes. Whereas most bacteria possess combinations of two different FBPase classes, *Francisella* genomes encompass only one class II FBPase, encoded by the gene *glpX* (*FTN_0298* in *F. tularensis* subsp *novicida* or *F. novicida*). Remarkably, the gene *glpX* has been repeatedly identified in earlier genetic screens [performed in *F. novicida*, *F. tularensis* live vaccine strain (LVS) and *F. tularensis* SCHU S4 (Maier *et al*., 2006; Su *et al*., 2007; Weiss *et al*., 2007; Kadzhaev *et al*., 2009; Peng and Monack, 2010)] but its functional role in pathogenesis was never addressed. The data presented here reveal the importance of gluconeogenesis in intracellular adaptation of *Francisella*. Glucose availability appears as a critical component in the tug-of-war between this pathogen and the host macrophage.

Results

GlpX, a type II fructose 1,6-bisphosphatase (FBPase II)

The gene *glpX* (*FTN_0298* in *F. novicida*) is the last gene of a predicted operon that is highly conserved among *Francisella* subspecies (Fig. S1). The protein GlpX (FTN_0298 in *F. novicida*) shows 100% to 98% amino acid sequence identity with its orthologs in *F. tularensis* subspecies *mediasiatica*, *holarctica* and *tularensis* (FTM_0252, FTL_1701 and FTT_1631c, respectively) and 47% amino acid identity with the type II fructose 1,6-bisphosphatase (FBPase II) of *Escherichia coli* K12 (b3925) of known crystallographic structure (Brown *et al*., 2009). Of note, the putative FBPase II catalytic sites are conserved in the sequence of FTN_0298 (Fig. S1B), suggesting that FTN_0298 is a genuine FBPase II. Unlike *E. coli*, which also expresses a class I FBPase (Fbp, b4232), the *Francisella* genomes encode a unique class II FBPase.

*A Δ*glpX *mutant is unable to grow on gluconeogenic substrates*

We constructed an isogenic mutant of *glpX* in *F. novicida* by allelic replacement (see Experimental procedures) and evaluated the impact of *glpX* inactivation on bacterial growth, intracellular multiplication and, *in vivo*, in the mouse model. Inactivation of *glpX* had no impact on bacterial growth in rich medium (Fig. S2A). Growth of the Δ*glpX* mutant was also identical to that of the wild-type (WT) strain in chemically defined medium (CDM, Chamberlain, 1965) supplemented either with glucose, ribose (Fig. 1A and B) or sucrose as carbon sources (Fig. S2B). In contrast, the Δ*glpX* mutant showed a severe growth defect in all the media containing gluconeogenic substrates tested (i.e. glycerol, pyruvate or an amino acid cocktail; Fig. 1C–E respectively). WT growth was always restored in the Δ*glpX*-complemented strain, demonstrating the absence of polar effect of the mutation. These data confirmed that *glpX* is required for growth of *F. novicida* in culture, but only when gluconeogenic substrates are used as carbon sources.

We further tested whether WT *F. novicida* or Δ*glpX* strains could grow in CDM where glucose was substituted by each of the 20 amino acids, individually supplemented at a 30 mM final concentration (Fig. S3). In the absence of added amino acid, growth of the WT strain in CDM with no glucose was significantly reduced but still detectable, likely due to the presence of the amino acids present in the CDM (in the 3 mM range, see Experimental procedures). In contrast, growth of the Δ*glpX* mutant was essentially abolished. Supplementation with excess amino acids improved, with variable efficiencies, growth of the WT strain in the absence of glucose (e.g. threonine, proline, methionine, lysine, tyrosine, tryptophane, pheny-

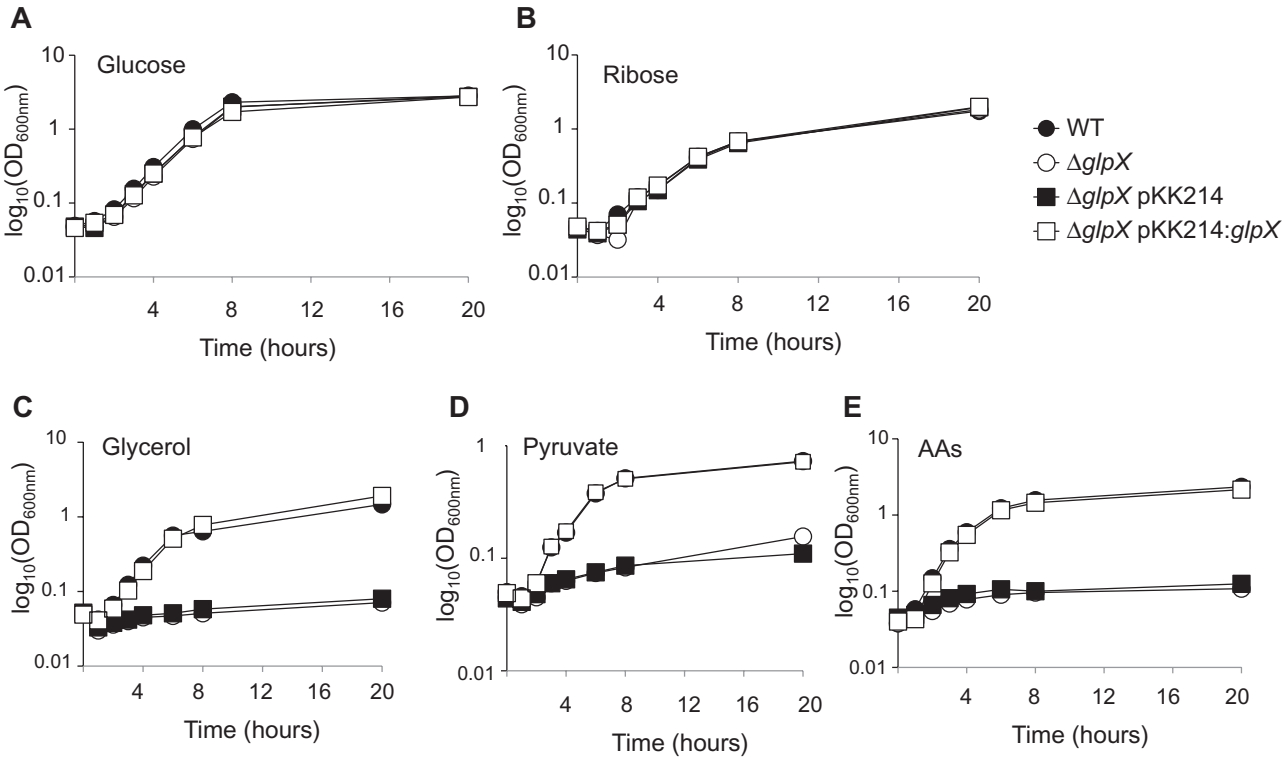

Fig. 1. Growth properties in CDM.
Wild-type *F. novicida* (WT, close circles), isogenic Δ*glpX* mutant (Δ*glpX*, open circles), Δ*glpX* containing empty pKK214 vector (Δ*glpX* pKK214, close square) and complemented Δ*glpX* strain (Δ*glpX* pKK214:*glpX*, open square) were grown in CDM supplemented with different carbon sources at a final concentration of 40 mM.
(A) Glucose, (B) ribose, (C) glycerol, (D) pyruvate, (E) amino acid cocktail (casamino acid solution at a final concentration of 5 g l^{-1}).

lalanine, asparagine or serine). Other amino acids did not improve growth of WT *F. novicida* in the absence of glucose (e.g. glutamine, glutamate, leucine, isoleucine, histidine or arginine). Of note, growth of WT *F. novicida* in CDM supplemented with 30 mM alanine was similar to that observed in CDM supplemented with glucose. Supplementation of the CDM lacking glucose with excess amino acids failed to restore growth of the Δ*glpX* mutant, demonstrating the utilization of amino acids as gluconeogenic substrates by *Francisella*. Under all conditions tested, functional complementation restored WT growth properties to the Δ*glpX* mutant (not shown).

Glucose metabolism in Francisella

We then evaluated the fate of glucose in *F. novicida* by an isotopic profiling approach. For this, WT *F. novicida* was grown in CDM supplemented with ^{13}C-labeled glucose. Labeling was performed with a mixture of [1-^{13}C]glucose and [U-$^{13}C_6$]glucose (see Experimental procedures for details). Altogether, the carbon isotopolog distribution (CID) indicated the simultaneous activity of glycolysis and gluconeogenesis (Fig. 2). The recycling of carbons through the pentose phosphate pathway (PPP) was visible in the gluconeogenic metabolites from fructose-1,6-biphosphate to glucose-1-phosphate (presence of isotopologs from M2 to M5 coming from carbon reassociation in the PPP) (Fig. 2). If glycolysis was the only pathway active, we would only find the isotopologs M1 and M6 for hexoses phosphates until fructose-bisphosphate (FBP). Actually, we could detect intermediate labeled forms from M2 to M5 and a small fraction of M0. These intermediate isotopologs can be formed by re-associations of carbons made by the enzyme of the non-oxidative PPP (transketolase, transaldolase). In contrast, 6-phosphogluconate (6PG) and pentose phosphates were not detected in this experiment, suggesting a low activity of the oxidative part of PPP, from 6PG to pentose-5-phospate. Indeed, production of P5P from the oxydative PPP should give large amount of unlabeled P5P (M0) after decarboxylation of 6PG. This M0 part of the P5P could be produced from the non-oxidative part of the PPP (from fructose-6-phosphate and glyceraldehyde-3-phosphate). Experimental labeling patterns of metabolites in C3 (2/3-phosphoglycerate and PEP) seemed very close to the theoretical labeling patterns that could be obtained in the hypothesis of an exclusive glycolytic flux (without any activity of the oxidative PPP). Indeed, in the case of an exclusive glycolytic flux,

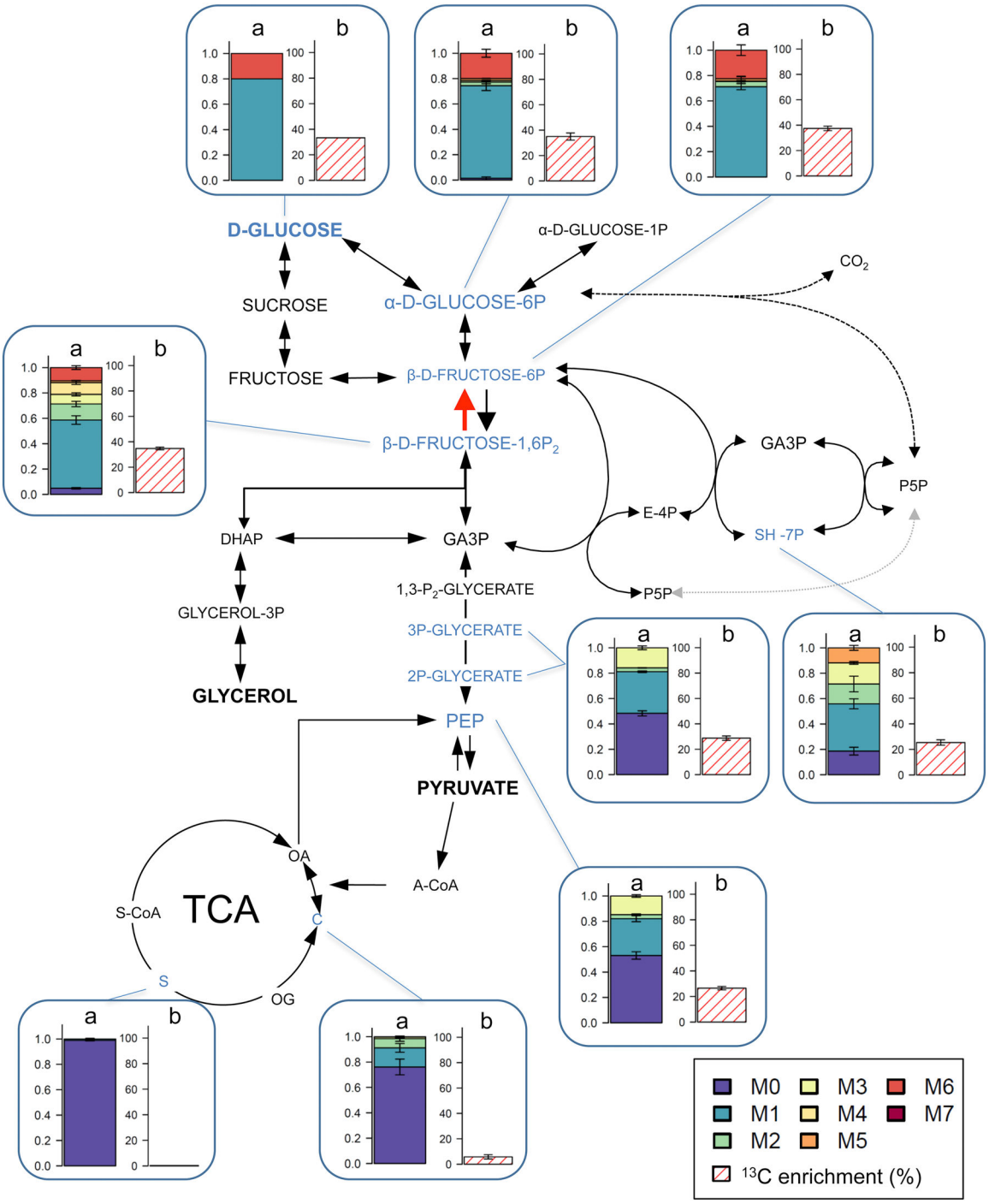

Fig. 2. Carbon isotopolog distribution of central metabolites.
A. CID of central metabolites ($n = 3$ mean ± sd). CID of central metabolites was determined after labelling of wild-type *F. novicida* grown in CDM with a mixture of [80% 1-^{13}C] glucose and 20% [U-^{13}C] glucose. CIDs were measured to obtain flux partition through the oxidative PPP since CO_2 loss within this pathway involves specific loss of the C1 of [1-^{13}C] glucose. The carbon isotopologs M0 to M7 refer to the isotopic isomers of metabolites having incorporated 0 to 7 ^{13}C atoms. The M0 abundances, corresponding to fraction of unlabeled molecules. CIDs are normalized to 1. The *glpX*-dependent step is indicated by a bold red arrow. The P5P correspond to the global pool of pentose-5-P (i.e. ribose-5-P + ribulose-5-P + xylulose-5-P).
B. ^{13}C enrichment of central metabolites. ^{13}C enrichment corresponds to the percentage of ^{13}C in a molecule. It is calculated from the carbon isotopolog distribution by the following formula: ^{13}C enrichment = $(0 \times M0 + 1 \times M1 + 2 \times M2 + \ldots + n \times Mn)/nC$. *nC* is the number of carbons in the molecule and Mn is the fraction of the corresponding isotopologue having incorporated n ^{13}C atoms. ^{13}C enrichments of central metabolites shown a significant enrichment dilution of TCA intermediates which seems to indicate a consumption of amino acids in the CDM medium diluting the ^{13}C coming from glycolysis.

theoretical labeling pattern of C3 compounds should be 40% M0, 40% M1 and 20% M3. An activity of the oxidative PPP should increase drastically the proportion of M0 over 40% on those C3 compounds, due to decarboxylation performed by the phosphogluconate dehydrogenase producing P5P. This increase of M0 in the C3 compounds is not significant in our results and comforts the hypothesis of a predominant activity of the glycolytic flux.

Finally, CID of the TCA metabolites shows an increase of the M0 forms probably due to a dilution of ^{13}C incorporation by consumption of amino acids present in the cultivation medium that are entering at multiple nodes of the TCA cycle. This dilution can clearly be identified by comparing ^{13}C enrichment of central metabolites (percentage of ^{13}C in metabolites calculated from measured CIDs; Table S3). The exploration of ^{13}C labeling information for flux profiling can indeed be limited by the utilization of non-minimal media without measuring every consumption flux. Nevertheless, regarding the previously discussed results on isotopic profiles of C3 compounds, gluconeogenic flux from TCA cycle seems to be limited in this condition.

In a second labeling experiment, WT *F. novicida* and Δ*gplX* knock-out strain were grown in CDM supplemented with ^{13}C-labeled pyruvate. Labeling was performed with [1-^{13}C]pyruvate in the presence of 1 mM glucose to support growth of the Δ*glpX* mutant (see Experimental procedures for details). CIDs measured from this experiment indicated an operational gluconeogenesis from pyruvate in the WT strain (Fig. S4). Indeed M1 isotopolog was clearly detected in the compounds of gluconeogenesis pathway after correction of the ^{13}C natural abundance. Nevertheless, M1 fraction in metabolites remained low (less than 15.4% in PEP, the first compound to be labeled from pyruvate), which is compatible with a low consumption of pyruvate from the medium by the cells. A significant dilution of the labeling was also detected in the metabolites of the upper part of gluconeogenesis. Hexoses-phosphates showed indeed a relative low proportion of M1 fraction (FBP: 6.9%, F6P: 3.7%, G6P: 2%), as compared with C3 compounds of the lower part of gluconeogenesis. These observations are consistent with the presence of 1 mM unlabeled glucose in the medium entering the glycolysis as well as the cocktail of unlabeled amino acids which could also be consumed by the cells for gluconeogenesis process and dilute the labeling coming from pyruvate. In this experiment, compounds of the PPP were not detected. The same experiment was performed on the Δ*glpX* mutant strain and the first significant observation is that neither G6P nor F6P were detected even with the presence of 1 mM of glucose in the medium. According to peak areas measured, we also detected a strong signal increase for compounds of gluconeogenesis below *gplX*-encoded type II fructose 1,6-bisphosphatase, from PEP to FBP (data not shown). In parallel, an increase in ^{13}C labeling was detected in the lower part of gluconeogenesis until FBP, most likely reflecting accumulation of these compounds in the mutant strain.

Altogether, these results support an effective blocking of gluconeogenesis and confirm the hypothesis of the critical role of *glpX* in gluconeogenic flux in *Francisella*.

*Intracellular multiplication of Δ*glpX *mutant is severely impaired in the presence of gluconeogenic substrates*

We next examined the ability of WT *F. novicida* and Δ*glpX* strains to survive and multiply in murine macrophage-like J774.1 cells, grown in cellular culture media supplemented either with glucose or glycerol (Fig. 3A and B). We used as a negative control a *F. novicida* mutant with a deletion of the entire *Francisella* pathogenicity island (FPI), designated Δ*FPI* mutant strain (Weiss *et al.*, 2007). This mutant is unable to escape from phagosomes and fails to grow in macrophages. In standard Dulbecco's modified Eagle's medium (DMEM) (i.e. containing glucose), the intracellular multiplication of the Δ*glpX* mutant was essentially identical to that of WT *F. novicida* (Fig. 3A). In contrast, when glucose was substituted either by glycerol (Fig. 3B) or pyruvate (not shown), multiplication of the Δ*glpX* mutant was severely impaired and comparable with that of the Δ*FPI* mutant. Indeed, after 24 h, cells infected with the Δ*glpX* mutant showed an approximately 100-fold reduction of intracellular bacteria in these media, as compared with cells infected with the WT strain.

The intracellular behavior of the Δ*glpX* mutant in THP-1 human monocytes (Fig. 3C and D) was quite similar to that in J774.1 cells. The Δ*glpX* mutant showed WT multiplication when cells were grown in cellular culture media supplemented with glucose (Fig. 3C), whereas it was severely impaired in the presence of glycerol (Fig. 3D). However, at 24 h, the mutant appeared to multiply in these cells almost to the same level as the complemented strain.

Finally, the intracellular behavior of the Δ*glpX* mutant was tested in bone marrow-derived macrophages (BMM) from BALB/c mice as well as in Hep G2 cells, a non-phagocytic human hepatocytic cell line currently used to study the intracellular properties of *Francisella* mutants (Qin and Mann, 2006; Qin *et al.*, 2008; 2009; Schulert *et al.*, 2009; Thomas-Charles *et al.*, 2013; Gesbert *et al.*, 2014). Intracellular multiplication of the Δ*glpX* mutant was also severely impaired in both cell types (Fig. 3F and H), when the culture medium was supplemented with glycerol. In contrast, when cells were supplemented with glucose, the multiplication defect of the Δ*glpX* mutant was essentially abolished in both cell types (Fig. 3E and G).

Functional complementation (i.e. introduction of a plasmid-born WT *glpX* allele into the Δ*glpX* mutant strain) restored normal intracellular bacterial replication in all cell

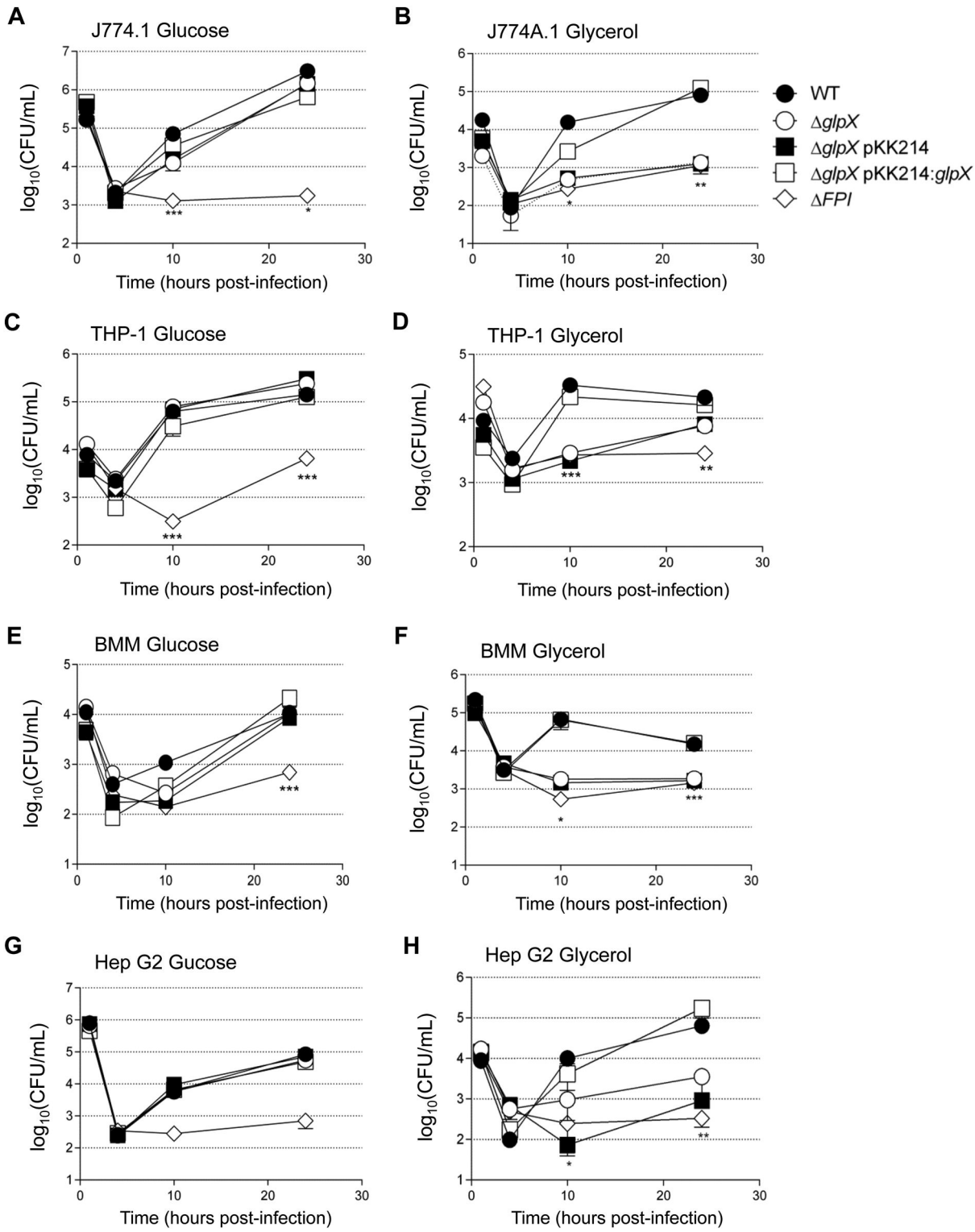

Fig. 3. *glpX* inactivation affects intracellular survival.
Intracellular bacterial multiplication of wild-type *F. novicida* (WT, close circles), isogenic Δ*glpX* mutant (Δ*glpX*, open circles), Δ*glpX* containing empty pKK214 vector (Δ*glpX* pKK214, close square) and complemented Δ*glpX* strain (Δ*glpX* pKK214:*glpX*, open square), and the Δ*FPI* negative control (open lozenge) was monitored during 24 h in J774A.1 macrophage cells (A, B), THP-1 macrophage cells (C, D), BMM from BALB/c mice (E, F) and Hep G2 hepatic cells (G, H).
DMEM (Dulbecco's modified Eagle medium) was supplemented with glucose (A, C, E, G) or glycerol (B, D, F, H).
$^{*}P < 0.05$; $^{**}P < 0.01$; $^{***}P < 0.001$ (determined by Student's *t*-test).

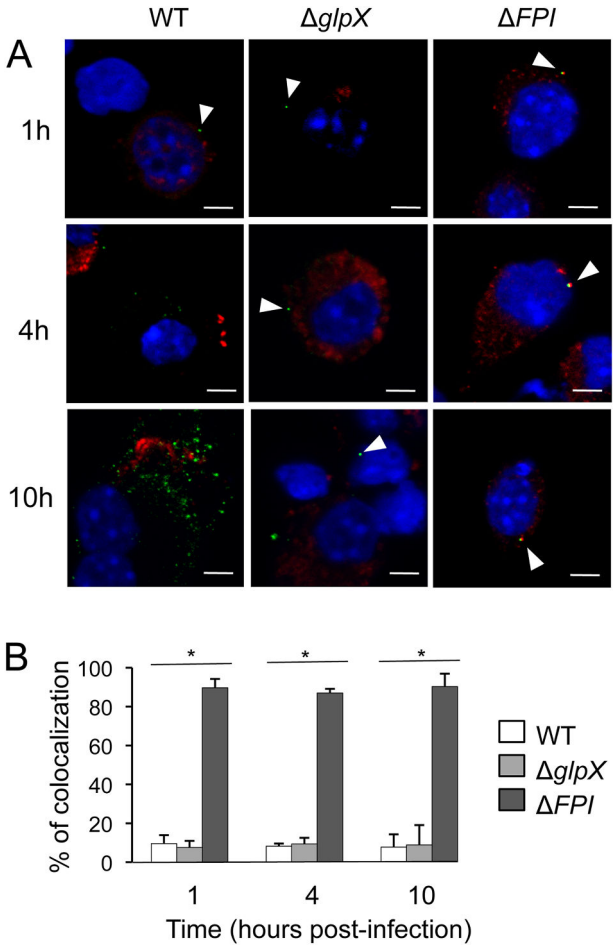

Fig. 4. Subcellular localization of the Δ*glpX* mutant.
A. J774.1 were infected for 30 min with wild-type *F. novicida* (WT), Δ*glpX* or Δ*FPI* strains, and their colocalization with the phagosomal marker LAMP1 was observed by confocal microscopy 1, 4 and 10 h, after beginning of the experiment. J774.1 were stained for *F. tularensis* (green), LAMP-1 (red) and host DNA (DAPI). Scale bars at the bottom right of each panel correspond to 5 μM.
B. Quantification of bacteria/phagosome colocalization at 1, 4 and 10 h for WT, Δ*glpX* and Δ*FPI* strains.
*$P < 0.001$ (determined by Student's *t*-test).

types tested. Altogether, these assays demonstrate that the Δ*glpX* mutant is unable to grow or to multiply when gluconeogenic substrates (glycerol, pyruvate or amino acids) are used as carbon sources (Figs. 1 and 3). In contrast, when non-gluconeogenic substrates are used, the growth defect of the Δ*glpX* mutant is completely suppressed.

To evaluate the capacity of the Δ*glpX* mutant to escape from phagosomal vacuoles, we labeled bacteria and the late phagosomal marker, LAMP-1, and evaluated their colocalization by confocal immunofluorescence microscopy (Fig. 4). Colocalization of *Francisella* and LAMP-1 was assayed at three time points, 1, 4 and 10 h (Fig. 4A). After 1 h of infection, only 9.5% and 7.5% of colocalization was recorded with WT *F. novicida* and Δ*glpX*, respectively, indicating that the Δ*glpX* mutant was able to escape phagosomes as fast as WT *F. novicida*. Colocalization remained still very low after 4 h (8.2% and 9.4%, respectively) and after 10 h (7.8% and 8.9% respectively). In contrast, the Δ*FPI* mutant strain remained trapped into phagosomes, as illustrated by high colocalization with LAMP-1 at all time points tested (89.6%, 87% and 90.3%, after 1, 4 and 10 h respectively) (Fig. 4B). These results indicate that the intracellular growth defect of the Δ*glpX* mutant is not due to altered phagosomal escape but to impaired cytosolic multiplication.

The glpX *mutant is attenuated in mice*

We evaluated the virulence of the *F. novicida* Δ*glpX* mutant in the mouse. For this, we first infected groups of five BALB/c mice by the intraperitoneal (i.p.) route with 2×10^2 colony forming units (CFUs) of Δ*glpX* or WT *F. novicida* and survival was followed over a 10 day period. Four out of five mice infected with the Δ*glpX* mutant strain were still alive and apparently healthy 10 days after infection. In contrast, all the mice infected with the WT strain died by the third day after infection (Fig. 5A).

The severe attenuation of virulence of the Δ*glpX* mutant was next confirmed by monitoring the bacterial burden in spleen and livers of BALB/c mice, 2.5 days after infection by the i.p. route with 2×10^2 CFUs. Mice infected with *F. novicida* WT strain had bacterial burdens close to 10^7 CFUs per organ (Fig. 5B). In contrast, mice infected with the Δ*glpX* mutant contained only between 10^3 and 10^4 CFUs per organ (i.e. 1000-fold lower amounts). Remarkably, the bacterial burdens in the organs of mice infected with the complemented strain were even slightly higher than those recorded with the WT strain (app. 10^8 CFUs per organ), demonstrating full *in vivo* functional complementation of the Δ*glpX* deletion by the plasmid-born WT *glpX* allele.

GlpX of F. tularensis *LVS is required for intracellular survival*

To further establish the importance of the *glpX* gene to *F. tularensis* pathogenesis, we constructed a chromosomal deletion mutant (Δ*FTL_1701*) in the *F. tularensis* subsp. *holarctica* LVS and evaluated its impact on intracellular multiplication. We first evaluated the impact of the mutation in standard CDM supplemented with glucose (Fig. 6A). Growth of the LVSΔ*glpX* mutant (Δ*FTL_1701*) was identical to that of WT LVS. Of note, unlike *F. novicida* (and *F. tularensis subsp tularensis*), *F. tularensis* LVS is unable to grow on glycerol. We therefore compared growth of the LVSΔ*glpX* mutant with that of WT in CDM supplemented with pyruvate (Fig. 6B). Growth of the

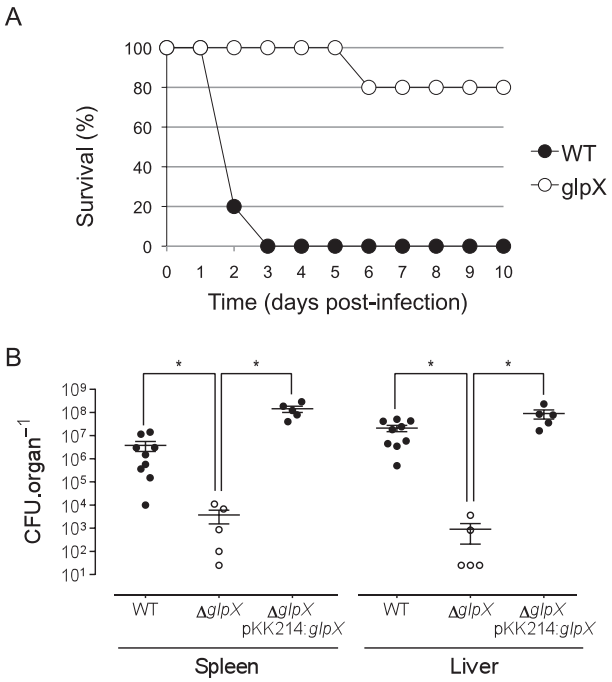

Fig. 5. *glpX* inactivation impairs virulence.
A. Groups of five BALB/c mice were infected by 2×10^2 *F. novicida* U112 (WT, close symbols) or *glpX* mutant (open symbols) by i.p. route. The survival of mice (%) was followed for 10 days after infection.
B. BALB/c mice were infected by 2×10^2 CFUs of wild-type *F. novicida* (10 mice, WT, close circles), Δ*glpX* mutant (5 mice, open circles) or Δ*glpX*-complemented strain (Δ*glpX* pKK214- glpX, 5 mice, closed circles) by i.p. route. After 2.5 days of infection, mice were sacrificed and the bacterial burden in spleen and liver was determined by plating tissue homogenates on chocolate agar.
*$P < 0.05$ (determined by Student's *t*-test)

LVSΔ*glpX* mutant was essentially abolished in this medium, demonstrating that pyruvate could no longer be used as a gluconeogenic substrate in the mutant strain. We next followed the kinetics of intracellular multiplication of the WT *F. tularensis* LVS and its Δ*glpX* derivative in J774.1 (Fig. 6C and D) and THP-1 macrophage cells (Fig. 6E and F). We used as a non-replicating control a Δ*iglC* mutant of LVS. The *ΔiglC* gene is part of the FPI (Nano and Schmerk, 2007). As with most of the other FPI mutants, *iglC* mutants fail to grow in macrophages and are deficient in their ability to escape from phagosomes (Santic *et al*., 2005).

In standard DMEM supplemented with glucose, the LVSΔ*glpX* mutant showed no significant defect in intracellular multiplication (Fig. 6C and E) in any of the two cell lines. In contrast, the LVSΔ*glpX* mutant showed a significant reduction in intracellular multiplication as compared with parental LVS, when DMEM was supplemented with pyruvate in both cell lines. In J774.1 cells, a 10-fold decrease in number of Δ*glpX* mutant relative to WT bacteria was recorded at 24 h (Fig. 6D); in THP-1 cells, a 20-fold decrease was recorded at 24 h and a 8-fold at 48 h (Fig. 6F). Complementation with the WT *glpX* allele almost restored WT multiplication. These results confirmed that *glpX* inactivation affected intracellular multiplication in the two *F. tularensis* subspecies. However, the intracellular multiplication defect provoked by *glpX* inactivation appears to be somewhat less severe in *F. tularensis* LVS. We next monitored the glucose levels in THP-1 and J774.1 macrophages (Fig. 7A and B) infected with WT *F. tularensis* LVS. Non-infected cells were used as control (see Experimental procedures). We observed a two- to threefold reduction in the glucose concentration in non-infected cells after 24 h, likely reflecting cellular glucose consumption. Comparable results were obtained in both cells types: infection with *F. tularensis* LVS led to approximately fivefold reduction in intracellular glucose at 24 h (as compared with non-infected cells) (Fig. 7).

Discussion

We recently demonstrated that acquisition of host-derived amino acids was essential for *Francisella* intracellular multiplication and virulence (Gesbert *et al*., 2014; 2015; Ramond *et al*., 2014; 2015). The data presented here unravel for the first time the critical role of the gluconeogenic pathway in *Francisella* pathogenesis and highlight the role of amino acids as major precursors for bacterial anabolic pathways.

Critical role of gluconeogenesis in Francisella *pathogenesis*

Central metabolism has been recently recognized as an essential component of the virulence of pathogenic microorganisms, and, in particular, of intracellular bacteria. Indeed, cytosolic bacterial multiplication not only relies on the ability to evade host innate defense mechanisms but also requires efficient utilization of nutrients available in the infected host (Eisenreich *et al*., 2010). The metabolism of mammalian cells involves a profusion of metabolites that could be used by intracellular bacteria as potential nutrients. Since the major anabolic and catabolic reactions of the host cells mainly take place in the cytosol, facultative intracellular bacterial pathogens with a cytosolic lifestyle, such as *Listeria*, *Shigella* and *Francisella*, have direct access to a broad variety of carbohydrates, amino acids, fatty acids and many other metabolites, to fulfill their nutritional needs. In spite of this common intracellular niche, these bacteria have evolved very different nutritional needs (Dandekar and Eisenreich, 2015). In particular, recent studies from our group (Gesbert *et al*., 2014; 2015; Ramond *et al*., 2014; 2015) and others (Wehrly *et al*., 2009; Raghunathan *et al*., 2010; Steele *et al*., 2013) have shown that amino acids are likely to represent major

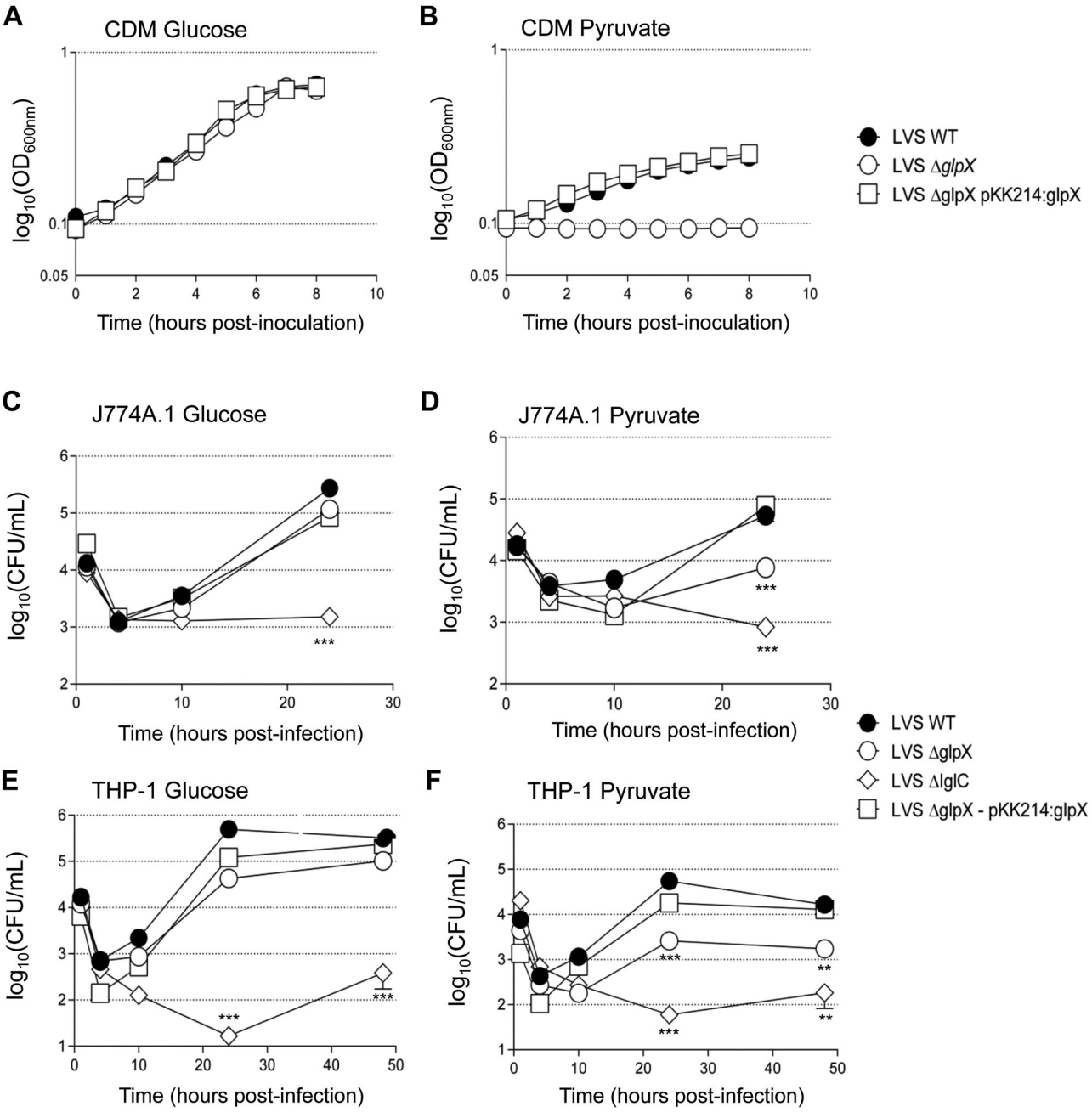

Fig. 6. The Δ*glpX* mutant of *F. tularensis* LVS.
Wild-type *F. tularensis* LVS (LVS, close circles), isogenic LVSΔ*glpX* mutant (Δ*glpX*, open circles) and complemented LVSΔ*glpX* strain (Δ*glpX* pKK214:*glpX*, open squares) were grown in CDM supplemented with (A) glucose or (B) pyruvate, at a final concentration of 40 mM. Intracellular bacterial multiplication of wild-type *F. tularensis* LVS (LVS, close circles), isogenic LVSΔ*glpX* mutant (Δ*glpX*, open circles), complemented LVSΔ*glpX* strain (Δ*glpX* pKK214:*glpX*, open squares) and the LVSΔ*iglC* negative control (Δ*iglC*, open lozenges) were monitored during 24 h in J774-1 (C, D) or 48 h THP-1 (E, F) macrophage cells in DMEM supplemented with glucose (C, E) or pyruvate (D, F). $^{**}P < 0.05$; $^{***}P < 0.001$ (determined by Student's *t*-test).

sources of carbon, nitrogen and energy for intracellular *Francisella*. By contrast, the majority of intracellular bacterial pathogens, which reside in a vacuole, do not have a direct access to the available nutrients and therefore have developed dedicated strategies to import their nutrients from the host cytosol into their subcellular compartment. For example, *Legionella pneumophila*, which mainly relies on amino acids as carbon and nitrogen sources, hijacks the conserved polyubiquitination and proteasomal degradation machinery to import amino acids and peptides into its

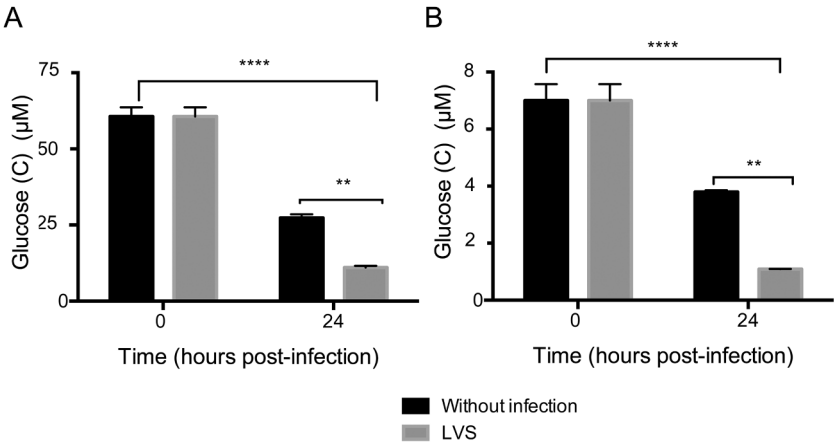

Fig. 7. Intracellular glucose concentration. The intracellular glucose concentration of (A) THP-1- or (B) J774.1-infected macrophages was determined by the Glucose Assay Kit. Macrophages were infected with wild-type *F. tularensis* LVS for 1 h. After 24 h, cells were lysed and intracellular glucose concentration was monitored. Non-infected cells were used as controls. The data presented are representative of three independent experiments ± the SD of triplicate samples. ****$P < 0.0001$, **$P < 0.01$ (determined by Student's *t*-test).

Legionella-containing vacuole (Price *et al.*, 2011; Abu Kwaik and Bumann, 2013). The *L. pneumophila* genome encodes multiple phagosomal transporters involved in the transport of these amino acids into its own cytoplasm (Fonseca and Swanson, 2014 and references therein). Other intravacuolar intracellular pathogens, such as *S. typhimurium* and *M. tuberculosis*, use both amino acids and carbohydrates as carbon sources. Indeed, *S. typhimurium* requires the simultaneous exploitation of numerous other host nutrients including amino acids to replicate within host phagocytes (Steeb *et al.*, 2013). *M. tuberculosis* utilizes glucose and fatty acid carbon and energy sources and like in other pathogens, carbon metabolism plays a critical role in virulence (Gouzy *et al.*, 2014). Nonetheless, the bacterium was also shown to critically rely on aspartate and asparagine as major nitrogen providers to support growth and virulence. Finally, some intravacuolar intracellular bacterial pathogens mostly rely on carbohydrates as nutritional sources. For example, numerous studies have highlighted the importance of carbohydrate metabolism for intracellular *Brucellae* (Barbier *et al.*, 2011; von Bargen *et al.*, 2012). Further supporting the notion that carbohydrates serve as major energy and/or carbon source, glucose uptake has been shown to be critical for efficient intracellular multiplication of *Brucella abortus* and for chronic infection (Xavier *et al.*, 2013). Of interest, very recent studies on *B. abortus* metabolism revealed that classical gluconeogenesis is not extensively used *in vivo* (Zuniga-Ripa *et al.*, 2014), suggesting complex metabolic adaptations of the pathogen throughout its intracellular life cycle.

The nutritional constraints of extracellular pathogens have also been recently addressed (Dandekar and Eisenreich, 2015). For example, it has been shown that gluconeogenesis and the TCA cycle were both required by uropathogenic *E. coli* during urinary tract infection (UTI) to catabolize available amino acids and peptides whereas glycolysis, the PPP and Entner–Doudoroff (ED) pathways were dispensable (Alteri *et al.*, 2009). In sharp contrast, another uropathogenic bacterium *Proteus mirabilis* requires these three pathways during UTI, thus illustrating that two pathogens sharing the same host environment and having access to the same nutrients may have quite divergent metabolic requirements (Alteri *et al.*, 2015).

By comparing the capacity of WT *F. novicida* and Δ*glpX* mutant bacteria to use amino acid as carbon sources in the absence of glucose, we found that several amino acids could serve as gluconeogenic substrates for *Francisella* (Fig. 8). In humans, the main gluconeogenic amino acid precursors are glutamine and alanine; and only leucine and glycine are not gluconeogenic amino acids. Glutamine is a non-essential amino acid in mammalian cells and one of the main substrates of anaplerotic reactions fueling the TCA cycle (Filomeni *et al.*, 2014). Alanine appeared to be the best carbon and energy source for *Francisella* grown in CDM lacking glucose. In contrast, glutamine was a poor substrate. We have recently shown that import of glutamate and its metabolism were critical for proper bacterial phagosomal escape (Ramond *et al.*, 2014), whereas asparagine utilization was strictly required for bacterial multiplication in the host cell cytosol (Gesbert *et al.*, 2014).

Our isotopic profiling data (using ^{13}C-labeled glucose and ^{13}C-labeled pyruvate) demonstrated that *Francisella* was capable of both glycolysis and gluconeogenesis. The data also indicated that the oxidative part of the PPP and the ED pathways was non-functional, at least during the *in vitro* conditions tested. Of note, both *F. tularensis* subsp *tularensis* and *F. novicida* can metabolize glycerol but not *F. tularensis* subsp *holaractica*, although the latter seems to possess all the genes required for its uptake and metabolism. The identification of a complete glycolytic pathway in *Francisella* is in perfect agreement with a recent study by Manoil and co-workers performed on a *F. novicida* trans-

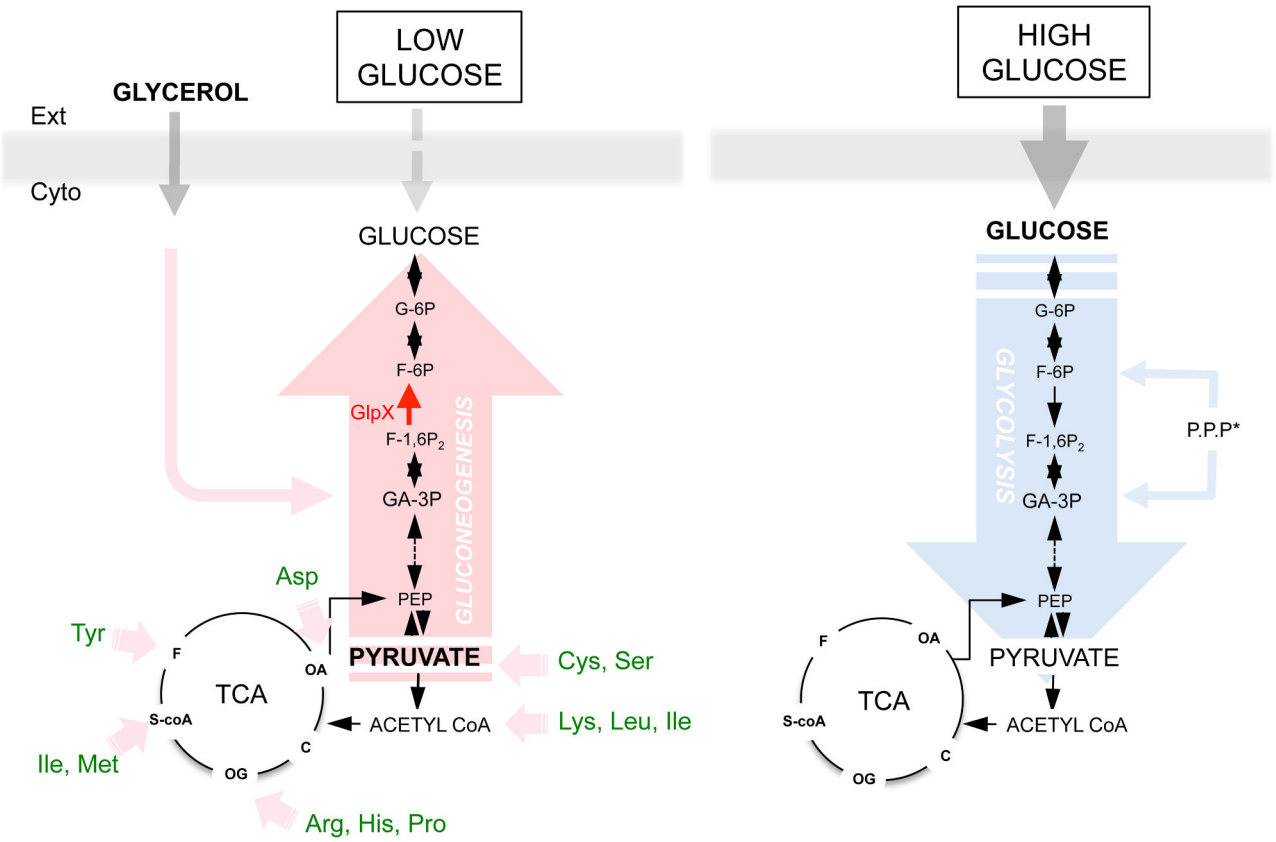

Fig. 8. Model of glucose biogenesis/catabolism in *Francisella*.
At low external glucose concentration (left part), gluconeogenesis is active (in pink) and requires GlpX (bold red arrow). The main gluconeogenic substrates are amino acids. Pyruvate and glycerol (in bold) also serve as gluconeogenic substrates. In green, the amino acids present in the CDM that may serve as gluconeogenic substrates. At high external glucose concentration (right part), glucose catabolism mainly occurs via the Embden–Meyerhoff pathway (glycolysis, in pale blue).
PPP*, non-oxidative part of the pentose phosphate pathway; TCA, tricarboxilic acid cycle.

poson mutant library grown on a variety of nutrient media (Enstrom *et al.*, 2012). Indeed, that study notably revealed that gene *FTN_1210* (originally annotated as encoding a putative ribokinase) encodes a phosphofructokinase most likely responsible for the non-initially predicted glycolytic reaction, converting fructose-6P to fructose-1,6P (and now designated *pfk*). Of note, the gene *pfk* has not been identified in earlier genetic screens. Since the protein Pfk is highly conserved among the different *F. tularensis* subspecies, this step of the glycolytic pathway may not be critical for the virulence of *Francisella* species.

The Δ*glpX* mutant normally escaped from the phagosome of infected macrophages even when cells were cultivated with glycerol instead of glucose, implying that gluconeogenesis is not involved in the escape process. Thus, it is likely that the amino acids that serve to fuel the gluconeogenic pathway mainly contribute to the later stages of the infectious cycle. The links between amino acid uptake and central metabolic pathways remain to be explored.

Host cell glucose homeostasis influences bacterial multiplication

Hexoses such as glucose are the preferred carbon and energy sources for many bacteria. Glucose uptake in bacteria can be mediated by multiple transport systems such as: (i) ATP-binding cassette (ABC) transporters (primary active transporters), (ii) secondary carriers (secondary active transporters), or (iii) group translocators (PEP:sugar PTS) (Jahreis *et al.*, 2008). To import glucose from the external medium, most bacterial species are equipped with multiple glucose uptake systems (Saier, 2000). Remarkably, *F. tularensis* genomes encode only a limited number of ABC transport system (none of which has been functionally characterized) and do not encode any putative PTS transport system (Meibom and Charbit, 2010). However, several secondary carriers, yet to be characterized, probably mediate glucose uptake since *Francisella* can use glucose as a carbon and energy source. *L. monocytogenes* possesses a transporter medi-

ating the uptake of glucose-6P (UhpT) that constitutes a key element of its cytosolic multiplication (Chico-Calero *et al.*, 2002). *F. tularensis* genomes do not encode any ortholog of the UhpT sugar phosphate transporter family. Furthermore, *F. novicida* and *F. tularensis* LVS are unable to ferment glucose-6P (A. Charbit, unpublished observations). Of note, *Francisella* genomes encode one putative glycerol uptake transporter (GlpF) and one glycerol-3 phosphate transporter (GlpT) that were recently shown to promote entry of the antibacterial drug fosfomycin (Mackie *et al.*, 2012). Thus, it is likely that in the absence of glucose, *Francisella* mainly uses available three carbon sources (such as pyruvate, glycerol and glycerol-3P) and amino acids as intracellular carbon and nitrogen sources (Fig. 8).

In all cell types tested, a severe intracellular multiplication defect of the Δ*glpX* mutant was observed when cells were supplemented with a gluconeogenic substrate such as pyruvate or glycerol. In contrast, WT multiplication was restored when the medium was supplemented with glucose.

Of note, a reduction in the intracellular glucose concentration was recorded in both J774.1 and THP-1 macrophages infected for 24 h with WT *F. tularensis* LVS (Fig. 7). The need for cytosolic *Francisella* to possess an active gluconeogenic pathway is consistent with the significant reduction in the available intracellular glucose pool observed upon infection. Supporting the notion of a nutritional immunity, it is conceivable that infected cells modify their metabolism to reduce the available glucose intracellular pool and, hence, limit bacterial proliferation. The role of cellular metabolism in macrophage activation is becoming an intense field of investigation. Notably, it has been demonstrated that aerobic glycolysis was essential to the activation of macrophages (Haschemi *et al.*, 2012). Since M1 activated macrophages produce high levels of proinflammatory cytokines and reactive oxygen and nitrogen species, it is thus possible that the decrease in the pool of intracellular glucose observed upon infection by *Francisella* might also reflect a strong increase in glycolysis required for the generation of oxygen radicals in activated macrophages. WT bacteria would thus critically need gluconeogenesis to obtain enough glucose for their metabolic purposes (biosynthesis of cell wall component or nucleotides, etc.) during intracellular multiplication and *in vivo* dissemination. At this stage, one cannot exclude that the lack of fructose biphosphatase in the Δ*glpX* mutant may also lead to the accumulation of metabolites (such as fructose 1,6 biphosphate or upstream gluconeogenic intermediates) that might inhibit other enzymatic reactions, thus concurring to the impaired virulence of the mutant. The enzymes involved in gluconeogenesis might thus constitute potential targets for therapeutic approaches against this pathogen. This work opens the way to future studies to dissect the tug of war between the pathogen and the host in the control of intracellular glucose homeostasis.

Experimental procedures

Ethics statement

All experimental procedures involving animals were conducted in accordance with guidelines established by the French and European regulations for the care and use of laboratory animals (Decree 87–848, 2001–464, 2001–486 and 2001–131 and European Directive 2010/63/UE) and approved by the INSERM Ethics Committee (Authorization Number: 75–906).

Strains and culture conditions

All strains used in this study are derivative from *F. tularensis* subsp. *novicida* U112 or *F. tularensis* subsp. *holarctica* LVS and are described in Table S1. Strains were grown at 37°C on pre-made chocolate agar PolyViteX plates (BioMerieux), tryptic soya broth (TSB) or CDM supplemented with the appropriate carbon source at a final concentration of 40 mM. The CDM used for *F. tularensis* subsp *novicida* corresponds to standard CDM (Chamberlain, 1965) without threonine and valine (Gesbert *et al.*, 2014). It contains (i) six essential amino acids (arginine, lysine, methionine, tyrosine at 0.4 g l^{-1}) and histidine, cysteine at 0.2 g l^{-1}) and (ii) five non-essential amino acids (isoleucine, serine, aspartate, leucine at 0.4 g l^{-1} and proline at 2 g l^{-1}).

For growth condition determination, bacterial strains were inoculated in the appropriate medium at an initial OD_{600} of 0.05 from an overnight culture in TSB for *F. novicida* or at an initial OD_{600} of 0.1 from an overnight culture in Schaedler K3 for *F. tularensis* LVS. Schaedler K3 medium is a rich medium that contains growth factors such as hemin, yeast extract and menadione (vitamin K3) as well as cysteine and glucose (Schaedler K3 medium, Biomerieux).

Construction of chromosomal deletion mutants

We inactivated the gene *glpX* in *F. novicida* (*FTN_0298*) by allelic replacement resulting in the deletion of the entire gene (start and six last codons were conserved). We constructed a recombinant polymerase chain reaction (PCR) product containing the upstream region of the gene *glpX* (*glpX*-UP), a kanamycin resistance cassette (*nptII* gene fused with *pGro* promoter) and the downstream region of the gene *glpX* (*glpX*-DN) by overlap PCR. Primers *glpX* upstream FW (p1) and *glpX* upstream (spl_K7) RV (p2) amplified the 1047 bp region upstream of position +4 of the *glpX* coding sequence (*glpX*-UP), primers *pGro* FW (p3) and *nptII* RV (p4) amplified the 1091 bp kanamycin resistance cassette (*nptII* gene fused with *pGro* promoter); and primers *glpX* downstream (spl_K7) FW (p5) and *glpX* downstream RV (p6) amplified the 633 bp region downstream of the position +970 of the *glpX* gene coding sequence (*glpX*-DN). Primers p2 and p5 have an overlapping sequence of 12 and 14 nucleotides with primers p3 and p4, respectively, resulting in fusion of *glpX*-UP and *glpX*-DN with the cassette after cross-over PCR. All single

fragment PCR reactions were realized using Phusion High-Fidelity DNA Polymerase (ThermoScientific) and PCR products were purified using NucleoSpin® Gel and PCR Clean-up kit (Macherey-Nagel). Overlap PCRs were realized using 100 ng of each purified PCR products and the resulting fragment of interest was purified from agarose gel. This fragment was then directly used to transform WT *F. novicida* by electroporation (Anthony *et al.*, 1991). Recombinant bacteria were isolated by spreading onto chocolate agar plates containing kanamycin (5 μg ml^{-1}). The mutant strains were checked for loss of the WT gene by PCR product direct sequencing (GATC-biotech) using appropriate primers.

For *F. tularensis* LVS, we used the pPV suicide plasmid (Golovliov *et al.*, 2003). The recombinant plasmid pPV-Δ*FTL_1701* was constructed by overlap PCR. Upstream and downstream regions of the gene *FTL_1701* were amplified using primer pairs LVS *glpX*up (Maurin *et al.*, 2000) FW/LVS *glpX*up(Spl_K7) RV and LVS *glpX*dn(Spl_K7) FW/LVS *glpX*dn (Maurin *et al.*, 2000) RV, respectively, and fused by overlap PCR with the kanamycin resistance cassette, as described earlier. The resulting fragment was cloned in pPV vector after *Sal*I restriction and transformed in *E. coli* TOP10 (Life Technologies). Plasmids from positive transformants were amplified and purified using NucleoSpin® Plasmid kit (Macherey-Nagel) and introduced into *F. tularensis* LVS by electroporation (Maier *et al.*, 2004). The standard two-step allelic exchange procedure was used to create the chromosomal Δ*FTL_1701* mutant (Golovliov *et al.*, 2003). Briefly, transformants were first selected at 37°C on chocolate agar plates containing chloramphenicol (1.5 μg ml^{-1}) and kanmycin (5 μg ml^{-1}) to select chromosomal integration of the recombinant plasmid (via a single crossing over). Single colonies were checked with appropriate pairs of primers and selected clones were subsequently passaged once on plates with selection, followed by one passage in liquid medium without selection (to allow recombination to occur). Next, bacteria were passaged once on agar plates containing 5% sucrose and kanamycin (5 μg ml^{-1}). Isolated colonies were checked for loss of the WT *glpX* gene by analyzing the size of the fragment obtained after PCR using appropriate primers. The mutant strains were finally checked for loss of the corresponding WT genes by PCR sequencing (GATC Biotech).

Functional complementation

The plasmid used for complementation of the *F. novicida*Δ*glpX* mutant (U112Δ*glpX*) and the *F. tularensis* strain LVSΔ*glpX* mutant (Δ*FTL_1701*), pKK-*glpX*$_{cp}$ is will be described later. Primers pGro[PstI] FW and pGro RV amplified the 279 bp of the *pGro* promoter and primers *glpX* FW/*glpX*[SpeI] RV amplified the 987 bp *glpX* gene from U112. PCR products were purified and PstI (*pGro* promoter) or SpeI (*glpX*) restricted in the presence of FastAP Thermosensitive Alkaline Phosphatase (ThermoScientific) to avoid self-ligation. A mixture of *pGro* promoter and interest gene fragments was then incubated in T4 polynucleotide kinase to allow blunt end ligation and fragments were then cloned in pKK214 vector after PstI/SpeI double restriction and transformed in *E. coli* TOP10. Recombinant plasmid pKK-*glpX*$_{cp}$ was purified and directly used for chemical transformation in *F. novicida* U112 (Gesbert *et al.*, 2015) or in *F. tularensis* LVS by electroporation. Recombinant colonies were selected on chocolate agar plates containing tetracycline (5 μg ml^{-1}) and kanamycin (5 μg ml^{-1}).

Isotopic profiling of F. novicida *by ion chromatography–mass spectrometry/mass spectrometry (IC–MS/MS)*

Firstly, we followed the fate of ^{13}C-labeled glucose in WT *F. novicida* grown in CDM containing 25 mM labeled glucose. Cultures for ^{13}C-labeling experiments used a mixture of 20% (mol mol^{-1}) [U-^{13}C] glucose and 80% (mol mol^{-1}) [1-^{13}C] glucose (Eurisotop, France). Next, we compared the fate of [1-^{13}C]-labeled pyruvate in WT *F. novicida* and Δ*glpX* mutant, grown in CDM containing 25 mM labeled pyruvate. In order to promote growth of the Δ*glpX* mutant, 1 mM of unlabeled glucose was added in both cultures.

Samples were collected at the mid-exponential phase to ensure isotopic and metabolic steady state. The metabolites selected for the isotopic profiling were glucose-1-P, glucose-6-P (G6P), fructose-6-P (F6P), FBP, pentoses-5-P = ribose-5P + ribulose-5P + xylulose-5P (P5P), ribose-1-P, sedoheptulose-7-P, glycerol-3-P, 1,3-diphosphoglycerate, 2 and 3-phosphoglycerate, phosphoenol-pyruvate (PEP), citrate, cis-aconitate, a-ketoglutarate, succinate, fumarate, malate and 6-phosphogluconate. Metabolite separation was performed by ionic chromatography (Dionex ICS 2500 ion chromatograph). Detection of mass isotopomers was performed by mass spectrometry on an Applied Biosystems 4000 Qtrap mass Spectrometer (ElectroSpray Ionisation on Negative mode; Detection mode: Multiple Reaction Monitoring). Isotopic profiles were corrected from the natural abundance of atom isotopes according to metabolites formulas by using IsoCor software (Millard *et al.*, 2012) to obtain CID of the metabolites.

Sampling and sample preparation

Cells were separated from the broth by centrifugation in a cold quenching solution composed of absolute ethanol precooled at –80°C. After quenching 120 μl of broth in 500 μl of quenching solution, cells were then centrifuged at 12 000 × *g* at –20°C for 5 min. Supernatants were then discarded and cell pellets were extracted by incubation in 5 ml ethanol/H_2O (75:25) at 96°C for min in closed tubes. This solvent mixture ensures a high reproducible metabolite extraction without significant degradation or interconversion of metabolites (Canelas *et al.*, 2009). To stop extraction, tubes were then transferred in a cooling bath of ethanol precooled at –80°C. Extracts were then centrifuged to remove cell debris at 12 000 × *g* at –20°C for 5 min; the supernatants were evaporated under vacuum in a SpeedVac (SC110A SpeddVac Plus) for 4 h. Dried extracts were then re-dissolved in 120 μl H_2O before injection and then stored at –80°C before analysis with IC-MS/MS.

Cell cultures and cell infection experiments

J774A.1 (ATCC® TIB-67™) and Hep G2 (ATCC® HB-8065™) cells were propagated in DMEM (PAA), containing 10% fetal bovine serum (FBS, PAA) unless otherwise stated. BMM from BALB/c mice and THP-1 (ATCC TIB-202)

were grown in Roswell Park Memorial Institute (RPMI-1640) or DMEM, containing 10% FBS. The day before infection, approximately 2×10^5 eukaryotic cells (i.e. J774A.1, THP-1, HepG2 and BMM) per well were seeded in 12-well cell issue plates (in appropriate cellular culture medium supplemented with the appropriate carbon source and bacterial strains were grown overnight in 5 ml of TSB at 37°C.

Infections were realized at a multiplicity of infection (MOI) of 100 and incubated for 1 h at 37°C in culture medium supplemented with the appropriate carbon source (glucose, glycerol or pyruvate). The amount of glucose in cell culture formulations ranges from 5.5 mM to as high as 55 mM (11 mM in RPMI and at 25 mM in DMEM). Therefore, we used in our assays DMEM without glucose supplemented either with glucose at 25 mM or with glycerol at the same molarity. For pyruvate supplementation, we used only 10 mM because higher concentrations were partially toxic to the cell.

After three washes with cellular culture medium, plates were incubated for 4, 10 and 24 h in fresh medium supplemented with gentamycin (10 μg ml^{-1}). At each kinetic point, cells were washed three times with culture medium and lysed by addition of 1 ml of distilled water for 10 min at 4°C. The titer of viable bacteria was determined by spreading preparations on chocolate plates. Each experiment was conducted at least twice in triplicates.

Confocal experiments

J774.1 macrophage cells were infected (MOI of 1000) with *Francisella tularensis subsp. novicida* U112, the Δ*glpX* isogenic mutant or an isogenic strain deleted for the *Francisella* pathogenicity island (Δ*FPI*) in DMEM without glucose and supplemented with glycerol (25 mM) for 30 min at 37°C. Cells were then washed three times with 1× PBS and maintained in fresh DMEM supplemented with gentamycin (10 μg ml^{-1}) until the end of the experiment. Three kinetic points (i.e. 1, 4 and 10 h) were sampled. For each point, cells were washed with 1× PBS, fixed 15 min with 4% paraformaldehyde and incubated 10 min in 50 mM NH_4Cl in 1× PBS to quench free aldehydes. Cells were then blocked and permeabilized with 1× PBS containing 0.1% saponin and 5% goat serum for 10 min at room temperature. Cells were then incubated for 30 min with anti-*F. novicida* mouse monoclonal antibody (1/500e final dilution, Creative Diagnostics) and anti-LAMP1 rabbit polyclonal antibody (1/100e, ABCAM). After washing, cells were incubated for 30 min with Alexa488-conjugated goat anti mouse and Alexa546 conjugated donkey anti-rabbit secondary antibodies (1/400e, AbCam). After washing, 4,6-diamidino-2-phenylindole (DAPI) was added (1/1000e) for 1 min and glass coverslips were mounted in Mowiol (Cityfluor Ltd.). Cells were examined using an ×63 oil-immersion objective on a LeicaTSP SP5 confocal microscope. Colocalization tests were quantified by using Image J software; and mean numbers were calculated on more than 500 cells for each condition. Confocal microscopy analyses were performed at the Cell Imaging Facility (Faculté de Médecine Necker Enfants-Malades).

Glucose assay

For determination of intracellular glucose levels, 5×10^7 THP-1 or J774.1 macrophages were infected or not by LVS, as described previously (Barel *et al.*, 2012). After extensive washing in PBS, pelleted cells were lyzed with 250 μl MilliQ water for 60 min at 4°C. After centrifugation at 12 000 × *g* for 15 min at 4°C, supernatants were collected and kept at –20°C until use. Glucose assay was performed with the Glucose Assay Kit (ABCAM, Cambridge, UK), as described by manufacturer. Briefly, 25 μl of each sample was diluted v:v with glucose assay buffer. Then, 50 μl of reaction mix was added. The reaction was performed on a rotating platform for 30 min at 37°C, protected from light. Absorbance was measured at 570 nm.

Mice infection

Wild-type *F. novicida* and Δ*glpX* mutant strain were grown in TSB to exponential growth phase and diluted to the appropriate concentrations. Six- to 8-week-old female BALB/c mice (Janvier) were intraperitoneally (i.p.) inoculated with 200 μl of a bacterial suspension containing 2×10^2 CFUs. Inoculum titers were checked spreading dilutions of the preparations in chocolate agar. For survival experiments conducted on 10 days, mice were checked for dead individuals every 12 h for the three first days and then every day.

For bacterial burden determination, mice were i.p. inoculated with 200 μl of bacterial suspension (2×10^2 bacteria per mouse). Mice infected with the complemented strain were treated with tetracycline to avoid loss of the complementing plasmid. For this, mice received one dose of tetracycline per day (1 mg per dose) i.e. 2 days before infection and every day until they were sacrificed. Homogenized preparations from spleen and liver were spread on chocolate plates.

Acknowledgements

We thank Dr A. Sjostedt for providing the *Francisella* strains U112 and LVS. These studies were supported by INSERM, CNRS and Université Paris Descartes Paris Cité Sorbonne. Elodie Ramond was funded by a fellowship from the 'Région Ile de France' and Terry Brissac by a financing from the 'Délégation Générale à l'Armement' (Grant ANR-12-ASTR-0018). The funders had no role in study design, data collection and analysis, decision to publish, or preparation of the manuscript.

References

Abu Kwaik, Y., and Bumann, D. (2013) Microbial quest for food in vivo: 'nutritional virulence' as an emerging paradigm. *Cell Microbiol* **15:** 882–890.

Abu Kwaik, Y., and Bumann, D. (2015) Host delivery of favorite meals for intracellular pathogens. *PLoS Pathog* **11:** e1004866.

Alteri, C.J., Smith, S.N., and Mobley, H.L. (2009) Fitness of *Escherichia coli* during urinary tract infection requires gluconeogenesis and the TCA cycle. *PLoS Pathog* **5:** e1000448.

Alteri, C.J., Himpsl, S.D., and Mobley, H.L. (2015) Preferential use of central metabolism in vivo reveals a nutritional basis for polymicrobial infection. *PLoS Pathog* **11:** e1004601.

Anthony, L.S., Gu, M.Z., Cowley, S.C., Leung, W.W., and

Nano, F.E. (1991) Transformation and allelic replacement in *Francisella* spp. *J Gen Microbiol* **137:** 2697–2703.
Barbier, T., Nicolas, C., and Letesson, J.J. (2011) *Brucella* adaptation and survival at the crossroad of metabolism and virulence. *FEBS Lett* **585:** 2929–2934.
Barel, M., Meibom, K., Dubail, I., Botella, J., and Charbit, A. (2012) *Francisella tularensis* regulates the expression of the amino acid transporter SLC1A5 in infected THP-1 human monocytes. *Cell Microbiol* **14:** 1769–1783.
von Bargen, K., Gorvel, J.P., and Salcedo, S.P. (2012) Internal affairs: investigating the *Brucella* intracellular lifestyle. *FEMS Microbiol Rev* **36:** 533–562.
Bowden, S.D., Rowley, G., Hinton, J.C., and Thompson, A. (2009) Glucose and glycolysis are required for the successful infection of macrophages and mice by *Salmonella* enterica serovar Typhimurium. *Infect Immun* **77:** 3117–3126.
Brown, G., Singer, A., Lunin, V.V., Proudfoot, M., Skarina, T., Flick, R., *et al*. (2009) Structural and biochemical characterization of the type II fructose-1,6-bisphosphatase GlpX from *Escherichia coli*. *J Biol Chem* **284:** 3784–3792.
Canelas, A.B., ten Pierick, A., Ras, C., Seifar, R.M., van Dam, J.C., van Gulik, W.M., and Heijnen, J.J. (2009) Quantitative evaluation of intracellular metabolite extraction techniques for yeast metabolomics. *Anal Chem* **81:** 7379–7389.
Chamberlain, R.E. (1965) Evaluation of live tularemia vaccine prepared in a chemically defined medium. *Appl Microbiol* **13:** 232–235.
Chico-Calero, I., Suarez, M., Gonzalez-Zorn, B., Scortti, M., Slaghuis, J., Goebel, W., and Vazquez-Boland, J.A. (2002) Hpt, a bacterial homolog of the microsomal glucose-6-phosphate translocase, mediates rapid intracellular proliferation in *Listeria*. *Proc Natl Acad Sci USA* **99:** 431–436.
Dandekar, T., and Eisenreich, W. (2015) Host-adapted metabolism and its regulation in bacterial pathogens. *Front Cell Infect Microbiol* **5:** 28.
Donahue, J.L., Bownas, J.L., Niehaus, W.G., and Larson, T.J. (2000) Purification and characterization of *glpX*-encoded fructose 1, 6-bisphosphatase, a new enzyme of the glycerol 3-phosphate regulon of *Escherichia coli*. *J Bacteriol* **182:** 5624–5627.
Eisenreich, W., Dandekar, T., Heesemann, J., and Goebel, W. (2010) Carbon metabolism of intracellular bacterial pathogens and possible links to virulence. *Nat Rev Microbiol* **8:** 401–412.
Enstrom, M., Held, K., Ramage, B., Brittnacher, M., Gallagher, L., and Manoil, C. (2012) Genotype-phenotype associations in a nonmodel prokaryote. *MBio* **3:** e00001-12. doi:10.1128/mBio.00001-12.
Filomeni, G., De Zio, D., and Cecconi, F. (2015) Oxidative stress and autophagy: the clash between damage and metabolic needs. *Cell Death Differ* **22:** 377–388.
Fonseca, M.V., and Swanson, M.S. (2014) Nutrient salvaging and metabolism by the intracellular pathogen *Legionella pneumophila*. *Front Cell Infect Microbiol* **4:** 12.
Gesbert, G., Ramond, E., Rigard, M., Frapy, E., Dupuis, M., Dubail, I., *et al*. (2014) Asparagine assimilation is critical for intracellular replication and dissemination of *Francisella*. *Cell Microbiol* **16:** 434–449.
Gesbert, G., Ramond, E., Tros, F., Dairou, J., Frapy, E., Barel, M., and Charbit, A. (2015) Importance of branched-chain amino Acid utilization in *Francisella* intracellular adaptation. *Infect Immun* **83:** 173–183.
Golovliov, I., Sjostedt, A., Mokrievich, A., and Pavlov, V. (2003) A method for allelic replacement in *Francisella tularensis*. *FEMS Microbiol Lett* **222:** 273–280.
Gouzy, A., Poquet, Y., and Neyrolles, O. (2014) Nitrogen metabolism in *Mycobacterium tuberculosis* physiology and virulence. *Nat Rev Microbiol* **12:** 729–737.
Grubmüller, S., Schauer, K., Goebel, W., Fuchs, T.M., and Eisenreich, W. (2014) Analysis of carbon substrates used by *Listeria monocytogenes* during growth in J774A.1 macrophages suggests a bipartite intracellular metabolism. *Front Cell Infect Microbiol* **4:** 156.
Haschemi, A., Kosma, P., Gille, L., Evans, C.R., Burant, C.F., Starkl, P., *et al*. (2012) The sedoheptulose kinase CARKL directs macrophage polarization through control of glucose metabolism. *Cell Metab* **15:** 813–826.
Jahreis, K., Pimentel-Schmitt, E.F., Bruckner, R., and Titgemeyer, F. (2008) Ins and outs of glucose transport systems in eubacteria. *FEMS Microbiol Rev* **32:** 891–907.
Kadzhaev, K., Zingmark, C., Golovliov, I., Bolanowski, M., Shen, H., Conlan, W., and Sjostedt, A. (2009) Identification of genes contributing to the virulence of *Francisella tularensis* SCHU S4 in a mouse intradermal infection model. *PLoS ONE* **4:** e5463.
Kingry, L.C., and Petersen, J.M. (2014) Comparative review of *Francisella tularensis* and *Francisella novicida*. *Front Cell Infect Microbiol* **4:** 35.
Lucchini, S., Liu, H., Jin, Q., Hinton, J.C., and Yu, J. (2005) Transcriptional adaptation of *Shigella flexneri* during infection of macrophages and epithelial cells: insights into the strategies of a cytosolic bacterial pathogen. *Infect Immun* **73:** 88–102.
Mackie, R.S., McKenney, E.S., and van Hoek, M.L. (2012) Resistance of *Francisella novicida* to fosmidomycin associated with mutations in the glycerol-3-phosphate transporter. *Front Microbiol* **3:** 226.
McLendon, M.K., Apicella, M.A., and Allen, L.A. (2006) *Francisella tularensis*: taxonomy, genetics, and Immunopathogenesis of a potential agent of biowarfare. *Annu Rev Microbiol* **60:** 167–185.
Maier, T.M., Havig, A., Casey, M., Nano, F.E., Frank, D.W., and Zahrt, T.C. (2004) Construction and characterization of a highly efficient *Francisella* shuttle plasmid. *Appl Environ Microbiol* **70:** 7511–7519.
Maier, T.M., Pechous, R., Casey, M., Zahrt, T.C., and Frank, D.W. (2006) In vivo Himar1-based transposon mutagenesis of *Francisella tularensis*. *Appl Environ Microbiol* **72:** 1878–1885.
Marrero, J., Rhee, K.Y., Schnappinger, D., Pethe, K., and Ehrt, S. (2010) Gluconeogenic carbon flow of tricarboxylic acid cycle intermediates is critical for *Mycobacterium tuberculosis* to establish and maintain infection. *Proc Natl Acad Sci USA* **107:** 9819–9824.
Maurin, M., Mersali, N.F., and Raoult, D. (2000) Bactericidal activities of antibiotics against intracellular *Francisella tularensis*. *Antimicrob Agents Chemother* **44:** 3428–3431.
Meibom, K.L., and Charbit, A. (2010) *Francisella tularensis*

metabolism and its relation to virulence. *Front Microbiol* **1:** 140.

Mercado-Lubo, R., Gauger, E.J., Leatham, M.P., Conway, T., and Cohen, P.S. (2008) A *Salmonella enterica serovar Typhimurium* succinate dehydrogenase/fumarate reductase double mutant is avirulent and immunogenic in BALB/c mice. *Infect Immun* **76:** 1128–1134.

Mercado-Lubo, R., Leatham, M.P., Conway, T., and Cohen, P.S. (2009) *Salmonella enterica serovar Typhimurium* mutants unable to convert malate to pyruvate and oxaloacetate are avirulent and immunogenic in BALB/c mice. *Infect Immun* **77:** 1397–1405.

Millard, P., Letisse, F., Sokol, S., and Portais, J.C. (2012) IsoCor: correcting MS data in isotope labeling experiments. *Bioinformatics* **28:** 1294–1296.

Nano, F.E., and Schmerk, C. (2007) The Francisella pathogenicity island. *Ann N Y Acad Sci* **1105:** 122–137.

Peng, K., and Monack, D.M. (2010) Indoleamine 2,3-dioxygenase 1 is a lung-specific innate immune defense mechanism that inhibits growth of *Francisella tularensis* tryptophan auxotrophs. *Infect Immun* **78:** 2723–2733.

Price, C.T., Al-Quadan, T., Santic, M., Rosenshine, I., and Abu Kwaik, Y. (2011) Host proteasomal degradation generates amino acids essential for intracellular bacterial growth. *Science* **334:** 1553–1557.

Puckett, S., Trujillo, C., Eoh, H., Marrero, J., Spencer, J., Jackson, M., *et al*. (2014) Inactivation of fructose-1,6-bisphosphate aldolase prevents optimal co-catabolism of glycolytic and gluconeogenic carbon substrates in *Mycobacterium tuberculosis*. *PLoS Pathog* **10:** e1004144.

Qin, A., and Mann, B.J. (2006) Identification of transposon insertion mutants of *Francisella tularensis* tularensis strain Schu S4 deficient in intracellular replication in the hepatic cell line HepG2. *BMC Microbiol* **6:** 69.

Qin, A., Scott, D.W., and Mann, B.J. (2008) *Francisella tularensis* subsp. tularensis Schu S4 disulfide bond formation protein B, but not an RND-type efflux pump, is required for virulence. *Infect Immun* **76:** 3086–3092.

Qin, A., Scott, D.W., Thompson, J.A., and Mann, B.J. (2009) Identification of an essential *Francisella tularensis* subsp. tularensis virulence factor. *Infect Immun* **77:** 152–161.

Raghunathan, A., Shin, S., and Daefler, S. (2010) Systems approach to investigating host-pathogen interactions in infections with the biothreat agent *Francisella*. Constraints-based model of *Francisella tularensis*. *BMC Syst Biol* **4:** 118.

Ramond, E., Gesbert, G., Rigard, M., Dairou, J., Dupuis, M., Dubail, I., *et al*. (2014) Glutamate utilization couples oxidative stress defense and the tricarboxylic acid cycle in *Francisella* phagosomal escape. *PLoS Pathog* **10:** e1003893.

Ramond, E., Gesbert, G., Guerrera, I.C., Chhuon, C., Dupuis, M., Rigard, M., *et al*. (2015) Importance of host cell arginine uptake in *Francisella* phagosomal escape and ribosomal protein amounts. *Mol Cell Proteomics* **4:** 870–881.

Saier, M.H., Jr (2000) Families of transmembrane sugar transport proteins. *Mol Microbiol* **35:** 699–710.

Santic, M., Molmeret, M., Klose, K.E., Jones, S., and Kwaik, Y.A. (2005) The *Francisella tularensis* pathogenicity island protein IglC and its regulator MglA are essential for modulating phagosome biogenesis and subsequent bacterial escape into the cytoplasm. *Cell Microbiol* **7:** 969–979.

Santic, M., Molmeret, M., Klose, K.E., and Abu Kwaik, Y. (2006) *Francisella tularensis* travels a novel, twisted road within macrophages. *Trends Microbiol* **14:** 37–44.

Schnappinger, D., Ehrt, S., Voskuil, M.I., Liu, Y., Mangan, J.A., Monahan, I.M., *et al*. (2003) Transcriptional adaptation of *Mycobacterium tuberculosis* within macrophages: insights into the phagosomal environment. *J Exp Med* **198:** 693–704.

Schulert, G.S., McCaffrey, R.L., Buchan, B.W., Lindemann, S.R., Hollenback, C., Jones, B.D., and Allen, L.A. (2009) *Francisella tularensis* genes required for inhibition of the neutrophil respiratory burst and intramacrophage growth identified by random transposon mutagenesis of strain LVS. *Infect Immun* **77:** 1324–1336.

Sjostedt, A. (2007) Tularemia: history, epidemiology, pathogen physiology, and clinical manifestations. *Ann N Y Acad Sci* **1105:** 1–29.

Sjostedt, A. (2011) Francisella tularensis *and tularemia. Front. Microbiol*., 25 April 2011. doi: 10.3389/fmicb.2011.00086.

Steeb, B., Claudi, B., Burton, N.A., Tienz, P., Schmidt, A., Farhan, H., *et al*. (2013) Parallel exploitation of diverse host nutrients enhances *Salmonella* virulence. *PLoS Pathog* **9:** e1003301.

Steele, S., Brunton, J., Ziehr, B., Taft-Benz, S., Moorman, N., and Kawula, T. (2013) *Francisella tularensis* harvests nutrients derived via ATG5-independent autophagy to support intracellular growth. *PLoS Pathog* **9:** e1003562.

Su, J., Yang, J., Zhao, D., Kawula, T.H., Banas, J.A., and Zhang, J.-R. (2007) Genome-wide identification of *Francisella tularensis* virulence determinants. *Infect Immun* **75:** 3089–3101.

Tchawa Yimga, M., Leatham, M.P., Allen, J.H., Laux, D.C., Conway, T., and Cohen, P.S. (2006) Role of gluconeogenesis and the tricarboxylic acid cycle in the virulence of *Salmonella enterica serovar Typhimurium* in BALB/c mice. *Infect Immun* **74:** 1130–1140.

Thomas-Charles, C.A., Zheng, H., Palmer, L.E., Mena, P., Thanassi, D.G., and Furie, M.B. (2013) FeoB-mediated uptake of iron by *Francisella tularensis*. *Infect Immun* **81:** 2828–2837.

Wehrly, T.D., Chong, A., Virtaneva, K., Sturdevant, D.E., Child, R., Edwards, J.A., *et al*. (2009) Intracellular biology and virulence determinants of *Francisella tularensis* revealed by transcriptional profiling inside macrophages. *Cell Microbiol* **11:** 1128–1150.

Weiss, D.S., Brotcke, A., Henry, T., Margolis, J.J., Chan, K., and Monack, D.M. (2007) In vivo negative selection screen identifies genes required for *Francisella* virulence. *Proc Natl Acad Sci USA* **104:** 6037–6042.

Xavier, M.N., Winter, M.G., Spees, A.M., den Hartigh, A.B., Nguyen, K., Roux, C.M., *et al*. (2013) PPARgamma-mediated increase in glucose availability sustains chronic *Brucella abortus* infection in alternatively activated macrophages. *Cell Host Microbe* **14:** 159–170.

Zhang, Y.J., and Rubin, E.J. (2013) Feast or famine: the host-pathogen battle over amino acids. *Cell Microbiol* **15:** 1079–1087.

Zuniga-Ripa, A., Barbier, T., Conde-Alvarez, R., Martinez-

Gomez, E., Palacios-Chaves, L., Gil-Ramirez, Y., *et al*. (2014) *Brucella abortus* depends on pyruvate phosphate dikinase and malic enzyme but not on Fbp and GlpX fructose-1,6-bisphosphatases for full virulence in laboratory models. *J Bacteriol* **196:** 3045–3057.

Supporting information

Additional supporting information may be found in the online version of this article at the publisher's web-site.

frontiers in Cellular and Infection Microbiology

REVIEW
published: 28 March 2017
doi: 10.3389/fcimb.2017.00096

Importance of Metabolic Adaptations in *Francisella* Pathogenesis

Jason Ziveri[1,2], *Monique Barel*[1,2] *and Alain Charbit*[1,2]*

[1] Sorbonne Paris Cité, Université Paris Descartes, Paris, France, [2] Institut National de la Santé et de la Recherche Médicale U1151 - Centre National de la Recherche Scientifique UMR 8253, Institut Necker-Enfants Malades, Team 11: Pathogenesis of Systemic Infections, Paris, France

Francisella tularensis is a highly infectious Gram-negative bacterium and the causative agent of the zoonotic disease tularemia. This bacterial pathogen can infect a broad variety of animal species and can be transmitted to humans in numerous ways with various clinical outcomes. Although, *Francisella* possesses the capacity to infect numerous mammalian cell types, the macrophage constitutes the main intracellular niche, used for *in vivo* bacterial dissemination. To survive and multiply within infected macrophages, *Francisella* must imperatively escape from the phagosomal compartment. In the cytosol, the bacterium needs to control the host innate immune response and adapt its metabolism to this nutrient-restricted niche. Our laboratory has shown that intracellular *Francisella* mainly relied on host amino acid as major gluconeogenic substrates and provided evidence that the host metabolism was also modified upon *Francisella* infection. We will review here our current understanding of how *Francisella* copes with the available nutrient sources provided by the host cell during the course of infection.

Keywords: *Francisella tularensis*, metabolism, glycolysis, nutrient uptake, virulence

OPEN ACCESS

Edited by:
Wolfgang Eisenreich, Technische Universität München, Germany

Reviewed by:
Jiri Stulik, University of Defence, Czechia
John-Demian Sauer, University of Wisconsin-Madison, USA

***Correspondence:**
Alain Charbit
alain.charbit@inserm.fr

Received: *30 January 2017*
Accepted: *13 March 2017*
Published: *28 March 2017*

Citation:
Ziveri J, Barel M and Charbit A (2017) Importance of Metabolic Adaptations in Francisella Pathogenesis. Front. Cell. Infect. Microbiol. 7:96. doi: 10.3389/fcimb.2017.00096

INTRODUCTION

Francisella tularensis is a small Gram-negative bacterium, causative agent of the zoonotic disease tularemia (Sjostedt, 2011). This facultative intracellular pathogen can infect humans by different modes, and notably direct contact with sick animals, inhalation, insect bites or ingestion of contaminated water or food (Foley and Nieto, 2010). *F. tularensis* is able to infect numerous cell types (Jones et al., 2012; Celli and Zahrt, 2013), including dendritic cells, neutrophils, macrophages as well as hepatocytes or endothelial cells but is thought to replicate *in vivo* mainly in macrophages (Santic et al., 2006). Four major subspecies of *F. tularensis* are currently listed: *tularensis*, *holarctica, mediasiatica, and novicida* (McLendon et al., 2006). These subspecies differ in virulence and geographical origin but all cause a fulminant disease in mice that is similar to tularemia in humans (Kingry and Petersen, 2014). Although, the subspecies *novicida* (here designated *F. novicida*) is rarely pathogenic in humans, its genome shares a high degree of nucleotide sequence conservation with the human pathogenic species and is thus widely used as a model to study highly virulent subspecies. The pathogenicity of *Francisella* is tightly associated to its capacity to multiply in the cytosolic compartment of infected macrophages (Celli and Zahrt, 2013). Different macrophage receptors involved in *Francisella* uptake have been identified (Moreau and Mann, 2013). After engulfment by phagocytic cells, *Francisella* transiently resides in a phagosomal compartment (**Figure 1**) that sequentially displays membrane markers of early (EEA1) and late endosomes/lysosomes (LAMP-1 and -2) but does not acquire the hydrolase cathepsin D or lysosomal tracers (Celli and Zahrt, 2013). Within the phagosome, *Francisella* must fight against

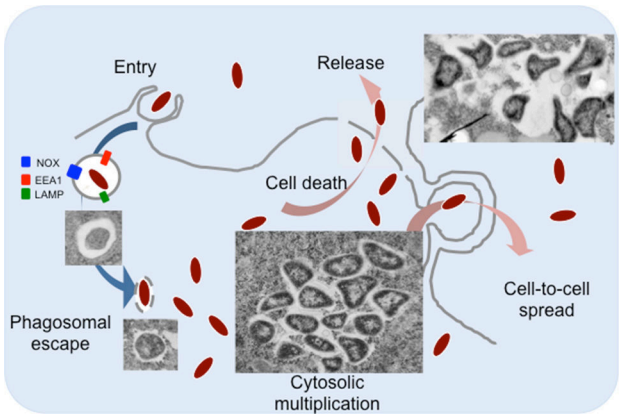

FIGURE 1 | The intracellular life cycle of *F. tularensis*. *Francisella* is internalized into macrophages by large pseudopodia. Inside cells, bacteria transiently reside in a phagosomal compartment that partially matures into a late phagocytic compartment, acquiring membrane markers of early (EEA1) and late endosomes/lysosomes (LAMP-1 and -2). Typical transmission electron microscopy images of intracellular *Francisella* are shown. Once in the host cell cytoplasm, *Francisella* takes advantage of available nutrients to actively multiply. Bacteria can be released from dead cells (by apoptosis and/or pyroptosis) or can be directly transferred by trogocytosis to neighboring cells.

several host antimicrobial defenses, including notably reactive oxygen species (ROS) produced by the NADPH oxidase (Kinkead and Allen, 2016). For this, *Francisella* is equipped with a series of enzymes that include superoxide dismutase, catalase and acid phosphatases (Jones et al., 2012). Phagosomal escape involves a number of additional factors among which its Type 6 secretion systems (T6SS) (Clemens et al., 2015; Rigard et al., 2016). The precise molecular contribution of the *Francisella* T6SS apparatus and/or effectors to phagosomal membrane disruption, as well as of additional non FPI-encoded proteins (Eshraghi et al., 2016) is not yet fully understood. The capacity of *Francisella* adaptation to the host cytosol nutritional environment has been coined "nutritional virulence" (Santic and Abu Kwaik, 2013).

Francisella belongs to a restricted family of bacteria that exclusively multiply in the cytosolic compartment of infected cells. This family, that notably includes *Listeria*, *Shigella*, and *Rickettsia*, have a direct access to the cytosolic elements necessary for their growth. In contrast, the majority of other (facultative or obligate) intracellular pathogens reside in vacuolar compartments (Creasey and Isberg, 2014) and must therefore first import their host-derived nutrients within this compartment before being able to utilize them. For example, *Legionella* takes advantage of proteasomal degradation, a natural host degradative pathway (Price et al., 2011), to obtain an abundant source of amino acids to fill-up the vacuolar compartment where it resides. Indeed, *Legionella pneumophila* has been shown to inject the effector AnkB into the infected host cells (Al-Quadan et al., 2012) which, after lipidation by the host farnesylation machinery, becomes anchored to the vacuolar membrane and serves as a platform for the assembly of Lys48-linked polyubiquitinated proteins. Proteasomal degradation then generates elevated levels of amino acids at the vacuolar membrane, which can be imported into the vacuole.

The host cytosol was initially considered as a nutrient-replete cellular compartment (Ray et al., 2009). However, numerous studies have now clearly established that it contains a number of nutrients in limiting amounts (Fonseca and Swanson, 2014; Abu Kwaik and Bumann, 2015; Eisenreich and Heuner, 2016). Invading intracellular pathogens have therefore evolved various strategies to take advantage of the available nutrient-limiting resources (Abu Kwaik and Bumann, 2013; Zhang and Rubin, 2013; Gouzy et al., 2014b,c; Miller and Celli, 2016).

After several rounds of active multiplication in the host cytosol, *Francisella* dissemination to adjacent cells occurs mainly after their release from lysed cells (Jones et al., 2012). Host guanylate-binding proteins (GBPs) have been shown to be involved in pyroptotic cell death by lysing cytosolic *Francisella* thereby, leading to the activation of the Absent in Melanoma 2 (AIM2) inflammasome (Meunier et al., 2015). Interestingly, a novel cell-to-cell dissemination mechanism has been also described very recently, by which *Francisella* can infect adjacent cells by trogocytosis (Steele et al., 2016). In this review, we will address the role of nutrient acquisition in *Francisella* intracellular adaptation and multiplication, focusing on amino acids and carbohydrates as nutrient supplies.

AMINO ACIDS CONSTITUTE A MAJOR CARBON SOURCE FOR INTRACELLULAR *FRANCISELLA*

Genome-scale genetic screens, performed in different cellular and/or animal models, have repeatedly identified genes encoding either metabolic pathways or predicted membrane proteins, highlighting the importance of metabolic adaptation and nutrient acquisition in intracellular survival of *Francisella* (Pechous et al., 2009; Meibom and Charbit, 2010). In 2009, we showed that *Francisella* used glutathione (a cysteine-containing tripeptide) as a source of intracellular cysteine to compensate its natural auxotrophy for cysteine (Alkhuder et al., 2009), thus providing the first demonstration that this pathogenic bacterium relied on host-derived compounds for intracellular survival. Because of its multiple auxotrophies (arginine, histidine, lysine, tyrosine, methionine, and cysteine), resulting from genetic alterations impairing biosynthetic pathways (Larsson et al., 2005), *Francisella* must acquire many other amino acids, including some available only in limiting concentrations within infected host cells. For this, the bacterium possesses high affinity dedicated uptake systems. Our previous genome analyses revealed that *F. tularensis* is mainly equipped with secondary carriers (Meibom and Charbit, 2010). This family of transporters encompasses several major families, including amino acid transporters, such as the amino acid-polyamine-organocation transporters (APC), the proton-dependent oligopeptide transporters (POT); the hydroxy/aromatic amino acid permeases (HAAAP); as well as the major facilitator superfamily (MFS) proteins, which is involved in a variety of transport functions, including amino acid uptake.

Since 2014, our laboratory has been able to characterize four amino acid transporters (two MFS members, AnsP and IleP;

and two APC members, GadC, and ArgP) and to elucidate their contribution to the major steps of *Francisella* intracellular life cycle. We will first briefly recall below their respective properties and then discuss how amino acid availability could be used by the bacterium to sense its intracellular environment.

*GadC, AnsP, IleP, and ArgP: all for one...*We first functionally characterized the glutamate permease GadC (Ramond et al., 2014) and showed that intracellular multiplication of a Δ*gadC* mutant was essentially abolished because the mutant bacteria remained trapped within the phagosomal compartment. Specifically, our experimental data revealed that GadC contributed, within this compartment, to resistance to reactive oxygen species (ROS). Direct quantification, of tricarboxylic acid (TCA) cycle intermediates present in the cytoplasm of the wild-type and Δ*gadC* strains, showed that inactivation of the *gadC* gene significantly affected succinate, fumarate, and oxoglutarate contents. These data supported the notion that imported glutamate is used by *Francisella* to feed the TCA cycle within the phagosomal compartment (Ramond et al., 2014). Imported glutamate can be converted into various compounds like glutamine, glutathione, GABA or oxoglutarate (OG), which is known to be a potent anti-oxidant molecule (Mailloux et al., 2009). Of note, we had previously shown that the AAA+ chaperone MoxR of *Francisella* (Dieppedale et al., 2013) interacted physically with the enzymes pyruvate dehydrogenase and oxoglutarate dehydrogenase and that this interaction was required for optimal activity of these two enzymes. Since *moxR* gene inactivation also impaired bacterial intracellular viability and stress resistance, one may assume that the activity of the TCA cycle contributes to stress defense and bacterial virulence. The role of the TCA cycle in stress defenses is currently investigated in other pathogenic bacterial species and a direct role of the oxoglutarate dehydrogenase in resistance to nitrosative stress has been recently demonstrated in *M. tuberculosis* (Maksymiuk et al., 2015).

In a parallel study, we identified a second permease, designated AnsP, specifically involved in asparagine uptake. In sharp contrast to GadC, AnsP appeared to be exclusively required for bacterial cytosolic multiplication. Impaired intracellular growth of the *F. novicida* Δ*ansP* mutant could be fully suppressed upon supplementation with an excess of asparagine, *in vitro* as well as *in vivo* (Gesbert et al., 2014). Of note, Neyrolles and co-workers have shown that *M. tuberculosis*, which is prototrophic for all 20 amino acids in broth, also relied on two paralogous amino acid transporters, one for aspartate and one for asparagine (designated AnsP1 and AnsP2, respectively) for intracellular survival and multiplication (Gouzy et al., 2013, 2014a,b,c). Interestingly, genetic inactivation of the gene encoding AnsP1 led to a severe decrease of mycobacterial fitness *in vivo*. In contrast, inactivation of the asparagine transporter AnsP2, although specifically involved in asparagine uptake at acidic pH, did not affect bacterial virulence *in vivo*.

The fact that *Francisella* is prototrophic for both glutamate and asparagine during growth in synthetic medium (and possesses intact biosynthetic pathways) suggests that the bacterium becomes "phenotypically" auxotrophic in infected cells, in agreement with the notion that uptake is generally preferred to synthesis. Whereas AnsP-dependent asparagine uptake was more specifically dedicated to protein synthesis, GadC-dependent glutamate transport was required for oxidative stress defense, indicating that amino acid acquisition contributes to multiple aspects of intracellular bacterial adaptation. The mechanisms down-regulating (or not up-regulating) the corresponding biogenesis pathways remain to be elucidated in intracellular bacteria.

More recently, we showed that two other amino acid permeases, IleP, and ArgP, were required in both phagosomal and cytosolic compartments. The orthologues of IleP, in the highly virulent strain *F. tularensis* Schu S4 and in *F. tularensis* LVS, had been shown to be required for normal bacterial replication in the hepatocytic human cell line HepG2 (Qin and Mann, 2006; Marohn et al., 2012). We found that the MFS permease IleP of *Francisella* mediated isoleucine uptake and was vital for bacterial intracellular multiplication and virulence (Gesbert et al., 2015). Remarkably, inactivation of the *ileP* gene in both *F. novicida* and *F. tularensis* LVS led to a delayed bacterial phagosomal escape and to a reduced cytosolic multiplication.

Genome comparisons showed that pathogenic *Francisella* subspecies possessed defective branched-chain amino acid (BCAA) pathways involved in leucine, isoleucine, and valine biosynthesis, relying thus exclusively on transporter-mediated acquisition of these amino acids from the host. At the opposite, *F. novicida* was equipped with an intact BCAA pathway and could use threonine as a precursor for their synthesis.

Of note, AnsP, and IleP proteins both belong to the Phagosomal transporter (Pht) subclass of MFS that is exclusively found among intracellular pathogenic bacteria (Chen et al., 2008). In *L. pneumophila*, the Pht protein PhtA has been shown to be required for threonine uptake in the Legionella-containing vacuole (Sauer et al., 2005). The *L. pneumophila* genome encodes 10 additional PhtA paralogues, some of which are also required during intracellular replication (Fonseca and Swanson, 2014). Interestingly, whereas PhtJ is required for acquisition of valine (Sauer et al., 2005), PhtC and PhtD were more recently shown to contribute to protecting *L. pneumophila* from dTMP starvation (Fonseca et al., 2014), indicating that Pht transporters are not strictly devoted to amino acid uptake.

We also showed that the permease ArgP of *Francisella* was a high affinity arginine transporter (Ramond et al., 2015). ArgP-mediated arginine uptake appeared to be crucial for efficient phagosomal escape. Arginine constitutes an essential amino acid for *Francisella* since the metabolic pathways, leading to- or coming to arginine, are predicted to be inactive, thus, highlighting the importance of essential amino acids during early stage infection. By using high-resolution mass spectrometry, we found that arginine limitation affected biogenesis of the majority of the ribosomal proteins. Indeed, in bacteria grown under arginine limiting conditions, the majority of the ribosomal proteins identified (app. 80%) were present in lower amount in the Δ*argP* mutant compared to wild-type, suggesting possible links between ribosomal proteins amounts and phagosomal escape (Ramond et al., 2015). Of note, ArgP is the closest paralogue of GadC within the APC family of transporter (Meibom and Charbit, 2010).

The contribution of the glycine cleavage system (GCS) to the pathogenesis of Francisella was addressed by Gerard Nau and co-workers (Brown et al., 2014). Genes encoding the GCS have been identified in genome-wide genetic screens developed to identify novel *Francisella* virulence genes (Meibom and Charbit, 2010). This pathway facilitates the degradation of glycine to acquire 5,10-methylene-tetrahydrofolate, a one carbon donor utilized in the production of serine, thymidine, and purines. Hence, the GCS is expected to contribute to pathogen fitness in conditions where these metabolites are limiting. In *F. tularensis* Schu S4, inactivation of the glycine cleavage system aminomethyltransferase T (GcvT) leads to serine auxotrophy, thus implying that the intact *serABC* pathway still present in the Δ*gcvT* mutant strain is either insufficiently active *in vitro* or not involved in serine biosynthesis in Francisella. The authors demonstrated that the *F. tularensis* GCS was essential for intracellular multiplication in conditions of serine limitation and contributed to *in vivo* pathogenesis. Of note, the GCS has been previously associated to persistence during chronic bacterial infection with Brucella abortus (Hong et al., 2000).

COULD AMINO ACIDS SERVE AS SENSORS OF THE INTRACELLULAR MILIEU?

The metabolism of branched chain amino acid lies at the crossroads of several other bacterial metabolic pathways in living cells. BCAAs are essential amino acids for humans and therefore must be supplied in the diet. Yet, BCAAs are among the most abundant amino acids in proteins; maintaining their pools is, thus, a prerequisite for high level synthesis of proteins. As mentioned above, in the pathogenic subsps *holarctica* and *tularensis*, BCAA degradation pathways were predicted to be nonfunctional, suggesting that exogenously acquired BCAAs could be used mainly for protein synthesis in these species. Interestingly, we found that the *F. tularensis* LVS triggered the uptake of important amounts of BCAAs upon entry into THP-1 macrophages (Gesbert et al., 2015). Indeed, the intracellular BCAA concentration sharply increased after 1 h of infection and strongly decreased after 24 h, suggesting that these amino acids had been consumed during the course of intracellular bacterial multiplication. We found that infection with *L. monocytogenes* EGD-e strain also triggered a significant (10-fold) rise in the concentration of each of the BCAAs in these cells but their concentration varied only very moderately over the course of infection. Of note, it has been previously reported that *L. monocytogenes* infection induced the BCAA pathway in macrophages (Lobel et al., 2012), suggesting that *L. monocytogenes* encountered limited amounts of BCAAs in the host cytosol. Furthermore, the pleiotropic isoleucine-responsive regulator CodY was found to be responsible for the upregulation of *L. monocytogenes* virulence genes under limiting concentrations of BCAAs in chemically defined medium. These observations led Herskovits and co-workers to propose that the limiting intracellular concentrations of BCAAs could represent a signal for the bacteria to sense their subcellular localization. More recently, these authors demonstrated that CodY directly bound the proximal portion of the coding sequence of the master virulence activator gene, *prfA*, and that this binding resulted in up-regulation of *prfA* transcription specifically under low concentrations of BCAA (Lobel et al., 2015), linking directly metabolism and virulence in this pathogen. *Francisella* genomes do not encode any CodY orthologue. Hence, one may speculate that intracellular isoleucine concentration influences *Francisella* genes expression via another, yet unidentified, regulatory mechanism.

Macrophages are able to synthesize their own arginine and to import it via constitutive and inducible cationic amino acid transporters CAT-1 (or SLC7A1) and CAT-2 (or SLC7A2), respectively (Ramond et al., 2015). Arginine serves either to produce nitrogen reactive species (NO, via NO synthases) or convert it to ornithine and urea (via type 1 arginase). The phagosome into which *Francisella* transiently resides is a dynamic compartment whose size and internal composition may considerably vary during the limited period of time spent by the bacterium. The arginine concentration available to *Francisella* in the phagosome might also progressively decrease during its maturation. One may suggest that intracellular *Francisella* respond to variations of arginine availability in this compartment by regulating their own ribosomal protein biogenesis. Indeed, repression of ribosomal protein synthesis in response to stresses, such as nutritional limitation, has been observed in all kingdoms of life (Conrad et al., 2014).

LINKING CARBOHYDRATE METABOLISM AND AMINO ACID UPTAKE

In mammalian cells, glycolysis and the oxidative branch of the pentose-phosphate pathway occur in the cytosol as the anabolic reactions (gluconeogenesis; and amino acid, nucleotide, fatty acids biosynthesis). In contrast, the TCA cycle and the electron-transfer chain, leading to oxidative phosphorylation, take place exclusively in the mitochondria and metabolites, such as pyruvate, are transferred from the cytosol to the mitochondria to feed the TCA. While several intracellular bacterial pathogens (such as enteroinvasive *Escherichia coli* and *Brucella*) mainly rely on glucose as a preferred carbon source for their intracellular metabolism (Abu Kwaik and Bumann, 2015), others simultaneously use multiple carbon sources (Abu Kwaik and Bumann, 2015). For example, *L. monocytogenes* has been shown to rely on two major carbon substrates, glycerol, and glucose-6P (Eisenreich et al., 2010; Grubmuller et al., 2014), but preferentially uses glycerol during its intracellular replication. Like *L. monocytogenes*, *Francisella* can use glucose as a carbon and energy sources. However, *L. monocytogenes* possesses a transporter (UhpT) specifically mediating the uptake of host glucose-6P that constitutes a key element of its cytosolic multiplication (Chico-Calero et al., 2002). *Francisella* genomes do not encode any orthologue of the UhpT sugar phosphate transporter family and *F. novicida* and *F. tularensis* LVS are even unable to ferment glucose-6P (Gesbert et al., 2014). This suggests that host-derived glucose-6P might not be utilizable

as a source of carbohydrate by *Francisella* during intracellular multiplication. In contrast, the non-pathogenic related species *Francisella philomiragia*, which has an environmental habitat, possesses a *uhpT* orthologous gene (Fphi_0883, unpublished observation), suggesting that this bacterium is able to utilize this sugar during its planktonic life.

Of note, *Francisella* genomes encode a glycerol uptake transporter (GlpF) and a glycerol-3 phosphate transporter (GlpT). Hence, in the absence of glucose, *Francisella* probably mainly uses the available carbon sources (such as pyruvate, glycerol and glycerol-3P), in addition to amino acids, as intracellular carbon and nitrogen sources. The mechanisms by which glucose or glycerol are taken up by *Francisella* are still unknown. Indeed, genome analyses indicate that *Francisella* is devoid of any carbohydrate PEP-dependent phosphotransferase (PTS) system (Meibom and Charbit, 2010) or other non-PTS putative glucose permease.

Gluconeogenesis, which allows glucose synthesis from non-sugar compounds such as amino acids or TCA cycle intermediates, is involved in virulence of several intracellular bacterial pathogens, including *M. tuberculosis* (Marrero et al., 2010; Puckett et al., 2014) but is dispensable for other bacteria such as *Brucella abortus* (Zuniga-Ripa et al., 2014). In *Francisella*, we recently showed that gluconeogenesis constituted a major pathway required for pathogenesis (Brissac et al., 2015). Indeed, inactivation of the gene *glpX*, encoding the unique class II fructose biphosphatase (FBPase) of *Francisella*, severely impaired intra-macrophagic bacterial multiplication, in the presence of gluconeogenic substrates and considerably attenuated virulence in the mouse mode. The strictly gluconeogenic enzyme is responsible for the conversion of fructose 1,6-bisphosphate into fructose 6-phosphate (**Figure 2**). A severe intracellular multiplication defect of a Δ*glpX* mutant was also observed when cells were supplemented with a gluconeogenic substrate (e.g., pyruvate or glycerol). In contrast, wild-type multiplication was restored when the medium was supplemented with glucose. In chemically defined medium (CDM), inactivation of *glpX* also led to a severe growth defect in all the media containing gluconeogenic substrates. Growth of the wild-type strain in CDM lacking glucose (CDMΔGlc) was significantly reduced but still detectable, due to the presence of the amino acids present in the 3 mM range whereas growth of the Δ*glpX* mutant was essentially abolished. Supplementation of CDMΔGlc with individually added excess amino acid (25 mM) improved to variable extents growth of the wild-type strain in the absence of glucose. Remarkably, alanine was the only amino acid to restore wild-type growth (Brissac et al., 2015) although no gene encoding a putative alanine dehydrogenase (catalyzing the

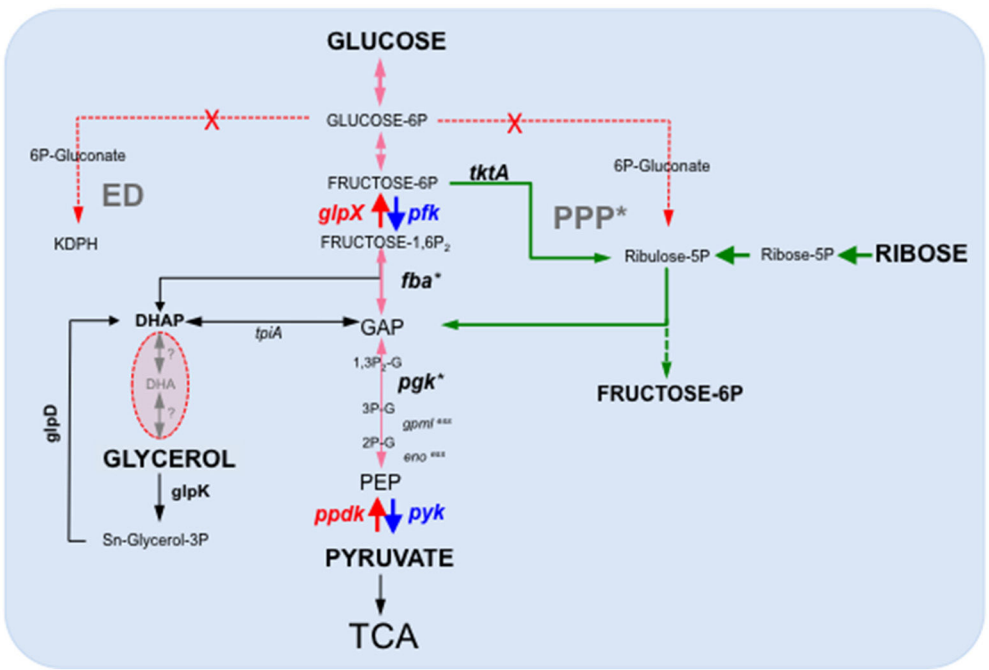

FIGURE 2 | Schematic depiction of the *Francisella* glycolytic and gluconeogenic pathways. *F. tularensis* possesses a complete glycolysis and gluconeogenesis pathways as well as an intact TCA cycle. In contrast, it lacks a functional Entner-Doudoroff (ED) pathway and the oxidative branch of the Pentose phosphate pathway (PPP), in red-dotted arrows. PPP*, the non-oxidative branch of the PPP is still functional. Ppdk and FBPase (in red) represent only two enzymatic steps specifically acting in the gluconeogenic direction. The dotted green arrows indicate the non-oxidative part of the Pentose Phosphate Pathway. Gene numbers in *F. novicida*: *pgm* (*FTN_0514*); *pgi* (*FTN_0663*); *gpmI* (*FTN_0648*); *eno* (*FTN_0621*); *glpX* (*FTN_0298*); *pfk* (*FTN_1210*); (*FTN_1631*); *glpD* (*FTN_1584*); *glpK* (*FTN_1585*). x^{ess}, essential genes. *Expression of *fba* and *pgK* have shown to be up-regulated in BMM (Wehrly et al., 2009). *F. tularensis Schu S4* and *F. novicida* U112 are able to ferment glycerol but the enzymes involved are unknown. *F. tularensis LVS* is unable to ferment glycerol. DHAP, Dihydroxyacetone phosphate (or Glycerone-Phosphate); GAP, glyceraldehyde 3-phosphate; PEP, phosphoenolpyruvate.

conversion of L-alanine to pyruvate) could be predicted in the *F. novicida* genome (unpublished observation). As expected, supplementation of the CDMΔGlc medium with any of the (individually added) twenty amino acids failed to restore growth of the Δ*glpX* mutant, strongly suggesting that amino acids served as gluconeogenic substrates by *Francisella*.

Isotopic profiling, using either ^{13}C-labeled glucose or ^{13}C-labeled pyruvate, revealed that *Francisella* possessed both active glycolysis and gluconeogenesis pathways in CDM (Brissac et al., 2015). The existence of a complete and functional glycolytic pathway in *Francisella* is in agreement with a genome-wide study which notably revealed that gene *FTN_1210* in *F. novicida* most likely encoded a phosphofructokinase, responsible for the conversion fructose-6P to fructose-1,6P (Enstrom et al., 2012). Indeed, this study, aimed at attributing novel non-predictable metabolic functions to non-essential genes, showed that inactivation of gene *FTN_1210* abolished growth on sugars but not on short-chain carbon sources, suggesting a block in glycolysis. Furthermore, the gene *FTN_1210* was shown to functionally complement the growth defect of an *E. coli pfk* mutant on sorbitol as the carbon source. Of note, the gene *FTN_1210,* now designated *pfk,* is still erroneously annotated as encoding a putative ribokinase in the KEGG database.

Our metabolomics analyses further indicated that the enzyme of the non-oxidative PPP (transketolase, transaldolase) were functional (**Figure 2**). However, 6-phosphogluconate (6-PG) and pentose phosphates were not detected, suggesting an absence of the oxidative part of PPP, from 6-PG to pentose-5-phospate, suggesting a major role of the Embden–Meyerhof (glycolysis) pathway in glucose catabolism in *Francisella*. Remarkably, a reduction in the intracellular glucose concentration was recorded in both J774.1 and THP-1 macrophages infected for 24 h with *F. tularensis* LVS (Brissac et al., 2015). The need for cytosolic *Francisella* to possess an active gluconeogenic pathway is thus consistent with the significant reduction in the available intracellular glucose pool observed upon infection. The control of the intracellular glucose homeostasis is likely to be a key issue for proper bacterial multiplication. Infected cells might modify their metabolism to reduce the available glucose intracellular pool and, hence, limit bacterial proliferation. Of particular interest, a very recent study (Sanman et al., 2016) demonstrated that *Salmonella typhimium* activated the NLRP3 inflammasome by disrupting the glycolytic flux upon infection of bone marrow-derived macrophages. The authors showed that this trigger occurred because intracellular bacteria were using the macrophage supply of glycolysis precursor molecules. This study suggests that glycolytic disruption may constitute a more general mechanism of inflammasome activation triggered in response to metabolic parasitism by microbes.

In conclusion, our recent studies have shown that amino acid uptake systems and carbohydrate metabolic pathways played both an important and complementary role in *Francisella* pathogenesis (**Figure 3**). Novel approaches are developed to translate multi-omics data into functional metabolic programs. For example, constraints-based systems analysis has been used on *Francisella* to integrate existing high-throughput data, *in silico* and experimental information (Raghunathan et al., 2010). This

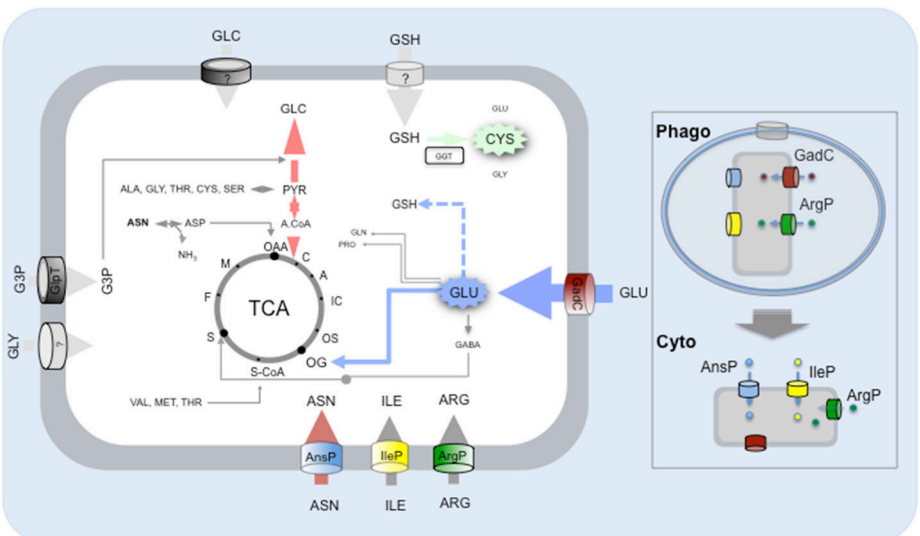

FIGURE 3 | Amino acid and carbohydrate uptake systems involved in *Francisella* intracellular survival. Schematic depiction of the carbohydrate and amino acid transporters (predicted or characterized) of *Francisella* and contribution of the imported amino acid and carbohydrates to metabolic pathways. Amino acids (ASN, asparagine; ILE, Isoleucine; ARG, Arginine; GLU, Glutamate) are taken up by *Francisella* via dedicated amino acid transporters and used to feed the TCA cycle (GLU) and/or as gluconeogenic substrates and/or as building blocks for protein synthesis (ASN, ARG, ILE). The imported carbohydrates (GLC, Glucose; GLY, Glycerol; G3P, Glyceraldehyde-3-Phosphate) are used to feed the glycolysis/gluconeogenesis pathways. Protein numbers of the represented transporters in *F. novicida*: GadC (FTN_ 0571), AnsP (FTN_1586), IleP (FTN_1654), ArgP (FTN-0848); G3P transporter GlpT (FTN_0636). Boxed to the right of the Figure, the respective contributions of the amino acid transporters to: (i) phagosomal survival and escape (upper part); (ii) cytosolic multiplication (lower part).

approach allowed the reconstruction of a genome-scale metabolic model, which identified significant changes of metabolism during *Francisella* intracellular growth in the infected macrophage. Altogether, a switch from oxidative metabolism, in the initial stages of infection, to glycolysis, fatty acid oxidation, and gluconeogenesis, during the later stages, could be deduced from their analyses.

Understanding the subtle interplay between bacterial and host metabolism will be a major challenge for future studies. Many important questions remain to be answered on the bacterial side to assess the contribution of other nutrient sources (such as lipids, ions) during intracellular multiplication. The molecular dissection of the links between metabolic alterations triggered by the pathogen and the modulation of the innate immune response constitutes a novel and very promising field of investigation.

AUTHOR CONTRIBUTIONS

AC and JZ wrote the paper, MB edited the paper.

ACKNOWLEDGMENTS

These studies were supported by INSERM, CNRS and Université Paris Descartes Paris Cité Sorbonne. JZ was funded by a fellowship from the "Délégation Générale à l'Armement." The funders had no role in study design, data collection and analysis, decision to publish, or preparation of the manuscript.

REFERENCES

Abu Kwaik, Y., and Bumann, D. (2013). Microbial quest for food *in vivo*: 'Nutritional virulence' as an emerging paradigm. *Cell. Microbiol.* 15, 882–890. doi: 10.1111/cmi.12138

Abu Kwaik, Y., and Bumann, D. (2015). Host delivery of favorite meals for intracellular pathogens. *PLoS Pathog.* 11:e1004866. doi: 10.1371/journal.ppat.1004866

Alkhuder, K., Meibom, K. L., Dubail, I., Dupuis, M., and Charbit, A. (2009). Glutathione provides a source of cysteine essential for intracellular multiplication of *Francisella tularensis*. *PLoS Pathog.* 5:e1000284. doi: 10.1371/journal.ppat.1000284

Al-Quadan, T., Price, C. T., and Abu Kwaik, Y. (2012). Exploitation of evolutionarily conserved amoeba and mammalian processes by *Legionella*. *Trends Microbiol.* 20, 299–306. doi: 10.1016/j.tim.2012.03.005

Brissac, T., Ziveri, J., Ramond, E., Tros, F., Kock, S., Dupuis, M., et al. (2015). Gluconeogenesis, an essential metabolic pathway for pathogenic *Francisella*. *Mol. Microbiol.* 98, 518–534. doi: 10.1111/mmi.13139

Brown, M. J., Russo, B. C., O'Dee, D. M., Schmitt, D. M., and Nau, G. J. (2014). The contribution of the glycine cleavage system to the pathogenesis of *Francisella tularensis*. *Microbes Infect.* 16, 300–309. doi: 10.1016/j.micinf.2013.12.003

Celli, J., and Zahrt, T. C. (2013). Mechanisms of *Francisella tularensis* intracellular pathogenesis. *Cold Spring Harb. Perspect. Med.* 3:a010314. doi: 10.1101/cshperspect.a010314

Chen, D. E., Podell, S., Sauer, J. D., Swanson, M. S., and Saier, M. H. Jr. (2008). The phagosomal nutrient transporter (Pht) family. *Microbiology* 154(Pt 1), 42–53. doi: 10.1099/mic.0.2007/010611-0

Chico-Calero, I., Suarez, M., Gonzalez-Zorn, B., Scortti, M., Slaghuis, J., Goebel, W., et al. (2002). Hpt, a bacterial homolog of the microsomal glucose- 6-phosphate translocase, mediates rapid intracellular proliferation in *Listeria*. *Proc. Natl. Acad. Sci. U.S.A.* 99, 431–436. doi: 10.1073/pnas.012363899

Clemens, D. L., Ge, P., Lee, B. Y., Horwitz, M. A., and Zhou, Z. H. (2015). Atomic structure of T6SS reveals interlaced array essential to function. *Cell* 160, 940–951. doi: 10.1016/j.cell.2015.02.005

Conrad, M., Schothorst, J., Kankipati, H. N., Van Zeebroeck, G., Rubio-Texeira, M., and Thevelein, J. M. (2014). Nutrient sensing and signaling in the yeast *Saccharomyces cerevisiae*. *FEMS Microbiol. Rev.* 38, 254–299. doi: 10.1111/1574-6976.12065

Creasey, E. A., and Isberg, R. R. (2014). Maintenance of vacuole integrity by bacterial pathogens. *Curr. Opin. Microbiol.* 17, 46–52. doi: 10.1016/j.mib.2013.11.005

Dieppedale, J., Gesbert, G., Ramond, E., Chhuon, C., Dubail, I., Dupuis, M., et al. (2013). Possible links between stress defense and the tricarboxylic acid (TCA) cycle in *Francisella* pathogenesis. *Mol. Cell. Proteomics* 12, 2278–2292. doi: 10.1074/mcp.M112.024794

Eisenreich, W., Dandekar, T., Heesemann, J., and Goebel, W. (2010). Carbon metabolism of intracellular bacterial pathogens and possible links to virulence. *Nat. Rev. Microbiol.* 8, 401–412. doi: 10.1038/nrmicro2351

Eisenreich, W., and Heuner, K. (2016). The life stage-specific pathometabolism of *Legionella pneumophila*. *FEBS Lett.* 590, 3868–3886. doi: 10.1002/1873-3468.12326

Enstrom, M., Held, K., Ramage, B., Brittnacher, M., Gallagher, L., and Manoil, C. (2012). Genotype-phenotype associations in a nonmodel prokaryote. *mBio* 3:e00001-12. doi: 10.1128/mbio.00001-12

Eshraghi, A., Kim, J., Walls, A. C., Ledvina, H. E., Miller, C. N., Ramsey, K. M., et al. (2016). Secreted effectors encoded within and outside of the *Francisella* Pathogenicity Island promote intramacrophage growth. *Cell Host Microbe* 20, 573–583. doi: 10.1016/j.chom.2016.10.008

Foley, J. E., and Nieto, N. C. (2010). Tularemia. *Vet. Microbiol.* 140, 332–338. doi: 10.1016/j.vetmic.2009.07.017

Fonseca, M. V., Sauer, J. D., Crepin, S., Byrne, B., and Swanson, M. S. (2014). The phtC-phtD locus equips *Legionella pneumophila* for thymidine salvage and replication in macrophages. *Infect. Immun.* 82, 720–730. doi: 10.1128/IAI.01043-13

Fonseca, M. V., and Swanson, M. S. (2014). Nutrient salvaging and metabolism by the intracellular pathogen *Legionella pneumophila*. *Front. Cell. Infect. Microbiol.* 4:12. doi: 10.3389/fcimb.2014.00012

Gesbert, G., Ramond, E., Rigard, M., Frapy, E., Dupuis, M., Dubail, I., et al. (2014). Asparagine assimilation is critical for intracellular replication and dissemination of *Francisella*. *Cell. Microbiol.* 16, 434–449. doi: 10.1111/cmi.12227

Gesbert, G., Ramond, E., Tros, F., Dairou, J., Frapy, E., Barel, M., et al. (2015). Importance of branched-chain amino acid utilization in Francisella intracellular adaptation. *Infect. Immun.* 83, 173–183. doi: 10.1128/IAI.02579-14

Gouzy, A., Larrouy-Maumus, G., Bottai, D., Levillain, F., Dumas, A., Wallach, J. B., et al. (2014a). *Mycobacterium tuberculosis* exploits asparagine to assimilate nitrogen and resist acid stress during infection. *PLoS Pathog.* 10:e1003928. doi: 10.1371/journal.ppat.1003928

Gouzy, A., Larrouy-Maumus, G., Wu, T. D., Peixoto, A., Levillain, F., Lugo-Villarino, G., et al. (2013). *Mycobacterium tuberculosis* nitrogen assimilation and host colonization require aspartate. *Nat. Chem. Biol.* 9, 674–676. doi: 10.1038/nchembio.1355

Gouzy, A., Poquet, Y., and Neyrolles, O. (2014b). Amino acid capture and utilization within the *Mycobacterium tuberculosis* phagosome. *Future Microbiol.* 9, 631–637. doi: 10.2217/fmb.14.28

Gouzy, A., Poquet, Y., and Neyrolles, O. (2014c). Nitrogen metabolism in *Mycobacterium tuberculosis* physiology and virulence. *Nat. Rev. Microbiol.* 12, 729–737. doi: 10.1038/nrmicro3349

Grubmuller, S., Schauer, K., Goebel, W., Fuchs, T. M., and Eisenreich, W. (2014). Analysis of carbon substrates used by *Listeria monocytogenes* during growth in J774A.1 macrophages suggests a bipartite intracellular metabolism. *Front. Cell. Infect. Microbiol.* 4:156. doi: 10.3389/fcimb.2014.00156

Hong, P. C., Tsolis, R. M., and Ficht, T. A. (2000). Identification of genes required for chronic persistence of *Brucella abortus* in mice. *Infect. Immun.* 68, 4102–4107. doi: 10.1128/IAI.68.7.4102-4107.2000

Jones, C. L., Napier, B. A., Sampson, T. R., Llewellyn, A. C., Schroeder, M. R., and Weiss, D. S. (2012). Subversion of host recognition and defense systems by *Francisella* spp. *Microbiol. Mol. Biol. Rev.* 76, 383–404. doi: 10.1128/MMBR.05027-11

Kingry, L. C., and Petersen, J. M. (2014). Comparative review of *Francisella tularensis* and *Francisella novicida*. *Front. Cell. Infect. Microbiol.* 4:35. doi: 10.3389/fcimb.2014.00035

Kinkead, L. C., and Allen, L. A. (2016). Multifaceted effects of *Francisella tularensis* on human neutrophil function and lifespan. *Immunol. Rev.* 273, 266–281. doi: 10.1111/imr.12445

Larsson, P., Oyston, P. C., Chain, P., Chu, M. C., Duffield, M., Fuxelius, H. H., et al. (2005). The complete genome sequence of *Francisella tularensis*, the causative agent of tularemia. *Nat. Genet.* 37, 153–159. doi: 10.1038/ng1499

Lobel, L., Sigal, N., Borovok, I., Belitsky, B. R., Sonenshein, A. L., and Herskovits, A. A. (2015). The metabolic regulator CodY links *Listeria monocytogenes* metabolism to virulence by directly activating the virulence regulatory gene prfA. *Mol. Microbiol.* 95, 624–644. doi: 10.1111/mmi.12890

Lobel, L., Sigal, N., Borovok, I., Ruppin, E., and Herskovits, A. A. (2012). Integrative genomic analysis identifies isoleucine and CodY as regulators of *Listeria monocytogenes* virulence. *PLoS Genet.* 8:e1002887. doi: 10.1371/journal.pgen.1002887

Mailloux, R. J., Singh, R., Brewer, G., Auger, C., Lemire, J., and Appanna, V. D. (2009). α-ketoglutarate dehydrogenase and glutamate dehydrogenase work in tandem to modulate the antioxidant α-ketoglutarate during oxidative stress in *Pseudomonas fluorescens*. *J. Bacteriol.* 191, 3804–3810. doi: 10.1128/JB.00046-09

Maksymiuk, C., Balakrishnan, A., Bryk, R., Rhee, K. Y., and Nathan, C. F. (2015). E1 of α-ketoglutarate dehydrogenase defends *Mycobacterium tuberculosis* against glutamate anaplerosis and nitroxidative stress. *Proc. Natl. Acad. Sci. U.S.A.* 112, E5834–E5843. doi: 10.1073/pnas.1510932112

Marohn, M. E., Santiago, A. E., Shirey, K. A., Lipsky, M., Vogel, S. N., and Barry, E. M. (2012). Members of the *Francisella tularensis* phagosomal transporter subfamily of major facilitator superfamily transporters are critical for pathogenesis. *Infect. Immun.* 80, 2390–2401. doi: 10.1128/IAI.00144-12

Marrero, J., Rhee, K. Y., Schnappinger, D., Pethe, K., and Ehrt, S. (2010). Gluconeogenic carbon flow of tricarboxylic acid cycle intermediates is critical for *Mycobacterium tuberculosis* to establish and maintain infection. *Proc. Natl. Acad. Sci. U.S.A.* 107, 9819–9824. doi: 10.1073/pnas.1000715107

McLendon, M. K., Apicella, M. A., and Allen, L. A. (2006). *Francisella tularensis*: taxonomy, genetics, and Immunopathogenesis of a potential agent of biowarfare. *Annu. Rev. Microbiol.* 60, 167–185. doi: 10.1146/annurev.micro.60.080805.142126

Meibom, K. L., and Charbit, A. (2010). *Francisella tularensis* metabolism and its relation to virulence. *Front. Microbiol.* 1:140. doi: 10.3389/fmicb.2010.00140

Meunier, E., Wallet, P., Dreier, R. F., Costanzo, S., Anton, L., Ruhl, S., et al. (2015). Guanylate-binding proteins promote activation of the AIM2 inflammasome during infection with *Francisella novicida*. *Nat. Immunol.* 16, 476–484. doi: 10.1038/ni.3119

Miller, C., and Celli, J. (2016). Avoidance and subversion of eukaryotic homeostatic autophagy mechanisms by bacterial pathogens. *J. Mol. Biol.* 428, 3387–3398. doi: 10.1016/j.jmb.2016.07.007

Moreau, G. B., and Mann, B. J. (2013). Adherence and uptake of *Francisella* into host cells. *Virulence* 4, 826–832. doi: 10.4161/viru.25629

Pechous, R. D., McCarthy, T. R., and Zahrt, T. C. (2009). Working toward the future: insights into *Francisella tularensis* pathogenesis and vaccine development. *Microbiol. Mol. Biol. Rev.* 73, 684–711. doi: 10.1128/MMBR.00028-09

Price, C. T., Al-Quadan, T., Santic, M., Rosenshine, I., and Abu Kwaik, Y. (2011). Host proteasomal degradation generates amino acids essential for intracellular bacterial growth. *Science* 334, 1553–1557. doi: 10.1126/science.1212868

Puckett, S., Trujillo, C., Eoh, H., Marrero, J., Spencer, J., Jackson, M., et al. (2014). Inactivation of fructose-1,6-bisphosphate aldolase prevents optimal co-catabolism of glycolytic and gluconeogenic carbon substrates in *Mycobacterium tuberculosis*. *PLoS Pathog.* 10:e1004144. doi: 10.1371/journal.ppat.1004144

Qin, A., and Mann, B. J. (2006). Identification of transposon insertion mutants of *Francisella tularensis* strain Schu S4 deficient in intracellular replication in the hepatic cell line HepG2. *BMC Microbiol.* 31:69. doi: 10.1186/1471-2180-6-69

Raghunathan, A., Shin, S., and Daefler, S. (2010). Systems approach to investigating host-pathogen interactions in infections with the biothreat agent *Francisella*. Constraints-based model of *Francisella tularensis*. *BMC Syst. Biol.* 4:118. doi: 10.1186/1752-0509-4-118

Ramond, E., Gesbert, G., Guerrera, I. C., Chhuon, C., Dupuis, M., Rigard, M., et al. (2015). Importance of host cell arginine uptake in Francisella phagosomal escape and ribosomal protein amounts. *Mol. Cell. Proteomics* 14, 870–881. doi: 10.1074/mcp.M114.044552

Ramond, E., Gesbert, G., Rigard, M., Dairou, J., Dupuis, M., Dubail, I., et al. (2014). Glutamate utilization couples oxidative stress defense and the tricarboxylic acid cycle in *Francisella* phagosomal escape. *PLoS Pathog.* 10:e1003893. doi: 10.1371/journal.ppat.1003893

Ray, K., Marteyn, B., Sansonetti, P. J., and Tang, C. M. (2009). Life on the inside: the intracellular lifestyle of cytosolic bacteria. *Nat. Rev. Microbiol.* 7, 333–340. doi: 10.1038/nrmicro2112

Rigard, M., Broms, J. E., Mosnier, A., Hologne, M., Martin, A., Lindgren, L., et al. (2016). *Francisella tularensis* IglG belongs to a novel family of PAAR-Like T6SS proteins and harbors a unique N-terminal extension required for virulence. *PLoS Pathog.* 12:e1005821. doi: 10.1371/journal.ppat.1005821

Sanman, L. E., Qian, Y., Eisele, N. A., Ng, T. M. van der Linden, W. A., Monack, D. M., et al. (2016). Disruption of glycolytic flux is a signal for inflammasome signaling and pyroptotic cell death. *Elife* 5:e13663. doi: 10.7554/elife.13663

Santic, M., and Abu Kwaik, Y. (2013). Nutritional virulence of *Francisella tularensis*. *Front. Cell. Infect. Microbiol.* 3:112. doi: 10.3389/fcimb.2013.00112

Santic, M., Molmeret, M., Klose, K. E., and Abu Kwaik, Y. (2006). *Francisella tularensis* travels a novel, twisted road within macrophages. *Trends Microbiol.* 14, 37–44. doi: 10.1016/j.tim.2005.11.008

Sauer, J. D., Bachman, M. A., and Swanson, M. S. (2005). The phagosomal transporter A couples threonine acquisition to differentiation and replication of *Legionella pneumophila* in macrophages. *Proc. Natl. Acad. Sci. U.S.A.* 102, 9924–9929. doi: 10.1073/pnas.0502767102

Sjostedt, A. (2011). Special topic on *Francisella tularensis* and tularemia. *Front. Microbio.* 2:86. doi: 10.3389/fmicb.2011.00086

Steele, S., Radlinski, L., Taft-Benz, S., Brunton, J., and Kawula, T. H. (2016). Trogocytosis-associated cell to cell spread of intracellular bacterial pathogens. *Elife* 5:e10625. doi: 10.7554/elife.10625

Wehrly, T. D., Chong, A., Virtaneva, K., Sturdevant, D. E., Child, R., Edwards, J. A., et al. (2009). Intracellular biology and virulence determinants of *Francisella tularensis* revealed by transcriptional profiling inside macrophages. *Cell. Microbiol.* 11, 1128–1150. doi: 10.1111/j.1462-5822.2009.01316.x

Zhang, Y. J., and Rubin, E. J. (2013). Feast or famine: the host–pathogen battle over amino acids. *Cell. Microbiol.* 15, 1079–1087. doi: 10.1111/cmi.12140

Zuniga-Ripa, A., Barbier, T., Conde-Alvarez, R., Martinez-Gomez, E., Palacios-Chaves, L., Gil-Ramirez, Y., et al. (2014). *Brucella abortus* depends on pyruvate phosphate dikinase and malic enzyme but not on Fbp and GlpX fructose-1,6-bisphosphatases for full virulence in laboratory models. *J. Bacteriol.* 196, 3045–3057. doi: 10.1128/JB.01663-14

Conflict of Interest Statement: The authors declare that the research was conducted in the absence of any commercial or financial relationships that could be construed as a potential conflict of interest.

BIBLIOGRAPHIE

A

Abd, H., Johansson, T., Golovliov, I., Sandstrom, G., and Forsman, M. (2003). Survival and Growth of Francisella tularensis in Acanthamoeba castellanii. Appl. Environ. Microbiol. *69*, 600–606.

Abu Kwaik, Y., and Bumann, D. (2015). Host Delivery of Favorite Meals for Intracellular Pathogens. PLOS Pathog. *11*, e1004866.

Akira, S., Uematsu, S., and Takeuchi, O. (2006). Pathogen Recognition and Innate Immunity. Cell *124*, 783–801.

Alkhuder, K., Meibom, K.L., Dubail, I., Dupuis, M., and Charbit, A. (2009). Glutathione Provides a Source of Cysteine Essential for Intracellular Multiplication of Francisella tularensis. PLoS Pathog. *5*, e1000284.

Al-Quadan, T., Price, C.T., and Kwaik, Y.A. (2012). Exploitation of evolutionarily conserved amoeba and mammalian processes by Legionella. Trends Microbiol. *20*, 299–306.

Ancuta, P., Pedron, T., Girard, R., Sandström, G., and Chaby, R. (1996). Inability of the Francisella tularensis lipopolysaccharide to mimic or to antagonize the induction of cell activation by endotoxins. Infect. Immun. *64*, 2041–2046.

Andersson, J.O., and Andersson, S.G. Insights into the evolutionary process of genome degradation. 8.

Anthony, L.D., Burke, R.D., and Nano, F.E. (1991). Growth of Francisella spp. in rodent macrophages. Infect. Immun. *59*, 3291–3296.

Arnoult, D., Soares, F., Tattoli, I., and Girardin, S.E. (2011). Mitochondria in innate immunity. EMBO Rep. *12*, 901–910.

Asare, R., and Kwaik, Y.A. (2010). Molecular Complexity Orchestrates Modulation of Phagosome Biogenesis and Escape to the Cytosol of macrophages by Francisella tularensis. Environ. Microbiol. *12*, 2559–2586.

Ashida, H., Mimuro, H., Ogawa, M., Kobayashi, T., Sanada, T., Kim, M., and Sasakawa, C. (2011). Cell death and infection: A double-edged sword for host and pathogen survival. J. Cell Biol. *195*, 931–942.

Assari, T. (2006). Chronic Granulomatous Disease; fundamental stages in our understanding of CGD. Med. Immunol. *5*, 4.

B

Balagopal, A., MacFarlane, A.S., Mohapatra, N., Soni, S., Gunn, J.S., and Schlesinger, L.S. (2006). Characterization of the Receptor-Ligand Pathways Important for Entry and Survival of Francisella tularensis in Human Macrophages. Infect. Immun. *74*, 5114–5125.

Banga, S., Gao, P., Shen, X., Fiscus, V., Zong, W.-X., Chen, L., and Luo, Z.-Q. (2007). Legionella pneumophila inhibits macrophage apoptosis by targeting pro-death members of the Bcl2 protein family. Proc. Natl. Acad. Sci. U. S. A. *104*, 5121–5126.

Barel, M., Hovanessian, A.G., Meibom, K., Briand, J.-P., Dupuis, M., and Charbit, A. (2008). A novel receptor – ligand pathway for entry of Francisella tularensis in monocyte-like THP-1 cells: interaction between surface nucleolin and bacterial elongation factor Tu. BMC Microbiol. *8*, 145.

Bargen, K. von, Gorvel, J.-P., and Salcedo, S.P. (2011). Internal affairs: investigating the

Brucella intracellular lifestyle. FEMS Microbiol. Rev. *36*, 533–562.
Barker, J.R., and Klose, K.E. (2007). Molecular and Genetic Basis of Pathogenesis in Francisella Tularensis. Ann. N. Y. Acad. Sci. *1105*, 138–159.
Baron, G.S., and Nano, F.E. (1998). MglA and MglB are required for the intramacrophage growth of Francisella novicida. Mol. Microbiol. *29*, 247–259.
Basler, M., Pilhofer, M., Henderson, G.P., Jensen, G.J., and Mekalanos, J.J. (2012). Type VI secretion requires a dynamic contractile phage tail-like structure. Nature *483*, 182–186.
Bauckman, K.A., Owusu-Boaitey, N., and Mysorekar, I.U. (2015). Selective Autophagy: Xenophagy. Methods San Diego Calif *75*, 120–127.
Beckstrom-Sternberg, S.M., Auerbach, R.K., Godbole, S., Pearson, J.V., Beckstrom-Sternberg, J.S., Deng, Z., Munk, C., Kubota, K., Zhou, Y., Bruce, D., et al. (2007). Complete Genomic Characterization of a Pathogenic A.II Strain of Francisella tularensis Subspecies tularensis. PLoS ONE *2*, e947.
Bell, B.L., Mohapatra, N.P., and Gunn, J.S. (2010). Regulation of Virulence Gene Transcripts by the Francisella novicida Orphan Response Regulator PmrA: Role of Phosphorylation and Evidence of MglA/SspA Interaction. Infect. Immun. *78*, 2189–2198.
Bergstrom, S., Robbins, K., Koomey, J.M., and Swanson, J. (1986). Piliation control mechanisms in Neisseria gonorrhoeae. Proc. Natl. Acad. Sci. *83*, 3890–3894.
Bethani, I., Lang, T., Geumann, U., Sieber, J.J., Jahn, R., and Rizzoli, S.O. (2007). The specificity of SNARE pairing in biological membranes is mediated by both proof-reading and spatial segregation. EMBO J. *26*, 3981–3992.
Borgeaud, S., Metzger, L.C., Scrignari, T., and Blokesch, M. (2015). The type VI secretion system of Vibrio cholerae fosters horizontal gene transfer. Science *347*, 63–67.
Bosio, C.M., Bielefeldt-Ohmann, H., and Belisle, J.T. (2007). Active Suppression of the Pulmonary Immune Response by Francisella tularensis Schu4. J. Immunol. *178*, 4538–4547.
Brissac, T., Ziveri, J., Ramond, E., Tros, F., Kock, S., Dupuis, M., Brillet, M., Barel, M., Peyriga, L., Cahoreau, E., et al. (2015). Gluconeogenesis, an essential metabolic pathway for pathogenic *F rancisella*: Gluconeogenesis in *Francisella* virulence. Mol. Microbiol. *98*, 518–534.
Brissac, T., Ziveri, J., Ramond, E., Tros, F., Kock, S., Dupuis, M., Brillet, M., Barel, M., Peyriga, L., Cahoreau, E., et al. Gluconeogenesis, an essential metabolic pathway for pathogenic Francisella. Mol. Microbiol. *98*, 518–534.
Brodmann, M., Dreier, R.F., Broz, P., and Basler, M. (2017). Francisella requires dynamic type VI secretion system and ClpB to deliver effectors for phagosomal escape. Nat. Commun. *8*.
Bröms, J.E., Sjöstedt, A., and Lavander, M. (2010a). The Role of the Francisella Tularensis Pathogenicity Island in Type VI Secretion, Intracellular Survival, and Modulation of Host Cell Signaling. Front. Microbiol. *1*.
Bröms, J.E., Sjöstedt, A., and Lavander, M. (2010b). The Role of the Francisella Tularensis Pathogenicity Island in Type VI Secretion, Intracellular Survival, and Modulation of Host Cell Signaling. Front. Microbiol. *1*.
Bröms, J.E., Meyer, L., Sun, K., Lavander, M., and Sjöstedt, A. (2012). Unique Substrates Secreted by the Type VI Secretion System of Francisella tularensis during Intramacrophage Infection. PLOS ONE *7*, e50473.
Brotcke, A., Weiss, D.S., Kim, C.C., Chain, P., Malfatti, S., Garcia, E., and Monack, D.M. (2006). Identification of MglA-Regulated Genes Reveals Novel Virulence Factors in Francisella tularensis. Infect. Immun. *74*, 6642–6655.
de Bruin, O.M., Duplantis, B.N., Ludu, J.S., Hare, R.F., Nix, E.B., Schmerk, C.L., Robb, C.S.,

Boraston, A.B., Hueffer, K., and Nano, F.E. (2011). The biochemical properties of the Francisella pathogenicity island (FPI)-encoded proteins IglA, IglB, IglC, PdpB and DotU suggest roles in type VI secretion. Microbiology *157*, 3483–3491.
Brzostek, A., Pawelczyk, J., Rumijowska-Galewicz, A., Dziadek, B., and Dziadek, J. (2009). Mycobacterium tuberculosis Is Able To Accumulate and Utilize Cholesterol. J. Bacteriol. *191*, 6584–6591.
Buchan, B.W., McCaffrey, R.L., Lindemann, S.R., Allen, L.-A.H., and Jones, B.D. (2009). Identification of migR, a Regulatory Element of the Francisella tularensis Live Vaccine Strain iglABCD Virulence Operon Required for Normal Replication and Trafficking in Macrophages. Infect. Immun. *77*, 2517–2529.

C

Casadevall, A. (2008a). Evolution of intracellular pathogens. Annu. Rev. Microbiol. *62*, 19–33.
Casadevall, A. (2008b). Evolution of Intracellular Pathogens. Annu. Rev. Microbiol. *62*, 19–33.
Cassat, J.E., and Skaar, E.P. (2013). Iron in Infection and Immunity. Cell Host Microbe *13*, 509–519.
Cazalet, C., Rusniok, C., Brüggemann, H., Zidane, N., Magnier, A., Ma, L., Tichit, M., Jarraud, S., Bouchier, C., Vandenesch, F., et al. (2004). Evidence in the *Legionella pneumophila* genome for exploitation of host cell functions and high genome plasticity. Nat. Genet. *36*, 1165.
Celli, J. (2015). The changing nature of the Brucella-Containing Vacuole. Cell. Microbiol. *17*, 951–958.
Celli, J., and Zahrt, T.C. (2013). Mechanisms of Francisella tularensis Intracellular Pathogenesis. Cold Spring Harb. Perspect. Med. *3*, a010314–a010314.
Cellier, M.F., Courville, P., and Campion, C. (2007). Nramp1 phagocyte intracellular metal withdrawal defense. Microbes Infect. *9*, 1662–1670.
Chamaillard, M., Hashimoto, M., Horie, Y., Masumoto, J., Qiu, S., Saab, L., Ogura, Y., Kawasaki, A., Fukase, K., Kusumoto, S., et al. (2003). An essential role for NOD1 in host recognition of bacterial peptidoglycan containing diaminopimelic acid. Nat. Immunol. *4*, 702–707.
Chang, Y.-W., Rettberg, L.A., Ortega, D.R., and Jensen, G.J. (2017). In vivo structures of an intact type VI secretion system revealed by electron cryotomography. EMBO Rep. *18*, 1090–1099.
Charity, J.C., Costante-Hamm, M.M., Balon, E.L., Boyd, D.H., Rubin, E.J., and Dove, S.L. (2007). Twin RNA Polymerase–Associated Proteins Control Virulence Gene Expression in Francisella tularensis. PLoS Pathog. *3*.
Checroun, C., Wehrly, T.D., Fischer, E.R., Hayes, S.F., and Celli, J. (2006). Autophagy-mediated reentry of Francisella tularensis into the endocytic compartment after cytoplasmic replication. Proc. Natl. Acad. Sci. U. S. A. *103*, 14578–14583.
Chong, A., Wehrly, T.D., Nair, V., Fischer, E.R., Barker, J.R., Klose, K.E., and Celli, J. (2008). The Early Phagosomal Stage of Francisella tularensis Determines Optimal Phagosomal Escape and Francisella Pathogenicity Island Protein Expression. Infect. Immun. *76*, 5488–5499.
Choy, A., Dancourt, J., Mugo, B., O'Connor, T.J., Isberg, R.R., Melia, T.J., and Roy, C.R. (2012). The Legionella Effector RavZ Inhibits Host Autophagy Through Irreversible Atg8 Deconjugation. Science *338*, 1072–1076.
Christoforidis, S., Miaczynska, M., Ashman, K., Wilm, M., Zhao, L., Yip, S.-C., Waterfield, M.D., Backer, J.M., and Zerial, M. (1999). Phosphatidylinositol-3-OH kinases are Rab5 effectors. Nat. Cell Biol. *1*, 249–252.

Christopher, Cieslak, Pavlin, and Eitzen (1997). Ovid: Biological Warfare: A Historical Perspective.
Clemens, D.L., and Horwitz, M.A. (2007). Uptake and Intracellular Fate of Francisella tularensis in Human Macrophages. Ann. N. Y. Acad. Sci. *1105*, 160–186.
Clemens, D.L., Lee, B.-Y., and Horwitz, M.A. (2004). Virulent and Avirulent Strains of Francisella tularensis Prevent Acidification and Maturation of Their Phagosomes and Escape into the Cytoplasm in Human Macrophages. Infect. Immun. *72*, 3204–3217.
Clemens, D.L., Lee, B.-Y., and Horwitz, M.A. (2005). Francisella tularensis Enters Macrophages via a Novel Process Involving Pseudopod Loops. Infect. Immun. *73*, 5892–5902.
Clemens, D.L., Ge, P., Lee, B.-Y., Horwitz, M.A., and Zhou, Z.H. (2015). Atomic Structure of T6SS Reveals Interlaced Array Essential to Function. Cell *160*, 940–951.
Clemens, D.L., Lee, B.-Y., and Horwitz, M.A. (2018). The Francisella Type VI Secretion System. Front. Cell. Infect. Microbiol. *8*.
Colquhoun, D.J., and Duodu, S. (2011). Francisella infections in farmed and wild aquatic organisms. Vet. Res. *42*, 47.
Coolen, J.P.M., Sjödin, A., Maraha, B., Hajer, G.F., Forsman, M., Verspui, E., Frenay, H.M.E., Notermans, D.W., Vries, M.C. de, Reubsaet, F.A.G., et al. (2013). Draft genome sequence of Francisella tularensis subsp. holarctica BD11-00177. Stand. Genomic Sci. *8*, 539.
Cossart, P., and Sansonetti, P.J. (2004). Bacterial Invasion: The Paradigms of Enteroinvasive Pathogens. Science *304*, 242–248.
Cossart, P., Vicente, M.F., Mengaud, J., Baquero, F., Perez-Diaz, J.C., and Berche, P. (1989). Listeriolysin O is essential for virulence of Listeria monocytogenes: direct evidence obtained by gene complementation. Infect. Immun. *57*, 3629–3636.
Cremer, T.J., Amer, A., Tridandapani, S., and Butchar, J.P. (2009). Francisella tularensis regulates autophagy-related host cell signaling pathways. Autophagy *5*, 125–128.
Cuthbert, B.J., Ross, W., Rohlfing, A.E., Dove, S.L., Gourse, R.L., Brennan, R.G., and Schumacher, M.A. (2017). Dissection of the molecular circuitry controlling virulence in Francisella tularensis. Genes Dev. *31*, 1549–1560.

D

Dennis, D.T., Inglesby, T.V., Henderson, D.A., Bartlett, J.G., Ascher, M.S., Eitzen, E., Fine, A.D., Friedlander, A.M., Hauer, J., Layton, M., et al. (2001). Tularemia as a Biological Weapon: Medical and Public Health Management. JAMA *285*, 2763.
Deussing, J., Roth, W., Saftig, P., Peters, C., Ploegh, H.L., and Villadangos, J.A. (1998). Cathepsins B and D are dispensable for major histocompatibility complex class II-mediated antigen presentation. Proc. Natl. Acad. Sci. U. S. A. *95*, 4516–4521.
van der Does, A.M., Beekhuizen, H., Ravensbergen, B., Vos, T., Ottenhoff, T.H.M., van Dissel, J.T., Drijfhout, J.W., Hiemstra, P.S., and Nibbering, P.H. (2010). LL-37 Directs Macrophage Differentiation toward Macrophages with a Proinflammatory Signature. J. Immunol. *185*, 1442–1449.
Dunn, W.A.J. (1990). Studies on the mechanisms of autophagy: formation of the autophagic vacuole. J. Cell Biol. *110*, 1923–1933.
Durand, E., Nguyen, V.S., Zoued, A., Logger, L., Péhau-Arnaudet, G., Aschtgen, M.-S., Spinelli, S., Desmyter, A., Bardiaux, B., Dujeancourt, A., et al. (2015). Biogenesis and structure of a type VI secretion membrane core complex. Nature *523*, 555–560.

E

Eisenreich, W., Dandekar, T., Heesemann, J., and Goebel, W. (2010). Carbon metabolism of intracellular bacterial pathogens and possible links to virulence. Nat. Rev. Microbiol. *8*, 401–412.

Eisenreich, W., Rudel, T., Heesemann, J., and Goebel, W. (2017). To Eat and to Be Eaten: Mutual Metabolic Adaptations of Immune Cells and Intracellular Bacterial Pathogens upon Infection. Front. Cell. Infect. Microbiol. *7*.

Engel, J., and Eran, Y. (2011). Subversion of Mucosal Barrier Polarity by Pseudomonas Aeruginosa. Front. Microbiol. *2*.

Escoll, P., and Buchrieser, C. (2018). Metabolic reprogramming of host cells upon bacterial infection: Why shift to a *Warburg-like* metabolism? FEBS J.

Eshraghi, A., Kim, J., Walls, A.C., Ledvina, H.E., Miller, C.N., Ramsey, K.M., Whitney, J.C., Radey, M.C., Peterson, S.B., Ruhland, B.R., et al. (2016). Secreted Effectors Encoded within and outside of the Francisella Pathogenicity Island Promote Intramacrophage Growth. Cell Host Microbe *20*, 573–583.

F

Felisberto-Rodrigues, C., Durand, E., Aschtgen, M.-S., Blangy, S., Ortiz-Lombardia, M., Douzi, B., Cambillau, C., and Cascales, E. (2011). Towards a Structural Comprehension of Bacterial Type VI Secretion Systems: Characterization of the TssJ-TssM Complex of an Escherichia coli Pathovar. PLoS Pathog. *7*.

Fonseca, M.V., and Swanson, M.S. (2014). Nutrient salvaging and metabolism by the intracellular pathogen Legionella pneumophila. Front. Cell. Infect. Microbiol. *4*.

Forbes, J.R. (2003). Iron, manganese, and cobalt transport by Nramp1 (Slc11a1) and Nramp2 (Slc11a2) expressed at the plasma membrane. Blood *102*, 1884–1892.

Forsberg, A., and Guina, T. (2007). Type II secretion and type IV pili of Francisella. Ann. N. Y. Acad. Sci. *1105*, 187–201.

Forsman, M., Sandström, G., and Sjöstedt, A. (1994). Analysis of 16S ribosomal DNA sequences of Francisella strains and utilization for determination of the phylogeny of the genus and for identification of strains by PCR. Int. J. Syst. Bacteriol. *44*, 38–46.

G

Geier, H., and Celli, J. (2011). Phagocytic Receptors Dictate Phagosomal Escape and Intracellular Proliferation of Francisella tularensis ▿. Infect. Immun. *79*, 2204–2214.

Gesbert, G., Ramond, E., Rigard, M., Frapy, E., Dupuis, M., Dubail, I., Barel, M., Henry, T., Meibom, K., and Charbit, A. (2014). Asparagine assimilation is critical for intracellular replication and dissemination of Francisella. Cell. Microbiol. *16*, 434–449.

Girardin, S.E., Boneca, I.G., Carneiro, L.A.M., Antignac, A., Jéhanno, M., Viala, J., Tedin, K., Taha, M.-K., Labigne, A., Zähringer, U., et al. (2003a). Nod1 detects a unique muropeptide from gram-negative bacterial peptidoglycan. Science *300*, 1584–1587.

Girardin, S.E., Boneca, I.G., Viala, J., Chamaillard, M., Labigne, A., Thomas, G., Philpott, D.J., and Sansonetti, P.J. (2003b). Nod2 Is a General Sensor of Peptidoglycan through Muramyl Dipeptide (MDP) Detection. J. Biol. Chem. *278*, 8869–8872.

Gouzy, A., Larrouy-Maumus, G., Wu, T.-D., Peixoto, A., Levillain, F., Lugo-Villarino, G., Gerquin-Kern, J.-L., de Carvalho, L.P.S., Poquet, Y., and Neyrolles, O. (2013). Mycobacterium

tuberculosis nitrogen assimilation and host colonization require aspartate. Nat. Chem. Biol. *9*.
Gouzy, A., Larrouy-Maumus, G., Bottai, D., Levillain, F., Dumas, A., Wallach, J.B., Caire-Brandli, I., de Chastellier, C., Wu, T.-D., Poincloux, R., et al. (2014). Mycobacterium tuberculosis Exploits Asparagine to Assimilate Nitrogen and Resist Acid Stress during Infection. PLoS Pathog. *10*, e1003928.
Grubmüller, S., Schauer, K., Goebel, W., Fuchs, T.M., and Eisenreich, W. (2014). Analysis of carbon substrates used by Listeria monocytogenes during growth in J774A.1 macrophages suggests a bipartite intracellular metabolism. Front. Cell. Infect. Microbiol. *4*.
Guaní-Guerra, E., Santos-Mendoza, T., Lugo-Reyes, S.O., and Terán, L.M. (2010). Antimicrobial peptides: General overview and clinical implications in human health and disease. Clin. Immunol. *135*, 1–11.

H

Hajjar, A.M., Harvey, M.D., Shaffer, S.A., Goodlett, D.R., Sjöstedt, A., Edebro, H., Forsman, M., Byström, M., Pelletier, M., Wilson, C.B., et al. (2006). Lack of In Vitro and In Vivo Recognition of Francisella tularensis Subspecies Lipopolysaccharide by Toll-Like Receptors. Infect. Immun. *74*, 6730–6738.
Hamon, M.A., Ribet, D., Stavru, F., and Cossart, P. (2012). Listeriolysin O: the Swiss army knife of Listeria. Trends Microbiol. *20*, 360–368.
Hancock, R.E.., and Diamond, G. (2000). The role of cationic antimicrobial peptides in innate host defences. Trends Microbiol. *8*, 402–410.
Hansson, C., and Ingvarsson, T. (2002). Two cases of tularaemia after an orienteering contest on the non-endemic Island of Bornholm. Scand. J. Infect. Dis. *34*, 76.
He, C., Bartholomew, C.R., Zhou, W., and Klionsky, D.J. (2009). Assaying autophagic activity in transgenic GFP-Lc3 and GFP-Gabarap zebrafish embryos. Autophagy *5*, 520–526.
Henderson, B. (2014). An overview of protein moonlighting in bacterial infection. Biochem. Soc. Trans. *42*, 1720–1727.
Henry, T., Brotcke, A., Weiss, D.S., Thompson, L.J., and Monack, D.M. (2007). Type I interferon signaling is required for activation of the inflammasome during Francisella infection. J. Exp. Med. *204*, 987–994.
Hersh, D., Monack, D.M., Smith, M.R., Ghori, N., Falkow, S., and Zychlinsky, A. (1999). The Salmonella invasin SipB induces macrophage apoptosis by binding to caspase-1. Proc. Natl. Acad. Sci. U. S. A. *96*, 2396–2401.
Hilbi, H. (2006). Modulation of phosphoinositide metabolism by pathogenic bacteria. Cell. Microbiol. *8*, 1697–1706.
Hollis, D.G., Weaver, R.E., Steigerwalt, A.G., Wenger, J.D., Moss, C.W., and Brenner, D.J. (1989). Francisella philomiragia comb. nov. (formerly Yersinia philomiragia) and Francisella tularensis biogroup novicida (formerly Francisella novicida) associated with human disease. J. Clin. Microbiol. *27*, 1601–1608.
Hood, A.M. (1977). Virulence factors of Francisella tularensis. J. Hyg. (Lond.) *79*, 47–60.
Hood, M.I., and Skaar, E.P. (2012). Nutritional immunity: transition metals at the pathogen-host interface. Nat. Rev. Microbiol. *10*.
Hovel-Miner, G., Faucher, S.P., Charpentier, X., and Shuman, H.A. (2010). ArgR-Regulated Genes Are Derepressed in the Legionella-Containing Vacuole. J. Bacteriol. *192*, 4504–4516.

I

Inohara, N., Ogura, Y., Fontalba, A., Gutierrez, O., Pons, F., Crespo, J., Fukase, K., Inamura, S., Kusumoto, S., Hashimoto, M., et al. (2003). Host Recognition of Bacterial Muramyl Dipeptide Mediated through NOD2: IMPLICATIONS FOR CROHN'S DISEASE. J. Biol. Chem. *278*, 5509–5512.

J

Jabado, N., Jankowski, A., Dougaparsad, S., Picard, V., Grinstein, S., and Gros, P. (2000). Natural Resistance to Intracellular Infections. J. Exp. Med. *192*, 1237–1248.

Jones, C.M., and Niederweis, M. (2011). Mycobacterium tuberculosis Can Utilize Heme as an Iron Source. J. Bacteriol. *193*, 1767–1770.

Juttukonda, L.J., and Skaar, E.P. (2015). Manganese Homeostasis and Utilization in Pathogenic Bacteria. Mol. Microbiol. *97*, 216–228.

K

Kingry, L.C., and Petersen, J.M. (2014). Comparative review of Francisella tularensis and Francisella novicida. Front. Cell. Infect. Microbiol. *4*.

Kroken, A.R., Chen, C.K., Evans, D.J., Yahr, T.L., and Fleiszig, S.M.J. (2018). The Impact of ExoS on Pseudomonas aeruginosa Internalization by Epithelial Cells Is Independent of fleQ and Correlates with Bistability of Type Three Secretion System Gene Expression. *9*, 21.

Kudryashev, M., Wang, R.Y.-R., Brackmann, M., Scherer, S., Maier, T., Baker, D., DiMaio, F., Stahlberg, H., Egelman, E.H., and Basler, M. (2015). Structure of the Type VI secretion system contractile sheath. Cell *160*, 952–962.

L

Laguna, R.K., Creasey, E.A., Li, Z., Valtz, N., and Isberg, R.R. (2006). A Legionella pneumophila-translocated substrate that is required for growth within macrophages and protection from host cell death. Proc. Natl. Acad. Sci. U. S. A. *103*, 18745–18750.

Lai, X.-H., and Sjöstedt, A. (2003). Delineation of the Molecular Mechanisms of Francisella tularensis-Induced Apoptosis in Murine Macrophages. Infect. Immun. *71*, 4642–4646.

Lai, X.-H., Golovliov, I., and Sjöstedt, A. (2004). Expression of IglC is necessary for intracellular growth and induction of apoptosis in murine macrophages by Francisella tularensis. Microb. Pathog. *37*, 225–230.

Lamason, R.L., and Welch, M.D. (2017). Actin-based motility and cell-to-cell spread of bacterial pathogens. Curr. Opin. Microbiol. *35*, 48–57.

Larsson, P., Oyston, P.C.F., Chain, P., Chu, M.C., Duffield, M., Fuxelius, H.-H., Garcia, E., Hälltorp, G., Johansson, D., Isherwood, K.E., et al. (2005). The complete genome sequence of Francisella tularensis, the causative agent of tularemia. Nat. Genet. *37*, 153–159.

Larsson, P., Elfsmark, D., Svensson, K., Wikström, P., Forsman, M., Brettin, T., Keim, P., and Johansson, A. (2009). Molecular Evolutionary Consequences of Niche Restriction in Francisella tularensis, a Facultative Intracellular Pathogen. PLoS Pathog. *5*.

Lauriano, C.M., Barker, J.R., Yoon, S.-S., Nano, F.E., Arulanandam, B.P., Hassett, D.J., and Klose, K.E. (2004). MglA regulates transcription of virulence factors necessary for Francisella tularensis intraamoebae and intramacrophage survival. Proc. Natl. Acad. Sci. U. S. A. *101*, 4246–4249.

Law, H.T., Lin, A.E.-J., Kim, Y., Quach, B., Nano, F.E., and Guttman, J.A. (2011). Francisella

tularensis Uses Cholesterol and Clathrin-Based Endocytic Mechanisms to Invade Hepatocytes. Sci. Rep. *1*.
Leon-Sicairos, N., Reyes-Cortes, R., Guadrón-Llanos, A.M., Madueña-Molina, J., Leon-Sicairos, C., and Canizalez-Román, A. (2015). Strategies of Intracellular Pathogens for Obtaining Iron from the Environment. BioMed Res. Int. *2015*, 1–17.
Lindemann, S.R., Peng, K., Long, M.E., Hunt, J.R., Apicella, M.A., Monack, D.M., Allen, L.-A.H., and Jones, B.D. (2011). *Francisella tularensis* Schu S4 O-Antigen and Capsule Biosynthesis Gene Mutants Induce Early Cell Death in Human Macrophages. Infect. Immun. *79*, 581–594.
Lindgren, H., Shen, H., Zingmark, C., Golovliov, I., Conlan, W., and Sjöstedt, A. (2007). Resistance of Francisella tularensis Strains against Reactive Nitrogen and Oxygen Species with Special Reference to the Role of KatG. Infect. Immun. *75*, 1303–1309.
Lindgren, M., Bröms, J.E., Meyer, L., Golovliov, I., and Sjöstedt, A. (2013). The Francisella tularensis LVS ΔpdpCmutant exhibits a unique phenotype during intracellular infection. BMC Microbiol. *13*, 20.
Lo, K.Y.-S., Chua, M.D., Abdulla, S., Law, H.T., and Guttman, J.A. (2013). Examination of in vitro epithelial cell lines as models for Francisella tularensis non-phagocytic infections. J. Microbiol. Methods *93*, 153–160.
Lovewell, R.R., Sassetti, C.M., and VanderVen, B.C. (2016). Chewing the fat: lipid metabolism and homeostasis during M. tuberculosis infection. Curr. Opin. Microbiol. *29*, 30–36.
Ludu, J.S., Nix, E.B., Duplantis, B.N., Bruin, O.M.D., Gallagher, L.A., Hawley, L.M., and Nano, F.E. (2007). Genetic elements for selection, deletion mutagenesis and complementation in Francisella spp. FEMS Microbiol. Lett. *278*, 86–93.

M

Ma, A.T., McAuley, S., Pukatzki, S., and Mekalanos, J.J. (2009). Translocation of a Vibrio cholerae Type VI Secretion Effector Requires Bacterial Endocytosis by Host Cells. Cell Host Microbe *5*, 234–243.
MacIntyre, D.L., Miyata, S.T., Kitaoka, M., and Pukatzki, S. (2010). The Vibrio cholerae type VI secretion system displays antimicrobial properties. Proc. Natl. Acad. Sci. U. S. A. *107*, 19520–19524.
Mailloux, R.J., Singh, R., Brewer, G., Auger, C., Lemire, J., and Appanna, V.D. (2009). α-Ketoglutarate Dehydrogenase and Glutamate Dehydrogenase Work in Tandem To Modulate the Antioxidant α-Ketoglutarate during Oxidative Stress in Pseudomonas fluorescens. J. Bacteriol. *191*, 3804–3810.
Malik, A., and Kanneganti, T.-D. (2017). Inflammasome activation and assembly at a glance. J Cell Sci *130*, 3955–3963.
Manske, C., Schell, U., and Hilbi, H. (2016). Metabolism of myo-inositol by Legionella pneumophila promotes infection of amoeba and macrophages. Appl. Environ. Microbiol. AEM.01018-16.
Mariathasan, S., Newton, K., Monack, D.M., Vucic, D., French, D.M., Lee, W.P., Roose-Girma, M., Erickson, S., and Dixit, V.M. (2004). Differential activation of the inflammasome by caspase-1 adaptors ASC and Ipaf. Nature *430*, 213–218.
Mariathasan, S., Weiss, D.S., Dixit, V.M., and Monack, D.M. (2005). Innate immunity against Francisella tularensis is dependent on the ASC/caspase-1 axis. J. Exp. Med. *202*, 1043–1049.
Martínez-Cano, D.J., Reyes-Prieto, M., Martínez-Romero, E., Partida-Martínez, L.P., Latorre, A., Moya, A., and Delaye, L. (2015). Evolution of small prokaryotic genomes. Front. Microbiol. *5*.

Maxfield, F.R., and Yamashiro, D.J. (1987). Endosome acidification and the pathways of receptor-mediated endocytosis. Adv. Exp. Med. Biol. *225*, 189–198.
McBride, H.M., Rybin, V., Murphy, C., Giner, A., Teasdale, R., and Zerial, M. (1999). Oligomeric Complexes Link Rab5 Effectors with NSF and Drive Membrane Fusion via Interactions between EEA1 and Syntaxin 13. Cell *98*, 377–386.
McKinney, J.D., oz-ElÂõas, E.J.M., Miczak, A., Chen, B., Chan, W.-T., Swenson, D., Sacchettini, J.C., and Jacobs, W.R. (2000). Persistence of Mycobacterium tuberculosis in macrophages and mice requires the glyoxylate shunt enzyme isocitrate lyase. *406*, 4.
Meibom, K.L., and Charbit, A. (2010). Francisella Tularensis Metabolism and its Relation to Virulence. Front. Microbiol. *1*.
Meibom, K.L., Forslund, A.-L., Kuoppa, K., Alkhuder, K., Dubail, I., Dupuis, M., Forsberg, Å., and Charbit, A. (2009). Hfq, a Novel Pleiotropic Regulator of Virulence-Associated Genes in Francisella tularensis. Infect. Immun. *77*, 1866–1880.
Melillo, A.A., Bakshi, C.S., and Melendez, J.A. (2010). Francisella tularensis Antioxidants Harness Reactive Oxygen Species to Restrict Macrophage Signaling and Cytokine Production. J. Biol. Chem. *285*, 27553–27560.
Mellouk, N., Weiner, A., Aulner, N., Schmitt, C., Elbaum, M., Shorte, S.L., Danckaert, A., and Enninga, J. (2014). Shigella Subverts the Host Recycling Compartment to Rupture Its Vacuole. Cell Host Microbe *16*, 517–530.
Méndez-Samperio, P. (2008). Role of antimicrobial peptides in host defense against mycobacterial infections. Peptides *29*, 1836–1841.
Merhej, V., Angelakis, E., Socolovschi, C., and Raoult, D. (2014). Genotyping, evolution and epidemiological findings of Rickettsia species. Infect. Genet. Evol. J. Mol. Epidemiol. Evol. Genet. Infect. Dis. *25*, 122–137.
Miao, E.A., Leaf, I.A., Treuting, P.M., Mao, D.P., Dors, M., Sarkar, A., Warren, S.E., Wewers, M.D., and Aderem, A. (2010). Caspase-1-induced pyroptosis is an innate immune effector mechanism against intracellular bacteria. Nat. Immunol. *11*, 1136–1142.
Miller, S.I., Ernst, R.K., and Bader, M.W. (2005). LPS, TLR4 and infectious disease diversity. Nat. Rev. Microbiol. *3*, 36–46.
Mougous, J.D., Gifford, C.A., Ramsdell, T.L., and Mekalanos, J.J. (2007). Threonine phosphorylation post-translationally regulates protein secretion in *Pseudomonas aeruginosa*. Nat. Cell Biol. *9*, 797–803.

N

Nano, F.E., and Schmerk, C. (2007). The Francisella Pathogenicity Island. Ann. N. Y. Acad. Sci. *1105*, 122–137.
Nano, F.E., Zhang, N., Cowley, S.C., Klose, K.E., Cheung, K.K.M., Roberts, M.J., Ludu, J.S., Letendre, G.W., Meierovics, A.I., Stephens, G., et al. (2004). A Francisella tularensis Pathogenicity Island Required for Intramacrophage Growth. J. Bacteriol. *186*, 6430–6436.
Nazarov, S., Schneider, J.P., Brackmann, M., Goldie, K.N., Stahlberg, H., and Basler, M. (2018). Cryo-EM reconstruction of Type VI secretion system baseplate and sheath distal end. EMBO J. *37*, e97103.
Niu, H., Xiong, Q., Yamamoto, A., Hayashi-Nishino, M., and Rikihisa, Y. (2012). Autophagosomes induced by a bacterial Beclin 1 binding protein facilitate obligatory intracellular infection. Proc. Natl. Acad. Sci. U. S. A. *109*, 20800–20807.

Nunes, P., Demaurex, N., and Dinauer, M.C. Regulation of the NADPH Oxidase and Associated Ion Fluxes During Phagocytosis. Traffic *14*, 1118–1131.

O

Ohya, T., Miaczynska, M., Coskun, Ü., Lommer, B., Runge, A., Drechsel, D., Kalaidzidis, Y., and Zerial, M. (2009). Reconstitution of Rab- and SNARE-dependent membrane fusion by synthetic endosomes. Nature *459*, 1091–1097.
Okan, N.A., and Kasper, D.L. (2013). The atypical lipopolysaccharide of Francisella. Carbohydr. Res. *378*, 79–83.
Olsufjev, N.G. (1970). Taxonomy and characteristic of the genus Francisella Dorofeev, 1947. J. Hyg. Epidemiol. Microbiol. Immunol. *14*, 67–74.
Osborne, S.E., Sit, B., Shaker, A., Currie, E., Tan, J.M.J., Rijn, J. van, Higgins, D.E., and Brumell, J.H. Type I interferon promotes cell-to-cell spread of Listeria monocytogenes. Cell. Microbiol. *19*, e12660.
Ottem, K.F., Nylund, A., Karlsbakk, E., Friis-Møller, A., and Kamaishi, T. (2009). Elevation of Francisella philomiragia subsp. noatunensis Mikalsen et al. (2007) to Francisella noatunensis comb. nov. [syn. Francisella piscicida Ottem et al. (2008) syn. nov.] and characterization of Francisella noatunensis subsp. orientalis subsp. nov., two important fish pathogens. J. Appl. Microbiol. *106*, 1231–1243.
Owens, C.P., Chim, N., and Goulding, C.W. (2013). Insights on how the Mycobacterium tuberculosis heme uptake pathway can be used as a drug target. Future Med. Chem. *5*.
Oyston, P.C.F., Sjöstedt, A., and Titball, R.W. (2004). Tularaemia: bioterrorism defence renews interest in Francisella tularensis. Nat. Rev. Microbiol. *2*, 967–978.
Ozanic, M., Marecic, V., Abu Kwaik, Y., and Santic, M. (2015). The Divergent Intracellular Lifestyle of Francisella tularensis in Evolutionarily Distinct Host Cells. PLOS Pathog. *11*, e1005208.

P

Pandey, A.K., and Sassetti, C.M. (2008). Mycobacterial persistence requires the utilization of host cholesterol. Proc. Natl. Acad. Sci. U. S. A. *105*, 4376–4380.
Parsa, K.V.L., Ganesan, L.P., Rajaram, M.V.S., Gavrilin, M.A., Balagopal, A., Mohapatra, N.P., Wewers, M.D., Schlesinger, L.S., Gunn, J.S., and Tridandapani, S. (2006). Macrophage Pro-Inflammatory Response to Francisella novicida Infection Is Regulated by SHIP. PLoS Pathog. *2*.
Pechous, R.D., McCarthy, T.R., and Zahrt, T.C. (2009). Working toward the Future: Insights into Francisella tularensis Pathogenesis and Vaccine Development. Microbiol. Mol. Biol. Rev. *73*, 684–711.
Petersen, J.M., and Schriefer, M.E. (2005). Tularemia: emergence/re-emergence. Vet. Res. *36*, 455–467.
Petrosino, J.F., Xiang, Q., Karpathy, S.E., Jiang, H., Yerrapragada, S., Liu, Y., Gioia, J., Hemphill, L., Gonzalez, A., Raghavan, T.M., et al. (2006). Chromosome Rearrangement and Diversification of Francisella tularensis Revealed by the Type B (OSU18) Genome Sequence. J. Bacteriol. *188*, 6977–6985.
Pillay, C.S., Elliott, E., and Dennison, C. (2002). Endolysosomal proteolysis and its regulation. Biochem. J. *363*, 417.
Pitt, A., Mayorga, L.S., Stahl, P.D., and Schwartz, A.L. (1992). Alterations in the protein

composition of maturing phagosomes. J. Clin. Invest. *90*, 1978–1983.
Pizarro-Cerdá, J., Charbit, A., Enninga, J., Lafont, F., and Cossart, P. (2016). Manipulation of host membranes by the bacterial pathogens Listeria, Francisella, Shigella and Yersinia. Semin. Cell Dev. Biol. *60*, 155–167.
Popov, S.G., Villasmil, R., Bernardi, J., Grene, E., Cardwell, J., Wu, A., Alibek, D., Bailey, C., and Alibek, K. (2002). Lethal toxin of Bacillus anthracis causes apoptosis of macrophages. Biochem. Biophys. Res. Commun. *293*, 349–355.
Preston, J.A., and Dockrell, D.H. (2008). Virulence factors in pneumococcal respiratory pathogenesis. Future Microbiol. *3*, 205–221.
Price, C.T.D., Al-Quadan, T., Santic, M., Rosenshine, I., and Abu Kwaik, Y. (2011). Host proteasomal degradation generates amino acids essential for intracellular bacterial growth. Science *334*, 1553–1557.
Pukatzki, S., Ma, A.T., Sturtevant, D., Krastins, B., Sarracino, D., Nelson, W.C., Heidelberg, J.F., and Mekalanos, J.J. (2006). Identification of a conserved bacterial protein secretion system in Vibrio cholerae using the Dictyostelium host model system. Proc. Natl. Acad. Sci. U. S. A. *103*, 1528–1533.
Pukatzki, S., Ma, A.T., Revel, A.T., Sturtevant, D., and Mekalanos, J.J. (2007). Type VI secretion system translocates a phage tail spike-like protein into target cells where it cross-links actin. Proc. Natl. Acad. Sci. U. S. A. *104*, 15508–15513.

R

Raetz, C.R.H., Guan, Z., Ingram, B.O., Six, D.A., Song, F., Wang, X., and Zhao, J. (2009). Discovery of new biosynthetic pathways: the lipid A story. J. Lipid Res. *50*, S103–S108.
Rajaram, M.V.S., Butchar, J.P., Parsa, K.V.L., Cremer, T.J., Amer, A., Schlesinger, L.S., and Tridandapani, S. (2009). Akt and SHIP Modulate Francisella Escape from the Phagosome and Induction of the Fas-Mediated Death Pathway. PLOS ONE *4*, e7919.
Ramond, E., Gesbert, G., Rigard, M., Dairou, J., Dupuis, M., Dubail, I., Meibom, K., Henry, T., Barel, M., and Charbit, A. (2014). Glutamate Utilization Couples Oxidative Stress Defense and the Tricarboxylic Acid Cycle in Francisella Phagosomal Escape. PLoS Pathog. *10*, e1003893.
Ramond, E., Gesbert, G., Guerrera, I.C., Chhuon, C., Dupuis, M., Rigard, M., Henry, T., Barel, M., and Charbit, A. (2015). Importance of Host Cell Arginine Uptake in Francisella Phagosomal Escape and Ribosomal Protein Amounts. Mol. Cell. Proteomics MCP *14*, 870–881.
Randow, F., and Münz, C. (2012). Autophagy in the regulation of pathogen replication and adaptive immunity. Trends Immunol. *33*, 475–487.
Renesto, P., Ogata, H., Audic, S., Claverie, J.-M., and Raoult, D. (2005). Some lessons from *Rickettsia* genomics. FEMS Microbiol. Rev. *29*, 99–117.
Rigard, M., Bröms, J.E., Mosnier, A., Hologne, M., Martin, A., Lindgren, L., Punginelli, C., Lays, C., Walker, O., Charbit, A., et al. (2016). Francisella tularensis IglG Belongs to a Novel Family of PAAR-Like T6SS Proteins and Harbors a Unique N-terminal Extension Required for Virulence. PLOS Pathog. *12*, e1005821.
Rink, J., Ghigo, E., Kalaidzidis, Y., and Zerial, M. (2005). Rab Conversion as a Mechanism of Progression from Early to Late Endosomes. Cell *122*, 735–749.
Robinson, C.G., and Roy, C.R. Attachment and fusion of endoplasmic reticulum with vacuoles containing Legionella pneumophila. Cell. Microbiol. *8*, 793–805.
Rodriguez, G.M. (2006). Control of iron metabolism in Mycobacterium tuberculosis. Trends Microbiol. *14*, 320–327.

Rohmer, L., Fong, C., Abmayr, S., Wasnick, M., Larson Freeman, T., Radey, M., Guina, T., Svensson, K., Hayden, H.S., Jacobs, M., et al. (2007). Comparison of Francisella tularensis genomes reveals evolutionary events associated with the emergence of human pathogenic strains. Genome Biol. *8*, R102.
Rohmer, L., Hocquet, D., and Miller, S.I. (2011). Are pathogenic bacteria just looking for food? Metabolism and microbial pathogenesis. Trends Microbiol. *19*, 341–348.
Rollin, G., Tan, X., Tros, F., Dupuis, M., Nassif, X., Charbit, A., and Coureuil, M. (2017). Intracellular Survival of Staphylococcus aureus in Endothelial Cells: A Matter of Growth or Persistence. Front. Microbiol. *8*.
Rowe, H.M., and Huntley, J.F. (2015). From the Outside-In: The Francisella tularensis Envelope and Virulence. Front. Cell. Infect. Microbiol. *5*.
Rubinsztein, D.C., Codogno, P., and Levine, B. (2012). Autophagy modulation as a potential therapeutic target for diverse diseases. Nat. Rev. Drug Discov. *11*, 709–730.

S

Salomonsson, E.N., Forslund, A.-L., and Forsberg, Å. (2011). Type IV Pili in Francisella – A Virulence Trait in an Intracellular Pathogen. Front. Microbiol. *2*.
Sampath, V., McCaig, W.D., and Thanassi, D.G. (2018). Amino acid deprivation and central carbon metabolism regulate the production of outer membrane vesicles and tubes by *Francisella*: Regulated production of membrane vesicles and tubes. Mol. Microbiol. *107*, 523–541.
Sana, T.G., Baumann, C., Merdes, A., Soscia, C., Rattei, T., Hachani, A., Jones, C., Bennett, K.L., Filloux, A., Superti-Furga, G., et al. (2015). Internalization of *Pseudomonas aeruginosa* Strain PAO1 into Epithelial Cells Is Promoted by Interaction of a T6SS Effector with the Microtubule Network. MBio *6*, e00712-15.
Sansonetti, P.J., Phalipon, A., Arondel, J., Thirumalai, K., Banerjee, S., Akira, S., Takeda, K., and Zychlinsky, A. (2000). Caspase-1 Activation of IL-1β and IL-18 Are Essential for Shigella flexneri–Induced Inflammation. Immunity *12*, 581–590.
Santic, M., Molmeret, M., and Kwaik, Y.A. (2005a). Modulation of biogenesis of the Francisella tularensis subsp. novicida-containing phagosome in quiescent human macrophages and its maturation into a phagolysosome upon activation by IFN-γ. Cell. Microbiol. *7*, 957–967.
Santic, M., Molmeret, M., Klose, K.E., Jones, S., and Kwaik, Y.A. (2005b). The Francisella tularensis pathogenicity island protein IglC and its regulator MglA are essential for modulating phagosome biogenesis and subsequent bacterial escape into the cytoplasm. Cell. Microbiol. *7*, 969–979.
Santic, M., Asare, R., Skrobonja, I., Jones, S., and Kwaik, Y.A. (2008). Acquisition of the Vacuolar ATPase Proton Pump and Phagosome Acidification Are Essential for Escape of Francisella tularensis into the Macrophage Cytosol. Infect. Immun. *76*, 2671–2677.
Sato, H., Okinaga, K., and Saito, H. (1988). Role of Pili in the Pathogenesis of Pseudomonas aeruginosa Burn Infection. Microbiol. Immunol. *32*, 131–139.
Sauer, J.-D., Shannon, J.G., Howe, D., Hayes, S.F., Swanson, M.S., and Heinzen, R.A. (2005). Specificity of Legionella pneumophila and Coxiella burnetii Vacuoles and Versatility of Legionella pneumophila Revealed by Coinfection. Infect. Immun. *73*, 4494–4504.
Schroder, K., and Tschopp, J. (2010). The Inflammasomes. Cell *140*, 821–832.
Schulert, G.S., and Allen, L.-A.H. (2006). Differential infection of mononuclear phagocytes by Francisella tularensis: role of the macrophage mannose receptor. J. Leukoc. Biol. *80*, 563–

571.
Schunder, E., Gillmaier, N., Kutzner, E., Herrmann, V., Lautner, M., Heuner, K., and Eisenreich, W. (2014). Amino Acid Uptake and Metabolism of *Legionella pneumophila* Hosted by *Acanthamoeba castellanii*. J. Biol. Chem. *289*, 21040–21054.
Schwarz, S., West, T.E., Boyer, F., Chiang, W.-C., Carl, M.A., Hood, R.D., Rohmer, L., Tolker-Nielsen, T., Skerrett, S.J., and Mougous, J.D. (2010). Burkholderia Type VI Secretion Systems Have Distinct Roles in Eukaryotic and Bacterial Cell Interactions. PLOS Pathog. *6*, e1001068.
Schwarz, S., Singh, P., Robertson, J.D., LeRoux, M., Skerrett, S.J., Goodlett, D.R., West, T.E., and Mougous, J.D. (2014). VgrG-5 Is a Burkholderia Type VI Secretion System-Exported Protein Required for Multinucleated Giant Cell Formation and Virulence. Infect. Immun. *82*, 1445–1452.
Seveau, S. (2014). Multifaceted Activity of Listeriolysin O, the Cholesterol-Dependent Cytolysin of Listeria monocytogenes. Subcell. Biochem. *80*, 161–195.
Sies, H. (1991). Oxidative stress: from basic research to clinical application. Am. J. Med. *91*, 31S-38S.
Smith, G.A., Marquis, H., Jones, S., Johnston, N.C., Portnoy, D.A., and Goldfine, H. (1995). The two distinct phospholipases C of Listeria monocytogenes have overlapping roles in escape from a vacuole and cell-to-cell spread. Infect. Immun. *63*, 4231–4237.
So, E.C., Mattheis, C., Tate, E.W., Frankel, G., and Schroeder, G.N. (2015). Creating a customized intracellular niche: subversion of host cell signaling by *Legionella* type IV secretion system effectors. Can. J. Microbiol. *61*, 617–635.
Steeb, B., Claudi, B., Burton, N.A., Tienz, P., Schmidt, A., Farhan, H., Mazé, A., and Bumann, D. (2013). Parallel Exploitation of Diverse Host Nutrients Enhances Salmonella Virulence. PLoS Pathog. *9*, e1003301.
Steele, S., Brunton, J., Ziehr, B., Taft-Benz, S., Moorman, N., and Kawula, T. (2013). Francisella tularensis Harvests Nutrients Derived via ATG5-Independent Autophagy to Support Intracellular Growth. PLOS Pathog. *9*, e1003562.
Steele, S., Radlinski, L., Taft-Benz, S., Brunton, J., and Kawula, T.H. (2016). Trogocytosis-associated cell to cell spread of intracellular bacterial pathogens. ELife *5*.
Stenmark, H. (2009). Rab GTPases as coordinators of vesicle traffic. Nat. Rev. Mol. Cell Biol. *10*, 513–525.
Stevens, J.M., Galyov, E.E., and Stevens, M.P. (2006). Actin-dependent movement of bacterial pathogens. Nat. Rev. Microbiol. *4*, 91–101.
Stundick, M.V., Albrecht, M.T., Houchens, C.R., Smith, A.P., Dreier, T.M., and Larsen, J.C. (2013). Animal Models for *Francisella tularensis* and *Burkholderia* Species: Scientific and Regulatory Gaps Toward Approval of Antibiotics Under the FDA Animal Rule. Vet. Pathol. *50*, 877–892.
Surewaard, B.G.J., Deniset, J.F., Zemp, F.J., Amrein, M., Otto, M., Conly, J., Omri, A., Yates, R.M., and Kubes, P. (2016). Identification and treatment of the Staphylococcus aureus reservoir in vivo. J. Exp. Med. *213*, 1141–1151.
Suter, E. (1956). INTERACTION BETWEEN PHAGOCYTES AND PATHOGENIC MICROORGANISMS. *20*, 39.
Svensson, K., Larsson, P., Johansson, D., Byström, M., Forsman, M., and Johansson, A. (2005). Evolution of Subspecies of Francisella tularensis. J. Bacteriol. *187*, 3903–3908.

T

Tamilselvam, B., and Daefler, S. (2008). Francisella targets cholesterol-rich host cell membrane domains for entry into macrophages. J. Immunol. Baltim. Md 1950 *180*, 8262–8271.
Tattoli, I., Sorbara, M.T., Yang, C., Tooze, S.A., Philpott, D.J., and Girardin, S.E. (2013). *Listeria* phospholipases subvert host autophagic defenses by stalling pre-autophagosomal structures: *Listeria* phospholipases subvert host autophagic defenses. EMBO J. *32*, 3066–3078.
Taylor, N.M.I., Prokhorov, N.S., Guerrero-Ferreira, R.C., Shneider, M.M., Browning, C., Goldie, K.N., Stahlberg, H., and Leiman, P.G. (2016). Structure of the T4 baseplate and its function in triggering sheath contraction. Nature *533*, 346–352.
Taylor, R.K., Miller, V.L., Furlong, D.B., and Mekalanos, J.J. (1987). Use of phoA gene fusions to identify a pilus colonization factor coordinately regulated with cholera toxin. Proc. Natl. Acad. Sci. U. S. A. *84*, 2833–2837.
Titball, R.W., Johansson, A., and Forsman, M. (2003). Will the enigma of Francisella tularensis virulence soon be solved? Trends Microbiol. *11*, 118–123.
Travassos, L.H., Carneiro, L.A.M., Ramjeet, M., Hussey, S., Kim, Y.-G., Magalhães, J.G., Yuan, L., Soares, F., Chea, E., Le Bourhis, L., et al. (2010). Nod1 and Nod2 direct autophagy by recruiting ATG16L1 to the plasma membrane at the site of bacterial entry. Nat. Immunol. *11*, 55–62.
Tseng, T.-T., Tyler, B.M., and Setubal, J.C. (2009). Protein secretion systems in bacterial-host associations, and their description in the Gene Ontology. BMC Microbiol. *9*, S2.
Tullius, M.V., Harmston, C.A., Owens, C.P., Chim, N., Morse, R.P., McMath, L.M., Iniguez, A., Kimmey, J.M., Sawaya, M.R., Whitelegge, J.P., et al. (2011). Discovery and characterization of a unique mycobacterial heme acquisition system. Proc. Natl. Acad. Sci. *108*, 5051–5056.
Tunio, S.A., Oldfield, N.J., Berry, A., Ala'Aldeen, D.A.A., Wooldridge, K.G., and Turner, D.P.J. (2010). The moonlighting protein fructose-1, 6-bisphosphate aldolase of Neisseria meningitidis: surface localization and role in host cell adhesion. Mol. Microbiol. *76*, 605–615.

V

Valentin-Hansen, P., Eriksen, M., and Udesen, C. MicroReview: The bacterial Sm-like protein Hfq: a key player in RNA transactions. Mol. Microbiol. *51*, 1525–1533.
Vettiger, A., Winter, J., Lin, L., and Basler, M. (2017). The type VI secretion system sheath assembles at the end distal from the membrane anchor. Nat. Commun. *8*.
Vieira, O.V., Bucci, C., Harrison, R.E., Trimble, W.S., Lanzetti, L., Gruenberg, J., Schreiber, A.D., Stahl, P.D., and Grinstein, S. (2003). Modulation of Rab5 and Rab7 Recruitment to Phagosomes by Phosphatidylinositol 3-Kinase. Mol. Cell. Biol. *23*, 2501–2514.
Vonderheit, A., and Helenius, A. (2005). Rab7 Associates with Early Endosomes to Mediate Sorting and Transport of Semliki Forest Virus to Late Endosomes. PLoS Biol. *3*.

W

Wang, J., Brackmann, M., Castaño-Díez, D., Kudryashev, M., Goldie, K.N., Maier, T., Stahlberg, H., and Basler, M. (2017). Cryo-EM structure of the extended type VI secretion system sheath–tube complex. Nat. Microbiol. *2*, 1507–1512.
Weber, B., Hasic, M., Chen, C., Wai, S.N., and Milton, D.L. Type VI secretion modulates quorum sensing and stress response in Vibrio anguillarum. Environ. Microbiol. *11*, 3018–3028.
Wehrly, T.D., Chong, A., Virtaneva, K., Sturdevant, D.E., Child, R., Edwards, J.A., Brouwer, D.,

Nair, V., Fischer, E.R., Wicke, L., et al. (2009). Intracellular biology and virulence determinants of Francisella tularensis revealed by transcriptional profiling inside macrophages. Cell. Microbiol. *11*, 1128–1150.
Weinert, L.A., and Welch, J.J. (2017). Why Might Bacterial Pathogens Have Small Genomes? Trends Ecol. Evol. *32*, 936–947.
Weiss, G., and Schaible, U.E. (2015). Macrophage defense mechanisms against intracellular bacteria. Immunol. Rev. *264*, 182–203.
Welch, M.D., and Way, M. (2013). Arp2/3-mediated actin-based motility: a tail of pathogen abuse. Cell Host Microbe *14*, 242–255.
Wells, R.M., Jones, C.M., Xi, Z., Speer, A., Danilchanka, O., Doornbos, K.S., Sun, P., Wu, F., Tian, C., and Niederweis, M. (2013). Discovery of a Siderophore Export System Essential for Virulence of Mycobacterium tuberculosis. PLoS Pathog. *9*, e1003120.
Wenren, L.M., Sullivan, N.L., Cardarelli, L., Septer, A.N., and Gibbs, K.A. (2013). Two Independent Pathways for Self-Recognition in Proteus mirabilis Are Linked by Type VI-Dependent Export. MBio *4*, e00374-13.
Wernegreen, J.J. (2015). Endosymbiont evolution: Predictions from theory and surprises from genomes. Ann. N. Y. Acad. Sci. *1360*, 16–35.
Wherry, W.B., and Lamb, B.H. (2004). Infection of man with Bacterium tularense. 1914. J. Infect. Dis. *189*, 1321–1329.
Whitney, J.C., Beck, C.M., Goo, Y.A., Russell, A.B., Harding, B., De Leon, J.A., Cunningham, D.A., Tran, B.Q., Low, D.A., Goodlett, D.R., et al. (2014). Genetically distinct pathways guide effector export through the type VI secretion system. Mol. Microbiol. *92*, 529–542.
Willis, L.M., and Whitfield, C. (2013). Structure, biosynthesis, and function of bacterial capsular polysaccharides synthesized by ABC transporter-dependent pathways. Carbohydr. Res. *378*, 35–44.

Y

Yilmaz, Ö., Sater, A.A., Yao, L., Koutouzis, T., Pettengill, M., and Ojcius, D.M. (2010). ATP-dependent activation of an inflammasome in primary gingival epithelial cells infected by Porphyromonas gingivalis. Cell. Microbiol. *12*, 188–198.
Yoshikawa, Y., Ogawa, M., Hain, T., Yoshida, M., Fukumatsu, M., Kim, M., Mimuro, H., Nakagawa, I., Yanagawa, T., Ishii, T., et al. (2009). Listeria monocytogenes ActA-mediated escape from autophagic recognition. Nat. Cell Biol. *11*, 1233–1240.

Z

Zheng, J., and Leung, K.Y. (2007). Dissection of a type VI secretion system in Edwardsiella tarda. Mol. Microbiol. *66*, 1192–1206.
Zheng, Y.T., Shahnazari, S., Brech, A., Lamark, T., Johansen, T., and Brumell, J.H. (2009). The Adaptor Protein p62/SQSTM1 Targets Invading Bacteria to the Autophagy Pathway. J. Immunol. *183*, 5909–5916.
Ziveri, J., Barel, M., and Charbit, A. (2017). Importance of Metabolic Adaptations in Francisella Pathogenesis. Front. Cell. Infect. Microbiol. *7*.
Zogaj, X., Chakraborty, S., Liu, J., Thanassi, D.G., and Klose, K.E. (2008). Characterization of the Francisella tularensis subsp. novicida type IV pilus. Microbiology *154*, 2139–2150.
Zoued, A., Durand, E., Brunet, Y.R., Spinelli, S., Douzi, B., Guzzo, M., Flaugnatti, N., Legrand, P., Journet, L., Fronzes, R., et al. (2016). Priming and polymerization of a bacterial contractile

tail structure. Nature *531*, 59–63.

Résumé

Francisella tularensis est l'agent étiologique responsable de la tularémie, une zoonose endémo-épidémique dans l'hémisphère Nord, capable d'infecter un grand nombre d'espèces animales (mammifères, oiseaux, insectes,…) et potentiellement hautement pathogène pour l'homme. Cette pathologie encore mal connue a des manifestations très polymorphes, pouvant aller de formes bénignes jusqu'à des formes pulmonaires mortelles. Lors de l'infection de mammifères, *Francisella* se multiplie principalement à l'intérieur des cellules macrophagiques. Cependant, au cours de sa dissémination systémique, elle est capable d'infecter de nombreux autres types cellulaires, y compris non phagocytaires (épithéliales, hépatocytes,…). Pour cela, *Francisella* a développé des mécanismes lui permettant d'échapper à la lyse dans le phagosome et de se multiplier dans le cytoplasme des cellules infectées où elle obtient certains éléments essentiels à sa croissance.

Dans une première partie, nous nous sommes intéressés à l'adaptation métabolique de *Francisella* au cours de son cycle intracellulaire et notamment au rôle d'une enzyme clé de la Glycolyse/Gluconéogenèse, la fructose-1,6-biphosphate aldolase (FBA). Au-delà de son rôle ménager dans le métabolisme, nous démontrons que FBA est importante pour la multiplication bactérienne dans les macrophages en présence de substrats gluconéogèniques. De plus, nous mettons en évidence un rôle direct de cette enzyme métabolique dans la régulation de la transcription des gènes *katG* et *rpoA*, codant respectivement pour la catalase et une sous-unité de l'ARN polymérase. Nous proposons un modèle dans lequel FBA participe au contrôle de l'homéostasie redox de l'hôte et à la réponse immunitaire inflammatoire.

Dans une seconde partie, nous nous sommes intéressés au système de sécrétion de type VI (SST6) de *Francisella*. De nombreuses bactéries à Gram négatif utilisent le SST6 pour transloquer des protéines effectrices dans des cellules eucaryotes ou procaryotes. *Francisella* possède un SST6 non-canonique codé sur l'îlot de pathogénicité FPI qui est essentiel pour la sortie du phagosome et permet à la bactérie de se multiplier dans le cytosol de la cellule hôte. En utilisant une approche phosphoprotéomique globale chez la sous-espèce *novicida*, nous avons identifié un site de phosphorylation unique sur la tyrosine 139 de IglB, un composant clé de la gaine contractile du SST6. Nos résultats suggèrent que le statut de phosphorylation de IglB joue un rôle important dans l'assemblage d'un SST6 fonctionnel. Nous proposons que cette modification post-traductionnelle du composant majeur de la gaine pourrait constituer un nouveau mécanisme permettant de moduler la dynamique d'assemblage/désassemblage du SST6.

Mots Clés : *Francisella tularensis*, Métabolisme, Fructose-1,6-biphosphate aldolase, Système de Sécrétion de Type VI, IglB, Modification post-traductionnelle